Université Lille1
Sciences et Technologies

Ecole Docrorale Sciences Pour l'Ingénieur de Lille **no d'ordre :41230**

Commande Intelligente Tolérante aux Fautes des Systèmes Multi-Sources d'Energie

THÉSE

Présentée et Soutenue Publiquement le 15 Novembre 2013
pour l'obtention du

Doctorat de l'Université Lille 1 Sciences et Technologies

(Spécialité Automatique, Génie Informatique, Traitement de Signal et Images)

par

Elkhatib Kamal Abdelfatah IBRAHIM

Composition du Jury

Rapporteurs :	**Fernando Tadeo**	Professeur à l'Université de Valladolid
	Ahmed El Hajjaji	Professeur à l'Université Jules Verne Picardie
Examinateurs:	**Mustapha Ouladsine**	Professeur à l'Université Aix Marseille III
	Christophe Saudemont	Professeur à l'Ecole à HEI Lille
Directeur de Thèse :	**Abdel Aitouche**	Professeur à l'Ecole à HEI Lille
Co-Directeur	**Mireille Bayart**	Professeur à l'Université Lille 1

Laboratoire d'Automatique, Génie Informatique et Signal-CNRS UMR 8219

LAGIS

Université Lille1
Sciences et Technologies

Ecole Docrorale Sciences Pour l'Ingénieur de Lille **Order No.:41230**

Intelligent Fault Tolerant Control of Multi-Sources Energy Systems

Being a thesis submitted for the degree of

Doctor of Philosophy

In the University of Lille 1 Sciences and Technologies, France
(Speciality: Automatic Control, Computer Engineering, Signal Processing and Images)

by

Elkhatib Kamal Abdelfatah IBRAHIM

Jury members

Reporters:	**Fernando Tadeo**	Professor at the University of Valladolid
	Ahmed El Hajjaji	Professor at the University of Jules Verne Picardie
Examiners:	**Mustapha Ouladsine**	Professor at the University of Aix Marseille III
	Christophe Saudemont	Professor at the School for HEI Lille
Thesis supervisor :	**Abdel Aitouche**	Professor at the School for HEI Lille
Co-supervisor	**Mireille Bayart**	Professor at the University of Lille 1

(November 2013)

Laboratoire d'Automatique, Génie Informatique et Signal-CNRS UMR 8219

LAGIS

ABSTRACT

This thesis presents stability analysis for a class of uncertain nonlinear systems and a method for designing robust fuzzy controllers to stabilize the multivariable multi-sources of energy systems subject to parameter uncertainties, sensor faults, actuator faults/unknown inputs and/or wind disturbance. First, the Takagi–Sugeno (TS) fuzzy model is adopted for fuzzy modeling of the uncertain nonlinear system. Next, we propose a Fuzzy Dedicated Observers (FDOS) method and a Fuzzy Proportional-Integral Estimation Observer (FPIEO) with a Fuzzy Fault Tolerant Control (FFTC) algorithm for TS systems. FDOS provide residuals for detection and isolation of sensor faults which can affect a TS model and FPIEO estimates the actuator faults which fed to the FDOS to reconfigure the controller. The TS fuzzy model is adopted for fuzzy modeling of the uncertain nonlinear system and establishing fuzzy state observers. The concept of the Parallel Distributed Compensation (PDC) is employed to design FFTC and fuzzy observers from the TS fuzzy models. TS fuzzy systems are classified into three families based on the input matrices and a FFTC synthesis is proposed for each family. In each family, sufficient conditions are derived for robust stabilization, in the sense of Taylor series stability and Lyapunov method, for the TS fuzzy system with parametric uncertainties, sensor faults, actuator faults/unknown inputs and/or wind disturbance. The sufficient conditions are formulated in the format of Linear Matrix Inequalities (LMIs) and Linear Matrix Equalities (LMEs). Important issues for the stability analysis and design are presented. The effectiveness of the proposed controller design methodology is finally demonstrated through a Hybrid Wind-Diesel System (HWDS), Wind Energy System (WES) with Doubly Fed Induction Generators (DFIG) and Photovoltaic (PV) generation system to illustrate the effectiveness of the proposed method.

***Index Terms*--** DFIG, Fuzzy Controller, FTC, Fuzzy Observer, LMIs, Parameters Uncertainties, Sensor Faults, Actuator Faults, TS Fuzzy Model, Unknown Inputs, PV.

ACKNOWLEDGEMENT

It is a pleasure to thank those who made this thesis possible. First, I owe many thanks for all the moral support, academic guidance that was given me by my supervisor, Professor Abdel Aitouche, in different matter during my study. Many thanks for his supervision expertise with numerous invaluable discussions and advice sessions that taught me how to do engineering research. It is really a wonderful feeling and honor to do research under his supervision. Thanks are extended to my second supervisor, Professor Mireille Bayart and Dr. Reza Ghorbani for their motivations and their helpful advice. I would like also to thank the head of the Department Professor Vincent Cocquempot for his dedication and help my thank goes to all colleagues at the Department of Engineering, especially people in LAGIS, the University of Lille1.

I would also like to thank Professor Abdul-Azim Ibrahim and Professor Magdy Koutb for their continual encouragement and for their great efforts beginning with selecting the topic of research and continuing during the course of the work.

I want to express my gratitude to my friends Judge Mostafa Nagy, Dr. Amr Hassan and Dr. Mohamed Gaber, for their friendship during all these years, also for their support and valuable advice.

I gratefully acknowledge the financial support of my PhD study from the Egypt ministry of higher education and scientific research.

I also owe a great debt of gratitude to my dearest ones my parent, my brother Nagy, my wife, my daughter, my son, and my parent in-law for their love and patient.

CONTENTS

CHAPTER 1

INTRODUCTION

CHAPTER 2

ROBUST CONTROL OF MULTI-SOURCES OF ENERGY SYSTEMS: STABILITY ANALYSIS AND DESIGN

CHAPTER 3

ROBUST FUZZY FAULT-TOLERANT CONTROL OF WES SUBJECT TO SENSOR FAULTS

CHAPTER 4

INTELLIGENT RFFTC OF WES SUBJECT TO ACTUATOR AND SENSOR FAULTS

CHAPTER 5

CONCLUSIONS

REFERENCES

AUTHOR'S PUBLICATIONS

INTERNATIONAL JOURNAL

[1] **Elkhatib Kamal**, A. Aitouche, and D. Abbes. Robust fuzzy scheduler fault tolerant control of wind energy systems subject to sensor and actuator faults, International Journal of Electrical Power and Energy Systems vol. 55, no.1, pp. 402-419, 2014. IF: 3,447.

http://authors.elsevier.com/sd/article/S0142061513004031

[2] **Elkhatib Kamal**, A. Aitouche. Fuzzy Fault-Tolerant Control of Wind-Diesel Hybrid Systems Subject to Sensor Faults, IEEE Transactions on Sustainable Energy, vol. 4, no 4, pp. 857-866, Oct.2013. IF: 1,217, http://ieeexplore.ieee.org/xpl/login.jsp?tp=&arnumber=6496183&url=http%3A%2F%2Fieeexplore.ieee.org%2Fiel7%2F5165391%2F5433168%2F06496183.pdf%3Farnumber%3D6496183

[3] **Elkhatib Kamal,** A. Aitouche. Robust Fault tolerant Control of DFIG Wind Energy Systems With Unknown Inputs. Renewable Energy, vol. 56, pp.2-15, 2013, IF(Impact factor): 2,978.

http://www.sciencedirect.com/science/article/pii/S0960148112006696

[4] **Elkhatib Kamal,** A. Aitouche. Robust Scheduler Fuzzy Controller of DFIG Wind Energy Systems, IEEE Transactions on Sustainable Energy, vol. 4, no 3, pp. 706-715, 2013. IF: 1,217.

http://ieeexplore.ieee.org/xpl/articleDetails.jsp?arnumber=6471277

[5] **Elkhatib Kamal**, A. Aitouche, R. Ghorbani and M. Bayart. Robust Nonlinear Control of Wind Energy Conversion Systems, International Journal of Electrical Power and Energy Systems, 44, no.1, pp. 202-209, Jan. 2013. IF: 3,432. http://www.sciencedirect.com/science/article/pii/S0142061512003699

[6] **Elkhatib Kamal**, A. Aitouche, R. Ghorbani and M. Bayart. Fuzzy Scheduler Fault Tolerant Control for Wind Energy Conversion Systems. IEEE Transactions on Control Systems Technology, TCST-2011-0526, Issue: 99, IF: 2.(This article has been accepted for inclusion in a future issue of this journal. Content is final as presented, with the exception of pagination).

http://ieeexplore.ieee.org/xpl/articleDetails.jsp?arnumber=6472050

[7] **Elkhatib Kamal**, A. Aitouche, R. Ghorbani and M. Bayart. Robust Fuzzy Fault Tolerant Control of Wind Energy Conversion Systems Subject to Sensor Faults, IEEE Transactions on Sustainable Energy, vol. 3, no 2, pp. 231-241, 2012. IF: 1,217.

http://ieeexplore.ieee.org/xpl/articleDetails.jsp?arnumber=6170986

[8] **Elkhatib Kamal**, A. Aitouche and M. Bayart. Intelligent Control of WECS subject to Parameter Uncertainties, Actuator and Sensor Faults, Acta Press, Control and Intelligent Systems, vol. 40, no 3, pp. 1-9, 2012. IF: 0,31

http://hal.archives-ouvertes.fr/view_by_stamp.php?&halsid=dj52ls4krqig51g8gj2tlcvbc3&label=LAGIS&langue=en&action_todo=view&id=hal-00742122&version=1

[9] **Elkhatib Kamal**, A. Aitouche, R. Ghorbani and M. Bayart. Robust Fuzzy Logic Control of Wind Energy Conversion Systems with Unknown Inputs. Acta Press, International Journal Power and Energy Systems, vol. 32, no 2, pp. 71-81, 2012. IF: 0,17.

http://hal.archives-ouvertes.fr/view_by_stamp.php?&halsid=5ap105ipmkf8duptgaughfaud1&label=LAGIS-STF&langue=fr&action_todo=view&id=hal-00742123&version=1

CHAPTER BOOK

[1] A. Aitouche, **Elkhatib Kamal** and M. Bayart. Intelligent Control of Wind Energy Conversion Systems,Wind Farm /Book 2, ISBN 978-953-307-467-2, Open Acces Publisher, Intechweb (available on line at 14th June 2011)

COLLECTIVE BOOK

[1] **Elkhatib Kamal,** A. Aitouche and M. Bayart. Design of Maximum Power Fuzzy Controller for PV Systems Based on the LMI-Based Stability International Conference on Diagnostics Processes and Systems, Intelligent Systems in Technical and Medical Diagnostics, Editors Jozef Korbicz and Marek Kowal, Springer, 2013.

[2] **Elkhatib Kamal**, A. Aitouche and M. Bayart. Fault Tolerant Control of Wind Energy Conversion Systems Subject to Sensor Faults. International Conference on Sustainability in Energy and Buildings,1-3 June 2011, Marseille, France.http://seb.sustainedenergy.org/

INTERNATIONAL CONFERENCE

[1] **Elkhatib Kamal,** A. Aitouche, R. Ghorbani and M. Bayart. Fuzzy Scheduler Fault Tolerant Control Method for WES subject to instrument faults, 2013 American Control Conference (ACC 2013), Washington, DC, USA, June 17-19 June, 2013, http://a2c2.org/conferences/acc2013/index.html.

[2] **Elkhatib Kamal, and** A. Aitouche,. Robust fuzzy control of PV systems with parametric uncertainties, IET Control and Automation Conference 2013, Conference Aston Lakeside Centre, Birmingham, UK, June 4-5 June, 2013, http://conferences.theiet.org/control/index.cfm.

[3] **Elkhatib Kamal**, A. Aitouche and Oena Kuzmych . Robust Fuzzy Controller For Photovoltaic Maximum Power Point Tracking, 21st Mediterranean Conference on Control and Automation, Platanias-Chania, Crete - Greece, June 25 - 28, 2013, http://www.med2013.org

[4] **Elkhatib Kamal,** A. Aitouche and M. Bayart. Fault Tolerant Control of WES Parametric Uncertainties, 2nd International Conference on Systems and Computer Science, Villeneuve d'Ascq, France, August 26-27, 2013, http://www.acs.pub.ro/icscs2013/

[5] **Elkhatib Kamal** and A. Aitouche**.** Nonlinear Control of PV Systems for Power Regulation, 3rd International Conference on Systems and Control, ICSC'2013 to be held in Algiers, Algeria, October 29-31, 2013,http://lias.labo.univ-poitiers.fr/icsc/icsc2013/

[6] **Elkhatib Kamal,** A. Aitouche, R. Ghorbani and M. Bayart. Unknown input observer with fuzzy fault tolerant control for wind energy system, SAFEPROCESS 2012, 29 August-31 August, 2012, Mexico. http://safeprocess2012.unam.mx

[7] **Elkhatib Kamal,** Abdel Aitouche, Reza Ghorbani, Mireille Bayart. Fuzzy Fault Tolerant Control For Wind Energy System Subject to Parameters Uncertainties and Unknown Inputs. 20th Mediterranean Conference on Control and Automation, 3-6 July, 2012, Barcelona, Spain. http://www.med2012.org

[8] **Elkhatib Kamal**, Abdel Aitouche, Reza Ghorbani, Mireille Bayart. Fault Tolerant Control of Wind Energy System Subject To Actuator Faults and Time Varying Parameters, 20th Mediterranean Conference on Control and Automation, 3-6 July, 2012, Barcelona, Spain. http://www.med2012.org

[9] **Elkhatib Kamal,** A. Aitouche, R. Ghorbani and M. Bayart. Fuzzy Scheduler Control for Wind Energy Conversion systems subject to Parameter

Uncertainties, 14th IFAC Symposium on Information Control Problems in Manufacturing, INCOM 2012, 23-25 May 2012, Bucharest, Romania. http://www.incom12.ro

[10] **Elkhatib Kamal,** A. Aitouche, M. Ouediat, A. Jouni. Fuzzy Maximum Power Control of PV System, International Conference on Renewable Energies, REDEC-2012, Nov 28, Nov 29, 2012 , http://www.ise.fraunhofer.de/en/events-and-trade-fairs/2012/redec-2012.

[11] **Elkhatib Kamal**, A. Aitouche, R. Ghorbani and M. Bayart. Output Regulation of PV Power System via a TS Fuzzy Model-based Approach, 2nd International Conference on Systems and Control Conference (ICSC 2012), marrakech, Morocco , 20th to 22nd June 2012, http://lias.labo.univ-poitiers.fr/icsc/icsc2012/

[12] **Elkhatib Kamal**, A. Aitouche and M. Bayart. Intelligent Fault Tolerant Control of Wind Energy Conversion Systems. Papyrus, First Workshop on “Fault Diagnosis and Fault Tolerant Control in large scale processing industries" , 6-7 October 2011, Porticcio, Corsica, France.

[13] **Elkhatib Kamal**, A. Aitouche and M. Bayart. A fuzzy Approach for Actuator Fault Tolerant Control of Wind Energy Conversion Systems. 19th Mediterranean Conference on Control and Automation, Acquis Corfu Holliday Palace, Corfu, Greece, 20-23 June, 2011, pp.120-125. http://www.med2011.org

[14] **Elkhatib Kamal**, A. Aitouche and M. Bayart.A Fault Tolerant Control of Wind Energy Conversion Systems subject to Parametric Uncertainties and Sensor Faults. 19th Mediterranean Conference on Control and Automation, Acquis Corfu Holliday Palace, Corfu, Greece, 20-23 June, 2011, pp.126-131. http://www.med2011.org

[15] **Elkhatib Kamal**, A. Aitouche and M. Bayart. A Fuzzy Scheduler Fault Tolerant Control for WECS subject to Sensor Faults and Parametric Uncertainties. 19th Mediterranean Conference on Control and Automation, Acquis Corfu Holliday Palace, Corfu, Greece, 20-23 June, 2011, pp. 1122-1127. http://www.med2011.org

[16] **Elkhatib Kamal**, A. Aitouche and M. Bayart. A Fuzzy Approach for Sensor Fault-Tolerant Control of wind energy conversion Systems, The 7th conference of the European Society for Fuzzy Logic and Technology (EUSFLAT-2011), 18-22 July 2011, Aix-Les-Bains, France. http://www.polytech.univ-savoie.fr/index.php?id=eusflat2011

[17] **Elkhatib Kamal**, A. Aitouche and M. Bayart. Robust Control of Wind Energy Conversion Systems. IEEE CCCA'11, International Conference on Communications Computing and Control Applications, 3-5 March, 2011, Hammamet, Tunisia.http://www.hypersciences.org/ccca11/

LIST OF SYMBOLS

$M_{\varepsilon i} q_{\varepsilon}(x(t))$	The grade of membership of $q_{\varepsilon}(x(t))$ in $M_{\varepsilon i}$
$N_{\alpha i}$ and $M_{\varepsilon i}$	Fuzzy set
$u(t)$	Control input; input vector
$x(t)$, X(t)	System state vectors
$y(t)$, Y(t)	Output state vectors
A_i	System matrix
B_i	Input matricx
C_i	Output vector
ΔA_i	Parameter uncertainties of the system matrices
ΔB, ΔB_i	Parameter uncertainties of the input matrices/vectors
c, p	Number of IF-Then rules
W	Noise distribution matrix
$d(t)$	Measurement noise
z_k, G_j	Controller gain matrices
$r(t)$	Reference input (set point)
H_{ij}, H_i	Closed-loop system matrices
ΔH_{ij}, ΔH_j	Closed-loop system parameter uncertainties matrices
$[\upsilon, \sigma, \delta, \partial, \theta, \varphi]$	Nonzero positive constants
T	Transformation matrix
$\gamma_{\max}$	The largest eigenvalue
$\|.\|$	l_2 vector norm or induced matrix norm
$\|.\|_{\max}$	Maximum l_2 vector norm or induced matrix norm
t	Time
t_0	Initial time

P	Symmetric positive definite matrix
P_m	Aerodynamic power
ρ	Air density
R	Rotor radius
v	Wind speed
β	Blade pitch angle of the wind turbine
λ	TSR
C_p	Power coefficient
Ω_r	Turbine rotational speed
λ_{opt}	Optimal TSR
$C_{p(\max)}$	Maximum power coefficient
T_r	The aerodynamic torque
$\xi = (1-L_m^2)/L_sL_r$	Leakage coefficient
f_s	Stator frequency
ω_s and ω_r	Stator and rotor angular frequencies, respectively
Ω_g	Mechanical generator speed
n_p	Number of pole pairs
i_{sd} and i_{rd}	Sator and rotor currents, respectively in axis *d*, respectively
i_{sq} and i_{rq}	Stator and rotor currents in axis *q*, respectively
R_s, and R_r	Stator and rotor resistance, respectively
L_s, L_r, and L_m	Stator, rotor leakage and magnetizing inductances, respectively
V_s	Stator voltage magnitude
τ_g	Time constant of the mode
T_h	High-speed shaft torque
n_b	Gearbox ratio

D_r, D_g, and D_{ls}	Damping constants for the rotor, generator, and the equivalent Low-speed shaft, respectively
K_{ls}	Equivalent torsional stiffness of the low-speed shaft
J_r and J_g	Moments of inertia of the rotor and generator, respectively
T_g and $T_{g,ref}$	Generator torque and required generator torque, respectively
P_s	Stator active power
Q_s	Stator reactive power
$\Delta a_{\upsilon\varsigma}^{\max or \min}$	Denotes $\Delta a_{\upsilon\varsigma}^{\max}$ or $\Delta a_{\upsilon\varsigma}^{\min}$
$\Delta b_{\upsilon o}^{\max or \min}$	Denotes $\Delta b_{\upsilon o}^{\max}$ or $\Delta b_{\upsilon o}^{\min}$
$\Delta a_{\upsilon\varsigma}^{\max}$, $\Delta b_{\upsilon o}^{\max}$	Denote the maximum values of $\Delta a_{\upsilon\varsigma}$, $\Delta b_{\upsilon o}$ (i.e. the element of ΔA and ΔB) respectively
$\Delta a_{\upsilon\varsigma}^{\min}$, $\Delta b_{\upsilon o}^{\min}$	Denote the minimum values of $\Delta a_{\upsilon\varsigma}$, $\Delta b_{\upsilon o}$, respectively
σ	The robustness index
$e(t)$	Observation error
H_m	Stable matrix to be designed
Q_m	Symmetric positive definite matrix
n_p and n_s	Number of the parallel and series cells, respectively
K_b	Boltzmanns' constant,
T_c	Cell temperature
φ_p	p-n Junction characteristic
q_p	Electron charge
i_{pv} and v_{pv}	Output current and the PV array voltage on the capacitance C_{pv}
I_{ph} and I_{rs}	Photocurrent and reverse saturation current, respectively

I_{sc} and I_{or}	Short-circuit cell current at reference temperature and insolation and the reverse saturation current at the reference temperature T_r
E_{gp}	Semiconductor band-gap energy
K_I	Short-circuit current temperature coefficient
λ_I	Insolation in *mW/*cm2
v_o and i_L	Capacitance voltage C_o and the inductance current L respectively
u_d	Duty ratio of the Pulse-Width-Modulated (PWM) signal to control the switching MOSFET
R_M, R_o and R_L	Internal resistances on the power MOSFET, the capacitance C_o and the inductance L, respectively
V_D	Forward voltage of the power diode
$I_b=1-i_o/i_L$, i_o	Measurable load current
$Z(t)$	Measurable output composed of v_{pv} and i_L, v_o is immeasurable due to the presence of the R_o
$f_s(t)$	Sensor faults which is assumed to be bounded
$f_a(t)$	Actuator faults which is assumed to be bounded
E_{si} and E_{si}	Sensor fault matrix and actuator fault matrix, respectively
$\overline{D_i}$	Known matrices of actuator faults
$\overline{F_{si}}$	Known sensor fault matrix
R_{obs1} and R_{obsg}	Residual signals for observer 1 and observer g
R_{res}	Residual between the actual output and the estimated output
th	Threshold values
N_i	FDOS gains
$\hat{x}(t)$	Estimated state vector by the FDOS
$\hat{y}(t)$	Final output of the FDOS

A_r	Constant stable system matrix
B_r	Constant input matrix
C_r and $\bar{y}(t)$	Constant output matrix and the reference output, respectively
V_c	AC side voltage of the converter
E_{fd}	SG field voltage
ω_s	Angular speed, which is proportional to frequency f_r
J_s and D_s	Inertia and frictional damping of SG, respectively
i_{sd} and i_{sq}	Direct and quadrature current components of SG, respectively
L_d and L_f	Stator d-axis and rotor inductances of SG, respectively
L_{md}	d-axis field mutual inductance
τ	Transient open circuit time constant
r_a	Rotor resistance of SG
P_{ind}	Power of the induction generator
P_{load}	Power of the load
I_{ref}	Direct current set point
V_b	Bus voltage
C_a	Capacitor bank
I_{ref}	Direct-current set point of the converter
$d(t)$	Wind disturbance
$Wd(t)$	Disturbance term
$\hat{x}_u(t)$	Estimated state vector by unknown fuzzy observer
K_i	Observation error matrices
L_i	Are their corresponding integral gains to be determined
$\hat{y}_u(t)$	Final output of the unknown fuzzy observer
$\hat{x}_o(t)$	Estimated state vector by the FDOS
$\hat{y}_o(t)$	Final output of the FDOS

LIST OF FIGURES

LIST OF TABLES

ABBREVIATIONS

TS	Takagi–Sugeno
FDOS	Fuzzy Dedicated Observers
UIFO	Nonlinear Unknown Input Fuzzy Observer
FPIEO	Proportional-Integral Estimation Observer
PDC	Parallel Distributed Compensation
LMIs	Linear Matrix Inequalities
LMEs	Linear Matrix Equalities
HWDS	Hybrid Wind-Diesel System
SG and IG	Synchronous Generator, Induction Generator, respectively,
WES	Wind Energy System
DFIG	Doubly Fed Induction Generators
PV	Photovoltaic
RFC	Robust Fuzzy Controller
RFSC	Robust Fuzzy Scheduled Controller
RFSC	Robust Fuzzy Scheduled Controller
FTC	Fault Tolerant Control
FSFTC	Fuzzy Scheduler Fault Tolerant Controller
DFFTC	Dynamic Fuzzy Fault Tolerant Control
RDFFTC	Robust Dynamic Fuzzy Fault Tolerant Control
RFFTC	Robust Fuzzy Fault Tolerant Control
RFSFTC	Robust Fuzzy Scheduler Fault Tolerant Controller
MPPT	Maximum Power Point Tracking
WG	Wind-Generator
LQG	Linear Quadratic Gaussian
TSR	Tip Speed Ratio

COG	Center of Gravity
FDI	Fault Detection and Isolation
FDD	Fault Detection and Diagnosis

CHAPTER 1

CHAPTER 1

INTRODUCTION

In remote areas and small islands, diesel generators are often the main source of electric power. Diesel fuel has several drawbacks, it is expensive because the transportation to remote areas adds extra cost, and it causes air pollution by engine exhaust. Providing a feasible, economical, and environmentally friendly solution to diesel generators is important. A hybrid system of wind power and diesel generators or the PV generation can benefit islands or other isolated communities and increase fuel savings. Wind is, however, a natural energy source that produces a fluctuating power output. The excessive fluctuation of power output adversely affects the quality of power in the distribution system, particularly frequency and voltage [1], [2].

Wind turbines form complex nonlinear mechanical systems exposed to uncontrolled wind profiles. This makes turbine controller design a challenging task [3]. As such, control of Wind Energy System (WES) is difficult due to the lack of systematic methods to identify requisite robust and sufficiently stable conditions, to guarantee performance. The problem becomes more complex when plant parameters become uncertain. The parameter uncertainties may come with the change of environment (temperature change, pressure change, load change and etc.). They make the values of the parameters deviate from the nominal values and may worsen system performance or even cause instability of the system. The mentioned parameter uncertainties may be considered to be measurable or unmeasurable depending on the implementation of sensors. For instance, the temperature change can be measured by thermal sensors. Some other parameter changes such as the resistance change of a power converter, ageing of components and measurement errors are difficult to measure and are treated as unmeasurable parameter uncertainties. Moreover, the parameter

uncertainties will become unmeasurable if sensors cannot be used due to some physical constraints or cost considerations. Fuzzy control is one of the techniques which deals with this class of systems. The stability of fuzzy systems formed by a fuzzy plant model and a fuzzy controller has recently been investigated. Various stability conditions have been obtained through the employment of Lyapunov stability theory [4], [5], fuzzy gain-scheduling controllers [6]-[8], switching controllers [9] and by other methods [10], [11]. Nonlinear controllers [12]-[14] have also been proposed for the control of WES represented by fuzzy models.

In addition to stability, robustness is also an important requirement to be considered in the study of uncertain nonlinear WES control systems. Robustness in fuzzy-model-based control has been extensively studied, such as stability robustness versus modelling errors and other various control techniques for TS fuzzy models [15].

In order to overcome nonlinearities and uncertainties, various schemes have been developed in the past two decades [16]-[19]. Reference [16] Addressing problems of output power regulation in fixed-pitch variable-speed wind energy conversion systems with parameter uncertainties. The design of Linear Matrix Inequalities (LMIs)-based robust controllers to control variable-speed, variable-pitch wind turbines, while taking into account parameter uncertainties in the aerodynamic model has been presented [17]. In [18] comparing several linear and nonlinear control strategies, with the aim of improving wind energy conversion systems. Reference [19] has also investigated fuzzy logic controls to reduce uncertainties faced by classical control methods.

Furthermore, although the problem of control in the maximization of power generation in Variable-Speed Wind Energy Systems (VS-WES) has been greatly studied, such control still remains an active research area [20]-[31]. References [20]-[24], Maximum Power Point Tracking (MPPT) algorithms for wind turbine systems have been presented. In [25] the design methodology for

TS fuzzy models is presented. This design methodology is based on fuzzy clustering methods for partitioning the input-output space, combined with Genetic Algorithms (GA), and recursive Least-Squares (LS) optimization methods for model parameter adaptation. A maximum power tracking algorithm for wind turbine systems, including a Matrix Converter (MC) has been presented in [26]. A Wind-Generator (WG) MPPT system has also been presented [27], consisting of a high efficiency buck-type DC/DC converter and a microcontroller-based control unit running the MPPT function. An advanced maximum power-tracking controller of WES [28], achieved though the implementation of fuzzy logic control techniques, also appears promising. The input to the controller consists in the difference between the maximum output power from the WES and the output power from the asynchronous link and, the derivative of this difference. The output of the controller is thus the firing angle of the line-commutated inverter, which transfers the maximum tracked power to the utility grid. Fuzzy controllers also permit the increase of captured wind energy under low and high wind speeds [29], [30]. The fuzzy controller is employed to regulate, indirectly, the power flow in the grid connected WES by regulating the DC current flows in the interconnected DC link. Sufficiently stable conditions are expressed in terms of LMIs. Reference [31] to maximize the energy captured by the wind turbine under low to medium wind speeds by tracking the desired pitch angle and rotor speed, when the wind turbine system nonlinearities structurally uncertain.

In addition, PV power generation has stimulated considerable interest over the past two decades. While solar energy is the only available energy source in space, it is an important alternative for many terrestrial applications. At a given temperature and insolation level, PV cells supply maximum power at one particular operation point called the Maximum Power Point (MPP). Unlike conventional energy sources, it is desirable to operate PV systems at its MPP. However, the MPP locus varies over a wide range, depending on PV array

temperature and insolation intensity. MPPT play an important role in PV power systems because they maximize the power output from a PV system for a given set of conditions, and therefore maximize the array efficiency. Thus, an MPPT can minimize the overall system cost. MPPTs find and maintain operation at the maximum power point, using an MPPT algorithm. Many MPPT techniques have been proposed, the Perturb-and-Observe (PO) [32], modified PO, incremental conductance methods [33], [34], Constant Voltage (CV) [35], incremental conductance and CV combined [35], Short Current Pulse [36], open circuit voltage [37], the Temperature Method [38]. These techniques are easily implemented and have been widely adopted for low-cost applications.

Concerning other studies, due to the strong requirements of the wind energy field, FTC of variable speed wind turbine systems has received significant attention in recent years [39]-[44]. To maintain the function of closed-loop control during faults and system changes, it is necessary to generate information about changes in a supervision scheme. Therefore, the objective of FTC is to maintain current performances close to desirable performances and preserve stability conditions in the presence of fault component and/or instrument. FTC systems must have the ability to adjust off-nominal behaviour, which might occur during sensor, actuator, or other component faults. A residual based scheme has been presented [39] to detect and accommodate faults in wind turbines. An observer based scheme [40] has been proposed to detect and isolate sensor faults in wind turbine drive trains. A study of fault tolerant power converter topology [41] and fault identification and compensation for a WES with Doubly Fed Induction Generators (DFIG), has also been done. In addition, a survey on failures of wind turbine systems in Sweden, Finland and Germany [42], has been carried out, where the data are from real maintenance records over the last two decades. Robust fault tolerant controllers based on the two-frequency loop have also been designed [43]. The

low-frequency-loop adopts a PI steady-state optimization control strategy, and the high-frequency-loop adopts a robust fault tolerant control approach, thus ensuring the actuator part of the system during failure in normal operation. Fault signature analysis to detect errors in the DFIG of a wind turbine has again been presented [44].

It is well known that observer based design is a very important problem in control systems. Since in many practical nonlinear control systems, state variables are often unavailable, output feedback or observer-based control is necessary and these aspects have received much interest [40], [45]-[50] fuzzy observer designs for TS fuzzy control systems have been studied, and prove that a state feedback controller and observer always result in a stabilizing output feedback controller, provided that the stabilizing property of the control and asymptotic convergence of the observer are guaranteed through the Lyapunov method. However, in the above output feedback fuzzy controllers, the parameter uncertainties for TS fuzzy control systems have not been considered. As such robustness of the closed-loop system may not be guaranteed.

This thesis presents different procedures of finding a robust nonlinear controller and fault tolerant control for nonlinear systems. Stability analysis will be carried on a closed-loop system formed by a nonlinear plant and a nonlinear controller. In this chapter 2, we investigate three different approaches in order to tackle this class of systems, a stable and robust parameter uncertainty. In first case, we present stability analysis for a class of uncertain nonlinear WES and a method for designing robust fuzzy controllers to stabilize the uncertain nonlinear systems. First, the Takagi-Sugeno (TS) fuzzy model is adopted for fuzzy modeling of the uncertain nonlinear system. Next, new stability conditions for a generalized class of uncertain systems are derived from robust control techniques such LMIs and Linear Matrix Equalities

(LMEs). The derived stability conditions are used to analyze the stability of TS fuzzy control systems with uncertainty which can be regarded as a generalized class of uncertain nonlinear systems. The design method employs the so-called Parallel Distributed Compensation (PDC).

However, in this case our goal is to study the problem of Robust Fuzzy Controller (RFC) design for TS models subject to parameter uncertainties and maximize the output power from the wind turbine. We are concerned with presenting a variety of LMIs-based controller design methods for uncertain nonlinear systems described by the TS fuzzy models. A part of the proposed methods is some what related with the method of [51]-[53], which will become clear after the explanations in section 2.2.2 in chapter 2. For clear and convenient presentation of our results, we classify the TS fuzzy systems into three families based on how diverse their input matrices and a unique RFC controller synthesis procedure is developed for each of the families. First, the TS fuzzy systems with their input matrices on a one-dimensional cone are considered. For this family, we show that a slight modification of the control law of the TS fuzzy control leads to a significant ease in the controller synthesis. The family of the TS fuzzy systems with the different input matrices constitutes the second family. Next, the complement set of the second family is considered, and a new RFC controller is proposed for the stabilization of the family, and it is observed that the TS fuzzy controllers which stabilize the systems in the family can be found by solving a simple set of LMIs. It is shown that in each family, sufficient conditions are derived for robust stabilization in the sense of Lyapunov and Taylor series stability, for the TS fuzzy system with parametric uncertainties. Important issues for the stability analysis and design are remarked. To illustrate the effectiveness of the proposed method the proposed controller design methodology is finally demonstrated through the WES with DFIG.

In second case, the Robust Fuzzy Scheduled Controller (RFSC) is proposed for nonlinear system which is robust enough to stabilize an uncertain nonlinear system and give an acceptable closed-loop performance in the presence of parametric uncertainties, disturbances, and state variables unavailable for measurements. The TS fuzzy model system with parameter uncertainties is adopted for modeling the nonlinear WES with a DFIG and establishing fuzzy state observers. Sufficient conditions are derived for robust stabilization in the sense of Lyapunov stability and are formulated with LMIs. RFSC is considered adaptive controllers because changes its parameters as the membership function values change with the uncertain plant parameters.

In case three, we develop a Robust Nonlinear Fuzzy Control (RNFC) for stand-alone solar Photovoltaic (PV) systems and also present a TS fuzzy model-based maximum power control approach. First, the maximum-power-voltage-based control scheme and direct maximum power control scheme are introduced for the MPPT. Furthermore, the MPPT robustness is also discussed to cope with varying atmosphere and system uncertainties. Second, the nonlinear system with parameter uncertainties is represented by the TS fuzzy model. Next, in order to reduce the number of measured signals, a TS fuzzy observer is established for state feedback. Then, the concept of PDC is employed to design RNFC from the TS fuzzy models. The sufficient conditions are formulated in the format of LMIs [54] to obtain the observer and controller gains. As indicated in chapter 2 in section 2.4 the nonlinear gains, which are the grades of membership of the fuzzy controller in case 1, correspondingly, can have positive and negative values which in indicated the main difference between RFC and RNFC. The effectiveness of the proposed controller design methodology is finally demonstrated through a photovoltaic panel array to maximize the PV power. Chapter 2 presents the three cases in detailed.

In chapter 3, new three different proposed Fault Tolerant Control (FTC) algorithms, namely, Fuzzy Fault Tolerant Control (FFTC), Fuzzy Scheduler Fault Tolerant Controller (FSFTC) and Dynamic Fuzzy Fault Tolerant Control (DFFTC) are proposed for nonlinear WES systems subject to sensor faults, parameter uncertainties, wind disturbance and/or state variables unavailable for measurements. The algorithm based on reconfiguration mechanism is then investigated for detection, isolation and accommodation of sensor faults. TS fuzzy model is employed to represent the nonlinear multi-sources of energy systems, and then a model based proposed FTC design uses the concept of PDC. A system that comprises a TS fuzzy plant model and a proposed FTC connected in closed-loop is first considered. The TS fuzzy plant model represents a faulty multivariable nonlinear system subject to the parameter uncertainties as a weighted sum of a number of sub-systems. Similarly, the proposed FTC is a weighted sum of a number of sub-controllers. Difficulties have been found on analysing and designing this class of nonlinear systems using the conventional control theories. This is because the interactions of the plant among the sub-control systems, which are related to the nonlinearities, have to be considered. Moreover, the parameter uncertainties of the nonlinear plants make the analysis more difficult to be carried out, especially when the ranges of the parameter uncertainties are large. TS fuzzy systems are classified into three families based on the input matrices and a proposed FTC synthesis procedure is given for each family. In each family, sufficient conditions are derived for robust stabilization, in the sense of Taylor series stability and Lyapunov method, for the TS fuzzy system with parametric uncertainties, and sensor faults.

The problem becomes more complex if the uncertain nonlinear system is subject to the sensor faults and or/ actuator faults /the unknown inputs, which are quite common in many physical systems. In chapter 4, we present three different algorithms to solve this problem. Moreover, the stability and

robustness conditions of fuzzy fault tolerant control systems subject to large parameter uncertainties have been determined. Based on the analysis results in chapter 2 and chapter 3, three approaches that are capable of controlling uncertain nonlinear systems subject to sensor faults and/or, actuator faults, unknown inputs and wind disturbance are derived namely, Robust Fuzzy Fault Tolerant Control (RFFTC), Robust Fuzzy Scheduler Fault Tolerant Controller (RFSFTC) and Robust Dynamic Fuzzy Fault Tolerant Control (RDFFTC). This class of nonlinear plants cannot be controlled satisfactorily by simple robust fuzzy controllers. A conclusion to the whole thesis will be given in chapter 5.

In view of the aforementioned difficulties, different methods of solving the control problem of multivariable nonlinear multi-sources of energy systems are proposed in this thesis. The work can be divided into five parts: (a) to develop ways of conducting stability and robustness analyses on fuzzy control systems subject to the parameter uncertainties, (b) stability and robustness analyses on fuzzy control systems subject to the sensor, wind disturbance and the parameter uncertainties are developed, (c) to develop methods of controlling nonlinear plants subject to parameter uncertainties, sensor, actuator faults and/or the unknown inputs, (d) to develop systematic design methodologies of FFTC with guaranteed closed-loop stability, (e) the algorithm maximizes the power coefficient for a fixed pitch, moreover, it reduces the voltage ripple and stabilizes the system over a wide range of wind speed variations are developed.

Different methods to tackle the nonlinear system subject to parameter uncertainties, sensor faults, actuator faults and/or unknown inputs and wind disturbance are investigated. This summarized as following:

1.1. Robust Fuzzy Control Systems

Based on the TS fuzzy plant model, a RFC can be designed using one of three proposed design approaches. We will present the stability analysis for a class of uncertain nonlinear systems and a method for designing robust fuzzy

controllers to stabilize the uncertain nonlinear systems. First, the TS fuzzy model is adopted for fuzzy modeling of the uncertain nonlinear system. Next, new stability conditions for a generalized class of uncertain systems are derived from robust control techniques such LMIs. The derived stability conditions are used to analyze the stability of Takagi and Sugeno's fuzzy control systems with uncertainties which can be regarded as a generalized class of uncertain nonlinear systems. The details about the analysis and the design approaches of the robust fuzzy systems will be given in chapter 2, section 2.2. To probe further, RNFC is proposed in section 2.4. Under this design, the number of LMIs to be solved is reduced. In section 2.3, RFSC approach is proposed and is presented in the next section.

1.2. Robust Fuzzy Scheduled Control Systems

This section is dedicated to the design of a Robust Fuzzy Scheduler Control (RFSC) strategy for an uncertain nonlinear system described by TS models. The main idea is that the fuzzy scheduler controller can be designed such that the states of the closed-loop system will follow those of a user-defined reference input despite the presence of wind disturbances and parameter uncertainties. The proposed algorithm is implemented as a state feedback controller based on the fuzzy model and utilizes the concept of PDC. Based on the analysis results of the robust fuzzy control systems in section 2.2 in chapter 2, the RFC for each TS fuzzy plant model is designed. A fuzzy scheduler is proposed to infer the control action from the outputs of the RFC. Stability criteria and robustness conditions of the fuzzy scheduled system will then be derived so as to formulate a design procedure. All details about the fuzzy scheduled systems will be given in section 2.3 in chapter 2.

1.3. Robust Fuzzy Fault Tolerant Control Systems

As an alternative way to tackle multivariable nonlinear systems subject to parameter uncertainties, sensor faults and/or actuator faults /unknown inputs and wind disturbance, a FFTC, FSFTC and DFFTC approaches are proposed. The effectiveness of the proposed controller design methodology is demonstrated through a wind energy system with DFIG to illustrate the effectiveness of the proposed method. FSFTC design is based on combine a number of FFTC together such that the FSFTC fuzzy control system is guaranteed to be stable within the large specified parameter space, sensor faults, actuator faults and/or unknown inputs and wind disturbance. The specified parameter space will be partitioned into smaller parameter subspaces. A stable and robust fuzzy controller is associated with each parameter sub-space. The fuzzy fault tolerant controller will be used when the operating parameters are inside its parameter subspaces. Stability criteria and robustness conditions of the fuzzy fault tolerant control system will be derived, and a procedure for designing this FFTC and FSFTC will be presented. All details about fuzzy fault tolerant control systems will be given in chapter 3 and chapter 4.

Also in these chapters (chapter 3 and chapter 4), DFFTC based on a FPIO design is presented to achieve fault estimation in TS fuzzy models with sensor faults and/or actuator faults/unknown inputs, wind disturbance and parameter uncertainties.

To test the obtained results and the developed methods, applications on Hybrid Wind–Diesel System (HWDS), WES with DFIG and PV generation system have been studied and will be given as illustrative examples in this thesis. The achievements can be summarized as follows.

(a) To study The stability and robustness of fuzzy control systems, which designed the fuzzy controller for uncertain nonlinear systems.

(b) A Fuzzy Dedicated Observers (FDOS) and Fuzzy Proportional-Integral Estimation Observer (FPIEO) design is proposed to achieve fault estimation of TS models.

(c) To design the proposed nonlinear FFTC gains that is based on the TS fuzzy plant model has been presented. The number of matrix inequalities is reduced.

(d) To compensate the effect of the sensor faults and/or actuator faults, wind disturbance and parameter uncertainties within given ranges, FSFTC have been realized based on the analysis results of the FFTC approach. FSFTC has a number of FFTC embedded inside, and the control signal is obtained based on these FFTC outputs. The FSFTC is considering adaptive controllers, since the fuzzy scheduler changes its parameters as the membership function values change with the uncertain plant parameters. In this case also, the closed-loop system stability has been proven.

(e) To maximize the power coefficient for a fixed pitch to obtain the maximum output power from the multi-sources energy system and reduces the voltage ripple, a maximum power controller has been proposed.

CHAPTER 2

CHAPTER 2

ROBUST CONTROL OF MULTI-SOURCES OF ENERGY SYSTEMS: STABILITY ANALYSIS AND DESIGN

2.1. Introduction

Various control system option have been applied in response to uncertain nonlinear wind turbine control problem [3], [8], [18], [19], [40], [55]-[66]. Robust gain scheduled controller synthesis for pitch regulated variable speed wind turbine is presented in [8], [55]. The problem of designing robust control system for wind turbines in the presence of uncertainties using minimax Linear Quadratic Gaussian (LQG) design methodology has been presented in [3], [56]. A robust controller is developed [37], which is proven to yield a globally uniformly ultimately bounded stable closed-loop system via Lyapunov-based analysis. Variable Structure Systems (VSS) theory for wind power regulation is further investigated in [18] and dynamical controller is presented for low-speed output power regulation which overcomes the practical limitations of previous control solutions. Fuzzy sliding mode method is presented in [57] and applied to a large-scale variable speed wind power system with uncertain parameters and external disturbances. In [19] two different methods of the LMIs-based robust controllers to control a variable-speed variable-pitch wind turbine, while taking into account parameter uncertainties in the aerodynamic model are adopted, of which the first method assumes full state information and therefore requires a separate observer to be designed, whereas the second method relies only on measured variables. H_∞ optimal controller based on the linear model

of a three bladed, horizontal axis wind turbine has designed in [58]. In [59] compares between the multivariable controllers for a WES using H_2 and H_∞ methodologies. Comparing Proportional-Integral (PI), Proportional-Integral-Derivative (PID) and robust control pitch controllers on a wind turbine is illustrated in [60] and [61]. Linear robust control has been presented in [20], [62], [63]. However, the performance of these linear controllers is limited by the highly nonlinear characteristics of wind turbine. Typical power regulation control schemes use blade pitch angle as the only controller input. Generator torque is sometimes controlled according to the method employed for the below-rated wind speed conditions, known as the indirect control in torque technique. Most controllers hold the generator torque constant at its nominal value, making the controller monovariable in pitch only [61], [64], [65]. These monovariable controllers are unable to meet the multiple objectives of regulating electrical power and rotor speed. A multivariable controller is therefore presented in this work. Its principle is to combine a PID pitch controller with the nonlinear torque controller that we have suggested in [66].

In addition, there are also many papers that are reporting solutions to maximization the power generation in WES [1], [2], [14], [67]-[70]. A lucid mathematical deduction of optimal rotor speed to maximize the energy yield of wind machines with passively stall regulated fixed speed scheme are presented in [67]. Reference [68] presents a MPPT control method for variable-speed constant-frequency WES based on sliding mode extremum seeking control. The model of DC-DC converter (buck converter) is developed in [69], which allows the MPPT controller output (duty cycle) adjusts the voltage input of the converter to track the MPPT of the wind generator. A Lyapunov-based approach is adopted in [70] to choose the set point change direction so that power capture can be maximized for the given wind speed and environmental parameters. In [1], [2], [14] investigate robustness and power quality performance of a simple HWDS. DFIG has become a widely used generator

type in wind energy conversion. Considerable research has been done on the modeling and control of wind turbines with DFIG [71]-[74], since it features a simple structure, high-energy efficiency, reliable operation, and high power density. However, the DFIG drive system is a nonlinear system which is characterized by multiple variables and a strong coupling with profuse dynamics.

Advances in Photovoltaic (PV) technology made necessary the design of more powerful control systems. This is in order to improve PV behavior, namely to make them more profitable and more reliable. The major part of the existing research works concerning PV control deals with the optimization of the extracted power. Many approaches have been proposed to adjust the duty cycle of the converter for MPPT [75]-[80]

In this chapter, three different approaches for robust fuzzy controllers are proposed for multi-sources of energy systems subject to parameter uncertainties. Based on the aforementioned studies, the contributions of this chapter are in twofold; i) The design of a RFC, RFSC and RNFC subject to a wide range of wind variation, wind disturbance, parameter uncertainties; ii) The use of the Linear LMEs approach which, based on the TS fuzzy model and LMIs [53] is used to obtain control gains. This modification leads to simplification of the solution of Riccati type equations. The robustness index σ plays a very important role in controlling the system to a high degree of uncertainty and will be viewed in the in section 2.3, and the simulation in section 2.3.6.

This chapter is organized as follows. Section 2.2 studies the first approach to investigate the RFC of WES provides the TS fuzzy model with parameter uncertainties. The second approach which studies the RFSC for the WES subject to parameter uncertainties and wind disturbance is given in section 2.3. Section 2.4 addressed the third proposed approach RNFC for a TS fuzzy

method for stand-alone solar PV systems subject to the parameter uncertainties. A conclusion will be drawn in section 2.5.

2.2. RFC of WES With DFIG

The main contribution of this section is a simple way sufficient condition as LMIs and a systematic design procedure for the controller design for a general nonlinear system with parametric uncertainties, for continuous-time TS fuzzy systems. Specifically, this section proposes some new solutions to the robust stabilization problem for a class of nonlinear systems with norm-bounded parametric uncertainties. The WES is used as a platform for illustration of the proposed ideas, techniques, and procedures. Based on the exact fuzzy modeling technique [53], the TS fuzzy systems are classified into three families based on the input matrices and an unique controller synthesis procedure is developed for each family [37], [52]. To illustrate the merits of the proposed controllers, they are applied to WES subject to uncertain parameters and wind disturbance. We include the derivation of the proposed algorithms. Some sufficient conditions for stabilization of the continuous-time TS fuzzy models are derived, subject to system parametric uncertainties. The stability conditions for nominal nonlinear systems are extended here to general nonlinear systems with parametric uncertainties, which are likewise formulated in the LMIs format. The overall proposed design methodology presents a systematic and effective framework for continuous-time control of complex dynamic systems such as WES.

This section is organized as follows. Section 2.2.1 provides the TS fuzzy model with parameter uncertainties. The modified algorithm of RFC is given in section 2.2.2. Section 2.2.3 shows the stability and robustness conditions for the proposed algorithm and the calculation of state feedback gains of the proposed fuzzy controller is presented. Section 2.2.4 shows simulation example.

2.2.1. TS Fuzzy Model With Parametric Uncertainties

This sub-section is dedicated to a brief presentation of TS models. Consider a nonlinear system described by

$$\begin{cases} \dot{x}(t) = f(x(t),u(t)) \\ y(t) = f(x(t),u(t)) \end{cases} \quad (2.1)$$

Where $x(t)$ and $y(t)$ are the state and output vector, respectively, $u(t)$ is the control input and $f(x(t),u(t))$ is the nonlinear function. A fuzzy dynamic model proposed by TS [81] is often used to represent a nonlinear system (2.1) by the interpolation of a set of linear sub-models. The TS fuzzy model is a piecewise interpolation of several linear models through membership functions. The fuzzy model is described by fuzzy If–Then rules and will be employed here to deal with the control design problem for the nonlinear system. The TS fuzzy systems can be classified into three families based on the diversity of their input matrices B_i [37], [52]. Consider the input matrices are defined as follows

$$B_1/\alpha_1 = B_2/\alpha_2 = \ldots = B_p/\alpha_p = B \quad (2.2)$$

where $\alpha_1,\ldots,\alpha_p$ are positive values and $B \in \kappa^{nxm}$. Let p the number of fuzzy rules. The ith rule of the fuzzy model for the nonlinear system is given by [48]:

Plant Rule i: IF $q_1(x(t))$ is M_{1i} AND … AND $q_\varepsilon(x(t))$ is $M_{\varepsilon i}$

$$\text{Then} \quad \begin{cases} \dot{x}(t) = (A_i + \Delta A_i)\,x(t) + \alpha_i(B + \Delta B)u(t) + Wd(t) & i = 1,2,\ldots,p \\ y(t) = C_i\,x(t) & i = 1,2,\ldots,p \end{cases} \quad (2.3)$$

Here, $M_{\ni i}$ is the fuzzy set ($i=1,2,..,p$; $\ni=1,2,\ldots,\varepsilon$), p is the number of the rules, $x(t) \in \kappa^{nx1}$ is the state vector, $u(t) \in \kappa^{mx1}$ is the input vector, $y(t) \in \kappa^{gx1}$ is the output vector, $A_i \in \kappa^{nxn}$ is the system matrix, $C_i \in \kappa^{gxn}$ is the output matrix, $q_1(x(t)),\ldots,q_\varepsilon(x(t))$ are known premise variables and p is the number of IF-Then rules. Each linear consequent equation represented by $A_ix(t)+B_iu(t)$ is called a

subsystem and $\Delta A_i \in \kappa^{nxn}$ and $\Delta B_i \in \kappa^{nxm}$ are the uncertainties of the constant system matrices $A_i \in \kappa^{nxn}$ and $B_i \in \kappa^{nxm}$, respectively, which are non time-varying parametric uncertainties in the plant model. These uncertainties are admissibly norm-bounded and structured and *W* is the disturbance matrix which is assumed to be known and *d(t)* is the measurement disturbance and *Wd(t)* is the disturbance part. The main feature of a TS fuzzy model is to express the local dynamics of each fuzzy implication (rule) by a linear system model. The overall fuzzy model of the system is achieved by fuzzy "blending" of the linear system models. In this tutorial, the reader will find, by example in sub-section 2.2.4.3, that almost all nonlinear dynamical systems can be represented by TS fuzzy models to high degree of precision. Each sub-model contributes to the global behavior of the nonlinear system through a weighting function $\mu_i(q(x(t)))$.

The TS structure is given by

$$\dot{x}(t) = \frac{\sum_{i=1}^{p} \varpi_i(q(x(t)))[(A_i + \Delta A_i)\,x(t) + \alpha_i(B + \Delta B)u(t) + Wd(t)]}{\sum_{i=1}^{p} \varpi_i(q(x(t)))}$$

$$= \sum_{i=1}^{p} \mu_i(q(t))[(A_i + \Delta A_i)\,x(t) + \alpha_i(B + \Delta B)u(t) + Wd(t)] \qquad (2.4)$$

$$y(t) = \frac{\sum_{i=1}^{p} \varpi_i(q(x(t)))C_i\,x(t)}{\sum_{i=1}^{p} \varpi_i(q(x(t)))}$$

$$y(t) = \sum_{i=1}^{p} \mu_i(q(x(t)))C_i\,x(t) \qquad (2.5)$$

where $q(x(t))=[q_1(x_1(t))\ \ q_2(x_2(t))\ \ \dots\ \ q_\varepsilon(x(t))]$

$$\varpi_i(q(x(t))) = \prod_{\ni=1}^{\varepsilon} M_{\varepsilon i}(q_\varepsilon(x(t))), \quad \mu_i(q(x(t))) = \frac{\varpi_i(q(x(t)))}{\sum_{i=1}^{p} \varpi_i(q(x(t)))},$$

for all *t*, the term $M_{\varepsilon i}q_\varepsilon(x(t))$ is the grade of membership of $q_\varepsilon(x(t))$ in $M_{\varepsilon i}$. Since

$$\begin{cases} \sum_{i=1}^{p} \varpi_i (q(x(t))) > 0 \\ \varpi_i (q(x(t))) \geq 0 \qquad i = 1,2,...,p \end{cases} \tag{2.6}$$

It is clear that

$$\begin{cases} \mu_i (q(x(t))) \geq 0 \\ \sum_{i=1}^{p} \mu_i (q(x(t))) = 1 \qquad i = 1,2,..., p \end{cases} \tag{2.7}$$

For the first family, we consider the input matrices on a one-dimensional cone, therefore the $\alpha_1, ..., \alpha_p > 0$. Therefore the plant dynamics is then described by (2.4) and (2.5).

For the second family, we consider the input matrices are not all the same, therefore, from (2.2) $\alpha_1 \neq \alpha_2 \cdots \neq \alpha_i$, thus $B_i = \alpha_i B$ and the state equation of the TS fuzzy systems can be described by,

$$\dot{x}(t) = \sum_{i=1}^{p} \mu_i (q(x(t)))[(A_i + \Delta A_i) x(t) + (B_i + \Delta B_i) u(t) + W d(t)]$$

$$y(t) = \sum_{i=1}^{p} \mu_i (q(x(t))) C_i x(t) \tag{2.8}$$

For the third family, to consider the input matrices are common input matrix, from (2.2), $\alpha_1 = \alpha_2 \cdots = \alpha_i = 1$, so the plant dynamics are then described by:

$$\dot{x}(t) = \sum_{i=1}^{p} \mu_i (q(x(t))) [(A_i + \Delta A_i) x(t) + (B + \Delta B) u(t) + W d(t)]$$

$$y(t) = \sum_{i=1}^{p} \mu_i (q(x(t))) C_i x(t) \tag{2.9}$$

2.2.2. The Proposed Modified RFC Algorithm

The goal is to design the robust fuzzy controller such that the system states are stable in the presence of parameter uncertainties and wind disturbance. In this sub-section, an unique controller synthesis procedure is developed for each of the TS family. It is more reliable and has larger freedom on finding the robust fuzzy controller to deal with a wide range of wind, parameter uncertainties and wind disturbance.

2.2.2.1. PDC Technique

The concept of PDC in [53] is utilized to design fuzzy controllers to stabilize fuzzy system (2.4) and (2.5). The idea of PDC is to associate a compensator for each rule of the fuzzy model. The resulting overall fuzzy controller is a fuzzy blending of each individual linear controller. The fuzzy controller shares the same fuzzy sets with the fuzzy system (2.4) and (2.5).

2.2.2.2. Proposed RFC

For the fuzzy model (2.4) and (2.5) we construct the following fuzzy controller via the PDC. It is used when the membership functions are known and the rule antecedents of the TS fuzzy plant model and the fuzzy controller are the same [19], [53]. It is assumed that the fuzzy system (2.3) is locally controllable. A fuzzy controller with p fuzzy rules is to be designed for the plant. The *ith* rule of the fuzzy controller is given by:

Controller Rule *i:* IF $q_1(x(t))$ is M_{1i} AND … AND $q_\varepsilon(x(t))$ is $M_{\varepsilon i}$

Then $u(t)=-[G_i x(t)+r(t)]/\alpha_i \qquad i=1,2,..,p$ (2.10)

where $G_i \epsilon \kappa^{mxn}$ are feedback gain vectors of rule i and $r(t)$ is the reference input. The final output of the modified RFC becomes

$$u(t)=\frac{\sum_{i=1}^{p}\mu_i(q(x(t)))[G_i x(t)+r(t)]}{\sum_{i=1}^{p}\alpha_i\mu_i(q(t))} \tag{2.11}$$

For the second family, the overall output of the RFC is given by,

$$\dot{u}(t)= z_k\, u(t)+\sum_{i=1}^{p}\mu_i(q(x(t)))[G_i x(t)+r(t)] \tag{2.12}$$

where z_k and G_i are controller matrices and computed by solving the LMI constant.

For the last family, the RFC is given by,

$$u(t)=\sum_{i=1}^{p}\mu_i(q(x(t)))[-G_i\, x(t)+r(t)] \tag{2.13}$$

2.2.2.3. The Fuzzy Control System

In order to carry out the analysis, the closed-loop fuzzy system should be obtained first. In order to establish the stability conditions for each TS family, in the following, $\mu_i(q(x(t)))$ is written as μ_i. When the input matrices are on one dimensional cone, using (2.4) and (2.11), the fuzzy control system is given by,

$$\dot{x}(t)=\sum_{i=1}^{p}\mu_i(A_i+\Delta A_i)\,x(t)+Wd(t)+\left\{\sum_{i=1}^{p}\alpha_i\,\mu_i\right\}(B+\Delta B)\left\{\sum_{i=1}^{p}\mu_i[-G_j\,x(t)+r(t)]\right\}/\left\{\sum_{i=1}^{p}\alpha_i\mu_i\right\} \tag{2.14}$$

where, $H_i=A_i+BG_i$, $\Delta H_i=\Delta A_i+\Delta BG_i$

when the input matrices are different, using (2.8) and (2.12), the fuzzy control system is given by,

$$\dot{X}(t)=\sum_{i=1}^{p}\mu_i[(H_i+\Delta H_i)X(t)+Qr(t)+\psi d(t)\,] \tag{2.15}$$

where $X(t)=\begin{bmatrix}x(t)\\u(t)\end{bmatrix}, H_{ij}=\begin{bmatrix}A_i & B_i\\G_i & z_k\end{bmatrix}, H_i=\begin{bmatrix}\Delta A_i & \Delta B_i\\0 & 0\end{bmatrix}, Q=\begin{bmatrix}0\\1\end{bmatrix}, \psi=\begin{bmatrix}W\\0\end{bmatrix}$

when the input matrices are all the same, using (2.9) and (2.13) and writing $\mu(q(t))$ as μ, the fuzzy control system is given by,

$$\dot{x}(t)=\sum_{i=1}^{p}\mu_i[(H_i+\Delta H_i)x(t)+(B+\Delta B)r(t)+Wd(t)\,] \tag{2.16}$$

where, $H_i=A_i+BG_i$, $\Delta H_i=\Delta A_i+\Delta BG_i$

2.2.3. Stability and Robustness for Nonlinear Systems with Parameter Uncertainties

In this sub-section, we derive the closed loop system stability conditions and calculate the robust fuzzy controller gains.

2.2.3.1. Derivation of the Stability and Robustness Conditions

In this sub-section, the stability and robustness analysis with reference to an uncertain fuzzy control system described by (2.14), (2.15) and (2.16) under PDC is summarized in the following lemma 2.1 and theorem 2.1.

The following lemma and the theorem must be satisfied for the fuzzy control system (2.14) become stable.

Lemma 2.1: the fuzzy control system as given by (2.14) with parameter uncertainty is stable if

$$m[TH_iT^{-1}] \le -\left\|T\Delta H_iT^{-1}\right\|\max - \upsilon \qquad \forall i \tag{2.17}$$

Also from (2.15), the system is stable if

$$m[TH_iT^{-1}] \le -\left\|T\Delta H_iT^{-1}\right\|\max - \theta \qquad \forall i \tag{2.18}$$

Also from (2.16), the system is stable if

$$m[TH_iT^{-1}] \le -\left\|T\Delta H_iT^{-1}\right\|\max - \delta \qquad \forall i \tag{2.19}$$

Where $m[TH_iT^{-1}] = \lim_{\Delta t\to 0^+} \frac{\left\|I + TH_iT^{-1}\Delta t\right\| - 1}{\Delta t} = \gamma_{\max}\left(\frac{TH_iT^{-1} + (TH_iT^{-1})^*}{2}\right)$, υ, θ, δ are designed nonzero positive constant, where $T \in \kappa^{nxn}$ is a transformation matrix of rank *n*, the analysis given in the proof indicates that $\|x(t)\|$ will go to its steady state faster if we use larger values of υ, θ, δ. Thus the system performance with a larger υ, θ, δ is better than with smaller υ, θ, δ but from the lemma, the robust area is smaller for a larger υ, θ, δ than a smaller υ, θ, δ.

Theorem 2.1. The TS fuzzy system (2.14) is asymptotically stabilizable, if there exist symmetric and positive definite matrix *P*, some matrix G_i, such that the following LMIs is satisfied

$$O A_i^T + A_iO + (B_i\Theta_i)^T + (B_i\Theta_i) \le 0 \qquad P > 0, \forall i \tag{2.20}$$

where $O=P^{-1}$, $\Theta_i = G_iO$. In the same manner, the condition stability of the augmented fuzzy system for the second and the third families can be deduced.

Proof. The conditions imposed to develop the lemma 2.1 and theorem 2.1 are shown in the following,

For the lemma 2.1, the stability and robustness analyses with reference to an uncertain fuzzy control system for the first family under PDC will be considered. The analysis procedures for the second and the third family are similar to those for first family, and the results will be given without proof. Consider the Taylor series [53].

$$X(t+\Delta t) = X(t) + \dot{X}(t)\Delta t + \Phi(\Delta t) \tag{2.21}$$

Where $\Phi(\Delta t) = X(t+\Delta t) - X(t) - \dot{X}(t)\Delta t$ is the residual and $\Delta t > 0$

$$\lim_{\Delta t \to 0^+} \frac{\Phi(\Delta t)}{\Delta t} = 0 \tag{2.22}$$

Let $T^T = T$, $P = TT$ [33], from (2.14**)** and (2.21), and multiplying a transformation matrix $T \epsilon R^{nxn}$ of rank n to both sides, and taking the norm on both sides, we have

$$\|T(X(t+\Delta t))\| \le \left\| \sum_{i=1}^{p} \mu_i (I + TH_i T^{-1} \Delta t) \right\| \|Tx(t)\| + \left\| \sum_{i=1}^{p} \mu_i [([T\Delta H_i X(t) + T(B+\Delta B)r(t) + TWd(t)]\ \Delta t \right\| + \|T\Phi(\Delta t)\| \tag{2.23}$$

Where $\|.\|$ denotes the L_2 norm for vectors and L_2 induced norm for matrices from (2.23)

$$\lim_{\Delta t \to 0^+} (\|T(x(t+\Delta t))\| - \|Tx(t)\|)/\Delta t \le \lim_{\Delta t \to 0^+} \{ \sum_{i=1}^{p} \mu_i (\left\| I + TH_i T^{-1} \Delta t \right\| - 1) \|TX(t)\| \}/\Delta t + \lim_{\Delta t \to 0^+} \{ + \left\| \sum_{i=1}^{p} \mu_i [([T\Delta H_i X(t) + T(B+\Delta B)r(t) + TWd(t)]\ \Delta t \right\| + \|T\Phi(\Delta t)\| \}/\Delta t \tag{2.24}$$

From (2.22) and (2.24), we obtain

$$\frac{d\|Tx(t)\|}{dt} \le \sum_{i=1}^{p} \mu_i m[TH_i T^{-1}] \|Tx(t)\| + \left\| \sum_{i=1}^{p} \mu_i [T\Delta H_i x(t) + T(B+\Delta B)r(t) + TWd(t) \right\| \tag{2.25}$$

Where $m[TH_i T^{-1}] = \lim_{\Delta t \to 0^+} \frac{\left\| I + TH_i T^{-1} \Delta t \right\| - 1}{\Delta t} = \gamma_{\max} (\frac{TH_i T^{-1} + (TH_i T^{-1})^*}{2})$ (2.26)

is the corresponding matrix measure [82] of the induced matrix norm of $\left\|TH_i T^{-1}\right\|$ (or the logarithmic derivative of $\left\|TH_i T^{-1}\right\|$), $\gamma_{\max}(.)$ is the largest eigen value, and * is the conjugate transpose. From (2.25)

$$d\|TX(t)\|/dt \le \sum_{i=1}^{p} \mu_i\{\, m[TH_i T^{-1}] + \left\|T\Delta H_i T^{-1}\right\| \}\|Tx(t)\| + \|T(B+\Delta B)r(t)\| + \|TWd(t)\| \quad (2.27)$$

if $m[TH_i T^{-1}]$ satisfies the following inequality:

$$m[TH_i T^{-1}] \le -\left\|T\Delta H_i T^{-1}\right\|\max - \upsilon \qquad \forall i \quad (2.28)$$

where $\left\|T\Delta H_i T^{-1}\right\|\max$ is the maximum value of $\left\|T\Delta H_i T^{-1}\right\|$, and υ is a nonzero positive constant. From (2.27) and (2.28), we obtain

$$\frac{d}{dt}(\|Tx(t)\|e^{\upsilon(t-t_0)}) \le (\|T(B+\Delta B)r(t)\| + \|TWd(t)\|)e^{\upsilon(t-t_o)} \quad (2.29)$$

where $t_o<t$ is an arbitrary initial time. Based on (2.29) there are two cases to investigate the system behavior $r=0$, $d(t)=0$ and $r(t)\neq 0, d(t)\neq 0$, If the condition (A.8) is satisfied the closed loop system (2.14) is stable, and $\|x(t)\|\to 0$ as $t\to\infty$ if $r=0$, and $d(t)=0$ since from (2.24)

$$\|Tx(t)\| \le \|Tx(t_o)\|e^{-\upsilon(t-t_o)} \quad (2.30)$$

and when $r(t)\neq 0, d(t)\neq 0$, from (2.29) and based on (2.28), we investigate that

$$\|Tx(t)\| \le \|TX(t_o)\|e^{-\upsilon(t-t_o)} + (\frac{\|T(\hat{B}+\Delta\hat{B})r(t)\|}{\upsilon} + \frac{\|TWd(t)\|}{\upsilon}(1-e^{-\upsilon(t-t_o)}) \quad (2.31)$$

where $\|T(\hat{B}+\Delta\hat{B})r(t)\| \ge \max_i \|T(B+\Delta B)r(t)\|_{\max} \ge \|T(B+\Delta B)r(t)\|$,

$\|T\hat{W}d(t)\| \ge \max_i \|TWd(t)\|_{\max} \ge \|\|TWd(t)\|\|$

Since the right-hand side of (2.31) is bounded if $r(t)$ and $d(t)$ are bounded, then the system (2.14) is also bounded, then the system is stable. In the same manner we investigate the condition for the second and third family as given in (2.18) and (2.19) in lemma 2.1.

For the theorem 2.1, we will calculate the gains for the nonlinear RFC. In order to analyse the convergence of the generalized equilibrium of a fuzzy

control system (2.14) using the control law (2.11), let us consider the following quadratic Lyapunov candidate function *V(t)*:

$$V(x(t)) = x(t)^T Px(t) \tag{2.32}$$

where *P* is time-invariant, symmetric and positive definite matrices. The time derivative of *V(x(t))* is

$$\dot{V}(x(t)) = \dot{x}(t)^T Px(t) + x(t)^T P\dot{x}(t)$$

By substituting (2.14), one obtain

$$\dot{V}(x(t)) = \left\{ \sum_{i=1}^{p} \mu_i[(H_i + \Delta H_i)x(t) + (B + \Delta B)r(t) + Wd(t)\ ] \right\}^{\mathrm{T}} \times \mathrm{P}X(\mathrm{t}) + X(t)^T P\left\{ \sum_{i=1}^{p} \mu_i[(H_i + \Delta H_i)x(t) + (B + \Delta B)r(t) + Wd(t)\ ] \right\}$$

The problem of robust state is to find the gains G_j, of the controller to ensure an asymptotic convergence of *x(t)* toward zero when *r=0*, *d(t)=0*. This problem is reduced to find *P* verifying *V(x(t))< 0*, ie.

$$H_i{}^T P + PH_i < 0 \qquad \forall i \tag{2.33}$$

where, $H_i=A_i+BG_i$. Equation (2.33) for a common $P = P^T$ forms a set of bilinear matrix inequalities (BMIs). The BMIs in (2.33) should be transformed into pure LMIs as follows: By multiplying (2.28) from left and right by $O= P^{-1}$ and applying the change of variable $\Theta_i = G_i O$, the LMIs (2.20) in the theorem 2.1 is obtained.

In this Proof, we will find T in Lemma 2.1. *T* should be found such that the system without uncertainty is stable. Moreover, that minimizes $m[TH_iT^{-1}] + \left\| T\Delta H_i T^{-1} \right\| \max$ for all *i* such that

so *T* should give us the maximum robust area. In view of these properties and Lemma, the nonlinear matrix inequality problem can be stated as follows.

$m[TH_iT^{-1}] + \left\| T\Delta H_i T^{-1} \right\| \max$ for all *i* such that

$$TH_iT^{-1} + T^{-1^T} H_i^T T^T \text{ is negative for all } i \tag{2.34}$$

The proof of condition (2.34) can be obtained by considering that $m[TH_iT^{-1}]<0$ from (2.26), the maximum eigenvalue of

$$\{TH_iT^{-1}+T^{-1^T}H_i^TT^T\}/2<0 \tag{2.35}$$

(2.35) can be reduced to a LMIs problem if $T = T^T$. In this case, Lemma will be reduced to the stability condition in [51] when an uncertainty free fuzzy control system is considered.

$m[TH_iT^{-1}]<0$ then $TH_iT^{-1}+T^{-1^T}H_i^TT^T<0$, then if $T=T^T$,

$$T\times\{TH_iT^{-1}+T^{-1^T}H_i^TT^T\}\times T<0 \tag{2.36}$$

$$TTH_i+H_i^TTT<0 \qquad \text{for all } i \tag{2.37}$$

Let $TT = P$ (P is symmetric positive definite), the problem of finding the stability condition can be formulated as follows:

$$PH_i+H_i^TP<0 \tag{2.38}$$

2.2.3.2. Procedure for Finding RFC

Based on the analysis above we can design RFC as the following.

a) TS fuzzy plant model is obtained.
b) The ranges of the parameter uncertainties are determine.
c) Solve (2.20) to obtain Θ, and O ($G_i=\Theta_iO^{-1}$).
d) Construct the RFC (2.11), (2.12) and (2.13).

2.2.4. Application Example A

To show the effectiveness of the proposed controller design techniques, WES model system with DFIG [71]-[74] with parametric uncertainties is simulated.

2.2.4.1. The Wind Turbine Characteristics and Modeling

The mechanical output power at a given wind speed is drastically affected by the turbine's Tip Speed Ratio (TSR), which is defined as the ratio of turbine rotor tip speed to the wind speed. At a given wind speed, the maximum turbine

energy conversion efficiency occurs at an optimal TSR. Therefore, as wind speed changes, the turbine's rotor speed needs to change accordingly in order to maintain the optimal TSR and thus to extract the maximum power from the available wind resources [83]. The expression for aerodynamic power (P_m) captured by the wind turbine is given by the nonlinear expression [84]

$$P_m=0.5C_p(\lambda, \beta)\, \rho\pi R^2 v^3 \tag{2.39}$$

Where ρ is the air density (kg $\cdot$m^{-3}), R is the rotor radius (m), v is the wind speed (m$\cdot$s^{-1}), β is the blade pitch angle of the wind turbine, λ is TSR and C_p is the power coefficient defined by the following relation [18].

$$C_p = (0.44 - 0.0167\beta)\sin\left[\frac{\pi(\lambda - 3)}{15 - 0.3\beta}\right] - 0.00184(\lambda - 3)\beta \tag{2.40}$$

and TSR and is given by [18]:

$$\lambda = \Omega_r R / v \tag{2.41}$$

where Ω_r is the turbine rotational speed on the low-speed side of the gearbox. Referring to (2.40), optimal TSR λ_{opt} can be obtained as follow

$$\lambda_{opt} = \left(\frac{15 - 0.3\beta}{\pi}\right)\cos^{-1}\left[\frac{0.00184\beta(15 - 0.3\beta)}{\pi(0.44 - 0.167\beta)}\right] + 3 \tag{2.42}$$

Thus the maximum power captured from the wind is given by:

$$P_{m(\max)} = 0.5\, C_{p(\max)}(\lambda_{opt}, \beta)\rho\pi R^2 v^3 \tag{2.43}$$

A typical C_p- λ curve for different values of β is shown in Fig. 2.1. It can be seen that there is a maximum power coefficient $C_{p(\max)}$. If $C_{p(\max)} \approx 0.48$, the maximum value of C_p is achieved for $\beta=0^o$ and λ_{opt}. Normally, a variable speed wind turbine follows the $C_{p(\max)}$ to capture the maximum power up to the rated speed by varying the rotor speed to keep the system at λ_{opt}, then operates at the rated power with power control during the periods of high wind by the active control of the blade pitch angle or the passive regulation based on aerodynamic stall.

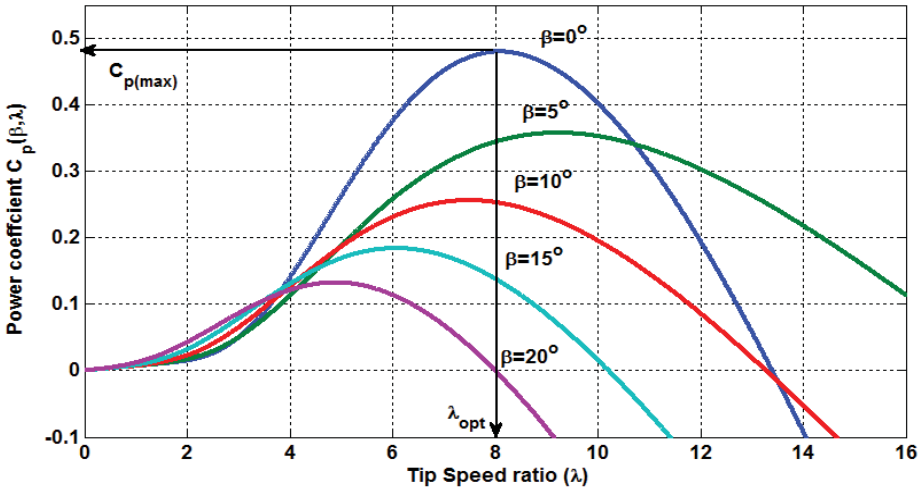

Fig. 2.1. Power coefficient C_p versus λ

2.2.4.2. WES Model System with DFIG in dq Coordinates

This section is devoted to the modeling of the mechanical and electrical system of a 1.5 MW wind turbine, and state space representation. The aerodynamic torque (T_r) on the wind turbine rotor can be obtained using the following relationships [66]:

$$T_r=P_m/\Omega_r=0.5C_p(\lambda, \beta)\, \rho\pi R^2\, v^3/\Omega_r \tag{2.44}$$

T_r at the optimal rotor speed $\Omega_{r(opt}$) is then given by

$$T_r = K_{opt}\, \Omega_r^2 \tag{2.45}$$

where $K_{opt}=0.5\rho\pi R^5 C_{p(max)}/\lambda_{opt}^2$

Since a commonly used model for induction generator converting power from the wind to serve the electric grid is shown in Fig.2.2 [71]-[74].The stator of the wound rotor induction machine is connected to the low voltage balanced grid and the rotor side is fed via the back-to-back voltage-source inverters with a common DC bus. These converters are voltage sourced converters that use force commutated power electronic devices to synthesize an AC voltage from a DC source. A capacitor connected on the DC side acts as the DC voltage source. The wind turbine catches the wind through its rotor blades and transfers

it to the rotor hub. The rotor hub is attached to a low speed shaft through a gear box. The high speed shaft drives an electric generator which converts the mechanical energy to electric energy and delivers it to the grid. As a summary, a doubly fed induction machine is a wound-rotor doubly fed electric machine and has several advantages over a conventional induction machine in wind power applications. First, as the rotor circuit is controlled by a power electronics converter, the induction generator is able to both import and export reactive power. This has important consequences for power system stability and allows the machine to support the grid during severe voltage disturbances. Second, the control of the rotor voltages and currents enables the induction machine to remain synchronized with the grid while the wind turbine speed varies. A variable speed wind turbine utilizes the available wind resource more efficiently than a fixed speed wind turbine, especially during light wind conditions. Third, the cost of the converter is low when compared with other variable speed solutions because only a fraction of the mechanical power, typically 25-30%, is fed to the grid through the converter, the rest being fed to grid directly from the stator. The efficiency of the DFIG is very good for the same reason.

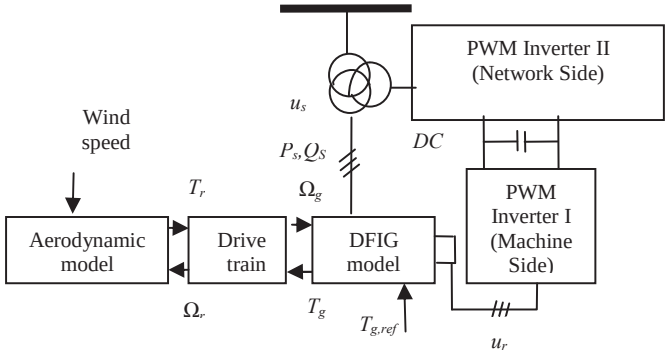

Fig. 2.2. Structure of the DFIG-based wind turbine system

In variable-speed wind turbines, the generator allows variable speed operation by providing an appropriate opposing torque T_g which follows the required value $T_{g,ref}$. However, modeling of the mechanical system of a 1.5

MW wind turbine, electrical modeling, mechanical modeling in dq coordinates can be expressed as a function of different state variables [71]-[74].

$$\frac{di_{sd}}{dt} = \frac{-R_s}{\xi L_s} i_{sd} + (\omega_s + \frac{1-\xi}{\xi} n_p \Omega_g) i_{sq} + \frac{R_r L_m}{\xi L_r L_s} i_{rd} + \frac{L_m}{\xi L_s} n_p \Omega_g i_{rq} + \frac{L_m}{\xi L_r L_s} u_{rd} - \frac{1}{\xi L_s} u_{sd}$$

$$\frac{di_{sq}}{dt} = \frac{-R_s}{\xi L_s} i_{sq} - (\omega_s + \frac{1-\xi}{\xi} n_p \Omega_g) i_{sd} + \frac{R_r L_m}{\xi L_r L_s} i_{rq} - \frac{L_m}{\xi L_s} n_p \Omega_g i_{rq} + \frac{L_m}{\xi L_r L_s} u_{rq} - \frac{1}{\xi L_s} u_{sq}$$

$$\frac{di_{rd}}{dt} = \frac{R_s L_m}{\xi L_r L_s} i_{sd} - \frac{L_m}{\xi L_r} n_p \Omega_g i_{sq} - \frac{R_r}{\xi L_r} i_{rd} + (\omega_s - \frac{1}{\xi} n_p \Omega_g) i_{rq} - \frac{1}{\xi L_r} u_{rd} + \frac{L_m}{\xi L_r L_s} u_{sd}$$

$$\frac{di_{rq}}{dt} = \frac{R_s L_m}{\xi L_r L_s} i_{sq} + \frac{L_m}{\xi L_r} n_p \Omega_g i_{sd} - \frac{R_r}{\xi L_r} i_{rq} - (\omega_s - \frac{1}{\xi} n_p \Omega_g) i_{rd} - \frac{1}{\xi L_r} u_{rq} + \frac{L_m}{\xi L_r L_s} u_{sq}$$

$$\frac{d\Omega_r}{dt} = (\frac{\mathrm{D_r}}{\mathrm{J_r}} + \frac{K_{opt}}{J_r} \Omega_r) \Omega_r - \frac{n_b}{J_r} T_h$$

$$\frac{d\Omega_g}{dt} = -\frac{\mathrm{D_g}}{\mathrm{J_g}} \Omega_g + \frac{1}{J_g} T_h - \frac{1}{J_g} T_g$$

$$\frac{dT_h}{dt} = \frac{1}{n_b}(K_{ls} - \frac{D_r D_{ls}}{J_r} + \frac{D_{lse} K_{opt}}{J_r} \Omega_r) \Omega_r - \frac{1}{n_b^2}(K_{ls} - \frac{D_g D_{ls}}{J_g}) \Omega_g - D_{ls}(\frac{1}{J_r} + \frac{1}{n_b^2 J_g}) T_h + \frac{D_{ls}}{n_b^2 J_g} Tg$$

$$\frac{dT_g}{dt} = -\frac{1}{\tau_g} T_g + \frac{1}{\tau_g} T_{g,ref} \tag{2.46}$$

where $\xi = (1-L_m^2)/L_s L_r$ is the leakage coefficient, $\omega_s = 2\pi f_s$, with f_s being the stator frequency, $\omega_r = n_p \Omega_g$, where ω_s and ω_r are the stator and rotor angular frequencies, respectively, Ω_g is the mechanical generator speed and n_p is the number of pole pairs. i_{sd} and i_{rd} denote the stator and rotor currents, respectively in axis d, i_{sq} and i_{rq} are stator and rotor currents in axis q, R_s, and R_r are stator and rotor resistance, L_s, L_r, and L_m are stator, rotor leakage and magnetizing inductances, respectively, V_s is the stator voltage magnitude, τ_g is the time constant of the model, T_h is the high-speed shaft torque, and n_b is the gearbox ratio. The gearbox is considered as a lossless device for this model. D_r, D_g, and D_{ls} denote damping constants for the rotor, generator, and the equivalent low-speed shaft, respectively, K_{ls} is the equivalent torsional stiffness of the low-speed shaft, J_r and J_g denote moments of inertia of the rotor and generator, respectively, and T_g and $T_{g,ref}$ are the generator torque and required generator torque, respectively. The used system parameters for the detailed

generator and wind turbine are shown in Table 2.1 and Table 2.2 [71]-[74], respectively. As far as the output of the system, the state will be assumed to be measurable. Moreover, other outputs of interest are the stator active power (P_s) and stator reactive power (Q_s). As usually done for the modeling of alternating current machines, the d-q reference frame is used [85], it is introduced by the well known 'Park Transformation' by which the three-phase variables of interest are transformed into the so called direct, quadrature and zero components as shown in [86],[87]. In the Park reference frame they can be shown to have the following expression:

$$P_s = -\frac{L_m V_s}{L_s} i_{qr}, \quad Q_s = \frac{V_s^2}{\omega_s L_s} - \frac{L_m V_s}{L_s} i_{rd} \tag{2.47}$$

The state space of a 1.5 MW wind turbine can be described by the following nonlinear equations from [71]-[74].

$$\dot{x}(t) = A(x)\,x(t) + Bu(t), \quad y(t) = C(x)\,x(t) \tag{2.48}$$

where $x(t) = \left[i_{sd}(t)\ i_{sq}(t)\ i_{rd}(t)\ i_{rq}(t)\ \Omega_r(t)\ \Omega_g(t)\ T_h(t)\ T_g(t) \right]^T$

$$= [x_1(t)\ x_2(t)\ x_3(t)\ x_4(t)\ x_5(t)\ x_6(t)\ x_7(t)\ x_8(t)]^T$$

$$B = \begin{bmatrix} -\frac{1}{\xi L_s} & 0 & \frac{L_m}{\xi L_r L_s} & 0 & 0 \\ 0 & -\frac{1}{\xi L_s} & 0 & \frac{L_m}{\xi L_r L_s} & 0 \\ \frac{L_m}{\xi L_r L_s} & 0 & -\frac{1}{\xi L_r} & 0 & 0 \\ 0 & \frac{L_m}{\xi L_r L_s} & 0 & -\frac{1}{\xi L_r} & 0 \\ 0 & 0 & 0 & 0 & 0 \\ 0 & 0 & 0 & 0 & 0 \\ 0 & 0 & 0 & 0 & 0 \\ 0 & 0 & 0 & 0 & \frac{1}{\tau_g} \end{bmatrix} \quad C(x(t)) = \begin{bmatrix} 0 & 0 & 0 & 0 & 1 & 0 & 0 & 0 \\ 0 & 0 & 0 & 0 & 0 & 1 & 0 & 0 \\ 0 & 0 & 0 & -\frac{L_m V_s}{L_s} & 0 & 0 & 0 & 0 \\ 0 & 0 & \frac{V_s^2}{i_{rd}(t)\omega_s L_s} & -\frac{L_m V_s}{L_s} & 0 & 0 & 0 & 0 \end{bmatrix},$$

$$A(x)=\begin{bmatrix}
\frac{-R_s}{\xi L_s} & \omega_s+\frac{(1-\xi)n_p\Omega_g(t)}{\xi} & \frac{L_m R_r}{\xi L_r L_s} & \frac{L_m}{\xi L_s}n_p\Omega_g(t) & 0 & 0 & 0 & 0\\
\frac{-R_s}{\xi L_s} & -(\omega_s+\frac{1-\xi}{\xi}n_p\Omega_g(t)) & \frac{R_r L_m}{\xi L_r L_s} & -\frac{L_m}{\xi L_s}n_p\Omega_g(t) & 0 & 0 & 0 & 0\\
\frac{R_s L_m}{\xi L_r L_s} & -\frac{L_m}{\xi L_r}n_p\Omega_g(t) & -\frac{R_r}{\xi L_r} & \omega_s-\frac{1}{\xi}n_p\Omega_g(t) & 0 & 0 & 0 & 0\\
\frac{R_s L_m}{\xi L_r L_s} & \frac{L_m}{\xi L_r}n_p\Omega_g(t) & -\frac{R_r}{\xi L_r} & -\omega_s+\frac{1}{\xi}n_p\Omega_g(t) & 0 & 0 & 0 & 0\\
0 & 0 & 0 & 0 & (\frac{D_r}{J_r}+\frac{K_{opt}}{J_r}\Omega_r(t)) & 0 & -\frac{n_b}{J_r} & 0\\
0 & 0 & 0 & 0 & 0 & \frac{-D_g}{J_g} & \frac{1}{J_g} & -\frac{1}{J_g}\\
0 & 0 & 0 & 0 & a75+\frac{D_{lse}K_{opt}}{n_b J_r}\Omega_r(t) & a76 & a77 & \frac{D_{ls}}{n_b^2 J_g}\\
0 & 0 & 0 & 0 & 0 & 0 & 0 & -\frac{1}{\tau_g}
\end{bmatrix},$$

$$y(t)=\begin{bmatrix}y_1\\y_2\\y_3\\y_4\end{bmatrix}=\begin{bmatrix}\Omega_r(t)\\\Omega_g(t)\\P_s(t)\\Q_s(t)\end{bmatrix},\ u(t)=\begin{bmatrix}u_{sd}(t)\\u_{sq}(t)\\u_{rd}(t)\\u_{rq}(t)\\T_{g,ref}(t)\end{bmatrix}=\begin{bmatrix}u_1(t)\\u_2(t)\\u_3(t)\\u_4(t)\\u_5(t)\end{bmatrix},\ a_{75}=\frac{1}{n_b}(K_{ls}-\frac{D_r D_{ls}}{J_r}),$$

$$a_{76}=-\frac{1}{n_b^2}(K_{ls}-\frac{D_g D_{ls}}{J_g}),\ a_{77}=-D_{ls}(\frac{1}{J_r}+\frac{1}{n_b^2 J_g})$$

TABLE 2.1
DFIG PARAMETERS

Quantity	Conversion from Gaussian and CGS EMU to SI
Rated power	1.5 [MW]
Rated apparent power	1.5 [MVA]
Rated voltage (line to line)	575 [V]
Frequency/Angular speed	2π60 [rad/sec]
Nominal system frequency	60 [Hz]
Stator resistance	0.0014 [Ω]
Stator leakage inductance	89.98[μH]
Rotor resistance	0.99187 [m Ω]
Rotor leakage inductance	82.088[μH]
Magnetizing inductance	1.526[mH]
Inertia of the generator	53.036[kg.m^2]
Pole pairs	3

TABLE 2.2
WIND TURBINE PARAMETERS

Quantity	Conversion from Gaussian and CGS EMU to SI
Wind turbine with a rotor diameter	70 [m]
Air density	0.55 [kg/m^3]
Cut-in wind speed	4 [m/s]
Cut-out wind speed	25 [m/s]
Rated wind speed	12 [m/s]
Rated rotor speed	19.7 [rpm]
Drivetrain torsion damper	1.0x10^7 [Nm/ sec]
Drivetrain torsion spring	5.6x10^9 [Nm/rad]
Inertia of the rotor	34.6x10^3 [kg.m^2]

2.2.4.3. TS Fuzzy WES Description

The following steps should be taken to derive the TS fuzzy model of (2.48). Here Ω_r, Ω_g, and $1/i_{rd}$ are nonlinear terms in the matrices $A(x(t))$ and $C(x(t))$ so we make them as our fuzzy variables. Generally they are denoted as $q_1(x_5(t))$, $q_2(x_6(t))$ and $q_3(x_3(t))$ are known as premise variables that may be functions of state variables. Therefore in our case, we have three nonlinear terms, $q_1(x_5(t))=\Omega_r(t)$, $q_2(x_6(t))=\Omega_g(t)$, and $q_3(x_3(t))=1/i_{rd}$. The first step for any kind of

fuzzy modeling is to determine the fuzzy variables and fuzzy sets or so-called membership functions. Although there is no general procedure for this step and it can be done by various methods predominantly trial and error, in exact fuzzy modeling using sector nonlinearity, it is quite routine. It is assumed in this tutorial that the premise variables are just functions of the state variables for the sake of simplicity. The TS fuzzy plant model which describes the dynamics of the given WES using a DFIG system has the following; we first represent the system (2.48) with a TS fuzzy model. The sector nonlinearity is as follows:

$$q_1(x_5(t))= \Omega_r(t)=M_1(q_1(x_5(t))).\ q_{1max}+ M_2(q_1(x_5(t)))\ q_{1min} \tag{2.49}$$

$$q_2(x_6(t))= \Omega g(t)=D_1(q_2(x_6(t))).q_{2max}+ D_2(q_2(x_6(t))).q_{2min} \tag{2.50}$$

$$q_3(x_3(t)) = 1/i_{rd}=N_1(q_3(x_3(t))).q_{3max}+ N_2(q_3(x_3(t))).q_{3min} \tag{2.51}$$

where M_1, M_2, D_1, D_2, N_1 and N_2 are the membership functions $q_1(x_5(t)) \in [q_{1\max} \quad q_{1\min}]$, $q_2(x_6(t)) \in [q_{2\max} \quad q_{2\min}]$ and $q_3(x_3(t)) \in [q_{3\max} \quad q_{3\min}]$

$$M_1 = \frac{q_1(x) - q_{1\min}}{q_{1\max} - q_{1\min}}, \quad M_2 = \frac{q_{1\max} - q_1(x)}{q_{1\max} - q_{1\min}} \tag{2.52}$$

$$D_1 = \frac{q_2(x) - q_{2\min}}{q_{2\max} - q_{2\min}}, \quad D_2 = \frac{q_{2\max} - q_2(x)}{q_{2\max} - q_{2\min}}, \tag{2.53}$$

$$N_1 = \frac{q_3(x) - q_{3\min}}{q_{3\max} - q_{3\min}}, \quad N_2 = \frac{q_{2\max} - q_2(x)}{q_{2\max} - q_{2\min}}, \tag{2.54}$$

The degree of membership function for state $q_1(x_5(t))$ is depicted in Fig. 2.3. Each membership function also represents model uncertainty for each sub-system. The degree of membership function for state $q_2(x_6(t))$ and $q_3(x_3(t))$ are implemented in the same manner. The dynamic equations of the model are known but some parameters (L_r, R_s and R_r) are uncertain. Then, the nonlinear WES using a DFIG (2.48) is represented by the following fuzzy model:

Rule 1: IF $q_1(x_5(t))$ is M_1 and $q_2(x_6(t))$ is D_1 and $q_3(x_3(t))$ is N_1

Then $\dot{x}(t) = (A_1 + \Delta A_1)x(t) + (B_1 + \Delta B_1)u(t)$, $y(t) = C_1 x(t)$ (2.55)

Rule 2: IF $q_1(x_5(t))$ is M_1 and $q_2(x_6(t))$ is D_1 and $q_3(x_3(t))$ is N_2

Then $\dot{x}(t) = (A_2 + \Delta A_2)x(t) + (B_2 + \Delta B_2)u(t)$, $y(t) = C_2 x(t)$ (2.56)

Rule 3: IF $q_1(x_5(t))$ is M_1 and $q_2(x_6(t))$ is D_2 and $q_3(x_3(t))$ is N_1

Then $\dot{x}(t) = (A_3 + \Delta A_3)x(t) + (B_3 + \Delta B_3)u(t)$, $y(t) = C_3 x(t)$ (2.57)

Rule 4: IF $q_1(x_5(t))$ is M_1 and $q_2(x_6(t))$ is D_2 and $q_3(x_3(t))$ is N_2

Then $\dot{x}(t) = (A_4 + \Delta A_4)x(t) + (B_4 + \Delta B_4)u(t)$, $y(t) = C_4 x(t)$ (2.58)

Rule 5: IF $q_1(x_5(t))$ is M_2 and $q_2(x_6(t))$ is D_1 and $q_3(x_3(t))$ is N_1

Then $\dot{x}(t) = (A_5 + \Delta A_5)x(t) + (B_5 + \Delta B_5)u(t)$, $y(t) = C_5 x(t)$ (2.59)

Rule 6: IF $q_1(x_5(t))$ is M_2 and $q_2(x_6(t))$ is D_1 and $q_3(x_3(t))$ is N_2

Then $\dot{x}(t) = (A_6 + \Delta A_6)x(t) + (B_6 + \Delta B_6)u(t)$, $y(t) = C_6 x(t)$ (2.60)

Rule 7: IF $q_1(x_5(t))$ is M_2 and $q_2(x_6(t))$ is D_2 and $q_3(x_3(t))$ is N_1

Then $\dot{x}(t) = (A_7 + \Delta A_7)x(t) + (B_7 + \Delta B_7)u(t)$, $y(t) = C_7 x(t)$ (2.61)

Rule 8: IF $q_1(x_5(t))$ is M_2 and $q_2(x_6(t))$ is D_2 and $q_3(x_3(t))$ is N_2

Then $\dot{x}(t) = (A_8 + \Delta A_8)x(t) + (B_8 + \Delta B_8)u(t)$, $y(t) = C_8 x(t)$ (2.62)

where

$$C_1 = C_3 = C_5 = C_7 = \begin{bmatrix} 0 & 0 & 0 & 0 & 1 & 0 & 0 \\ 0 & 0 & 0 & 0 & 0 & 1 & 0 \\ 0 & 0 & 0 & -\frac{L_m V_s}{L_s} & 0 & 0 & 0 \\ 0 & 0 & \frac{V_s^2}{\omega_s L_s} q_{3\max} & -\frac{L_m V_s}{L_s} & 0 & 0 & 0 & 0 \end{bmatrix},$$

$$C_2 = C_4 = C_6 = C_8 = \begin{bmatrix} 0 & 0 & 0 & 0 & 1 & 0 & 0 \\ 0 & 0 & 0 & 0 & 0 & 1 & 0 \\ 0 & 0 & 0 & -\frac{L_m V_s}{L_s} & 0 & 0 & 0 \\ 0 & 0 & \frac{V_s^2}{\omega_s L_s} q_{3\min} & -\frac{L_m V_s}{L_s} & 0 & 0 & 0 & 0 \end{bmatrix}$$

$$A_3+\Delta A_3=A_4+\Delta A_4=\begin{bmatrix}
-\frac{\bar{R}_s}{\xi L_s} & \omega_s+\frac{(1-\xi)n_p q_{2\min}}{\xi} & \frac{L_m\bar{R}_r}{\xi\bar{L}_r L_s} & \frac{L_m}{\xi L_s}n_p q_{2\min} & 0 & 0 & 0 & 0\\
-\frac{\bar{R}_s}{\xi L_s} & -(\omega_s+\frac{1-\xi}{\xi}n_p q_{2\min}) & \frac{\bar{R}_r L_m}{\xi\bar{L}_r L_s} & -\frac{L_m}{\xi L_s}n_p q_{2\min} & 0 & 0 & 0 & 0\\
\frac{\bar{R}_s L_m}{\xi\bar{L}_r L_s} & -\frac{L_m}{\xi\bar{L}_r}n_p q_{2\min} & -\frac{\bar{R}_r}{\xi\bar{L}_r} & \omega_s-\frac{1}{\xi}n_p q_{2\min} & 0 & 0 & 0 & 0\\
\frac{\bar{R}_s L_m}{\xi\bar{L}_r L_s} & \frac{L_m}{\xi\bar{L}_r}n_p q_{2\min} & -\frac{\bar{R}_r}{\xi\bar{L}_r} & -\omega_s+\frac{1}{\xi}n_p q_{2\min} & 0 & 0 & 0 & 0\\
0 & 0 & 0 & 0 & (\frac{D_r}{J_r}+\frac{K_{opt}}{J_r}q_{1\max}) & 0 & -\frac{n_b}{J_r} & 0\\
0 & 0 & 0 & 0 & 0 & -\frac{D_g}{J_g} & \frac{1}{J_g} & -\frac{1}{J_g}\\
0 & 0 & 0 & 0 & a75+\frac{D_{lse}K_{opt}}{n_b J_r}q_{1\max} & a76 & a77 & \frac{D_{ls}}{n_b^2 J_g}\\
0 & 0 & 0 & 0 & 0 & 0 & 0 & -\frac{1}{\tau_g}
\end{bmatrix},$$

$$B_i+\Delta B_i=\begin{bmatrix}
-\frac{1}{\xi L_s} & 0 & \frac{L_m}{\xi\bar{L}_r L_s} & 0 & 0\\
0 & -\frac{1}{\xi L_s} & 0 & \frac{L_m}{\xi\bar{L}_r L_s} & 0\\
\frac{L_m}{\xi\bar{L}_r L_s} & 0 & -\frac{1}{\xi\bar{L}_r} & 0 & 0\\
0 & \frac{L_m}{\xi\bar{L}_r L_s} & 0 & -\frac{1}{\xi\bar{L}_r} & 0\\
0 & 0 & 0 & 0 & 0\\
0 & 0 & 0 & 0 & 0\\
0 & 0 & 0 & 0 & 0\\
0 & 0 & 0 & 0 & \frac{1}{\tau_g}
\end{bmatrix}\quad i=1,2,...,8$$

$$A_5+\Delta A_5=A_6+\Delta A_6=\begin{bmatrix}
\frac{-\bar{R}_s}{\xi L_s} & \omega_s+\frac{(1-\xi)n_p q_{2\max}}{\xi} & \frac{L_m\bar{R}_r}{\xi\bar{L}_r L_s} & \frac{L_m}{\xi L_s}n_p q_{2\max} & 0 & 0 & 0 & 0\\
\frac{-\bar{R}_s}{\xi L_s} & -(\omega_s+\frac{1-\xi}{\xi}n_p q_{2\max}) & \frac{\bar{R}_r L_m}{\xi\bar{L}_r L_s} & -\frac{L_m}{\xi L_s}n_p q_{2\max} & 0 & 0 & 0 & 0\\
\frac{\bar{R}_s L_m}{\xi\bar{L}_r L_s} & -\frac{L_m}{\xi\bar{L}_r}n_p q_{2\max} & -\frac{\bar{R}_r}{\xi\bar{L}_r} & \omega_s-\frac{1}{\xi}n_p q_{2\max} & 0 & 0 & 0 & 0\\
\frac{\bar{R}_s L_m}{\xi\bar{L}_r L_s} & \frac{L_m}{\xi\bar{L}_r}n_p q_{2\max} & -\frac{\bar{R}_r}{\xi\bar{L}_r} & -\omega_s+\frac{1}{\xi}n_p q_{2\max} & 0 & 0 & 0 & 0\\
0 & 0 & 0 & 0 & (\frac{\mathrm{D_r}}{\mathrm{J_r}}+\frac{K_{opt}}{J_r}q_{1\min}) & 0 & -\frac{n_b}{J_r} & 0\\
0 & 0 & 0 & 0 & 0 & \frac{-\mathrm{D_g}}{\mathrm{J_g}} & \frac{1}{J_g} & -\frac{1}{J_g}\\
0 & 0 & 0 & 0 & a75+\frac{D_{lse}K_{opt}}{n_b J_r}q_{1\min} & a76 & a77 & \frac{D_{ls}}{n_b^2 J_g}\\
0 & 0 & 0 & 0 & 0 & 0 & 0 & -\frac{1}{\tau_g}
\end{bmatrix},$$

$$A_7+\Delta A_7=A_8+\Delta A_8=\begin{bmatrix}
\frac{-\bar{R}_s}{\xi L_s} & \omega_s+\frac{(1-\xi)n_p q_{2\min}}{\xi} & \frac{L_m\bar{R}_r}{\xi L_r\bar{L}_s} & \frac{L_m}{\xi L_s}n_p q_{2\min} & 0 & 0 & 0 & 0\\
\frac{-\bar{R}_s}{\xi L_s} & -(\omega_s+\frac{1-\xi}{\xi}n_p q_{2\min}) & \frac{\bar{R}_r L_m}{\xi\bar{L}_r L_s} & -\frac{L_m}{\xi L_s}n_p q_{2\min} & 0 & 0 & 0 & 0\\
\frac{\bar{R}_s L_m}{\xi L_r L_s} & -\frac{L_m}{\xi\bar{L}_r}n_p q_{2\min} & -\frac{\bar{R}_r}{\xi\bar{L}_r} & \omega_s-\frac{1}{\xi}n_p q_{2\min} & 0 & 0 & 0 & 0\\
\frac{\bar{R}_s L_m}{\xi\bar{L}_r L_s} & \frac{L_m}{\xi\bar{L}_r}n_p q_{2\min} & -\frac{\bar{R}_r}{\xi\bar{L}_r} & -\omega_s+\frac{1}{\xi}n_p q_{2\min} & 0 & 0 & 0 & 0\\
0 & 0 & 0 & 0 & (\frac{\mathrm{D_r}}{\mathrm{J_r}}+\frac{K_{opt}}{J_r}q_{1\min}) & 0 & -\frac{n_b}{J_r} & 0\\
0 & 0 & 0 & 0 & 0 & \frac{-\mathrm{D_g}}{\mathrm{J_g}} & \frac{1}{J_g} & -\frac{1}{J_g}\\
0 & 0 & 0 & 0 & a75+\frac{D_{lse}K_{opt}}{n_b J_r}q_{1\min} & a76 & a77 & \frac{D_{ls}}{n_b^2 J_g}\\
0 & 0 & 0 & 0 & 0 & 0 & 0 & -\frac{1}{\tau_g}
\end{bmatrix},$$

The inferred system is given by:

$$\dot{x}(t) = \sum_{i=1}^{8} \mu_i [(A_i + \Delta A_i)x(t) + (B_i + \Delta B_i)u(t)]$$

$$y(t) = \sum_{i=1}^{8} \mu_i C_i x(t) \qquad (2.63)$$

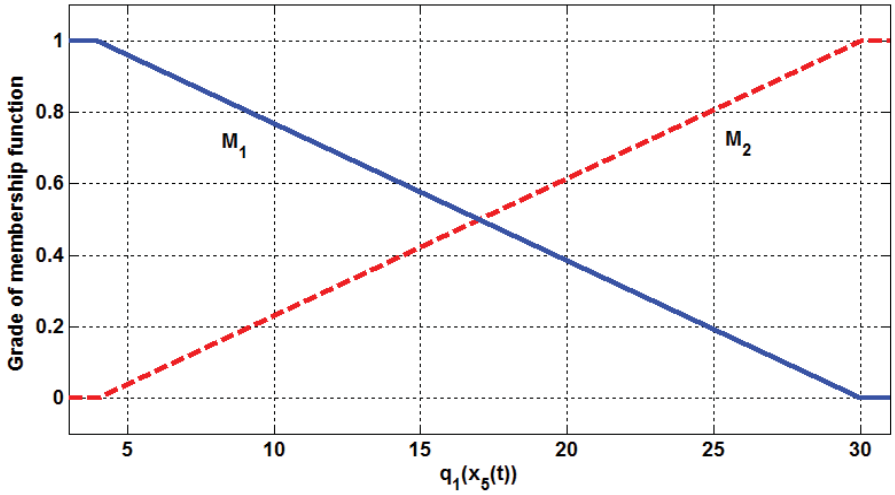

Fig. 2.3. Membership functions $M_1(q_1(x_5(t)))$ and $M_2(q_1(x_5(t)))$

With parameters q_{ji} for j = 1-3 and i = 1-8. The setting of the parameters q_{ji} with respect to each rule is addressed such that satisfy (2.55)-(2.62). The uncertain parameter $\overline{P}_u$ can be bounded in an interval with the upper and lower bounds of P_u^U and P_u^L, respectively, then $\overline{P}_u \in [P_u^L, P_u^U]$ is the range of the parameter uncertainties, and can be written in the following form $\overline{P}_u = P_o + \Delta P$, where P_o is the nominal value, ΔP is an uncertain value confined to the bounded range. $\overline{L}_r = L_r + \Delta L_r$, $\overline{R}_s = R_s + \Delta R_s$ and $\overline{R}_r = R_r + \Delta R_r$, where ΔL_r, ΔR_s and ΔR_r are denoted as the uncertainties introduced by system parameters L_r, R_s and R_r and changed within 35% of their nominal values, respectively. Since the input matrices are common, the first family is used. A eight fuzzy rules to implement the fuzzy controller are employed and the membership functions of

the fuzzy controller are chosen to be the same as those of the TS fuzzy plant model of (2.55)-(2.62). Eight rules of the fuzzy controller are as follows,

Rule j: IF $q_1(x_5(t))$ is $M_{э\,j}$ and $q_2(x_6(t))$ is $D_{э\,j}$ and $q_3(x_3(t))$ is $N_{э\,j}$

Then $u(t) = G_j x(t) + r(t)$ $j=1,2,\ldots,8$; $э=1,2$ (2.64)

PDC is used to design the fuzzy controller. Then, the overall fuzzy controller is described by

$$u(t) = \sum_{j=1}^{8} \mu_j G_j\, x(t) + r(t) \tag{2.65}$$

2.2.5. Simulation and Results

Simulations were performed in MATLAB using the nonlinear model provided in sub-Section 2.2.4. The proposed controller for the WES is tested for a random variation of wind speed as shown in Fig. 2.4. The control objective of this section is to design a RFC law for the system (2.48) to ensure that all signals in the closed-loop system are bounded.

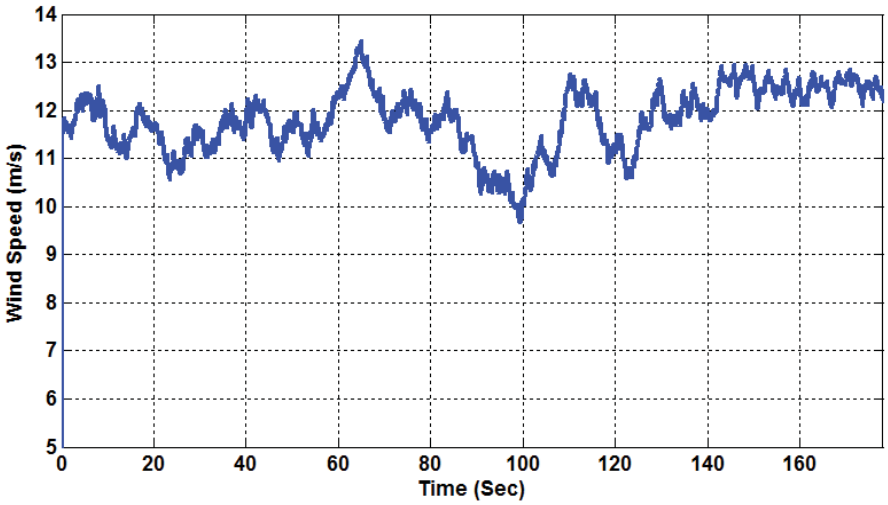

Fig. 2.4. Wind speed profile

Fig. 2.5 and Fig. 2.6 show the rotational speed of the wind turbine and generator (dashed line), respectively, in the presence of parametric

uncertainties. The parametric uncertainties L_r, R_s and R_r are considered within 35% of their nominal values. In order to obtain optimality, the $r(t)=\Omega_{gref}=\Omega_{opt}=\omega_s-n_b\lambda_{opt}v/R$ profile is chosen in such a way as to follow the optimal tip speed ratio (λ_{opt}) (solid line). From the simulation results using the proposed control scheme, we can observe that the outputs of the system are bounded and good tracking performance can be obtained through the uncertain nonlinearities of the system.

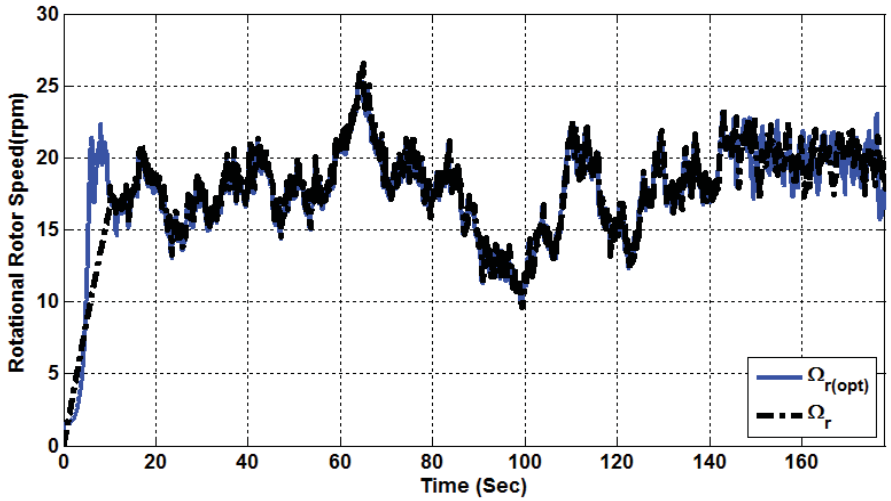

Fig. 2.5. The trajectories of Ω_r with proposed algorithm RFC strategy

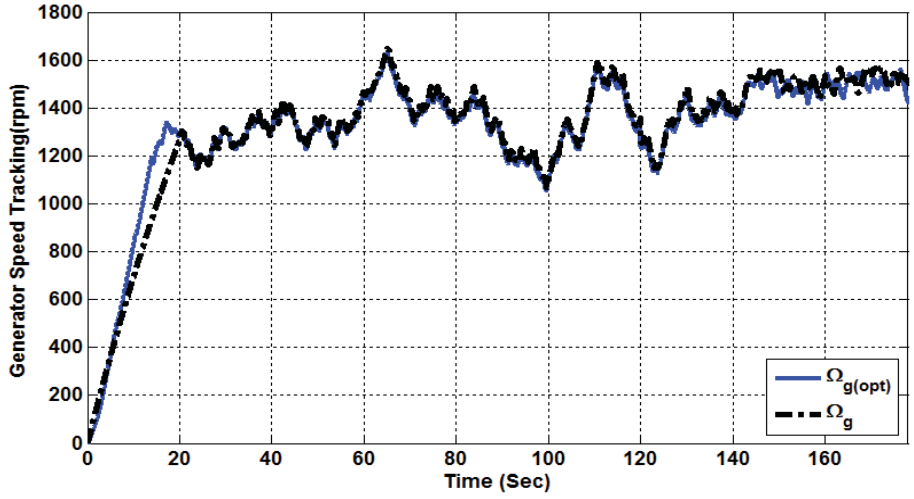

Fig. 2.6. The trajectories of Ω_g with proposed algorithm RFC strategy

Fig. 2.7 and Fig. 2.8 show the active power P_s and the reactive power Q_s, respectively. The power coefficient is shown in Fig. 2.9, it is clear that the $C_{p(\max)} \approx 0.48$.

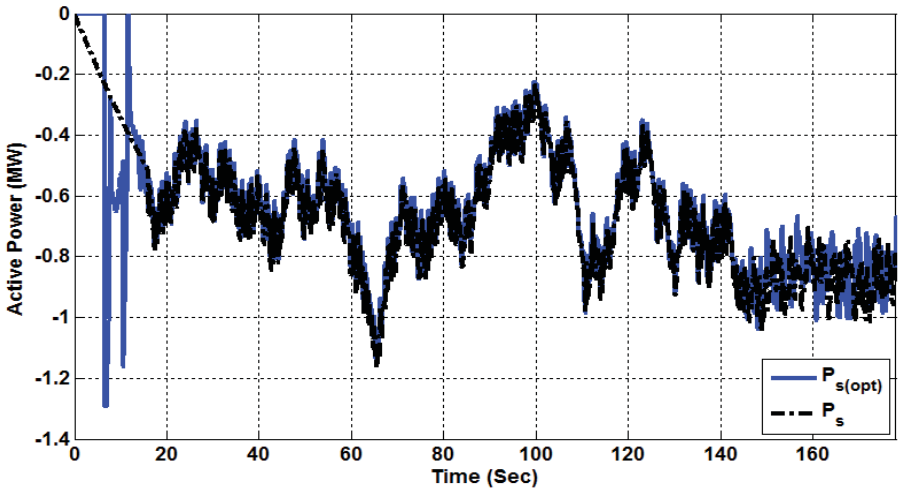

Fig. 2.7. The trajectories of P_s with proposed algorithm RFC strategy

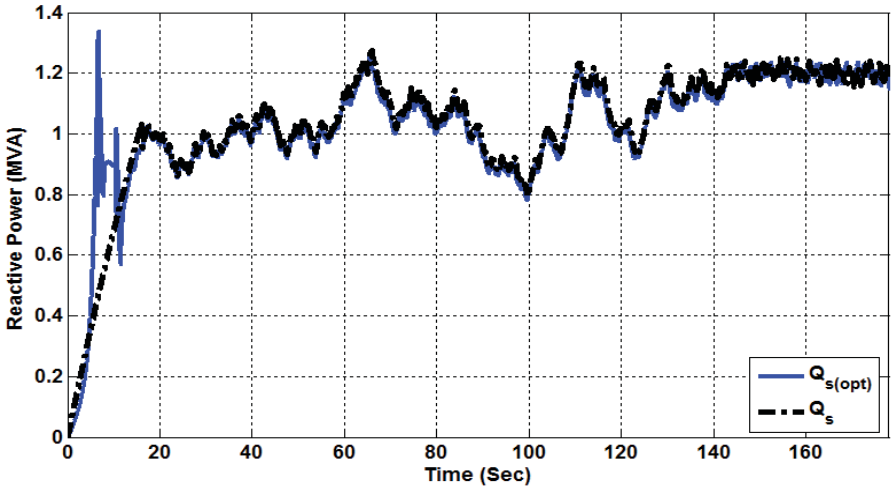

Fig. 2.8. The trajectories of Q_s with proposed algorithm RFC strategy

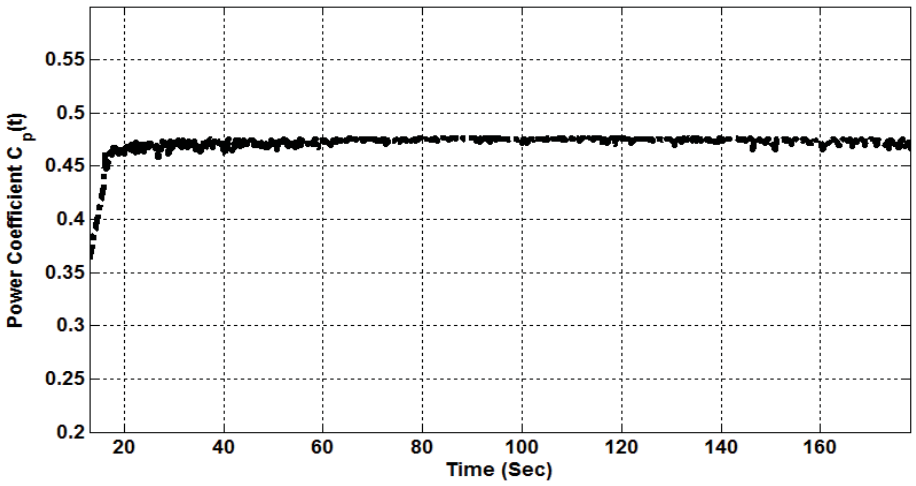

Fig. 2.9. Maximum power coefficient $C_{pmax)}$ with proposed RFC strategy

The simulation results demonstrate the effectiveness of the proposed control approach. The proposed control scheme can guarantee the stability of the closed-loop system and the convergence of the output tracking error. In addition, maximize the power coefficient and keep it at 0.48 as shown in Fig. 2.9. Adding an integral term to the control law guarantees obtaining a system that yields zero steady-state tracking error for the reference inputs, as long as closed-loop stability is maintained as presented in [14].

The major advantage of integral controllers is that they have the unique ability to return the controlled variable back to the exact set. Disadvantages of the integral control mode are that it responds relatively slowly to an error signal and that it can initially allow a large deviation at the instant the error is produced. This can lead to system instability and cyclic operation. For this reason, the integral control mode is not normally used alone, but is combined with another control mode.

In summary results, we can be seen that the system trajectory follows the trajectory of the reference input. Thus, the TS fuzzy model based controller is robust against norm-bounded parametric uncertainties, and wind disturbance. Comparing the results of the proposed algorithm, with that given in the

previous algorithms, it is obvious that the proposed controller has the following advantages:

(i) It can control the plant well over a wide range of the wind speeds.

(ii) It is stable over a wide range of uncertainty up to 35% compared with [1], [14] and wind disturbance.

2.3. RFSC of WES With DFIG

In this section, a RFSC for fuzzy TS systems subject to parametric. The TS fuzzy model is adopted for fuzzy modeling of the uncertain nonlinear system and establishing fuzzy state observers. The concept of PDC is employed to design RFSC from the TS fuzzy models. TS fuzzy systems are also classified into three families based on the input matrices and a RFSC is designed for each family.

The section is organized as follows; in section 2.3.1 the TS fuzzy plant model and the Fuzzy Regenerator Uncertainty (FRU) are given. In section 2.3.2, the proposed fuzzy scheduler will be presented. The fuzzy scheduled system and stability and robustness analyses of the fuzzy scheduled system will be presented in section 2.3.3. In this section also, the procedures for designing the RFSC will be summarized. In section 2.3.4, an application example on stabilizing a WES model system with DFIG. To illustrate the effectiveness of the proposed approach, Simulation and results will be given in section 2.3.5.

2.3.1. TS Fuzzy Plant Model and FRU

In this sub-section, we will present the TS fuzzy model and the FRU. The RFC [53], [88] will be used for designing the proposed fuzzy scheduler controller based on the fuzzy observer.

2.3.1.1. TS Fuzzy Model With Parametric Uncertainties

In sub-section 2.2, a TS fuzzy plant model representing an uncertain multivariable nonlinear system has been introduced. The TS fuzzy systems can

be also classified into three families based on the diversity of their input matrices, for the first family based on (2.2), the dynamics of TS fuzzy plant model is described by (2.4) which is restated as follows,

$$\dot{x}(t) = \sum_{i=1}^{p} \mu_i [(A_i + \Delta A_i)\, x(t) + \alpha_i (B + \Delta B) u(t) + W d(t)\ ] \tag{2.66}$$

In this sub-section, the TS fuzzy plant model of the following form is used,

$$\dot{x}(t) = \sum_{i=1}^{p} \mu_i [(A_i + \Delta A)\, x(t) + (\alpha_i B + \Delta B) u(t) + W d(t)] \tag{2.67}$$

where $\Delta A = \sum_{i=1}^{p} \mu_i \Delta A_i = \begin{bmatrix} \Delta a_{11} & \cdots & \Delta a_{1n} \\ \vdots & \ddots & \vdots \\ \Delta a_{n1} & \cdots & \Delta a_{nn} \end{bmatrix}$, $\Delta B = \sum_{i=1}^{p} \mu_i \Delta B_i = \begin{bmatrix} \Delta b_{11} & \cdots & \Delta b_{1m} \\ \vdots & \ddots & \vdots \\ \Delta b_{n1} & \cdots & \Delta b_{nm} \end{bmatrix}$ (2.68)

are the parameter uncertainties within given ranges. A_i and B_i are the nominal parameters. It should be noted that (2.66) and (2.67) are equivalent.

In the same manner we can restate the TS fuzzy plant model for the second and third family based on (2.8) and (2.9), respectively.

2.3.1.2. FRU

A FRU is a TS fuzzy model for regenerating the parameter uncertainties using fuzzy rules. It represents the parameter uncertainties as a weighted sum of the parameter uncertainty matrices in the specified parameter space. The *l*-th rule of the fuzzy uncertainty regenerator is of the following format [54],[82],

Rule *l: If* Δa_{11} *is* $N_{l\Delta a11}$ *and ... and* Δa_{nn} *is* $N_{l\Delta ann}$ *and* Δb_{11} *is* $N_{l\Delta b11}$ *and ... and* Δb_{nm} *is* $N_{l\Delta bnm}$

Then $\Delta A = \Delta \tilde{A}_l$ and $\Delta B = \Delta \tilde{B}_l$ (2.69)

where $N_{l\Delta a_{\theta\varsigma}}$ and $N_{l\Delta b_{\theta\zeta}}$ are the fuzzy term of rule for $\Delta a_{\theta\varsigma}, \Delta b_{\theta\zeta}$ (i.e. the element of ΔA and ΔB) respectively, $\theta = 1,2,\ldots,n$, $\varsigma = 1,2,\ldots,n$, $\zeta = 1,2,\ldots,m$. The final FRU are given by:

$$\Delta A = \sum_{l=1}^{s} h_l(\Delta A, \Delta B) \Delta \tilde{A}_l \ , \ \Delta B = \sum_{l=1}^{s} h_l(\Delta A, \Delta B) \Delta \tilde{B}_l \tag{2.70}$$

$$\sum_{l=1}^{s} h_l(\Delta A, \Delta B) = 1, \quad h_l(\Delta A, \Delta B) \in [0 \ \ 1] \quad \forall l \tag{2.71}$$

$$h_l(\Delta A, \Delta B) = \frac{\varpi_l(\Delta a, \Delta b)}{\sum_{l=1}^{c} \varpi_l(\Delta a, \Delta b)} \quad , \varpi_l(\Delta a, \Delta b) = N_{l\Delta a_{11}}(\Delta a_{11}) \times ... \times N_{l\Delta\Delta_{nn}}(\Delta a_{nn})$$

$$\times N_{l\Delta\Delta_{11}}(\Delta b_{11}) \times ... \times N_{l\Delta\Delta_{nm}}(\Delta b_{nm})$$

$s=2^b$ is the number of fuzzy rules, l= 1,2,...,s, b is the number of uncertain elements in ΔA and ΔB, h_l is a function of ΔA and ΔB, $\Delta\tilde{A}_l$ and $\Delta\tilde{B}_l$ are known constant matrices of ΔA and ΔB respectively, and are defined as,

$$\Delta\tilde{A}_l = \begin{bmatrix} \Delta a_{11}^{\max or \min} & \cdots & \Delta a_{1n}^{\max or \min} \\ \vdots & \ddots & \vdots \\ \Delta a_{n1}^{\max or \min} & \cdots & \Delta a_{nn}^{\max or \min} \end{bmatrix}, \Delta\tilde{B}_l = \begin{bmatrix} \Delta b_{11}^{\max or \min} & \cdots & \Delta b_{1m}^{\max or \min} \\ \vdots & \ddots & \vdots \\ \Delta b_{n1}^{\max or \min} & \cdots & \Delta b_{nm}^{\max or \min} \end{bmatrix} \tag{2.72}$$

where $\Delta a_{\upsilon\varsigma}^{\max or \min}$ denotes $\Delta a_{\upsilon\varsigma}^{\max}$ or $\Delta a_{\upsilon\varsigma}^{\min}$, $\Delta b_{\upsilon o}^{\max or \min}$ denotes $\Delta b_{\upsilon o}^{\max}$ or $\Delta b_{\upsilon o}^{\min}$; $\Delta a_{\upsilon\varsigma}^{\max}$, $\Delta b_{\upsilon o}^{\max}$, $\Delta a_{\upsilon\varsigma}^{\min}$, $\Delta b_{\upsilon o}^{\min}$ denote the maximum and minimum values of $\Delta a_{\upsilon\varsigma}$, $\Delta b_{\upsilon o}$ (i.e. the element of ΔA and ΔB) respectively, υ=1,2,...,n, ς =1,2,...,n, o =1,2,…,m. The choice of the superscript *max* or *min* depends on the location of the specified parameter space.

In the following, let $h_l(\Delta A, \Delta B)$ as h_l. To express the TS fuzzy plant model of (2.67) as a weighted sum of the robust fuzzy systems, we use the property $\sum_{i=1}^{p} \mu_i = \sum_{l=1}^{s} h_l = \sum_{i=1}^{p} \sum_{l=1}^{s} \mu_i h_l = 1$, ***for the first family,*** from (2.67) and (2.70) the TS fuzzy plant model becomes

$$\dot{x}(t) = \sum_{i=1}^{p} \sum_{l=1}^{s} \mu_i h_l [(A_i + \Delta\tilde{A}_l) x(t) + \alpha_i (B + \Delta\tilde{B}_l) u(t) + Wd(t)]$$

$$y(t) = \sum_{i=1}^{p} \mu_i C_i x(t) \tag{2.73}$$

In the same manner, we can induce the inferred output of the fuzzy scheduler system for the other two cases.

2.3.2. Proposed RFSC Based on RFC

A RFSC is used to derive the control signal by inferring the output signals from the RFC in sub-section 2.2.2. The RFC and the RFSC will be investigated as the following sub-section.

2.3.2.1. RFC Controller

A fuzzy controller in [53] is used to close the feedback loop of the robust fuzzy system then the fuzzy control system is obtained. Based on the analysis that discussed in sub-section 2.2.2.2, a fuzzy controller with *c* fuzzy rules can be developed via the PDC. For the first, second and third families the RFC are given in (2.11), (2.12) and (2.13).

2.3.2.2. Proposed RFSC Controllers

A fuzzy scheduler is based on the fuzzy controller outputs [53], [88] according to the fuzzy scheduler rules. The antecedents and the number of rules of the fuzzy scheduler and FRU are the same. ***For the first family***, the *l*-th rule of fuzzy scheduler is of the following format: Rule *l: If* Δa_{11} *is* $N_{l\Delta a11}$ *and ... and* Δa_{nn} *is* $N_{l\Delta ann}$ *and* Δb_{11} *is* $N_{l\Delta b11}$ *and ... and* Δb_{nm} *is* $N_{l\Delta bnm}$

Then $$u(t)=\frac{\sum_{j=1}^{c}\mu_j[-G_j\,x(t)+r(t)]}{\sum_{j=1}^{c}\alpha_j\mu_j} \qquad l=1,2,\ldots,s \qquad (2.74)$$

Based on (2.11), the inferred output of the fuzzy scheduler is given by:

$$u(t)=\frac{\sum_{l=1}^{s}\sum_{j=1}^{c}h_l\mu_j[-G_{jl}\,x(t)+r(t)]}{\sum_{l=1}^{s}\sum_{j=1}^{c}\alpha_j h_l\mu_j} \qquad (2.75)$$

In the same manner we can induce the inferred output of the RFSC for the other two cases as follows

For the second family, the RFSC base on (2.12), becomes

$$\dot{u}(t) = z_k\, u(t) + \sum_{l=1}^{s}\sum_{j=1}^{c} h_l \mu_j [-G_{jl}\, x(t) + r(t)] \tag{2.76}$$

For the last family, the RFSC based on (2.13) becomes

$$u(t) = \sum_{l=1}^{s}\sum_{j=1}^{c} h_l \mu_j [-G_{jl}\, x(t) + r(t)] \tag{2.77}$$

2.3.3. The Proposed RFSC Stability Analysis

In this section, the fuzzy scheduled system which is formed by the nonlinear plant represented by the augmented TS fuzzy plant model and the fuzzy scheduler connected in closed-loop is investigated. A block diagram of a fuzzy scheduled system, which consists of a nonlinear plant and a fuzzy scheduler, is shown in Fig. 2.10. Stability and robustness analyses will be conducted on this fuzzy scheduled system. In [53], PDC has been discussed to design the fuzzy controller. This approach can also be applied to develop the fuzzy scheduled controllers.

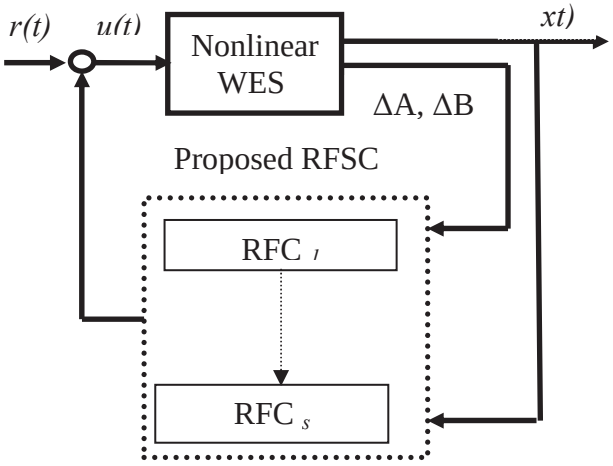

Fig. 2.10. Block diagram of a fuzzy scheduled system

2.3.3.1. Robust Fuzzy Scheduled Systems Under PDC

In this sub-section the fuzzy control system of the state can be obtained.

For the first family, from (2.73) and with the modified RFSC (2.75), the fuzzy scheduled system is given by

$$\dot{x}(t) = \sum_{i=1}^{p}\sum_{l=1}^{s} \mu_i h_l [(A_i + \Delta\tilde{A}_l)x(t) + Wd(t)]$$

$$+ \left\{\sum_{i=1}^{p}\sum_{l=1}^{s} \alpha_i \mu_i h_l\right\}(B + \Delta\tilde{B}_l)\left\{\sum_{l=1}^{s}\sum_{j=1}^{c} h_l \mu_j [-G_{jl}\, x(t) + r(t)]\right\} / \left\{\sum_{l=1}^{s}\sum_{j=1}^{c} \alpha_j h_l \mu_j\right\} \quad (2.78)$$

From (2.75) and (2.78), a TS fuzzy closed-loop can be observed:

$$\dot{x}(t) = \sum_{i=1}^{p}\sum_{j=1}^{c}\sum_{l=1}^{s} \mu_i \mu_j h_l [(\tilde{H}_{ijl} + \Delta\tilde{H}_{ijl})x(t) + (S + \Delta\tilde{S})r(t) + Wd(t)] \quad (2.79)$$

With $\Delta\tilde{H}_{ijl} = \tilde{A}_l - \Delta\tilde{B}_l G_{jl}$, $\tilde{H}_{ijl} = A_i - BG_{jl}$, $S = B$, $\tilde{S} = \Delta\tilde{B}$,

In the same manner, the augmented fuzzy system for the second and the third families can be deduced.

2.3.3.2. Stability Analysis of Fuzzy Scheduled Systems

The analysis procedures are the same as those in section 2.2.3, and so the analysis results will be presented without proof. The stability and robustness conditions are summarized into the following lemma 2.2 and theorem 2.2.

The fuzzy control system (2.79) becomes stable if the following lemma 2.2 and the theorem 2.2 are satisfied.

Lemma 2.2: the fuzzy control system as given by (2.79) with parameter uncertainty and state variables unavailable for measurements under PDC is stable if

$$m[T\tilde{H}_{ijl}T^{-1}] \le -\left\|T\Delta\tilde{H}_{ijl}T^{-1}\right\|_{\max} - \sigma \quad (2.80)$$

Also for the second family, the system is stable if

$$m[T\tilde{H}_{ijl}T^{-1}] \le -\left\|T\Delta\tilde{H}_{ijl}T^{-1}\right\|_{\max} - \phi \quad (2.81)$$

Also for the third family, the system is stable if

$$m[T\tilde{H}_{ijl}T^{-1}] \le -\left\|T\Delta\tilde{H}_{ijl}T^{-1}\right\|_{\max} - \varphi \quad (2.82)$$

where $\tilde{H}_{ijl}$ is defined by (2.77), σ, ϕ, φ are the robustness index, $m[T\tilde{H}_{ijl}T^{-1}]$ is the corresponding matrix measure [54],[82] of the induced matrix norm of

$\left\|T\tilde{H}_{ijl}T^{-1}\right\|$ (or the logarithmic derivative of $\left\|T\tilde{H}_{ijl}T^{-1}\right\|$), $\left\|T\Delta\tilde{H}_{ijl}T^{-1}\right\|_{\max}$ is the maximum value of the norm of the matrix $T\Delta\tilde{H}_{ijl}T^{-1}$.

Theorem 2.2: The fuzzy control system as given by (2.79) is stable if the controller gain are set to $G_{jl} = \Phi_{jl}\Re^{-1}$, with the matrices Φ, and $\Re$ satisfying the following LMEs.

$$\Re A_i^T + A_i\Re - (B_i\Phi_{jl})^T - (B_i\Phi_{jl}) = -\sigma I \tag{2.83}$$

Where $\Re = P^{-1}$, and σ is designed nonzero positive constant. By solving (2.83) related to the wind turbine system, the controller gains ($G_{jl} = \Phi_{jl}\Re^{-1}$) can be easily determined and we can see that the uncertainty is affected by σ as shown in Fig. 2.11 since at certain value of σ the control system is stable in spite of the large value of uncertainty. The general form of the Fig.2.11 is nearly the same for any model except that the robustness index σ and the percentage of the uncertainly are changed depend on the model and the robust controller [37].

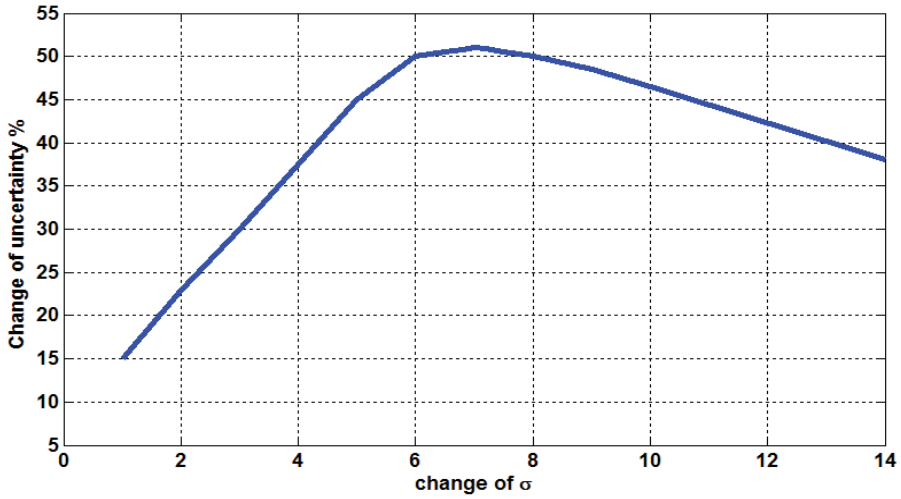

Fig.2.11 Change of uncertainty with σ

2.3.4. Design Procedure of the RFSC and Calculation Controller Gains

In this section, we calculate the controller gains and we investigate the procedure of the fuzzy scheduler. In order to analyse the convergence of the augmented state *X(t)*, consider the quadratic Lyapunov candidate function *V(t)*as given in (2.32), $X(t) \to 0$ if $\dot{V}(t) < 0$. $\dot{V}(t) < 0$ if the inequality satisfy

$$\tilde{H}_{ijl}^{\ T} P + P\tilde{H}_{ijl} < 0 \qquad \forall i, j, l \tag{2.84}$$

Assuming that *P>0*, by multiplying (2.84) from left and right by $\Re = P^{-1}$ and applying the change of variables $\Phi_{jl} = G_{jl}\Re$, the following LMIs conditions are obtained:

$$\Re A_i^{\ T} + A_i \Re - (B_i \Phi_{jl})^T - (B_i \Phi_{jl}) < 0 \tag{2.85}$$

By transforming the inequality (2.85) into equality, the above inequality will be rewritten as the LMEs (2.83) are obtained as given in the theorem 2.2. Based on the analysis above we can design the RFSC as the following

a) Classify the TS fuzzy systems into three families based on how divers their input matrices.

b) Solve (2.85) to obtain Φ, and Φ thus ($G_{jl} = \Phi_{jl}\Re^{-1}$).

a) Construct the RFSC (2.75) or (2.76) or (2.77).

2.3.5. Application Example B

The WES model with a DFIG system used in application example A of section 2. 2.4, will be used again here. However, the ranges of the uncertain parameters will be different in this section. Fig. 2.2 shows the WES Model with a DFIG system. Its dynamic equation is given by (2.48). The fuzzy scheduler is designed by following the procedure given in sub-section 2.3.4.2.

According to the analysis above, the procedure for finding the proposed RFSC is summarized as follows.

a) The dynamics of the nonlinear WES using a DFIG system is given in (2.48)

b) The TS fuzzy plant model which describes the dynamics of the given WES using a DFIG system has the following; we first represent the system (2.48) with a TS fuzzy model. The sector nonlinearity is given in (2.49), (2.50) and (2.51). The membership functions as given by (2.52), (2.53) and (2.54). The degree of membership function for state $q_1(x_5(t))$ is depicted in Fig. 2.3. Each membership function also represents model uncertainty for each sub-system. Then, the nonlinear WES using a DFIG (2.48) is represented by the following fuzzy model:

Rule 1: IF $q_1(x_5(t))$ is M_1 and $q_2(x_6(t))$ is D_1 and $q_3(x_3(t))$ is N_1

Then $\dot{x}(t) = (A_1 + \Delta A_1)x(t) + B_1 u(t)$, $y(t) = C_1 x(t)$ (2.86)

Rule 2: IF $q_1(x_5(t))$ is M_1 and $q_2(x_6(t))$ is D_1 and $q_3(x_3(t))$ is N_2

Then $\dot{x}(t) = (A_2 + \Delta A_2)x(t) + B_2 u(t)$, $y(t) = C_2 x(t)$ (2.87)

Rule 3: IF $q_1(x_5(t))$ is M_1 and $q_2(x_6(t))$ is D_2 and $q_3(x_3(t))$ is N_1

Then $\dot{x}(t) = (A_3 + \Delta A_3)x(t) + B_3 u(t)$, $y(t) = C_3 x(t)$ (2.88)

Rule 4: IF $q_1(x_5(t))$ is M_1 and $q_2(x_6(t))$ is D_2 and $q_3(x_3(t))$ is N_2

Then $\dot{x}(t) = (A_4 + \Delta A_4)x(t) + B_4 u(t)$, $y(t) = C_4 x(t)$ (2.89)

Rule 5: IF $q_1(x_5(t))$ is M_2 and $q_2(x_6(t))$ is D_1 and $q_3(x_3(t))$ is N_1

Then $\dot{x}(t) = (A_5 + \Delta A_5)x(t) + B_5\, u(t)$, $y(t) = C_5\, x(t)$ (2.90)

Rule 6: IF $q_1(x_5(t))$ is M_2 and $q_2(x_6(t))$ is D_1 and $q_3(x_3(t))$ is N_2

Then $\dot{x}(t) = (A_6 + \Delta A_6)x(t) + B_6 u(t)$, $y(t) = C_6\, x(t)$ (2.91)

Rule 7: IF $q_1(x_5(t))$ is M_2 and $q_2(x_6(t))$ is D_2 and $q_3(x_3(t))$ is N_1

Then $\dot{x}(t) = (A_7 + \Delta A_7)x(t) + B_7 u(t)$, $y(t) = C_7\, x(t)$ (2.92)

Rule 8: IF $q_1(x_5(t))$ is M_2 and $q_2(x_6(t))$ is D_2 and $q_3(x_3(t))$ is N_2

Then $\dot{x}(t) = (A_8 + \Delta A_8)x(t) + B_8 u(t)$, $y(t) = C_8\, x(t)$ (2.93)

where

$$A_1 = A_2 = \begin{bmatrix} \frac{-R_s}{\xi L_s} & \omega_s + \frac{(1-\xi)n_p q_{2\max}}{\xi} & \frac{L_m R_r}{\xi L_r L_s} & \frac{L_m}{\xi L_s} n_p q_{2\max} & 0 & 0 & 0 & 0 \\ \frac{-R_s}{\xi L_s} & -(\omega_s + \frac{1-\xi}{\xi} n_p q_{2\max}) & \frac{R_r L_m}{\xi L_r L_s} & -\frac{L_m}{\xi L_s} n_p q_{2\max} & 0 & 0 & 0 & 0 \\ \frac{R_s L_m}{\xi L_r L_s} & -\frac{L_m}{\xi L_r} n_p q_{2\max} & -\frac{R_r}{\xi L_r} & \omega_s - \frac{1}{\xi} n_p q_{2\max} & 0 & 0 & 0 & 0 \\ \frac{R_s L_m}{\xi L_r L_s} & \frac{L_m}{\xi L_r} n_p q_{2\max} & -\frac{R_r}{\xi L_r} & -\omega_s + \frac{1}{\xi} n_p q_{2\max} & 0 & 0 & 0 & 0 \\ 0 & 0 & 0 & 0 & (\frac{\mathrm{D_r}}{\mathrm{J_r}} + \frac{K_{opt}}{J_r} q_{1\max}) & 0 & -\frac{n_b}{J_r} & 0 \\ 0 & 0 & 0 & 0 & 0 & \frac{-\mathrm{D_g}}{\mathrm{J_g}} & \frac{1}{J_g} & -\frac{1}{J_g} \\ 0 & 0 & 0 & 0 & a75 + \frac{D_{lse} K_{opt}}{n_b J_r} q_{1\max} & a76 & a77 & \frac{D_{ls}}{n_b^2 J_g} \\ 0 & 0 & 0 & 0 & 0 & 0 & 0 & -\frac{1}{\tau_g} \end{bmatrix},$$

$$A_3 = A_4 = \begin{bmatrix}
\frac{-R_s}{\xi L_s} & \omega_s + \frac{(1-\xi)n_p q_{2\min}}{\xi} & \frac{L_m R_r}{\xi L_r L_s} & \frac{L_m}{\xi L_s} n_p q_{2\min} & 0 & 0 & 0 & 0 \\
\frac{-R_s}{\xi L_s} & -(\omega_s + \frac{1-\xi}{\xi} n_p q_{2\min}) & \frac{R_r L_m}{\xi L_r L_s} & -\frac{L_m}{\xi L_s} n_p q_{2\min} & 0 & 0 & 0 & 0 \\
\frac{R_s L_m}{\xi L_r L_s} & -\frac{L_m}{\xi L_r} n_p q_{2\min} & -\frac{R_r}{\xi L_r} & \omega_s - \frac{1}{\xi} n_p q_{2\min} & 0 & 0 & 0 & 0 \\
\frac{R_s L_m}{\xi L_r L_s} & \frac{L_m}{\xi L_r} n_p q_{2\min} & -\frac{R_r}{\xi L_r} & -\omega_s + \frac{1}{\xi} n_p q_{2\min} & 0 & 0 & 0 & 0 \\
0 & 0 & 0 & 0 & (\frac{\mathrm{D_r}}{\mathrm{J_r}} + \frac{K_{opt}}{J_r} q_{1\max}) & 0 & -\frac{n_b}{J_r} & 0 \\
0 & 0 & 0 & 0 & 0 & \frac{-\mathrm{D_g}}{\mathrm{J_g}} & \frac{1}{J_g} & -\frac{1}{J_g} \\
0 & 0 & 0 & 0 & a75 + \frac{D_{lse} K_{opt}}{n_b J_r} q_{1\max} & a76 & a77 & \frac{D_{ls}}{n_b^2 J_g} \\
0 & 0 & 0 & 0 & 0 & 0 & 0 & -\frac{1}{\tau_g}
\end{bmatrix},$$

$$A_5 = A_6 = \begin{bmatrix}
\frac{-R_s}{\xi L_s} & \omega_s + \frac{(1-\xi)n_p q_{2\max}}{\xi} & \frac{L_m R_r}{\xi L_r L_s} & \frac{L_m}{\xi L_s} n_p q_{2\max} & 0 & 0 & 0 & 0 \\
\frac{-R_s}{\xi L_s} & -(\omega_s + \frac{1-\xi}{\xi} n_p q_{2\max}) & \frac{R_r L_m}{\xi L_r L_s} & -\frac{L_m}{\xi L_s} n_p q_{2\max} & 0 & 0 & 0 & 0 \\
\frac{R_s L_m}{\xi L_r L_s} & -\frac{L_m}{\xi L_r} n_p q_{2\max} & -\frac{R_r}{\xi L_r} & \omega_s - \frac{1}{\xi} n_p q_{2\max} & 0 & 0 & 0 & 0 \\
\frac{R_s L_m}{\xi L_r L_s} & \frac{L_m}{\xi L_r} n_p q_{2\max} & -\frac{R_r}{\xi L_r} & -\omega_s + \frac{1}{\xi} n_p q_{2\max} & 0 & 0 & 0 & 0 \\
0 & 0 & 0 & 0 & (\frac{\mathrm{D_r}}{\mathrm{J_r}} + \frac{K_{opt}}{J_r} q_{1\min}) & 0 & -\frac{n_b}{J_r} & 0 \\
0 & 0 & 0 & 0 & 0 & \frac{-\mathrm{D_g}}{\mathrm{J_g}} & \frac{1}{J_g} & -\frac{1}{J_g} \\
0 & 0 & 0 & 0 & a75 + \frac{D_{lse} K_{opt}}{n_b J_r} q_{1\min} & a76 & a77 & \frac{D_{ls}}{n_b^2 J_g} \\
0 & 0 & 0 & 0 & 0 & 0 & 0 & -\frac{1}{\tau_g}
\end{bmatrix},$$

$$A_7 = A_8 = \begin{bmatrix} \frac{-R_s}{\xi L_s} & \omega_s + \frac{(1-\xi)n_p q_{2\min}}{\xi} & \frac{L_m R_r}{\xi L_r L_s} & \frac{L_m}{\xi L_s} n_p q_{2\min} & 0 & 0 & 0 & 0 \\ \frac{-R_s}{\xi L_s} & -(\omega_s + \frac{1-\xi}{\xi} n_p q_{2\min}) & \frac{R_r L_m}{\xi L_r L_s} & -\frac{L_m}{\xi L_s} n_p q_{2\min} & 0 & 0 & 0 & 0 \\ \frac{R_s L_m}{\xi L_r L_s} & -\frac{L_m}{\xi L_r} n_p q_{2\min} & -\frac{R_r}{\xi L_r} & \omega_s - \frac{1}{\xi} n_p q_{2\min} & 0 & 0 & 0 & 0 \\ \frac{R_s L_m}{\xi L_r L_s} & \frac{L_m}{\xi L_r} n_p q_{2\min} & -\frac{R_r}{\xi L_r} & -\omega_s + \frac{1}{\xi} n_p q_{2\min} & 0 & 0 & 0 & 0 \\ 0 & 0 & 0 & 0 & (\frac{D_r}{J_r} + \frac{K_{opt}}{J_r} q_{1\min}) & 0 & -\frac{n_b}{J_r} & 0 \\ 0 & 0 & 0 & 0 & 0 & \frac{-D_g}{J_g} & \frac{1}{J_g} & -\frac{1}{J_g} \\ 0 & 0 & 0 & 0 & a75 + \frac{D_{lse} K_{opt}}{n_b J_r} q_{1\min} & a76 & a77 & \frac{D_{ls}}{n_b^2 J_g} \\ 0 & 0 & 0 & 0 & 0 & 0 & 0 & -\frac{1}{\tau_g} \end{bmatrix},$$

$$C_1 = C_3 = C_5 = C_7 = \begin{bmatrix} 0 & 0 & 0 & 0 & 1 & 0 & 0 \\ 0 & 0 & 0 & 0 & 0 & 1 & 0 \\ 0 & 0 & 0 & -\frac{L_m V_s}{L_s} & 0 & 0 & 0 \\ 0 & 0 & \frac{V_s^2}{\omega_s L_s} q_{3\max} & -\frac{L_m V_s}{L_s} & 0 & 0 & 0 & 0 \end{bmatrix},$$

$$C_2 = C_4 = C_6 = C_8 = \begin{bmatrix} 0 & 0 & 0 & 0 & 1 & 0 & 0 \\ 0 & 0 & 0 & 0 & 0 & 1 & 0 \\ 0 & 0 & 0 & -\frac{L_m V_s}{L_s} & 0 & 0 & 0 \\ 0 & 0 & \frac{V_s^2}{\omega_s L_s} q_{3\min} & -\frac{L_m V_s}{L_s} & 0 & 0 & 0 & 0 \end{bmatrix}$$

$$B_i = \begin{bmatrix} -\frac{1}{\xi L_s} & 0 & \frac{L_m}{\xi L_r L_s} & 0 & 0 \\ 0 & -\frac{1}{\xi L_s} & 0 & \frac{L_m}{\xi L_r L_s} & 0 \\ \frac{L_m}{\xi L_r L_s} & 0 & -\frac{1}{\xi L_r} & 0 & 0 \\ 0 & \frac{L_m}{\xi L_r L_s} & 0 & -\frac{1}{\xi L_r} & 0 \\ 0 & 0 & 0 & 0 & 0 \\ 0 & 0 & 0 & 0 & 0 \\ 0 & 0 & 0 & 0 & 0 \\ 0 & 0 & 0 & 0 & \frac{1}{\tau_g} \end{bmatrix}_{i=1,2,...,8}$$

The inferred system is given by:

$$\dot{x}(t) = \sum_{i=1}^{8} \mu_i [(A_i + \Delta A_i)x(t) + B_i u(t)]$$

$$y(t) = \sum_{i=1}^{8} \mu_i C_i \, x(t) \qquad (2.94)$$

c) ΔA_i (l=1,2,…,16) represents the system parameters bounded uncertainties. The elements of ΔA_i are randomly varied within 40% of their nominal values corresponding to system parameter R_r, we considered only R_r to reduce the number of rules for the FRU. The ranges of the parameter uncertainties are

$$\Delta A = \begin{bmatrix} 0 & 0 & \Delta a_{13} & 0 & 0 & 0 & 0 & 0 \\ 0 & 0 & \Delta a_{23} & 0 & 0 & 0 & 0 & 0 \\ 0 & 0 & \Delta a_{33} & 0 & 0 & 0 & 0 & 0 \\ 0 & 0 & \Delta a_{43} & 0 & 0 & 0 & 0 & 0 \\ 0 & 0 & 0 & 0 & 0 & 0 & 0 & 0 \\ 0 & 0 & 0 & 0 & 0 & 0 & 0 & 0 \\ 0 & 0 & 0 & 0 & 0 & 0 & 0 & 0 \\ 0 & 0 & 0 & 0 & 0 & 0 & 0 & 0 \end{bmatrix}$$

$$\in \left(\begin{bmatrix} 0 & 0 & -0.3967 & 0 & 0 & 0 & 0 & 0 \\ 0 & 0 & -0.3967 & 0 & 0 & 0 & 0 & 0 \\ 0 & 0 & -0.3967 & 0 & 0 & 0 & 0 & 0 \\ 0 & 0 & -0.3967 & 0 & 0 & 0 & 0 & 0 \\ 0 & 0 & 0 & 0 & 0 & 0 & 0 & 0 \\ 0 & 0 & 0 & 0 & 0 & 0 & 0 & 0 \\ 0 & 0 & 0 & 0 & 0 & 0 & 0 & 0 \\ 0 & 0 & 0 & 0 & 0 & 0 & 0 & 0 \end{bmatrix}, \begin{bmatrix} 0 & 0 & 0.3967 & 0 & 0 & 0 & 0 & 0 \\ 0 & 0 & 0.3967 & 0 & 0 & 0 & 0 & 0 \\ 0 & 0 & 0.3967 & 0 & 0 & 0 & 0 & 0 \\ 0 & 0 & 0.3967 & 0 & 0 & 0 & 0 & 0 \\ 0 & 0 & 0 & 0 & 0 & 0 & 0 & 0 \\ 0 & 0 & 0 & 0 & 0 & 0 & 0 & 0 \\ 0 & 0 & 0 & 0 & 0 & 0 & 0 & 0 \\ 0 & 0 & 0 & 0 & 0 & 0 & 0 & 0 \end{bmatrix} \right)$$

$$= \sum_{i=1}^{16} \mu_i \Delta A_i = \sum_{l=1}^{16} \mathrm{h}_l \Delta \tilde{\mathrm{A}}_l \tag{2.95}$$

d) The fuzzy rules of the fuzzy uncertainty regenerator are as follows,

Rule 1*:* If Δa_{13} *is* $N^1{}_{\Delta a13}$ and Δa_{23} *is* $N^1{}_{\Delta a23}$ and Δa_{33} *is* $N^1{}_{\Delta a33}$ and Δa_{43} *is* $N^1{}_{\Delta a43}$

$$\text{Then} \quad \Delta A_1 = \begin{bmatrix} 0 & 0 & -0.3967 & 0 & 0 & 0 & 0 & 0 \\ 0 & 0 & -0.3967 & 0 & 0 & 0 & 0 & 0 \\ 0 & 0 & -0.3967 & 0 & 0 & 0 & 0 & 0 \\ 0 & 0 & -0.3967 & 0 & 0 & 0 & 0 & 0 \\ 0 & 0 & 0 & 0 & 0 & 0 & 0 & 0 \\ 0 & 0 & 0 & 0 & 0 & 0 & 0 & 0 \\ 0 & 0 & 0 & 0 & 0 & 0 & 0 & 0 \\ 0 & 0 & 0 & 0 & 0 & 0 & 0 & 0 \end{bmatrix} \tag{2.96}$$

Rule 2*:* If Δa_{13} *is* $N^2{}_{\Delta a13}$ and Δa_{23} *is* $N^2{}_{\Delta a23}$ and Δa_{33} *is* $N^2{}_{\Delta a33}$ and Δa_{43} *is* $N^2{}_{\Delta a43}$

$$\text{Then} \quad \Delta A_2 = \begin{bmatrix} 0 & 0 & -0.3967 & 0 & 0 & 0 & 0 & 0 \\ 0 & 0 & 0.3967 & 0 & 0 & 0 & 0 & 0 \\ 0 & 0 & -0.3967 & 0 & 0 & 0 & 0 & 0 \\ 0 & 0 & -0.3967 & 0 & 0 & 0 & 0 & 0 \\ 0 & 0 & 0 & 0 & 0 & 0 & 0 & 0 \\ 0 & 0 & 0 & 0 & 0 & 0 & 0 & 0 \\ 0 & 0 & 0 & 0 & 0 & 0 & 0 & 0 \\ 0 & 0 & 0 & 0 & 0 & 0 & 0 & 0 \end{bmatrix} \tag{2.97}$$

Rule 3*:* If Δa_{13} *is* $N^3{}_{\Delta a13}$ and Δa_{23} *is* $N^3{}_{\Delta a23}$ and Δa_{33} *is* $N^3{}_{\Delta a33}$ and Δa_{43} *is* $N^3{}_{\Delta a43}$

$$\text{Then} \quad \Delta A_3 = \begin{bmatrix} 0 & 0 & -0.3967 & 0 & 0 & 0 & 0 & 0 \\ 0 & 0 & -0.3967 & 0 & 0 & 0 & 0 & 0 \\ 0 & 0 & 0.3967 & 0 & 0 & 0 & 0 & 0 \\ 0 & 0 & -0.3967 & 0 & 0 & 0 & 0 & 0 \\ 0 & 0 & 0 & 0 & 0 & 0 & 0 & 0 \\ 0 & 0 & 0 & 0 & 0 & 0 & 0 & 0 \\ 0 & 0 & 0 & 0 & 0 & 0 & 0 & 0 \\ 0 & 0 & 0 & 0 & 0 & 0 & 0 & 0 \end{bmatrix} \tag{2.98}$$

Rule 4*:* If Δa_{13} *is* $N^4_{\Delta a13}$ and Δa_{23} *is* $N^4_{\Delta a23}$ and Δa_{33} *is* $N^4_{\Delta a33}$ and Δa_{43} *is* $N^4_{\Delta a43}$

$$\text{Then} \quad \Delta A_4 = \begin{bmatrix} 0 & 0 & -0.3967 & 0 & 0 & 0 & 0 & 0 \\ 0 & 0 & 0.3967 & 0 & 0 & 0 & 0 & 0 \\ 0 & 0 & 0.3967 & 0 & 0 & 0 & 0 & 0 \\ 0 & 0 & -0.3967 & 0 & 0 & 0 & 0 & 0 \\ 0 & 0 & 0 & 0 & 0 & 0 & 0 & 0 \\ 0 & 0 & 0 & 0 & 0 & 0 & 0 & 0 \\ 0 & 0 & 0 & 0 & 0 & 0 & 0 & 0 \\ 0 & 0 & 0 & 0 & 0 & 0 & 0 & 0 \end{bmatrix} \tag{2.99}$$

Rule 5*:* If Δa_{13} *is* $N^5_{\Delta a13}$ and Δa_{23} *is* $N^5_{\Delta a23}$ and Δa_{33} *is* $N^5_{\Delta a33}$ and Δa_{43} *is* $N^5_{\Delta a43}$

$$\text{Then} \quad \Delta A_5 = \begin{bmatrix} 0 & 0 & -0.3967 & 0 & 0 & 0 & 0 & 0 \\ 0 & 0 & -0.3967 & 0 & 0 & 0 & 0 & 0 \\ 0 & 0 & -0.3967 & 0 & 0 & 0 & 0 & 0 \\ 0 & 0 & 0.3967 & 0 & 0 & 0 & 0 & 0 \\ 0 & 0 & 0 & 0 & 0 & 0 & 0 & 0 \\ 0 & 0 & 0 & 0 & 0 & 0 & 0 & 0 \\ 0 & 0 & 0 & 0 & 0 & 0 & 0 & 0 \\ 0 & 0 & 0 & 0 & 0 & 0 & 0 & 0 \end{bmatrix} \tag{2.100}$$

Rule 6*:* If Δa_{13} *is* $N^6_{\Delta a13}$ and Δa_{23} *is* $N^6_{\Delta a23}$ and Δa_{33} *is* $N^6_{\Delta a33}$ and Δa_{43} *is* $N^6_{\Delta a43}$

$$\text{Then} \quad \Delta A_6 = \begin{bmatrix} 0 & 0 & -0.3967 & 0 & 0 & 0 & 0 & 0 \\ 0 & 0 & 0.3967 & 0 & 0 & 0 & 0 & 0 \\ 0 & 0 & -0.3967 & 0 & 0 & 0 & 0 & 0 \\ 0 & 0 & 0.3967 & 0 & 0 & 0 & 0 & 0 \\ 0 & 0 & 0 & 0 & 0 & 0 & 0 & 0 \\ 0 & 0 & 0 & 0 & 0 & 0 & 0 & 0 \\ 0 & 0 & 0 & 0 & 0 & 0 & 0 & 0 \\ 0 & 0 & 0 & 0 & 0 & 0 & 0 & 0 \end{bmatrix} \tag{2.101}$$

Rule 7*:* If Δa_{13} *is* $N^7_{\Delta a13}$ and Δa_{23} *is* $N^7_{\Delta a23}$ and Δa_{33} *is* $N^7_{\Delta a33}$ and Δa_{43} *is* $N^7_{\Delta a43}$

$$\text{Then} \quad \Delta A_7 = \begin{bmatrix} 0 & 0 & -0.3967 & 0 & 0 & 0 & 0 & 0 \\ 0 & 0 & -0.3967 & 0 & 0 & 0 & 0 & 0 \\ 0 & 0 & 0.3967 & 0 & 0 & 0 & 0 & 0 \\ 0 & 0 & 0.3967 & 0 & 0 & 0 & 0 & 0 \\ 0 & 0 & 0 & 0 & 0 & 0 & 0 & 0 \\ 0 & 0 & 0 & 0 & 0 & 0 & 0 & 0 \\ 0 & 0 & 0 & 0 & 0 & 0 & 0 & 0 \\ 0 & 0 & 0 & 0 & 0 & 0 & 0 & 0 \end{bmatrix} \tag{2.102}$$

Rule 8*:* If Δa_{13} *is* $N^{8}_{\Delta a13}$ and Δa_{23} *is* $N^{8}_{\Delta a23}$ and Δa_{33} *is* $N^{8}_{\Delta a33}$ and Δa_{43} *is* $N^{8}_{\Delta a43}$

$$\text{Then} \quad \Delta A_8 = \begin{bmatrix} 0 & 0 & -0.3967 & 0 & 0 & 0 & 0 & 0 \\ 0 & 0 & 0.3967 & 0 & 0 & 0 & 0 & 0 \\ 0 & 0 & 0.3967 & 0 & 0 & 0 & 0 & 0 \\ 0 & 0 & 0.3967 & 0 & 0 & 0 & 0 & 0 \\ 0 & 0 & 0 & 0 & 0 & 0 & 0 & 0 \\ 0 & 0 & 0 & 0 & 0 & 0 & 0 & 0 \\ 0 & 0 & 0 & 0 & 0 & 0 & 0 & 0 \\ 0 & 0 & 0 & 0 & 0 & 0 & 0 & 0 \end{bmatrix} \tag{2.103}$$

Rule 9*:* If Δa_{13} *is* $N^{9}_{\Delta a13}$ and Δa_{23} *is* $N^{9}_{\Delta a23}$ and Δa_{33} *is* $N^{9}_{\Delta a33}$ and Δa_{43} *is* $N^{9}_{\Delta a43}$

$$\text{Then} \quad \Delta A_9 = \begin{bmatrix} 0 & 0 & 0.3967 & 0 & 0 & 0 & 0 & 0 \\ 0 & 0 & -0.3967 & 0 & 0 & 0 & 0 & 0 \\ 0 & 0 & -0.3967 & 0 & 0 & 0 & 0 & 0 \\ 0 & 0 & -0.3967 & 0 & 0 & 0 & 0 & 0 \\ 0 & 0 & 0 & 0 & 0 & 0 & 0 & 0 \\ 0 & 0 & 0 & 0 & 0 & 0 & 0 & 0 \\ 0 & 0 & 0 & 0 & 0 & 0 & 0 & 0 \\ 0 & 0 & 0 & 0 & 0 & 0 & 0 & 0 \end{bmatrix} \tag{2.104}$$

Rule 10*:* If Δa_{13} *is* $N^{10}_{\Delta a13}$ and Δa_{23} *is* $N^{10}_{\Delta a23}$ and Δa_{33} *is* $N^{10}_{\Delta a33}$ and Δa_{43} *is* $N^{10}_{\Delta a41}$

$$\text{Then} \quad \Delta A_{10} = \begin{bmatrix} 0 & 0 & 0.3967 & 0 & 0 & 0 & 0 & 0 \\ 0 & 0 & 0.3967 & 0 & 0 & 0 & 0 & 0 \\ 0 & 0 & -0.3967 & 0 & 0 & 0 & 0 & 0 \\ 0 & 0 & -0.3967 & 0 & 0 & 0 & 0 & 0 \\ 0 & 0 & 0 & 0 & 0 & 0 & 0 & 0 \\ 0 & 0 & 0 & 0 & 0 & 0 & 0 & 0 \\ 0 & 0 & 0 & 0 & 0 & 0 & 0 & 0 \\ 0 & 0 & 0 & 0 & 0 & 0 & 0 & 0 \end{bmatrix} \tag{2.105}$$

Rule 11*:* If Δa_{13} *is* $N^{11}{}_{\Delta a13}$ and Δa_{23} *is* $N^{11}{}_{\Delta a23}$ and Δa_{33} *is* $N^{11}{}_{\Delta a33}$ and Δa_{43} *is* $N^{11}{}_{\Delta a41}$

$$\text{Then} \quad \Delta A_{11} = \begin{bmatrix} 0 & 0 & 0.3967 & 0 & 0 & 0 & 0 & 0 \\ 0 & 0 & -0.3967 & 0 & 0 & 0 & 0 & 0 \\ 0 & 0 & 0.3967 & 0 & 0 & 0 & 0 & 0 \\ 0 & 0 & -0.3967 & 0 & 0 & 0 & 0 & 0 \\ 0 & 0 & 0 & 0 & 0 & 0 & 0 & 0 \\ 0 & 0 & 0 & 0 & 0 & 0 & 0 & 0 \\ 0 & 0 & 0 & 0 & 0 & 0 & 0 & 0 \\ 0 & 0 & 0 & 0 & 0 & 0 & 0 & 0 \end{bmatrix} \tag{2.106}$$

Rule 12*:* If Δa_{13} *is* $N^{12}{}_{\Delta a13}$ and Δa_{23} *is* $N^{12}{}_{\Delta a23}$ and Δa_{33} *is* $N^{12}{}_{\Delta a33}$ and Δa_{43} *is* $N^{12}{}_{\Delta a43}$

$$\text{Then} \quad \Delta A_{12} = \begin{bmatrix} 0 & 0 & 0.3967 & 0 & 0 & 0 & 0 & 0 \\ 0 & 0 & 0.3967 & 0 & 0 & 0 & 0 & 0 \\ 0 & 0 & 0.3967 & 0 & 0 & 0 & 0 & 0 \\ 0 & 0 & -0.3967 & 0 & 0 & 0 & 0 & 0 \\ 0 & 0 & 0 & 0 & 0 & 0 & 0 & 0 \\ 0 & 0 & 0 & 0 & 0 & 0 & 0 & 0 \\ 0 & 0 & 0 & 0 & 0 & 0 & 0 & 0 \\ 0 & 0 & 0 & 0 & 0 & 0 & 0 & 0 \end{bmatrix} \tag{2.107}$$

Rule 13*:* If Δa_{13} *is* $N^{13}{}_{\Delta a13}$ and Δa_{23} *is* $N^{13}{}_{\Delta a23}$ and Δa_{33} *is* $N^{13}{}_{\Delta a33}$ and Δa_{43} *is* $N^{13}{}_{\Delta a43}$

$$\text{Then} \quad \Delta A_{13} = \begin{bmatrix} 0 & 0 & 0.3967 & 0 & 0 & 0 & 0 & 0 \\ 0 & 0 & -0.3967 & 0 & 0 & 0 & 0 & 0 \\ 0 & 0 & -0.3967 & 0 & 0 & 0 & 0 & 0 \\ 0 & 0 & 0.3967 & 0 & 0 & 0 & 0 & 0 \\ 0 & 0 & 0 & 0 & 0 & 0 & 0 & 0 \\ 0 & 0 & 0 & 0 & 0 & 0 & 0 & 0 \\ 0 & 0 & 0 & 0 & 0 & 0 & 0 & 0 \\ 0 & 0 & 0 & 0 & 0 & 0 & 0 & 0 \end{bmatrix} \tag{2.108}$$

Rule 14*:* If Δa_{13} *is* $N^{14}{}_{\Delta a13}$ and Δa_{23} *is* $N^{14}{}_{\Delta a23}$ and Δa_{33} *is* $N^{14}{}_{\Delta a33}$ and Δa_{43} *is* $N^{14}{}_{\Delta a43}$

$$\text{Then} \quad \Delta A_{14} = \begin{bmatrix} 0 & 0 & 0.3967 & 0 & 0 & 0 & 0 & 0 \\ 0 & 0 & 0.3967 & 0 & 0 & 0 & 0 & 0 \\ 0 & 0 & -0.3967 & 0 & 0 & 0 & 0 & 0 \\ 0 & 0 & 0.3967 & 0 & 0 & 0 & 0 & 0 \\ 0 & 0 & 0 & 0 & 0 & 0 & 0 & 0 \\ 0 & 0 & 0 & 0 & 0 & 0 & 0 & 0 \\ 0 & 0 & 0 & 0 & 0 & 0 & 0 & 0 \\ 0 & 0 & 0 & 0 & 0 & 0 & 0 & 0 \end{bmatrix} \tag{2.109}$$

Rule 15*:* If Δa_{13} *is* $N^{15}{}_{\Delta a13}$ and Δa_{23} *is* $N^{15}{}_{\Delta a23}$ and Δa_{33} *is* $N^{15}{}_{\Delta a33}$ and Δa_{43} *is* $N^{15}{}_{\Delta a43}$

$$\text{Then} \quad \Delta A_{15} = \begin{bmatrix} 0 & 0 & 0.3967 & 0 & 0 & 0 & 0 & 0 \\ 0 & 0 & -0.3967 & 0 & 0 & 0 & 0 & 0 \\ 0 & 0 & 0.3967 & 0 & 0 & 0 & 0 & 0 \\ 0 & 0 & 0.3967 & 0 & 0 & 0 & 0 & 0 \\ 0 & 0 & 0 & 0 & 0 & 0 & 0 & 0 \\ 0 & 0 & 0 & 0 & 0 & 0 & 0 & 0 \\ 0 & 0 & 0 & 0 & 0 & 0 & 0 & 0 \\ 0 & 0 & 0 & 0 & 0 & 0 & 0 & 0 \end{bmatrix} \tag{2.110}$$

Rule 16*:* If Δa_{13} *is* $N^{16}{}_{\Delta a13}$ and Δa_{23} *is* $N^{16}{}_{\Delta a23}$ and Δa_{33} *is* $N^{16}{}_{\Delta a33}$ and Δa_{43} *is* $N^{16}{}_{\Delta a43}$

$$\text{Then} \quad \Delta A_{16} = \begin{bmatrix} 0 & 0 & 0.3967 & 0 & 0 & 0 & 0 & 0 \\ 0 & 0 & 0.3967 & 0 & 0 & 0 & 0 & 0 \\ 0 & 0 & 0.3967 & 0 & 0 & 0 & 0 & 0 \\ 0 & 0 & 0.3967 & 0 & 0 & 0 & 0 & 0 \\ 0 & 0 & 0 & 0 & 0 & 0 & 0 & 0 \\ 0 & 0 & 0 & 0 & 0 & 0 & 0 & 0 \\ 0 & 0 & 0 & 0 & 0 & 0 & 0 & 0 \\ 0 & 0 & 0 & 0 & 0 & 0 & 0 & 0 \end{bmatrix} \tag{2.111}$$

The inferred output of the fuzzy uncertainty regenerator is,

$$\Delta A = \sum_{l=1}^{16} h_l \Delta \tilde{A}_l \tag{2.112}$$

where $h_l = \dfrac{N^l_{\Delta a_{13}} \times N^l_{\Delta a_{23}} \times N^l_{\Delta a_{33}} \times N^l_{\Delta a_{43}}}{\sum_{l=1}^{16} (N^l_{\Delta a_{13}} \times N^l_{\Delta a_{23}} \times N^l_{\Delta a_{33}} \times N^l_{\Delta a_{43}})}$, for l=1,2,…,16

$$N^1_{\Delta a_{13}} = N^2_{\Delta a_{13}} = N^3_{\Delta a_{13}} = N^4_{\Delta a_{13}} = N^5_{\Delta a_{13}} = N^6_{\Delta a_{13}} = N^7_{\Delta a_{13}} = N^8_{\Delta a_{13}} = \frac{-\Delta a_{13} + 0.3967}{0.7934} \tag{2.113}$$

$$N^9_{\Delta a_{13}} = N^{10}_{\Delta a_{13}} = N^{11}_{\Delta a_{13}} = N^{12}_{\Delta a_{13}} = N^{13}_{\Delta a_{13}} = N^{14}_{\Delta a_{13}} = N^{15}_{\Delta a_{13}} = N^{16}_{\Delta a_{13}} = \frac{\Delta a_{13} + 0.3967}{0.7934} \tag{2.114}$$

$$N^1_{\Delta a_{23}} = N^3_{\Delta a_{23}} = N^5_{\Delta a_{23}} = N^7_{\Delta a_{23}} = N^9_{\Delta a_{23}} = N^{11}_{\Delta a_{23}} = N^{13}_{\Delta a_{23}} = N^{15}_{\Delta a_{23}} = \frac{-\Delta a_{23} + 0.3967}{0.7934} \tag{2.115}$$

$$N^2_{\Delta a_{23}} = N^4_{\Delta a_{23}} = N^6_{\Delta a_{23}} = N^8_{\Delta a_{23}} = N^{10}_{\Delta a_{23}} = N^{12}_{\Delta a_{23}} = N^{14}_{\Delta a_{23}} = N^{16}_{\Delta a_{23}} = \frac{\Delta a_{23} + 0.3967}{0.7934} \tag{2.116}$$

$$N^1_{\Delta a_{33}} = N^2_{\Delta a_{33}} = N^5_{\Delta a_{33}} = N^6_{\Delta a_{33}} = N^9_{\Delta a_{33}} = N^{10}_{\Delta a_{33}} = N^{14}_{\Delta a_{33}} = \frac{-\Delta a_{33} + 0.3967}{0.7934} \tag{2.117}$$

$$N^3_{\Delta a_{33}} = N^4_{\Delta a_{33}} = N^7_{\Delta a_{33}} = N^8_{\Delta a_{33}} = N^{11}_{\Delta a_{33}} = N^{12}_{\Delta a_{33}} = N^{13}_{\Delta a_{33}} = N^{15}_{\Delta a_{33}} = N^{16}_{\Delta a_{33}} = \frac{\Delta a_{33} + 0.3967}{0.7934} \tag{2.118}$$

$$N^1_{\Delta a_{43}} = N^2_{\Delta a_{43}} = N^3_{\Delta a_{43}} = N^4_{\Delta a_{43}} = N^9_{\Delta a_{43}} = N^{10}_{\Delta a_{43}} = N^{11}_{\Delta a_{43}} = N^{12}_{\Delta a_{43}} = N^{14}_{\Delta a_{43}} = \frac{-\Delta a_{43} + 0.00056}{0.7934} \tag{2.119}$$

$$N^5_{\Delta a_{43}} = N^6_{\Delta a_{43}} = N^7_{\Delta a_{43}} = N^8_{\Delta a_{43}} = N^{13}_{\Delta a_{43}} = N^{15}_{\Delta a_{43}} = N^{16}_{\Delta a_{43}} = \frac{\Delta a_{43} + 0.00056}{0.7934} \tag{2.120}$$

They are shown in Fig. 2.12.

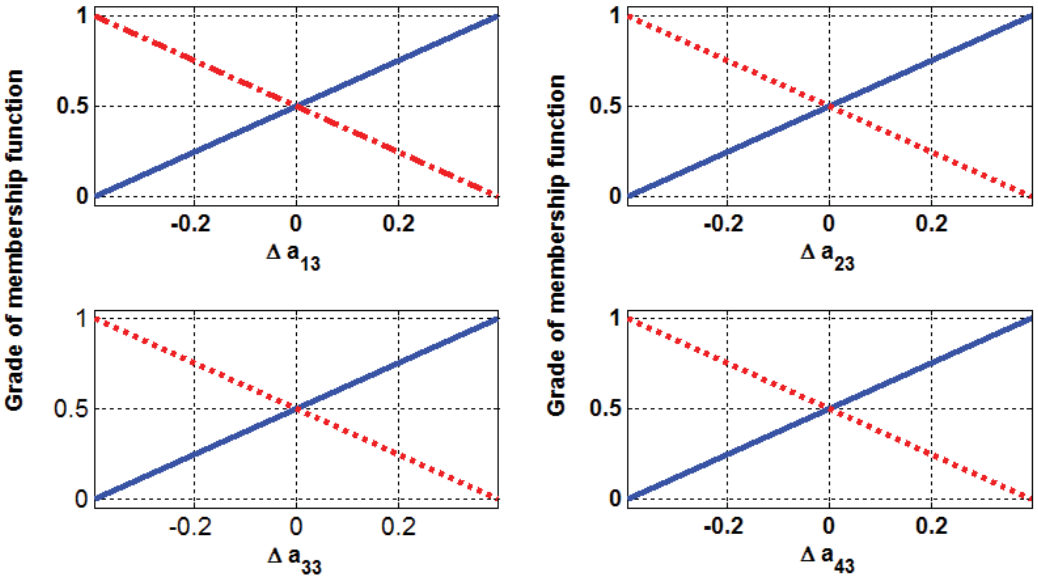

Fig.2.12. Membership function of the parameter uncertainties of 40% of their nominal values

Then, the augmented TS fuzzy plant model of (2.94) is given by

$$\dot{x}(t) = \sum_{i=1}^{8} \sum_{l=1}^{16} \mu_i h_l [(A_i + \Delta \tilde{A}_l) x(t) + B_i u(t)] \qquad (2.121)$$

e) Since the input matrices are common we use the third family.

f) The fuzzy controller is designed by PDC. Eight fuzzy rules are used to implement the RFSC of each fuzzy system. The membership functions of each RFSC are chosen to be the same as those of the TS fuzzy plant model of (2.94), i.e., the membership functions given by (2.52)-(2.54). The rules of the RFSC are as follows,

Rule j: IF $q_1(t)$is M_{1j} and $q_2(t)$is D_{1j} and $q_3(t)$is N_{1j}

Then $u(t) = -G_{jl}\, x(t) + r(t)$ j=1,2,…,8 (2.122)

The inferred output of the RFSC is given by,

$$u(t) = \sum_{j=1}^{8} \mu_j [-G_{jl}\, x(t) + r(t)] \qquad l=1,2,\ldots,16 \qquad (2.123)$$

g) The rules of the RFSC are as follows,

Rule *l:* If Δa_{13} *is* $N^{l}_{\Delta a13}$ and Δa_{23} *is* $N^{l}_{\Delta a23}$ and Δa_{33} *is* $N^{l}_{\Delta a33}$ and Δa_{43} *is* $N^{6}_{\Delta a43}$

$$\text{Then} \quad u(t) = \sum_{j=1}^{8} \mu_j [-G_{jl}\, x(t) + r(t)] \tag{2.124}$$

The inferred output of the RFSC is,

$$u(t) = -\sum_{j=1}^{8} \sum_{l=1}^{16} \mu_j h_l \, [-G_{jl}\, x(t) + r(t)] \tag{2.125}$$

2.3.6. Simulations and Results

We study the results of the proposed algorithm for same random profile of wind speed as shown in Fig. 2.4. We compared the results of the proposed algorithms RFSC and RFC with the previous algorithm [53] (dashed line) subject to parameter uncertainties including a large disturbance. The reference input ($\Omega_{ref}=\Omega_{opt}=\lambda_{opt}v/R$) is also applied to the controller to obtain the maximum power coefficient from the WES, Ω_{opt} is the reference rotational speed. As given in (2.95), the elements of ΔA_i achieve values within 40% of their nominal values corresponding to system parameter variations in parameter R_s, with $\Delta B_i=0$ and disturbance (20% of wind speed), as the following figures the time responses of the Ω_r and Ω_g of the WES (2.38) subject to parameter uncertainties including a large disturbance for the proposed algorithm RFSC (dotted line) and RFC (dashed-dotted line), the previous algorithm [53] (dashed line) and optimal tracking (solid line) are shown in Figs. 2.13 and 2.14, respectively.

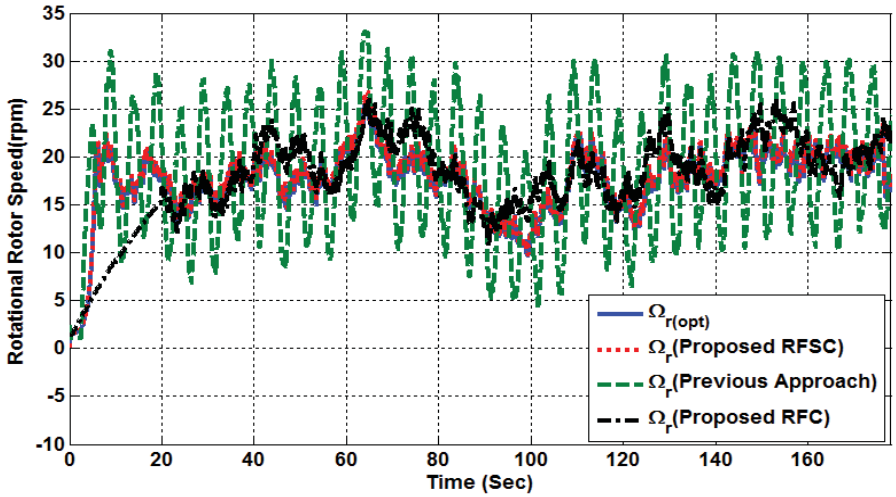

Fig. 2.13. The trajectory of Ω_r of the proposed RFSC (dotted line) and RFC (dashed-dotted line), previous approach (dashed line) [53] and optimal tracking (solid line)

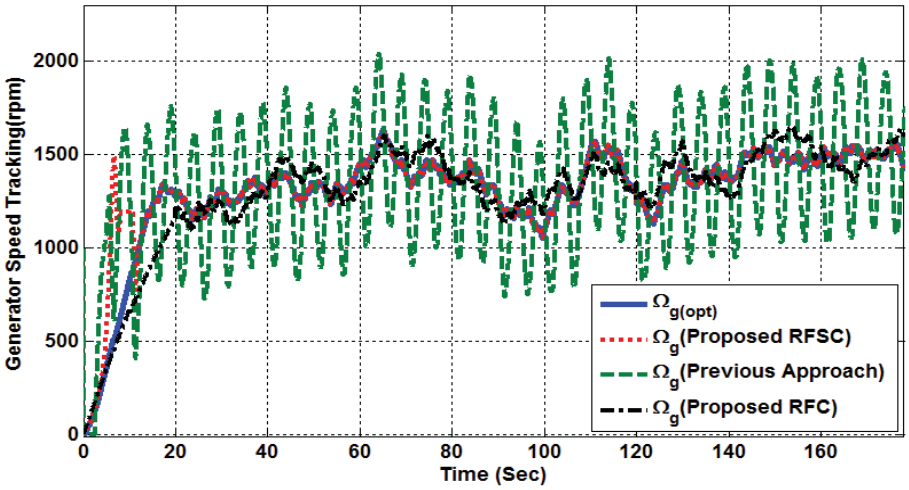

Fig. 2.14. The trajectory of Ω_g of the proposed RFSC (dotted line) and RFC (dashed-dotted line), previous approach (dashed line) [53] and optimal tracking (solid line)

Fig. 2.15 and Fig. 2.16 show the active power P_s and the reactive power Q_s for the proposed algorithm RFSC (dotted line) and RFC (dashed-dotted line), the previous algorithm [53] (dashed line) and optimal tracking (solid line), respectively. From the Fig. 2.15 and Fig. 2.16, it can be seen that the previous

algorithm [53] leads to system highly oscillation but the proposed algorithm gives a good robustness.

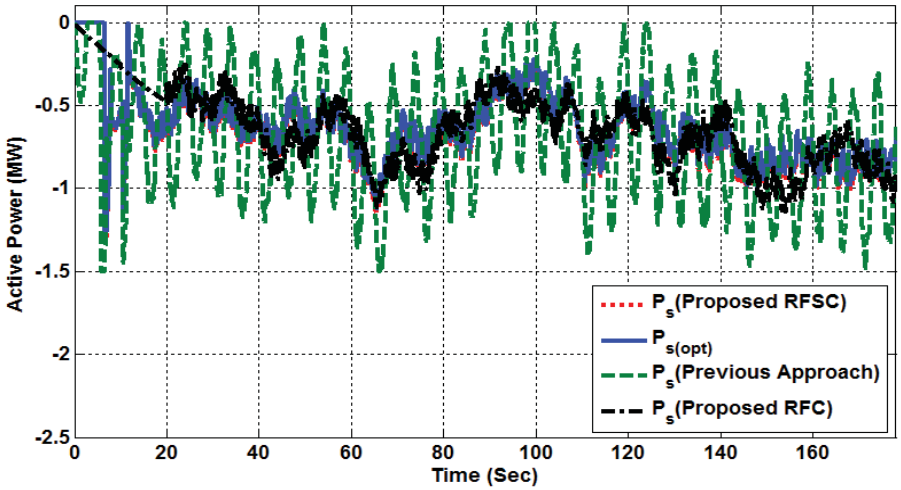

Fig. 2.15. The trajectory of P_s of the proposed RFSC (dotted line) and RFC (dashed-dotted line), previous approach (dashed line) [53] and optimal tracking (solid line)

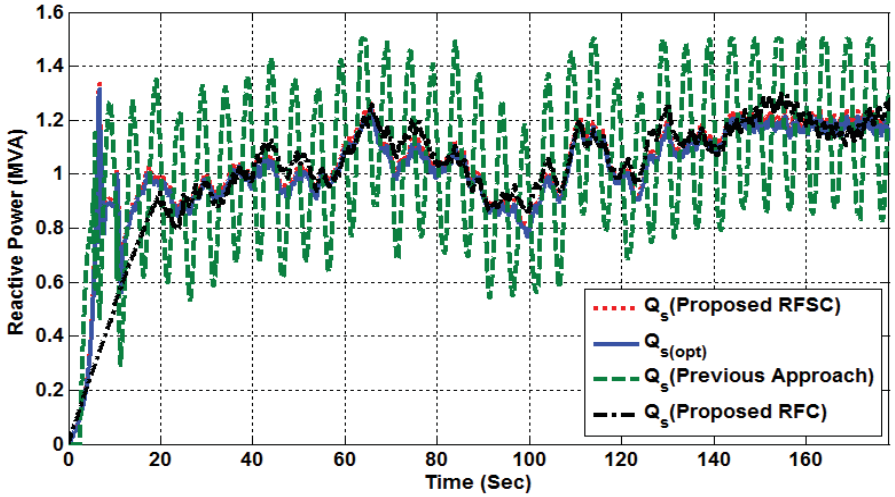

Fig. 2.16. The trajectory of Q_s of the proposed RFSC (dotted line) and RFC (dashed-dotted line), previous approach (dashed line) [53] and optimal tracking (solid line)

In order to obtain maximum output power from a wind turbine generator system, it is necessary to drive the wind turbine at an optimal rotor speed for a particular wind speed, and keep the power coefficient at 0.48, Fig. 2.17 shows the power coefficient, it can be seen that $C_{p(max)}$ ≈0.48, which prove the effectiveness of the proposed algorithm.

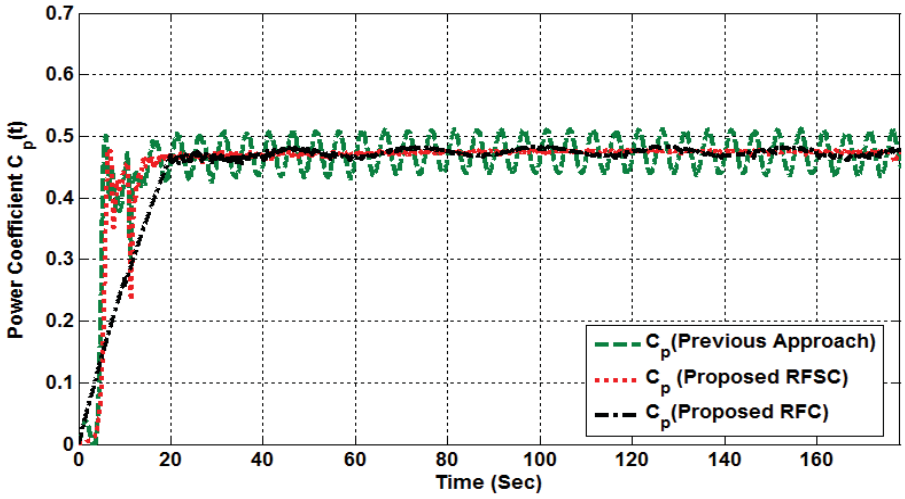

Fig. 2.17. Maximum power coefficient $C_{p(max)}$ of the proposed approach RFSC (dotted line) and RFC (dashed-dotted line), previous approach (dashed line) [53]

In summary, from Figs. 2.13 to 2.16, it can be seen that the proposed algorithms give a good tracking for the reference input whereas the previous algorithm [53] leads to system instability when parameter uncertainty R_s increased to 40% of their nominal values and the disturbance up to 20% of the wind speed.

We can observe also from Figs. 2.13 to 2.16 compare the output states of the system with RFSC (dashed lines), and with RSC (dashed lines-dotted lines). It can be seen that the RFSC provides a better performance.

The simulation results demonstrate the effectiveness of the proposed control approaches. The proposed control scheme can guarantee the stability of the closed-loop system and the convergence of the output tracking error.

2.4. Proposed RNFC of PV Based on TS Fuzzy Plant Model

This section addresses the RNFC problem for nonlinear systems in the presence of parametric uncertainties. The TS fuzzy model is adopted for fuzzy modeling of the nonlinear system and establishing fuzzy state observers. The concept of PDC is also employed to design RNFC from the TS fuzzy models. The sufficient conditions are formulated in the format of LMIs. The effectiveness of the proposed controller design methodology is finally demonstrated through a photovoltaic panel array to MPPT. In detail, we consider a DC/DC buck converter to regulate the output power of the photovoltaic panel array. Furthermore, when considering disturbance and uncertainty, robust MPPT is guaranteed by advanced gain design. Therefore, the proposed method provides an easier implementation form under strict stability analysis. Finally, the control performance is shown from the numerical simulation results.

The rest of the section is organized as follows. In sub-section 2.4.1, TS fuzzy model, fuzzy observer and the RNFC are presented. The stability analysis condition is given in sub-section 2.4.2. Sub-section 2.4.3 introduces the electric characteristic of PV array and TS fuzzy modeling of general solar PV power control systems. To show the control performance, numerical simulations are carried out in Sections 2.4.4.

2.4.1. TS Fuzzy Model and RNFC

TS fuzzy a multivariable non-linear control system which consists of a nonlinear plant and a RNFC connected in closed-loop.

2.4.1.1. TS Fuzzy Plant Model

The plant is represented by the TS fuzzy plant model as discussed in sub-section 2.2.1. In this section, assume $d(t)$=0, and TS fuzzy plant model (2.8) can rewrite as the following,

$$\dot{x}(t) = \sum_{i=1}^{p} \mu_i(q(t))[(A_i + \Delta A_i)\, x(t) + (B_i + \Delta B_i)\, u(t)]$$

$$y(t) = \sum_{i=1}^{p} \mu_i(q(t)) C_i\, x(t) \qquad (2.126)$$

2.4.1.2. TS Fuzzy Observer

This sub-section presents fuzzy observer design methodologies involving state estimation for TS fuzzy models. In practice, all states are not fully measurable, it is necessary to design a fuzzy observer in order to implement the RNFC, it is assumed that the fuzzy system model (2.126) is locally observable. PDC [53] is also employed to design the following observer structures. The i-th rule of the fuzzy observer is of the following format [46],

Rule i: IF $q_1(x(t))$ is M_{1i} AND … AND $q_\varepsilon(x(t))$ is $M_{\varepsilon i}$

Then $\dot{\hat{x}}(t) = A_i\hat{x}(t) + B_i u(t) + N_i(y(t)-\hat{y}(t))$

$$\hat{y}(t) = C_i\hat{x}(t) \qquad i=1, 2\ldots,p \qquad (2.127)$$

The inferred observer states are governed by:

$$\dot{\hat{x}}(t) = \sum_{i=1}^{p} \mu_i[A_i\hat{x}(t) + B_i u(t) + N_i(y(t)-\hat{y}(t))]$$

$$\hat{y}(t) = \sum_{i=1}^{p} \mu_i C_i\hat{x}(t) \qquad (2.128)$$

where $\hat{x}(t)$ is the estimated state vector by the fuzzy observer, $\hat{y}(t)$ is the final output of the fuzzy observer, and $N_i \in \kappa^{nxg}$ are the fuzzy observer gains.

2.4.1.3. Proposed RNFC

A nonlinear controller is to be designed for the nonlinear plant represented by the TS fuzzy plant model of (2.126) [54]. The nonlinear controller has a similar form as that of the fuzzy controller of (2.13) in section 2.2.2.1.

Rule j: IF $q_1(x(t))$ is M_{1j} AND … AND $q_\varepsilon(x(t))$ is $M_{\varepsilon j}$

Then $u(t) = -G_j x(t)$ (2.129)

where $G_j \epsilon \kappa^{mxn}$, $j = 1, 2, \ldots c$, are feedback gain vectors that are to be designed and the output of the fuzzy controller is given by,

$$u(t) = -\sum_{j=1}^{c} \mu_j(q(x(t)))\, G_j\, x(t) \tag{2.130}$$

where

$$\sum_{j=1}^{c} \mu_j(q(x(t))) = 1 \;,\; g_j(q(x(t))) = \prod_{\ni=1}^{\varepsilon} M_{\varepsilon j}(q_\varepsilon(x(t))) \tag{2.131}$$

$$\mu_j(q(x(t))) = \frac{g_j(q(x(t)))}{\sum_{j=1}^{c} g_j(q(x(t)))} \tag{2.132}$$

$g_j(q(x(t)))$ are nonlinear gains to be designed. From (2.128) we use the estimated state by the observer, then the final output of the fuzzy controller as follows,

$$u(t) = -\sum_{j=1}^{c} \mu_j(q(x(t)))\, G_j \hat{x}(t) \tag{2.133}$$

2.4.2. Stability Analysis for the Proposed RNFC Algorithm

A closed-loop system can be obtained by combining (2.126), (2.128) and (2.133). Writing $\mu_i(q(x(t)))$ as μ_i and $\mu_j(q(x(t)))$ as μ_i. Let observation error as the following [54],

$$e(t)=x(t)-\hat{x}(t) \tag{2.134}$$

From (2.126), (2.128), (2.133) and (2.134), we can obtain the fuzzy control system of state and the errors,

$$\dot{x}(t)=\sum_{i=1}^{p}\sum_{j=1}^{c}\mu_i\mu_j[(A_i-B_iG_j+\Delta A_i-\Delta B_iG_j)x(t)+(B_i+\Delta B_i)G_j\,e(t)] \tag{2.135}$$

$$\dot{e}(t)=\sum_{i=1}^{p}\sum_{j=1}^{c}\mu_i\mu_j[\Delta A_i-\Delta B_iG_jx(t)+(A_i-N_iC_j+\Delta B_iG_j)e(t)] \tag{2.136}$$

Combining (2.135) and (2.136) yields the following augmented nonlinear control system then becomes.

$$\dot{X}(t)=\sum_{i=1}^{p}\sum_{j=1}^{c}\mu_i\mu_j[(H_{ij}+\Delta H_{ij})X(t)] \tag{2.137}$$

where

$$X(t)=\begin{bmatrix}x(t)\\e(t)\end{bmatrix},\ H_{ij}=\begin{bmatrix}A_i-B_iG_j & B_iG_j\\0 & (A_i-N_iC_j)\end{bmatrix},\ \text{and,}\ \ \Delta H_{ij}=\begin{bmatrix}\Delta A_i-\Delta B_iG_j & \Delta B_iG_j\\\Delta A_i-\Delta B_iG_j & \Delta B_iG_j\end{bmatrix}$$

To investigate the stability of the nonlinear control system of (2.137), based on Lyapunov's function (2.32) is considered,

$$V(X(t))=0.5X(t)^TPX(t) \tag{2.138}$$

where $P\in\kappa^{nxn}$ is a symmetric positive definite matrix. Then,

$$\dot{V}(X(t))=0.5[\dot{X}(t)^TPX(t)+X(t)^TP\dot{X}(t)] \tag{2.139}$$

From (2.137), (2.139) and the property of $\sum_{i=1}^{p}\mu_i=\sum_{j=1}^{c}\mu_j=\sum_{i=1}^{p}\sum_{j=1}^{c}\mu_i\mu_j=1$

$$\dot{V}(X(t))=0.5\left[\left(\sum_{i=1}^{p}\sum_{j=1}^{c}\mu_i\mu_j(H_{ij}+\Delta H_{ij})X(t)\right)^TPX(t)\right.$$

$$+ X(t)^T P \sum_{i=1}^{p} \sum_{j=1}^{c} \mu_i \mu_j (H_{ij} + \Delta H_{ij}) X(t) \Big) \tag{2.140}$$

$$= 0.5 \Bigg[\Bigg(\sum_{i=1}^{p} \sum_{j=1}^{c} \mu_i \mu_j (H_{ij} + \Delta H_{ij} - H_m + H_m) X(t) \Bigg)^T P x(t)$$

$$+ X(t)^T P \sum_{i=1}^{p} \sum_{j=1}^{c} \mu_i \mu_j (H_{ij} + \Delta H_{ij} - H_m + H_m) X(t) \Big) \tag{2.141}$$

$$= 0.5 X(t)^T (H_m^T P + P H_m) X(t)$$
$$+ 0.5 \sum_{i=1}^{p} \sum_{j=1}^{c} \mu_i \mu_j \Big[(H_{ij} + \Delta H_{ij} - H_m)^T P + P(H_{ij} + \Delta H_{ij} - H_m) \Big] X(t)$$

$$= -0.5 X(t)^T Q_m X(t) - 0.5 \sum_{i=1}^{p} \sum_{j=1}^{c} \mu_i \mu_j X(t)^T (Q_{ij} - Q_m + \Delta Q_{ij})^T X(t) \tag{2.142}$$

where $H_m \in \kappa^{nxn}$ is a stable matrix to be designed. $Q_m \in \kappa^{nxn}$ is a symmetric positive definite matrix and $Q_{ij} \in \kappa^{nxn}$ is a symmetric matrix. They are defined as,

$$Q_{ij} = -(H_{ij}^T P + P H_{ij}) \ , \ Q_m = -(H_m^T P + P H_m) \tag{2.143}$$

$$\Delta Q_{ij} = -(\Delta H_{ij}^T P + P \Delta H_{ij}) \quad for \quad i = 1,2,...,p; \ \ j = 1,2,...,c \tag{2.144}$$

From (2.142)

$$\dot{V}(X(t)) \le -0.5 \lambda_{\min}(Q_m) \|X(t)\|^2 + 0.5 \sum_{i=1}^{p} \sum_{j=1}^{c} \mu_i \mu_j \left\| \Delta Q_{ij} \right\| \|X(t)\|^2$$

$$- 0.5 \sum_{j=1}^{c} \mu_j X(t)^T (\sum_{i=1}^{p} \mu_i Q_{ij} - Q_m) X(t) \tag{2.145}$$

where $\lambda_{\min}(Q_m)$ denotes the minimum eigcnvalne of Q_m, $\|\bullet\|$ denotes the l_2 norm for vectors and l_2 induced norm for matrices.

$$\dot{V}(X(t)) \le -0.5 \sum_{i=1}^{p} \sum_{j=1}^{c} \mu_i \mu_j [\lambda_{\min}(Q_m) - \max_{ij} \left\| \Delta Q_{ij} \right\|_{\max}] \|X(t)\|^2$$

$$- 0.5 \sum_{j=1}^{c} \mu_j X(t)^T (\sum_{i=1}^{p} \mu_i Q_{ij} - Q_m) X(t) \tag{2.146}$$

where $\max_{ij} \left\| \Delta Q_{ij} \right\|_{\max} \ge \left\| \Delta Q_{ij} \right\|_{\max} \ge \left\| \Delta Q_{ij} \right\|$

$$\dot{V}(X(t)) \le -0.5\varepsilon \|X(t)\|^2 - 0.5 \sum_{j=1}^{c} \mu_j X(t)^T (\sum_{i=1}^{p} \mu_i Q_{ij} - Q_m) X(t) \tag{2.147}$$

$$\text{where} \quad \lambda_{\min}(Q_m) - \max_{ij} \left\| \Delta Q_{ij} \right\|_{\max} = \varepsilon \tag{2.148}$$

Where ε is nonzero positive scalar and we design μ_j as the following,

$$\mu_j = \frac{X(t)^T (\sum_{i=1}^{p} \mu_i Q_{ij} - Q_m) X(t)}{\sum_{j=1}^{c} \left[X(t)^T (\sum_{i=1}^{p} \mu_i Q_{ij} - Q_m) X(t) \right]} \quad for \quad j = 1,2,...,c \tag{2.149}$$

Comparing (2.149) with (2.132), (2.149) gives the design of the gains of the nonlinear controller (2.133) such that

$$g_j(q(t)) = X(t)^T (\sum_{i=1}^{p} \mu_i Q_{ij} - Q_m) X(t) \tag{2.150}$$

Considering the denominator at the right hand side of (2.150),

$$\sum_{j=1}^{c} \left[X(t)^T (\sum_{i=1}^{p} \mu_i Q_{ij} - Q_m) X(t) \right] = \sum_{i=1}^{p} \mu_i \left[X(t)^T (\sum_{j=1}^{c} Q_{ij} - cQ_m) X(t) \right] \tag{2.151}$$

Q_{ij} and Q_m are designed such that,

$$\sum_{j=1}^{c} Q_{ij} - cQ_m > 0 \qquad for \quad i = 1,2,..., p \tag{2.152}$$

As $\mu_i \in [0\ 1]$ for all *i*, and at least one of the $\mu_i \neq 0$ (this is a property of the TS fuzzy plant model), (2.152) implies that (2.151) will be always greater than or equal to zero. It is equal to zero only when *X(t)*=0. Under this condition, the output of the nonlinear controller of (2.133) should be zero, and $\mu_j = \frac{1}{c}$ is chosen in order to satisfy the condition of (2.132). From (2.135) and (2.136),

$$\dot{V}(x(t)) = -0.5 X(t)^T Q_m X(t) - \frac{\sum_{j=1}^{c} \left[X(t)^T \left(\sum_{i=1}^{p} \mu_i Q_{ij} - Q_m \right) X(t) \right]^2}{2 \sum_{j=1}^{c} \left[X(t)^T (\sum_{i=1}^{p} \mu_i Q_{ij} - Q_m) X(t) \right]} \tag{2.153}$$

As the second term at the right side of (2.153) is greater than or equal to zero,

$$\dot{V}(x(t)) \le -0.5 X(t)^T Q_m X(t) \le 0 \tag{2.154}$$

Equality holds only when $X(t)=0$. Hence, it can be concluded that the nonlinear control system is globally asymptotically stable [89], [90]. The sufficient and necessary stability condition of the nonlinear control system (2.137) is summarized by the following lemma 2.3 and theorem 2.3.

Lemma 2.3: An uncertain nonlinear control system of (2.137) is guaranteed to be globally asymptotically stable,

i) if the gains of the nonlinear controller of (2.133) are chosen as,

$$\begin{cases} g_j(\mathrm{q(x(t))}) = X(t)^T \left(\sum_{i=1}^{p} \mu_i Q_{ij} - Q_m \right) X(t) \quad when \quad X(t) \neq 0 \\ g_j(\mathrm{q(x(t))}) = \dfrac{1}{\mathrm{c}} \quad when \quad X(t) = 0 \qquad for\ j = 1,2,...,c \end{cases} \tag{2.155}$$

and there is a common solution of P for the following LMIs,

$$\begin{cases} Q_m > 0 \\ \sum_{j=1}^{c} Q_{ij} - c\,Q_m > 0 \qquad for\ all\ i = 1,2,...,p \end{cases} \tag{2.156}$$

where $Q_m = -(H_m^T P + P H_m)$, $\Delta Q_{ij} = -(\Delta H_{ij}^{\ T} P + P \Delta H_{ij})$ (2.157)

$$Q_{ij} = -(H_{ij}^{\ T} P + P H_{ij}) , \tag{2.158}$$

ii) there exists nonzero positive scalar

$$\varepsilon = \lambda_{\min}(Q_m) - \max_{ij} \left\| \Delta Q_{ij} \right\|_{\max} \tag{2.159}$$

where $\max_{ij} \left\| \Delta Q_{ij} \right\|_{\max} \geq \left\| \Delta Q_{ij} \right\|_{\max} \geq \left\| \Delta Q_{ij} \right\|$

Lemma governs the way of designing the gains of the nonlinear controller of (2.133). The number of linear matrix inequalities is reduced to $p+1$, instead of $p(p+1)/2$ as stated in [53]. Depend on the derivation on section 2.2.31, and from (2.36) and (2.37), we can investigate the following theorem,

Theorem 2.3: The fuzzy control system as given by (2.137) is stable if the controller and the observer gains are set to $G_j=Y_jZ_{11}^{-1}$ and $N_i=P_{22}^{-1}O_i$ with the matrices Z_{11}, P_{22}, Y_j and O_i , satisfying the following LMIs.

$$Z_{11}A_i^T + A_i Z_{11} - (B_i Y_j)^T - (B_i Y_j) < 0 \tag{2.160}$$

$$A_i^T P_{22} + P_{22} A_i - (O_i C_j)^T - (O_i C_j) < 0 \tag{2.161}$$

where P=diag(P_{11},P_{22}) and Z_{11}= P_{11}^{-1}

2.4.3. Application Example C

To show the effectiveness of the proposed controller design techniques, PV model System [75]-[78] with parametric uncertainties are simulated.

2.4.3.1. PV Electric Characteristics

The current-voltage characteristic of a PV array conducts as a function of solar irradiance and cell temperature is described as follows [76]:

$$i_{pv} = n_p I_{ph} - n_p I_{rs} (\exp(q_p v_{pv} / n_s \varphi_p K_b T_c) - 1) \tag{2.162}$$

where n_p and n_s are the number of the parallel and series cells, respectively, K_b is the Boltzmanns' constant(K_b=1.3805x10^{-23}), T_c is the cell temperature, φ_p is the ideal *p-n* junction factor (φ_p=1-5), q_p is the electron charge(q_p =1.6x10^{-19}), i_{pv} and v_{pv} are the output current and the PV array voltage on the capacitance C_{pv}, I_{ph} and I_{rs} are the photocurrent and reverse saturation current, respectively and are given by

$$I_{ph} = (I_{sc} + K_I (T_c - T_r)) \frac{\lambda_I}{100} \tag{2.163}$$

$$I_{rs} = I_{or} (\frac{T_c}{T_r})^3 \exp(q_p E_{gp} (1/T_r - 1/T_c) / K_b T_c) \tag{2.164}$$

where I_{sc} and I_{or} is the short-circuit cell current at reference temperature and insolation and the reverse saturation current at the reference temperature T_r, E_{gp} is the semiconductor band-gap energy (E_{gp}=1.1eV), K_I is the short-circuit current temperature coefficient; and λ_I is the insolation in *mW/*cm2. The power generation of the PV array:

$$P_{pv} = i_{pv} v_{pv} = n_p I_{ph} v_{pv} - n_p I_{rs} v_{pv} (\exp(q_p v_{pv} / n_s \varphi_p K_b T_c) - 1) \tag{2.165}$$

The relationship of P_{pv} versus v_{pv}, for different values of the insolation and temperature is shown in Fig. 2.18 [77]. Obviously, the maximum power changes along various insolation and cell temperature. Moreover, there exists a

specific PV array voltage and that the PV array generated power is maximized under a certain insolation and temperature. According to the electric power equation (2.165), the power slope dP_{pv}/dv_{pv} can be expressed as follows:

$$\frac{dP_{pv}}{dv_{pv}} = i_{pv} + v_{pv}\frac{di_{pv}}{dv_{pv}} \tag{2.166}$$

$$= i_{pv} - n_p I_{rs} v_{pv}(q_p / n_s \varphi_p K_b T_c)(\exp(q_p v_{pv} / n_s \varphi_p K_b T_c) \tag{2.167}$$

When the power slope $dP_{pv}/dv_{pv}=0$, the system operates at the maximum power generation.

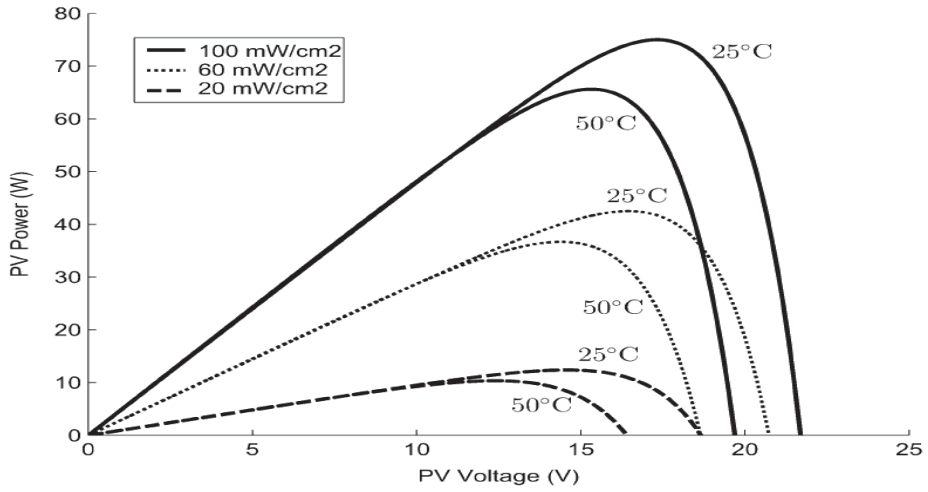

Fig. 2.18. Characteristics of the PV power with respect to the PV voltage

2.4.3.2. PV Modelling

A schematic overview of the PV energy system is shown in Fig. 2.19. This system consists of a PV array and a buck converter [76]. The dynamic equation can be expressed by the following differential equations [75]-[80]:

$$\dot{x}(t) = A(x)x(t) + B_1(x)u(t) + B_2 W_I$$

$$y(t) = Cx(t) \tag{2.168}$$

where $x(t)=\begin{bmatrix} v_{pv} \\ i_L \\ v_o \end{bmatrix}$, $A(x)=\begin{bmatrix} \frac{i_{pv}}{C_{pv}v_{pv}} & 0 & 0 \\ 0 & -\frac{1}{L}(R_L+R_oI_b) & -\frac{1}{L} \\ 0 & -\frac{1}{C_o}I_b & 0 \end{bmatrix}$,

$B_1(x)=\begin{bmatrix} \frac{-i_L}{C_{pv}} \\ \frac{1}{L}(V_D+v_{pv}-R_Mi_L) \\ 0 \end{bmatrix}$, $B_2=\begin{bmatrix} 0 \\ 1 \\ 0 \end{bmatrix}$, $C^T=\begin{bmatrix} 1 & 0 \\ 0 & 1 \\ 0 & 0 \end{bmatrix}$, $W_I=(\frac{-V_D}{L})$,

where, $x(t)\epsilon\kappa^{3x1}$ and $u(t)\epsilon\kappa^{1x1}$ are the state vectors and the control input, respectively, v_o and i_L are the capacitance voltage C_o and the inductance current L, respectively, u is the duty ratio of the Pulse-Width-Modulated (PWM) signal to control the switching MOSFET, $u \in \{0,1\}$ defines the switch position, R_M, R_o and R_L are the internal resistances on the power MOSFET, the capacitance C_o and the inductance L, respectively, V_D is the forward voltage of the power diode, $I_b=1-i_o/i_L$, i_o is a measurable load current and $y(t)$ is the measurable output composed of v_{pv} and i_L, v_o is immeasurable due to the presence of the R_o. The parameters of the system are shown in Table 2. 3 [75]-[78], where all system parameters are assumed with a 5% deviation.

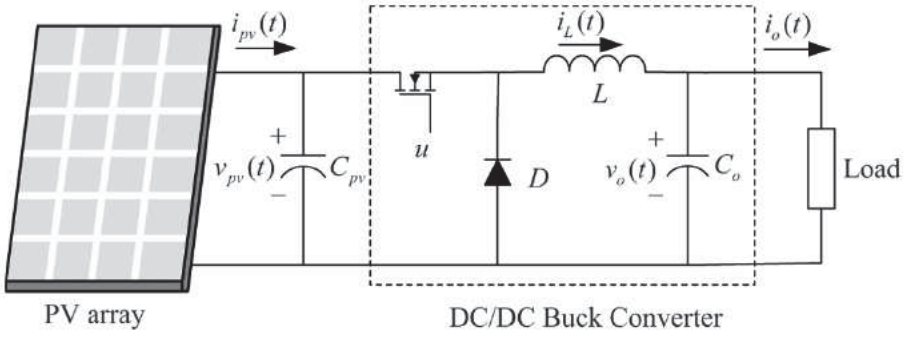

Fig. 2.19. PV power control system using a dc/dc buck converter

2.4.3.3. TS Fuzzy Model of PV

To design the fuzzy control, we must have a fuzzy model that represents the dynamics of PV. Therefore, we first represent the system with a TS fuzzy model. The system (2.168) is described by a TS fuzzy representation with the $q_1(t)= i_{pv}/v_{pv}$, $q_2(t)=I_b$, $q_3(t)=i_L$, and $q_4(t)=v_{pv}$, as the premise variables. Next, calculate the minimum and maximum values of $q_j(t)$, $q_{jmin} \leq q_j(t) \leq q_{jmax}$ (j=1,2,3,4), where q_{jmax} and q_{jmin} are the upper and the lower bounds of the variable $q_j(t)$. From the maximum and minimum values $q_j(t)$, can obtain the sector nonlinearity as follow,

$$q_j(t)=q_{jmax}\ M_{ji}(q_j(t))+q_{jmin}\ \overline{M}_{ji}(q_j(t))$$

where $M_{ji}(q_j(t))+\overline{M}_{ji}(q_j(t))=1$ and $M_{ji}(q_j(t)), \overline{M}_{ji}(q_j(t))$ are a fuzzy term of rule i and are given by;

$$M_{ji}(q_j(t))=\frac{q_{j\max}-q_j(t)}{q_{j\max}-q_{j\min}},\ \overline{M}_{ji}(q_j(t))=1-M_{ji}(q_j(t)) \tag{2.169}$$

The degree of membership function for $q_1(t)$ is depicted in Fig. 2.20. The degree of membership function for state $q_2(t)$, $q_3(t)$ and $q_4(t)$ are implemented in the same manner. Consequently the PV can be represented by a TS-fuzzy plant model having 16 rules. The *ith* rule can be written as follow (i=1,2,…,16),

Rule i: IF $q_1(t)$is M_{1i} and …and $q_j(t)$is $\overline{M}_{ji}$

$$\text{Then}\quad \dot{x}(t)=(A_i+\Delta A_i)\,x(t)+(B_{1i}+\Delta B_{1i})u(t)+B_2W \tag{2.170}$$

The system dynamics is described by

$$\dot{x}(t)=\sum_{i=1}^{16}\mu_i[(A_i+\Delta A_i)\,x(t)+(B_{1i}+\Delta B_{1i})u(t)+B_2W] \tag{2.171}$$

where

$$A_i = \begin{bmatrix} \frac{q_{1i}}{C_{pv}} & 0 & 0 \\ 0 & -\frac{1}{L}(R_L + R_o q_{2i}) & -\frac{1}{L} \\ 0 & -\frac{1}{C_o} q_{2i} & 0 \end{bmatrix}, \quad C^T = \begin{bmatrix} 1 & 0 \\ 0 & 1 \\ 0 & 0 \end{bmatrix}, \quad B_{1i}(x) = \begin{bmatrix} \frac{-q_{3i}}{C_{pv}} \\ \frac{1}{L}(V_D + q_{4i} - R_M q_{3i}) \\ 0 \end{bmatrix},$$

$$\Gamma^T = \begin{bmatrix} 1 & 0 \\ 0 & 1 \\ 0 & 0 \end{bmatrix}$$

ΔA_i and ΔB_{1i} ($i=1,2,...,16$) represents the system parameters bounded uncertainties. The elements of ΔA_i are randomly varied within 35% of their nominal values corresponding to system parameter R_L and R_M.

TABLE 2.3
PV SYSTEM PARAMETERS

Symbol	Quantity	Conversion from Gaussian and CGS EMU to SI
	Rated power	75[W]
	Rated voltage	17 [V]
	Rated current	4.4 [A]
	Short circuit current	4.8 [A]
	Open circuit voltage	21.7 [V]
	Short-circuit current	2.06[mA/^{o}K]
C_{pv}=C_o	The capacitance	1000 [μF]
R_L	Internal resistances on the inductance L	1[Ω]
R_o	internal resistances on the capacitance C_o	160 [mΩ]
R_M	internal resistances on the power MOSFET	0.27 [Ω]
V_D	the forward voltage of the power diode	0.57 [V]
L	The inductance	150 [μH]

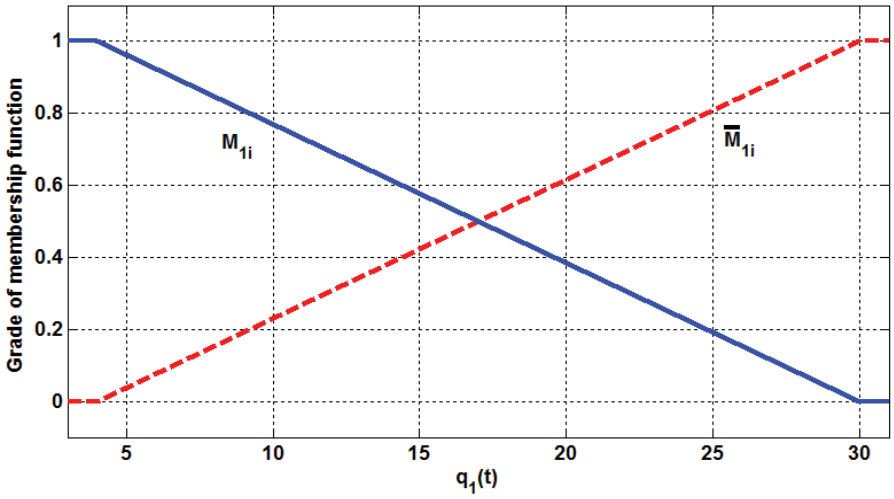

Fig. 2.20. Membership functions of variable $q_1(t)$

2.4.3.4. MPPT Control Method

In this section we will present the MPPT control method. The Incremental Conductance (IC) algorithm is based on the observation that the following equation holds at the MPP [33], [34]. The maximum power point satisfies the condition $dP_{pv}/dv_p=0$. However, due to the high nonlinearity, the maximum power point is difficult to be solved from (2.167). This is the reason why the MPPT cannot be achieved easily. The incremental conductance algorithm is derived by differentiating the PV array power with respect to voltage and setting the result equal to zero. Therefore,

$$\frac{dP_{pv}}{dv_{pv}} = 0 \Rightarrow i_{pv} + v_{pv}\frac{di_{pv}}{dv_{pv}} = 0 \quad \Rightarrow -\frac{i_{pv}}{v_{pv}} = \frac{di_{pv}}{dv_{pv}} \text{ at the MPP} \tag{2.172}$$

Where $-i_{pv}/v_{pv}$ is the opposite of instant conductance of PV cells and di_{pv}/dv_{pv} is the incremental conductance. From (2.172), at the MPPT, there are two quantities equal in magnitude, but opposite in sign. If the operating point is off of the MPPT, a set of inequalities can be derived from (2.172) that indicate whether the operating voltage is above or below the MPPT voltage. These relationships are summarized as the following equations.

$$\text{if } \frac{di_{pv}}{dv_{pv}} > -\frac{i_{pv}}{v_{pv}};\ \left(\frac{dP_{pv}}{dv_{pv}} > 0\right), \text{ Left of MPP, then increase } v_{pv} \tag{2.173}$$

$$\text{if } \frac{di_{pv}}{dv_{pv}} = -\frac{i_{pv}}{v_{pv}};\ \left(\frac{dP_{pv}}{dv_{pv}} = 0\right) \text{ at MPP, then } v_{pv} \text{ must remain constant} \tag{2.174}$$

$$\text{if } \frac{di_{pv}}{dv_{pv}} < -\frac{i_{pv}}{v_{pv}};\left(\frac{dP_{pv}}{dv_{pv}} < 0\right), \text{ Right of MPP, then decrease } v_{pv} \tag{2.175}$$

These changes in PV's voltage may be done by coupling a DC/DC converter to PV and controlling properly its duty cycle. Neglecting losses the output voltage of the buck converter is given by the $v_o=Dv_{pv}$, where D is the fraction of time that the switch is closed, therefore,

$$\frac{v_o}{v_{pv}} = D = fd \tag{2.176}$$

By using *fd*, the reference MPPT is determined from the incremental conductance method [33], [34]. The incremental conductance uses a search technique that changes a reference or a duty cycle so that v_{pv} changes and searches for the condition of (2.166) and at that condition the maximum power point has been found and searching will stop. Fig.2.21 shows a flowchart of the proposed maximum power point tracking.

2.4.3.5. Simulation and Results

In this section two cases of simulation are presented, we assume an ideal case with a fixed atmosphere ***in first case***, where the insolation is 80 mW/cm2. Consider that the output load current is i_o= (1/2)v_o and the cell temperature Tc = 323.18 K. Fig. 2.22 shows the power regulation responses generated by applying the proposed nonlinear controller, and the PV voltage and the control signal are given in Fig. 2.23 and Fig. 2.24, respectively. The estimation errors of the state are given in Figs. 2.25, 2.26 and 2.27, where all errors asymptotically converge to zero.

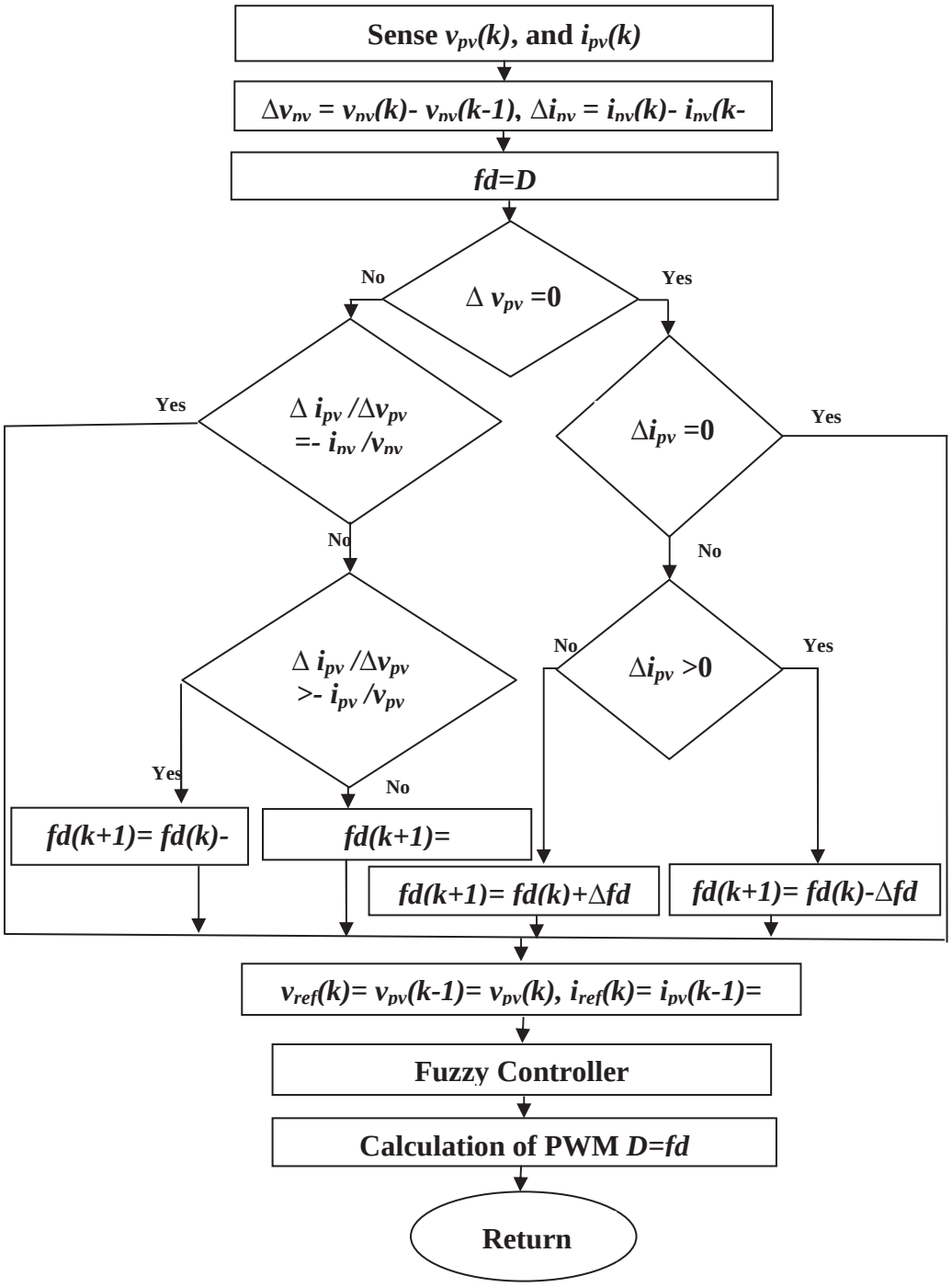

Fig.2.21. Incremental conductance algorithm and fuzzy controller flowchart

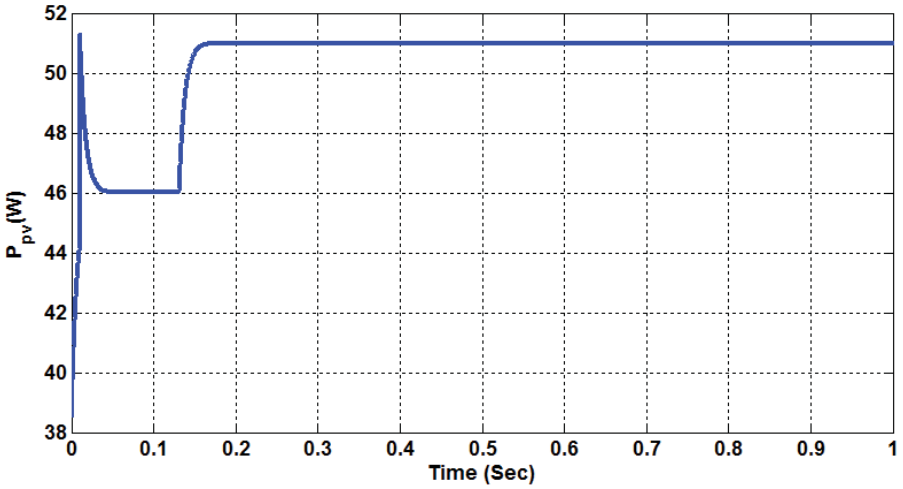

Fig. 2.22. Response of the PV power control

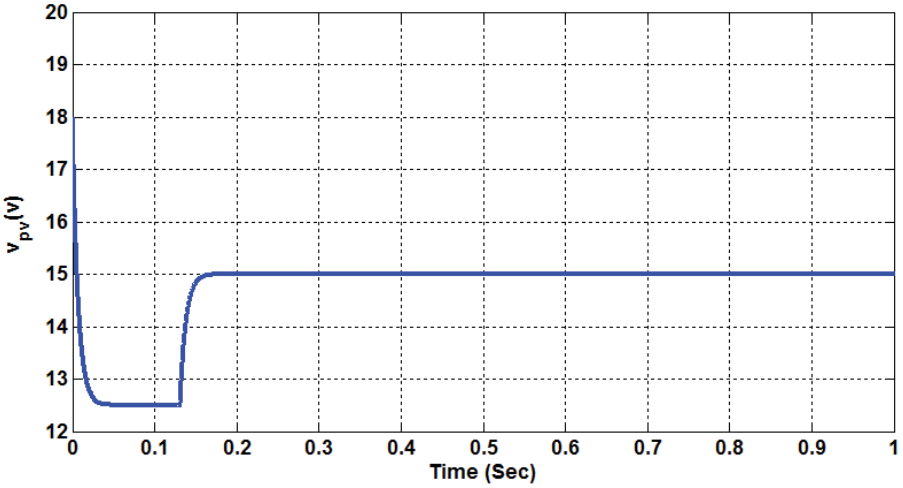

Fig. 2.23. PV voltage

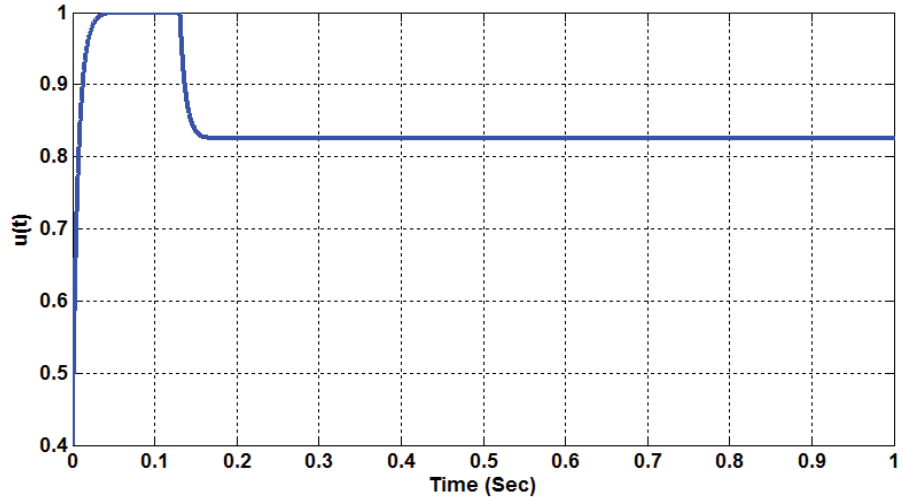

Fig. 2.24. Control signal

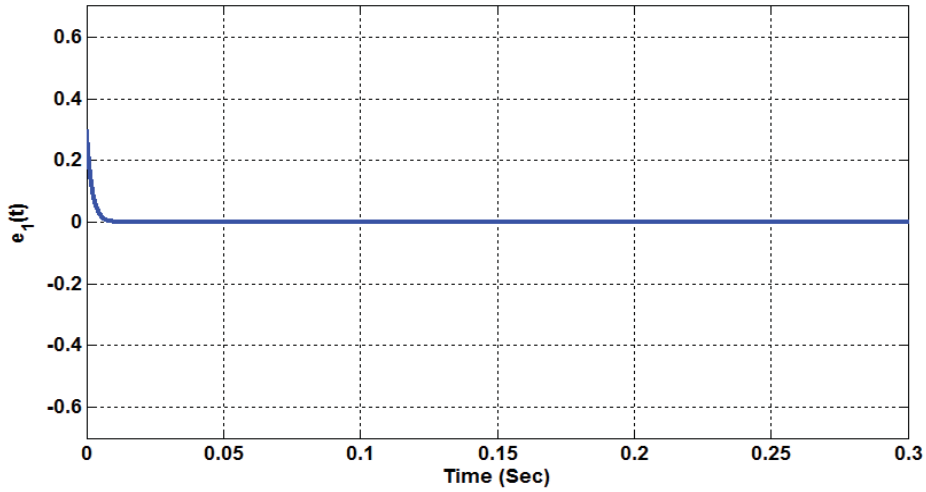

Fig. 2.25. Inductance current estimation error

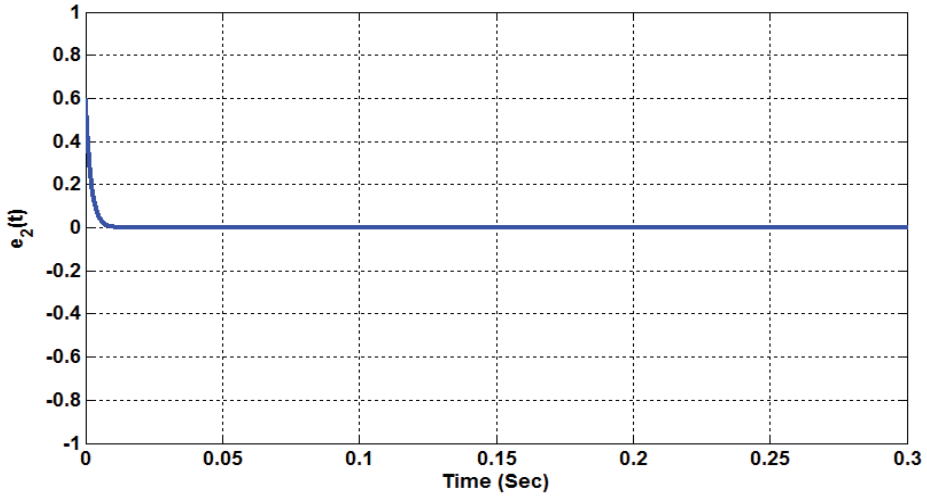

Fig. 2.26. PV array voltage estimation error

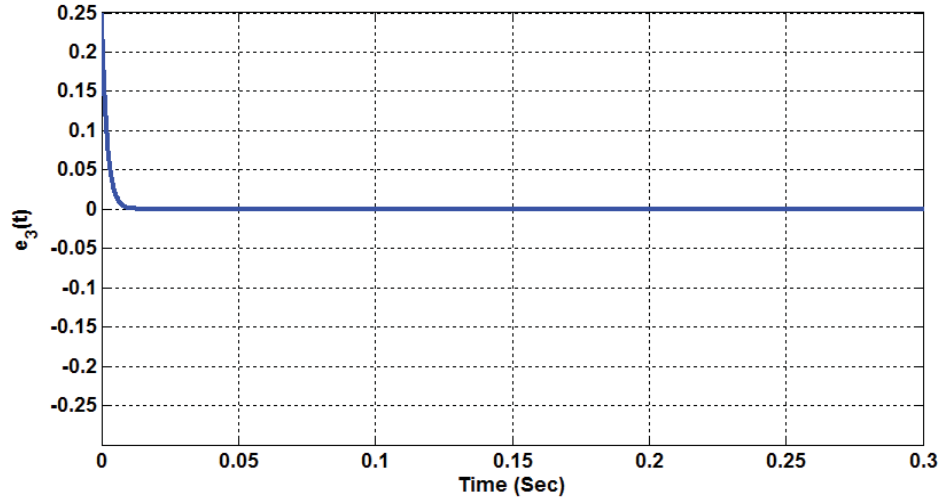

Fig. 2.27. Output capacitance voltage estimation error

In second case, consider varying insolation with constant temperature *Tc*= 323.18 *K* shown in Fig. 2.28. By applying the proposed control method, the power regulation response is shown in Fig. 2.29, where the PV array always provides a maximum power.

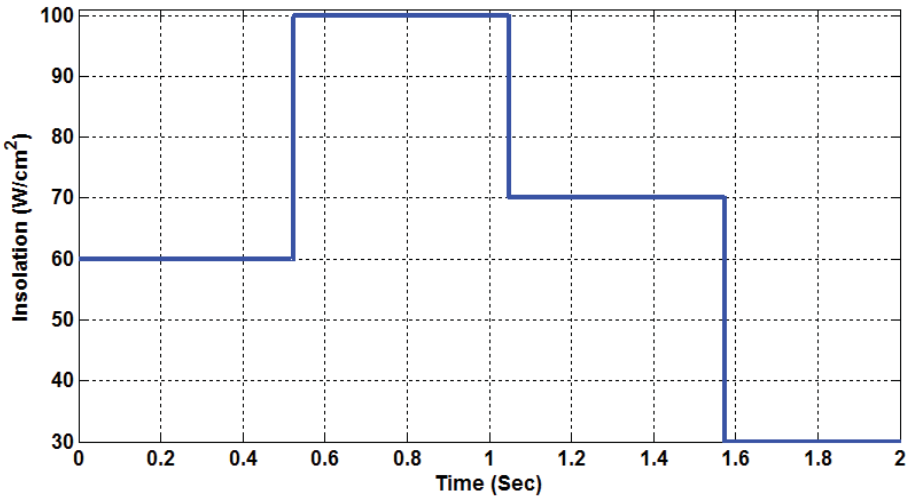

Fig. 2.28. Varying insolation

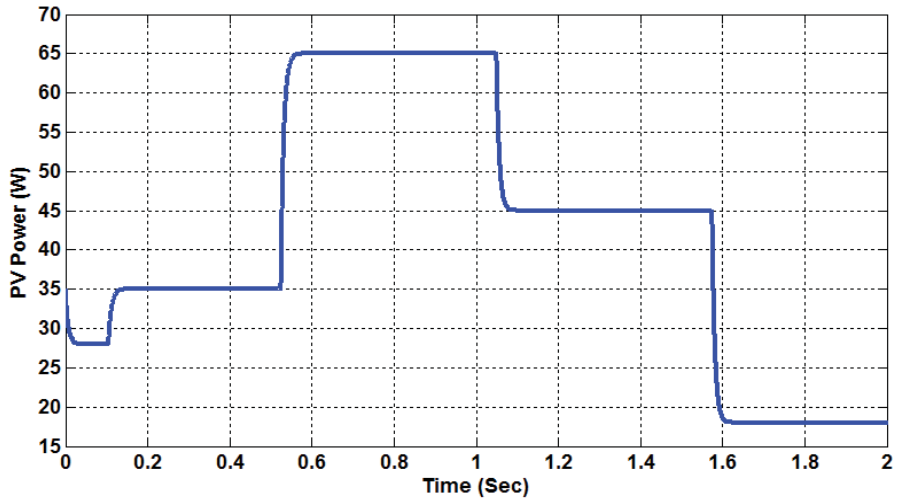

Fig. 2.29. Response of the power regulation

The nonlinear control systems have been presented and an improved stability analysis has been derived. Since by this proposed algorithm we are only needed to solve *p+1* LMIs to obtain the controller gains and the observer gains, where *p* is the number of rules of the TS fuzzy plant model. An application example on stabilizing a nonlinear of solar power generation systems has been given to illustrate the merits of the proposed nonlinear controller. Based on the TS fuzzy representation, the fuzzy controller is developed to maintain the maximum power voltage. The proposed control is achieved with asymptotic convergence. The advantages of the proposed controller include, the design is more systematic than traditional methods. In addition, the overall stability has strict analysis, which is lacked in traditional methods.

2.5. Chapter Conclusion

A new robust fuzzy controller design methodology for the control of continuous-time TS fuzzy models with parametric uncertainties are developed and analyzed in this chapter. TS fuzzy systems are classified into three families based on the input matrices and a robust controller synthesis procedure is given for each family. The robust fuzzy controllers are designed based the design approach discussed in [44], [47]. The sufficient conditions were derived and are formulated in the format of LMIs. The simulation results proved the effectiveness, robustness and better tracking performance of the proposed controller in controlling nonlinear systems with parametric uncertainties. Furthermore, based on the analysis results of this chapter, we investigate three proposed controllers, namely a FFTC, FSFTC and DFFTC to tackle nonlinear plants subject to large parameter uncertainties, sensor faults in chapter 3 and RFFTC, RFSFTC and RDFFTC to tackle nonlinear plants subject to actuator faults and/or unknown inputs, large parameter uncertainties and sensor faults in chapter 4.

CHAPTER 3

CHAPTER 3

ROBUST FUZZY FAULT-TOLERANT CONTROL OF WES SUBJECT TO SENSOR FAULTS

3.1. Introduction

Stability is one of the most important problems in the analysis and synthesis of control systems. Recently, the issue of stability of fuzzy control systems in nonlinear stability frameworks has been considered [51], [91]. Reference [51] presented a design method for the stabilization of a class of nonlinear systems as described by a TS fuzzy model. In order to design a fuzzy controller, they used the concept of the PDC and LMIs. Reference [82] also presented stability conditions satisfying decay rates for the TS fuzzy model.

Since faults are frequently a source of instability and are encountered in various engineering systems, robust fuzzy controller design for faulty nonlinear systems has received considerable interest [46], [47], [93]. References [47], [93] derived robust stability conditions for a fuzzy system with sensor faults. Active fault-tolerant control for nonlinear systems with sensor faults and a method for designing robust controllers to stabilize sensor faults in nonlinear systems were also presented [46].

A WES performance heavily depends on the sensors. A sudden failure in one of the current sensors decreases the performance of the system. In addition, if a fault is not detected and treated quickly, its effect leads to system disconnection. Hence, to reduce the rate of failures and to prevent unplanned

shutdowns, a real time fault detection, isolation, and compensation scheme could be adopted. During the last decade, various methods of Fault Detection and Isolation (FDI) and FTC have been well developed [41], [94]-[99]. References [41], [94] present a composite approach based on the Kalman filter to improve blade moment sensor fault detection and isolation for three-bladed horizontal axis wind turbines. The approach includes detection techniques for both additive and multiplicative faults, but the simulation is done with a linearized wind turbine model, a constant threshold, and the assumption that only one set of the sensors can have faults at a time. In addition, these approaches are limited to only one operating point and then do not take into account the nonlinearities of the system. The adaptive fault diagnosis observer approach is presented in [95] and [96]. One of the advantages of the adaptive fault diagnosis observer is that the estimation of the state vector and actuator fault vector can be achieved simultaneously. However, as shown in [96], the main problem encountered in the conventional adaptive fault estimation algorithm is that the performance requirements cannot be satisfied since it is only suitable for the constant fault case. However in practical situations, faults are time varying and sometimes may be fast time varying. Fault diagnosis filter design was investigated in detail in [97], [98], but the issue of fault estimation was not included. Therefore obtaining effective solutions to overcome the above difficulties is necessary and is the primary motivation for the study of this paper.

In addition, limited publications are concerned with energy storage systems combined with wind power generation [99], [100], along side an analysis of the dynamic stability of wind-battery hybrid systems in remote areas [101], [102]. These works do not provide sufficiently detailed dynamic models of the battery storage system suitable for stability analysis, nor for designing an effective controller. An energy storage system with a diesel powered-synchronous generator unit has been studied in [2], wherein the authors have not sufficiently

addressed the optimal membership functions for the fuzzy controller. In this paper, a nonlinear mathematical model of a wind-battery hybrid system is developed to design a more effective controller for power quality improvement and the reduction of bus voltages and frequency ripple relative to [14], [103].

In this chapter, three different methods of solving the fault tolerant control for the WES subject to the parameter uncertainties, and sensor faults are proposed. In first method and second method we use the FFTC and FSFTC we will be explain the two methods in section 3.2 and section 3.3, respectively, in the two methods the fault detection scheme is based on a bank of observer and is assumed that at any time one sensor only fails at the most. If the two sensors fail simultaneously, the controller cannot use the healthy one and the system becomes unstable. After that, the state variables are reconstructed from the output of the healthy sensor. But in the third method a modified DFFTC approach is designed such that to handle multi-sensor failure at any time but the in the FFTC and FSFTC assumed only one faulty sensor at any time. The proposed DFFTC strategy is based on the known of the fault estimate and the error between the faulty system state and a reference system state. A FPIO design is proposed to estimate the state and sensor's fault.

This chapter is organized as follows. Section 3.2 studies the first method to investigate the FFTC of WES subject to sensor faults, wind disturbance and parameter uncertainties. The second method which studies the FSFTC for the WES subject to parameter uncertainties, sensor faults and wind disturbance is given in section 3.3. Section 3.4 addressed the third method to design DFFTC of HWDSS subject to sensor faults and parameter uncertainties. A conclusion will be given in section 2.5.

3.2. FFTC for the WES Subject to Sensor Faults and Parameter Uncertainties

This section presents a new method for FFTC of nonlinear systems described by TS fuzzy systems subject to sensor faults, parameter uncertainties, and wind disturbance. The algorithm based on reconfiguration mechanism is then investigated for detection, isolation and accommodation of faults. The idea is to use a FDOS, and design a new control law to minimize the state deviation between healthy observers. This scheme requires the knowledge of the system states and the occurring faults. These signals are estimated from a FDOS Observers. TS fuzzy systems are classified into three families based on the input matrices and a design FFTC for each family. In each family, the fault tolerant control law is designed by using the Lyapunov method to obtain conditions which are given in LMIs formulation. The effectiveness of the proposed controller design methodology is finally demonstrated through a WES with DFIG to illustrate the effectiveness of the proposed method.

The section is organized as follows: the proposed scheme, TS fuzzy model and the structure of the fuzzy observers are presented in section 3.2.1. Section 3.2.2 shows the proposed nonlinear FFTC controller. Stability and robustness analysis are given section 3.2.3. In Section 3.2.4, the application example on the model of the WES with DFIG and its TS fuzzy description are presented. Section 3.2.5 presents simulation of the wind turbine with DFIG.

3.2.1. TS Fuzzy Model With Parameter Uncertainties and FDOS

In this section we present TS fuzzy models and fuzzy observers.

3.2.1.1. TS Fuzzy Plant Model With Parameter Uncertainties, and Sensor Faults

A nonlinear control system can be represented as a TS fuzzy plant model based system. It consists of a TS fuzzy plant model [91] and a fuzzy controller [53] connected in a closed-loop. In general the TS fuzzy system (2.3) [104], [105] subject to parameter uncertainties and sensor faults is rewritten as

Plant Rule *i:* IF $q_1(x(t))$ is M_{1i} AND … AND $q_{\varepsilon}(x(t))$ is $M_{\varepsilon i}$

$$\text{Then } \begin{cases} \dot{x}(t) = (A_i + \Delta A_i)x(t) + (B_i + \Delta B_i)u(t) + Wd(t) & i = 1,2,..., p \\ y(t) = C_i\, x(t) + \bar{F}_{si}\, f_s(t) & i = 1,2,..., p \end{cases} \tag{3.1}$$

where $f_s(t) \in \kappa^{sx1}$ represents the sensor faults which is assumed to be bounded, and $\bar{F}_{si} \in \kappa^{gxs}$ are the known sensor fault matrix, $\Delta A_i \in \kappa^{nxn}$ and $\Delta B_i \in \kappa^{nxm}$ are the uncertainties of the constant system matrices $A_i \in \kappa^{nxn}$ and $B_i \in \kappa^{nxm}$, respectively, which are non time-varying parametric uncertainties in the plant model, *W* is the disturbance matrix which is assumed to be known and *d(t)* is the measurement disturbance and *Wd(t)* is the disturbance par. The inferred system is given by

$$\dot{x}(t) = \sum_{i=1}^{p} \mu_i(q(x(t)))[(A_i + \Delta A_i)x(t) + (B_i + \Delta B_i)u(t) + Wd(t)]$$

$$y(t) = \sum_{i=1}^{p} \mu_i(q(x(t)))[C_i\, x(t) + \bar{F}_{si}\, f_s(t)] \tag{3.2}$$

For the first family, without loss the generality in order to investigate the proposed FFTC law we formulate the (3.2) based on (2.3) and (3.1) as the following,

$$\dot{x}(t) = \sum_{i=1}^{p} \mu_i(q(x(t)))[(A_i + \Delta A_i)x(t) + \alpha_i(B + \Delta B)u(t) + Wd(t)]$$

$$y(t) = \sum_{i=1}^{p} \mu_i(q(x(t)))[(I + F_s)\, C_i x(t)] \tag{3.3}$$

where F_s are faults which are modelled as proportional signals to sensor outputs, let

$$F_s=diag(\eta_1, \eta_2 ,\ldots, \eta_g),\ -0.1 \le \eta_a \le 0.1,\ a=1,2,\ldots,g; \quad (3.4)$$

which is the sensor fault vectors which is assumed to be bounded and $(I+F_s)$ is sensor gain. It is assumed that at any given time only one sensor fails at most, I is the identity matrix, the premise variables $q_1(x(t)),\ldots, q_\varepsilon(x(t))$ are also assumed measurable variables and do not depend on the faults.

As we explained before in chapter 2 we can deduce the plant dynamics for the second and the third family

3.2.1.2. TS Fuzzy Observer and the FFTC Scheme Design

In this sub-section we presented the proposed FFTC Scheme Design and Fuzzy Dedicated Observer.

3.2.1.2.1. TS Fuzzy of FDOS

As given in subsection 2.4.1.1, it is necessary to design a FDOS in order to implement the FFTC. To investigate the FFTC problem in the event of sensor faults and parameter uncertainties, the fault model must be established first. Letting sensor fault model as (3.4), if the state of the system (3.3) is unavailable, then we established fuzzy state observer for TS fuzzy model with parameter uncertainties and sensors faults as follows,

For the first family, the concept of PDC is also employed to design the following FDOS structures [48]:

Rule i: IF $q_1(x(t))$ is M_{1i} AND … AND $q_\varepsilon(x(t))$ is $M_{\varepsilon i}$

Then $\dot{\hat{x}}(t) = A_i\hat{x}(t) + \alpha_i Bu(t) + N_i(y(t)-\hat{y}(t))$

$$\hat{y}(t) = C_i\hat{x}(t) \qquad i= 1, 2,\ldots,p \quad (3.5)$$

where $\hat{x}(t)$ is the estimated state vector by the FDOS, $\hat{y}(t)$ is the final output of the FDOS, and $N_i C\kappa^{nxg}$ are the FDOS gains. The inferred FDOS states are governed by:

$$\dot{\hat{x}}(t) = \sum_{i=1}^{p} \mu_i [A_i \hat{x}(t) + \alpha_i Bu(t) + N_i (y(t) - \hat{y}(t))]$$

$$\hat{y}(t) = \sum_{i=1}^{p} \mu_i C_i \hat{x}(t) \tag{3.6}$$

In the same manner, we can induce the inferred output of the FDOS for the other two cases

3.2.1.2.2. TS Fuzzy Observer Structure –Based on FDI Design

It is important to be able to carry out fault detection and isolation before faults have a drastic effect on the system performance. Even in case of system changes, faults should be detected and isolated [104]. Observer based estimator schemes are used to generate residual signals corresponding to the difference between measured and estimated variables [106]. We also assume that at any time one sensor only fails at the most. The residual signals are processed using either deterministic (e.g. using fixed or variable thresholds) [107] or stochastic techniques (based upon decision theory) [108]. In this thesis we used the deterministic method. The method that we propose is illustrated in Fig.3.1, where it can be seen that the FDI functional block uses g FDOS observers each one is driven by a single sensor output. The failure is detected first, and then the faulty sensor is identified. After that, the state variables are reconstructed from the output of the healthy sensor. The WES control system enters the degraded mode that guaranteed stability and an acceptable level of performance. Figure 3.1 shows the block diagram of the proposed closed system, $y(t) = [\Omega_r, \Omega_g, P_s, Q_s]$ is the output vector of the system where Ω_r is the turbine rotational speed, Ω_g is the mechanical generator speed, P_s is the stator active power and Q_s is the stator reactive power. Four observers based controllers are designed, one based on the observer that uses the measurement of Ω_r and the other one based on the observer that uses the measurement of Ω_g , the third uses the measurement of P_s and the last one uses the measurement of Q_s. The FDI scheme developed in this study follows a classical strategy such as the well-established observer based FDI methods [109]-[111]. The residual

signals are used for the estimation of the model uncertainties and then, for the construction of model uncertainty indicators. The decision block is based on the analysis of these residual signals. Indeed faults are detected and then switching operates according to the following scheme:

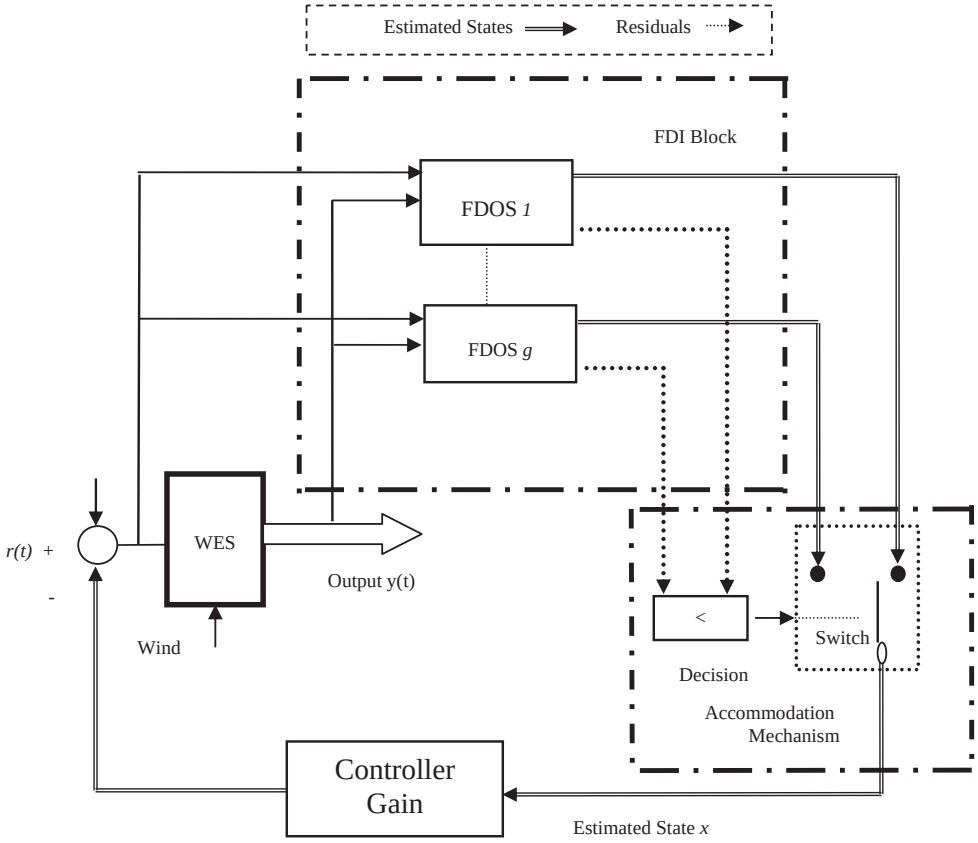

Fig. 3.1. Block diagram of the proposed scheme

3.2.1.2.2.1. Decision Block

It compares the residual values of R_{obs1},..., and R_{obsg} with the threshold value (*th*), where R_{obs1} ,…, and R_{obsg} are the residual signals for observer *1*,..., and observer *g*, respectively.

Residual: $R_{res}(t) = y(t)-\hat{y}(t)$

$$\left\|R_{res}(t)\right\| \begin{cases} \leq th & \text{if there is no sensor fault} \\ > th & \text{if there is sensor fault} \end{cases} \quad (3.7)$$

where R_{res} is the residual between the actual output ($y(t)$) and the estimated output ($\hat{y}(t)$) and th is threshold values.

3.2.1.2.2.2. Switching Block

If ($abs(R_{obs1}) > abs(R_{obs2})$), then switch to observer 2, else switch to observer1. Since sensor noise also contributes to nonzero residuals under the normal operation th must be large enough to avoid false alarm.

3.2.2. Proposed FFTC Controller Based on FDOS

In this section, a unique FFTC synthesis procedure is developed for each member of the TS family. It is more reliable and has larger range of freedom for finding the FFTC to deal with a wide range of uncertainties, sensor faults, and wind disturbance while maintaining the stability of the closed loop system.

3.2.2.1. Proposed Nonlinear FFTC

For the fuzzy model (3.3), we construct the following FFTC via the PDC. It is assumed that the fuzzy system (3.3) is locally controllable. Based on the designed controller **for the first family** in chapter 2 (2.11) and from the estimated state by the healthy observer from FDOS (3.6), then, the final output of the modified FFTC becomes

$$u(t) = \frac{\sum_{j=1}^{c} \mu_j [-G_j \hat{x}(t) + r(t)]}{\sum_{j=1}^{c} \alpha_j \mu_j} \tag{3.8}$$

Let c the number of fuzzy rules. By the same method, we can designed the FFTC by the following

For the second family, the overall output of the FFTC is given by,

$$\dot{u}(t) = z_k\, u(t) + \sum_{j=1}^{c} \mu_j [-G_j \hat{x}(t) + r(t)] \tag{3.9}$$

For the last family, the FFTC is given by,

$$u(t) = \sum_{j=1}^{c} \mu_j [-G_j \hat{x}(t) + r(t)] \tag{3.10}$$

3.2.2.2. The Augmented Fuzzy Control System

In order to carry out the analysis, the closed-loop fuzzy system should be obtained first by establishing the conditions for the asymptotic convergence of the observers (3.6).

For the first family, the fuzzy control system of the state and the errors can be obtained.

Let $$e(t) = x(t) - \hat{x}(t) \tag{3.11}$$

$$\dot{x}(t) = \sum_{i=1}^{p} \mu_i A_i x(t) + \left\{ \sum_{i=1}^{p} \alpha_i \mu_i \right\} (B + \Delta B) u(t) + \sum_{i=1}^{p} \mu_i \Delta A_i x(t) + W d(t) \tag{3.12}$$

With the modified TS fuzzy fault tolerant controller (3.8) employed, the TS fuzzy system (3.11) has the following closed-loop:

$$\dot{x}(t) = \sum_{i=1}^{p} \mu_i A_i x(t) + \sum_{i=1}^{p} \mu_i \Delta A_i x(t) + W d(t) + \left\{ \sum_{i=1}^{p} \alpha_i \mu_i \right\} (B + \Delta B) \left\{ \sum_{j=1}^{p} \mu_j [-G_j \hat{x}(t) + r(t)] \right\} / \left\{ \sum_{j=1}^{p} \alpha_j \mu_j \right\} \tag{3.13}$$

Let the output estimation errors be calculated as follows

$$R_{res}(t) = y(t) - \hat{y}(t) = \begin{cases} \sum_{i=1}^{p} \mu_i C_i e(t) & \text{if there is no sensor fault} \\ \sum_{i=1}^{p} \mu_i C_i e(t) + F C_i x(t) & \text{if there is sensor fault} \end{cases}$$

From (3.11) and (3.13), a TS fuzzy closed-loop can be observed:

$$\dot{x}(t) = \sum_{i=1}^{p} \sum_{j=1}^{c} \mu_i \mu_j [(A_i - B G_j) x(t) + (B + \Delta B) G_j e(t) + (B + \Delta B) r(t)] + \sum_{i=1}^{p} \mu_i [\Delta A_i - \Delta B G_j] x(t) + W d(t) \tag{3.14}$$

By taking the derivative of (3.11) and substituting from (3.3), (3.6) and (3.8), the following is obtained:

$$\dot{e}(t) = \sum_{i=1}^{p}\sum_{j=1}^{c}\mu_i\mu_j[(\Delta A_i - \Delta BG_j - N_i \mathrm{FC}_j)x(t) + (A_i - N_i C_j + \Delta BG_j)e(t) + \Delta B_i r(t)] + Wd(t) \quad (3.15)$$

The equations (3.14) and (3.15) can be written:

$$\dot{X}(t) = \sum_{i=1}^{p}\sum_{j=1}^{c}\mu_i\mu_j[(H_{ij} + \Delta H_{ij})X(t) + (S + \Delta S)r(t) + \Psi d(t)] \quad (3.16)$$

with $X(t) = \begin{bmatrix} x(t) \\ e(t) \end{bmatrix}$, $\Psi = \begin{bmatrix} W \\ 0 \end{bmatrix}$, $S = \begin{bmatrix} B \\ 0 \end{bmatrix}$, $\Delta S = \begin{bmatrix} \Delta B \\ \Delta B \end{bmatrix}$, $\Delta H_{ij} = \begin{bmatrix} \Delta A_i - \Delta BG_j & \Delta BG_j \\ \Delta A_i - N_i FC_j & \Delta BG_j \end{bmatrix}$,

$H_{ij} = \begin{bmatrix} (A_i - BG_j) & BG_j \\ 0 & (A_i - N_i C_j) \end{bmatrix}$

In the same manner, the augmented fuzzy system for the second and third family can be deduced.

3.2.3. Stability and Robustness Analysis and Calculation of Observer and the Proposed Controller Gains

Once the fuzzy fault tolerant system is formulated, its stability and robustness can be investigated. The analysis procedures are the same as those in chapter 2, section 2.2.3, and so the analysis results will be presented without proof. The main result for the global asymptotic stability of a TS fuzzy model with parameter uncertainties, sensor faults, and wind disturbance are summarized by the following theorem 3.1. The sufficient and necessary stability condition of the fuzzy control system (3.16) is guaranteed by lemma 2.1 and theorems 3.1 are satisfied.

Theorem 3.1: The fuzzy control system as given by (3.16) is stable if the controller and the observer gains are set to $G_j = Y_j M_{m11}^{-1}$ and $N_i = P_2^{-1} O_i$ with the matrices M_{11}, Y_j and O_i satisfying the following LMIs.

$$M_{m11}A_i^T + A_i M_{m11} - (B_i Y_j)^T - (B_i Y_j) < 0 \quad (3.17)$$

$$A_i^T P_2 + P_2 A_i - (O_i C_j)^T - (O_i C_j) < 0 \quad (3.18)$$

where $M_{m11} = P_1^{-1}$

3.2.3.1. Observer and the Proposed Controller Gains Calculation

In this sub-section, we calculate the observer and controller gains and we investigate the procedure of the FFTC. In order to analyse the convergence of the augmented state *X(t)*, consider the quadratic Lyapunov candidate function *V(t)* as given (2.32): $X(t) \to 0$ if $\dot{V}(t) < 0$. $\dot{V}(t) < 0$ if the inequality satisfy

$$H_{ij}{}^{T} P + P H_{ij} < 0 \qquad \forall i, j \tag{3.19}$$

Assuming that $P = \begin{bmatrix} P_1 & 0 \\ 0 & P_2 \end{bmatrix}$ and $P_1>0$ and $P_2>0$, by multiplying (3.19) from left and right by $M_{m11} = P_1^{-1}$ [1] and applying the change of variables $Y_j = G_j M_{m11}$, and $O_i = P_2 N_i$ the LMIs (3.17) and (3.18) are obtained as given in the theorem 3.1.

3.2.3.2. The Design Procedure of the FFTC

The procedure for finding the FFTC and the fuzzy observer based on the analysis above are summarized as follows:

a) Obtain the mathematical model of the WES to be controlled
b) Obtain the TS fuzzy plant model with parameter uncertainty and sensor fault information of the plant obtained first step
c) Solve (3.17) and (3.18) to obtain M_{m11},Y_i, P_2, and O_i thus ($Y_j = G_j M_{m11}$, and $O_i = P_2 N_i$)
d) Construct the fuzzy observer (3.6) and the FFTC (3.8), (3.9) and (3.10).

3.2.4. Application Example A

The WES model system with DFIG system used in application example A, in chapter 2 will be used as an application example. The nonlinear systems are subject to large parameter uncertainties and sensor faults. The objective here is

to conceive a sensor fault tolerant control for WECS with parameters uncertainties within 35% of the nominal values and disturbance (20% of wind speed). where ΔA_i ($i=1,2,\ldots,8$) represent the non time varying system parameters uncertainties (J_r, J_g, R_s and R_r) but bounded, the elements of $\Delta A_i(i=1,2,\ldots,8)$ randomly achieve the values within 35% of their nominal values corresponding to $A_i(i=1,2,\ldots,8)$; ΔB_i ($i=1,2,\ldots,8$) = 0. Faults are modelled as additive signals to generator speed sensor outputs as shown in Fig. 3.2, a proportional error on the generator speed sensors changes the sensor gain as shown below.

$$\Omega_{g,mes}(k_f) = (I + F_s)\Omega g(k) \quad rad/s \tag{3.20}$$

where $\Omega_{g,mes}(k)$ generator speed measurements [rad/s] and $k_f > k$.

3.2.5. Simulations and Results

The proposed controller for the WES is tested for the same random variation of wind speed as shown in Fig. 2.4 in chapter 2. The control objective of this section is to design a FFTC law for WES model system with DFIG (2.38) to ensure that all signals in the closed-loop system are bounded. Fig.3.2 shows the proportional signals that represent sensor failures which has been added to the output of sensor 6 between t=40sec and t=80sec. The magnitudes of faults are between ≈10% to ≈20% of the nominal values of the variables and the parametric uncertainties J_r, J_g, R_s and R_r are considered within 35% of their nominal values.

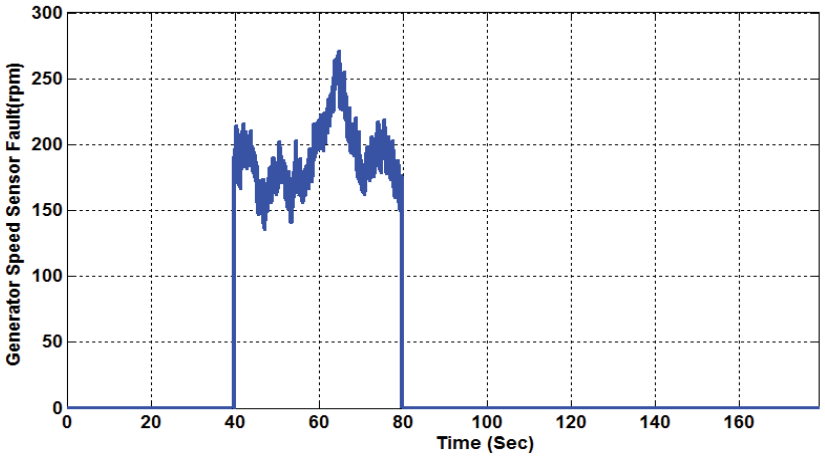

Fig. 3.2. Proportional error on the generator speed sensor

The simulation results are given in Figs. 3.3-3.6 with (left) and without (right) the switching block and all the simulations are realized on the nonlinear model given in (2.38) with the presence of non time varying parametric uncertainties, sensor faults and wind disturbance. In Figs. 3.3-3.6 (left) the control law is based on one observer (observer 2) without using the switching block. We can observe that between t =0 sec to t ≈<40 sec and t >≈ there are no faults, providing good tracking performance. However between t=40sec to t=80sec, we can see that the WES's performance is reduced right after the generator speed sensor and actuators became faulty. Figs. 3.3 and 3.4 (right) shows WES state variables and their estimated signals, when the law control is based on the bank observers (observer 5) with the switch block. We can note that the WES remains stable despite the presence of faults and parameter uncertainties, which shows the effectiveness of the proposed FFTC strategy. The rotational speed of the wind turbine and generator (dashed line), respectively, and their estimates (dotted lines) in the presence of parametric uncertainties, sensor faults and wind disturbance, are shown in Figs. 3.3 and 3.4. In order to obtain optimality, the $r(t)=\Omega_{gref}=\Omega_{opt}=\omega_s-n_b\lambda_{opt}\, v\, /R$ profile are chosen in such a way to follow the optimal tip speed ratio (λ_{opt}) (solid line).

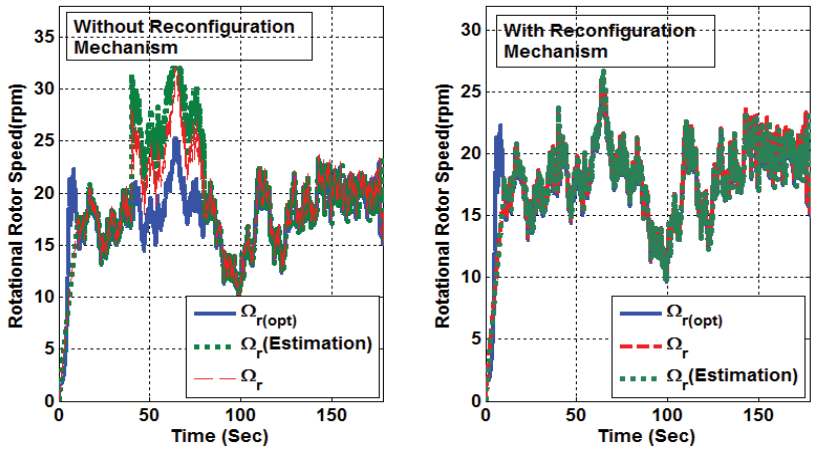

Fig. 3.3. The trajectories of Ω_r and its estimate without (left) and with (right) switching block

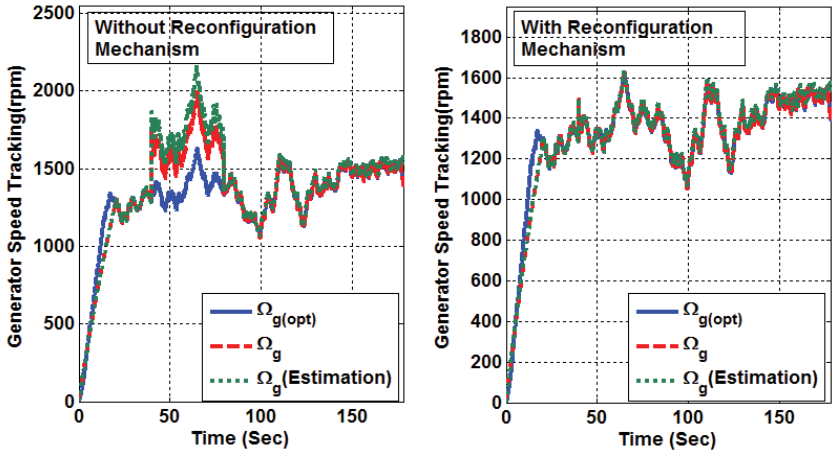

Fig. 3.4. The trajectories of Ω_g and its estimate without (left) and with (right) switching block

The switching from observer 2 to observer 1 is visualized clearly at t ≈ 40sec (Figs. 3.3-3.6 (right)). We notice that switching observers is carried out without loss of control of the system state.

Fig. 3.5 and Fig. 3.6 show the active power P_s (dashed line) and its estimate (dotted line) and the reactive power Q_s (dashed line) and its estimate (dotted

line), respectively. It can be seen that our design can get good tracking performance.

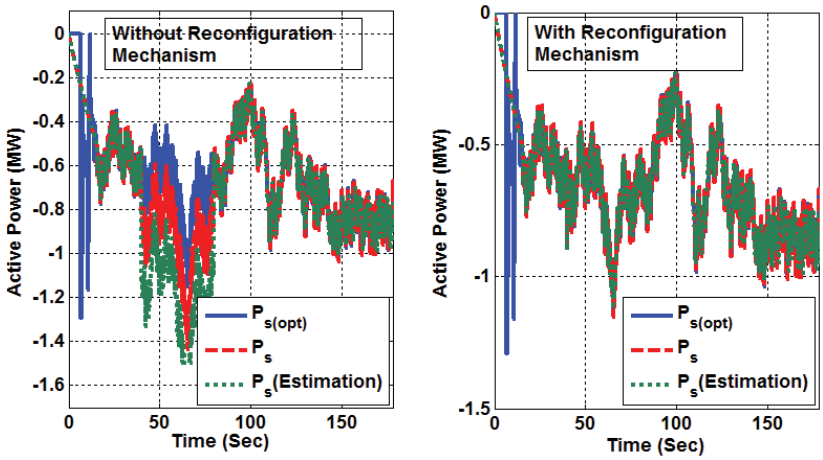

Fig. 3.5. The trajectories of P_s and its estimate without (left) and with (right) switching block

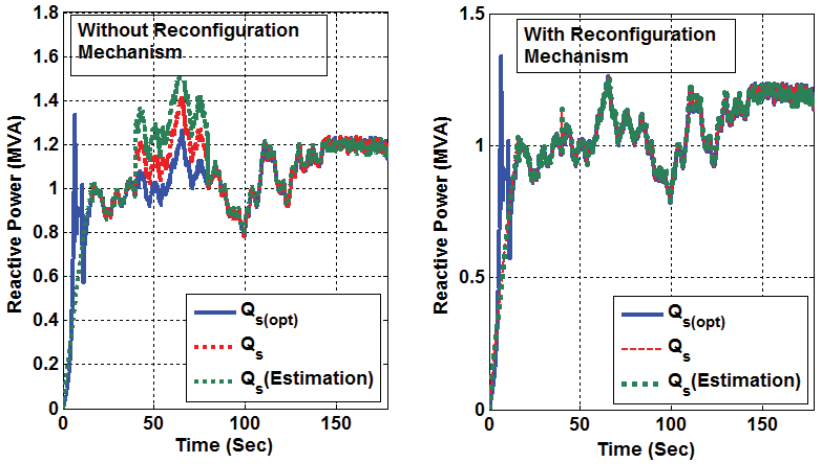

Fig. 3.6. The trajectories of Q_s (dashed line) and its estimate (dotted line) without (left) and with (right) switching block

From the simulation, it can be seen that without the reconfiguration mechanism, the WES lost its performance after the generator speed sensor became faulty. Whereas for the same reference input and by using the switching block strategy proposed, the WES remains stable in the presence of

sensor faults, parameter uncertainties and actuator faults. This demonstrates the effectiveness of the proposed FFTC strategy.

In summary, it has been shown that the proposed scheme is able to detect and isolate sensor faults, through a proper and feasible selection of the healthy observed variables. The simulation results demonstrate the effectiveness of the proposed control approach. The proposed control scheme can guarantee the stability of the closed-loop system and the convergence of the output tracking error. In addition, it maximizes the power coefficient and keeps it at 0.48.

3.3. FSFTC for WES Subject to Sensor Faults and Parameter Uncertainties

In this section, new FSFTC method is proposed for nonlinear systems subject to sensor faults, parameter uncertainties, wind disturbance and state variables unavailable for measurements. The algorithm based on reconfiguration mechanism is then investigated for detection, isolation and accommodation of sensor faults. TS fuzzy model is employed to represent the nonlinear WES, and then a model based fuzzy scheduler controller design uses the concept of PDC. Sufficient stability conditions are expressed in terms of LMEs which can be solved very efficiently using convex optimization techniques. The proposed algorithm maximizes the produced power and is able to maintain the system stable during the sensor faults, wind disturbance and parameter uncertainties. The design procedures are applied to a dynamics model of typical WES with DFIG to illustrate the effectiveness of the proposed control technique

This section is organized as follows. Section 3.3.1 provides the TS fuzzy model with wind disturbance, parameter uncertainties and sensor faults.

Section 3.3.2 shows the stability and robustness conditions for the proposed algorithm followed by the calculation of state FSFTC and FDOS gains. Section 3.3.3 shows Application example on WES model system with DFIG. Simulation and results are shown in section 3.3.4.

3.3.1. TS Fuzzy Model with Wind Disturbance, Parameter Uncertainties and Sensor Faults

In this section, the TS fuzzy plant model subject to parameter uncertainties, sensor faults, and wind disturbance will be expressed as a weighted sum of a number of fuzzy systems. In chapter 2, the inferred output of the fuzzy scheduler system for three families has been introduced. The TS fuzzy systems can be also classified into three families based on the diversity of their input matrices, for the first family based on (2.73) and (3.3) the dynamics of fuzzy scheduler fault system for the first family is given by,

$$\dot{x}(t) = \sum_{i=1}^{p} \sum_{l=1}^{s} \mu_i h_l [(A_i + \Delta\tilde{A}_l) x(t) + \alpha_i (B + \Delta\tilde{B}_l) u(t) + Wd(t)]$$

$$y(t) = \sum_{i=1}^{p} \mu_i (q(t))(I + F_s) C_i \; x(t) \tag{3.21}$$

In the same manner we can induce the inferred output of the fuzzy scheduler for the other two cases.

3.3.2. Stability and Analysis for the Proposed FSFTC Algorithm

In this section, a unique FSFTC synthesis procedure is developed for each member of the TS family deal with a wide range of parameter uncertainties,

sensor faults, and wind disturbance while maintaining the stability of the closed loop system.

3.3.2.1. Proposed FSFTC

The inferred output of the fuzzy scheduler controller has been presented in chapter 2 in section 2.3.2.2 for the first family based on (3.6) and (2.75) the inferred output of the FSFTC for the first family is given by,

$$u(t)=\frac{\sum_{l=1}^{s}\sum_{j=1}^{c} h_l \mu_j [-G_{jl}\,\hat{x}(t)+r(t)]}{\sum_{l=1}^{s}\sum_{j=1}^{c} \alpha_j h_l \mu_j} \tag{3.22}$$

In the same manner we can induce the inferred output of the FSFTC for the other two cases as follows,

For the second family, the FSFTC will be becomes

$$\dot{u}(t)= z_k\, u(t)+\sum_{l=1}^{s}\sum_{j=1}^{c} h_l \mu_j [-G_{jl}\hat{x}(t)+r(t)] \tag{3.23}$$

For the last family, the FSFTC is given by

$$u(t)=\sum_{l=1}^{s}\sum_{j=1}^{c} h_l \mu_j [-G_{jl}\,\hat{x}(t)+r(t)] \tag{3.24}$$

3.3.2.2. Stability Analysis for the Proposed FSFTC Algorithm

In order to carry out the analysis, the closed-loop fuzzy system should be obtained first by establishing the conditions for the asymptotic convergence of the observers. We use the same proposed scheme, illustrated in Fig. 3.1, but we will change the FFTC to FSFTC. The FDI scheme developed in this study follows a classical strategy such as the well-established observer based FDI methods [112].

For the first family, the fuzzy control system of the state and the errors can be obtained.

Let $$e(t)=x(t)-\hat{x}(t) \tag{3.25}$$

From (3.21), (3.6) and with the modified FSFTC (3.22), the fuzzy scheduled system is given by

$$\dot{x}(t) = \sum_{i=1}^{p}\sum_{l=1}^{s} \mu_i h_l (\mathrm{A}_i + \Delta\tilde{A}_l)\mathrm{x}(t) + Wd(t)$$

$$+\left\{\sum_{i=1}^{p}\sum_{l=1}^{s} \alpha_i \mu_i h_l\right\}(B+\Delta\tilde{B}_l)\left\{\sum_{j=1}^{c}\sum_{l=1}^{s} \mu_j h_l[-G_{jl}\,\hat{x}(t)+r(t)]\right\} / \left\{\sum_{j=1}^{c}\sum_{j=1}^{s} \alpha_j \mu_j h_l\right\} \tag{3.26}$$

From (3.25) and (3.26), the TS fuzzy system (3.26) has the following closed-loop:

$$\dot{x}(t) = \sum_{i=1}^{p}\sum_{j=1}^{c}\sum_{l=1}^{s} \mu_i \mu_j h_l [((A_i - BG_{jl} + (\Delta\tilde{A}_l - \Delta\tilde{B}_l G_{jl}))x(t)$$

$$+ (B + \Delta\tilde{B}_l)G_{jl} e(t) + (B + \Delta\tilde{B}_l)r(t) + Wd(t)] \tag{3.27}$$

By taking the derivative of (3.25) and substituting from (3.21), (3.6) and (3.22), the following is obtained:

$$\dot{e}(t) = \sum_{i=1}^{p}\sum_{j=1}^{c}\sum_{l=1}^{s} \mu_i \mu_j h_l [(\Delta\tilde{A}_l - \Delta\tilde{B}_l G_{jl})x(t)$$

$$+ \sum_{i=1}^{p}\sum_{j=1}^{q}\sum_{l=1}^{c} \mu_i \mu_j h_{[l}(A_i - N_i C_i + \Delta\tilde{B}_l G_{jl} - N_i FC_j)e(t) + \Delta B_i r(t)] \tag{3.28}$$

Therefore, the augmented FSFTC system can be expressed as the following form:

$$\dot{X}(t) = \sum_{i=1}^{p}\sum_{j=1}^{c}\sum_{l=1}^{s} \mu_i \mu_j h_l [(\tilde{H}_{ijl} + \Delta\tilde{H}_{ijl})\mathrm{X}(t) + (S + \Delta\tilde{S}_l)r(t) + \Psi d(t)] \tag{3.29}$$

where $X(t) = \begin{bmatrix} x(t) \\ e(t) \end{bmatrix}$, $\tilde{H}_{ijl} = \begin{bmatrix} A_i - BG_{jl} & BG_{jl} \\ 0 & (A_i - N_i C_i) \end{bmatrix}$, $\Delta\tilde{S}_l = \begin{bmatrix} \Delta\tilde{B}_l \\ \Delta\tilde{B}_l \end{bmatrix}$, $s = \begin{bmatrix} B \\ 0 \end{bmatrix}$,

$$\Delta\tilde{H}_{ijl} = \begin{bmatrix} \Delta\tilde{A}_l - \Delta\tilde{B}_l G_{jl} & \Delta\tilde{B}_l G_{jl} \\ \Delta\tilde{A}_l - \Delta\tilde{B}_l G_{jl} & \Delta\tilde{B}_l G_{jl} - N_i FC_j \end{bmatrix}, \Psi = \begin{bmatrix} W \\ 0 \end{bmatrix}$$

In the same manner, the augmented fuzzy system for the second and the third families can be deduced.

3.3.3. Derivation of the Stability and Robustness Conditions

The analysis procedures are the same as those in chapter 2, so the analysis results will be presented without proof. The main result for the global asymptotic stability of a TS fuzzy model with parameter uncertainties, sensor faults, and wind disturbance input are summarized by the following theorem 3.2. The sufficient and necessary stability condition is guaranteed for the fuzzy control system (3.29) if the lemma 2.2 and theorems 3.2 are satisfied.

Theorem 3.2: The fuzzy control system as given by (3.29) is stable if the controller and the observer gains are set to $G_{jl} = Y_{jl}\chi^{-1}$, $\mathrm{N_i} = P_2^{-1}O_i$ with the matrices χ, Y_j and O_i satisfying the following LMEs.

$$\chi A_i^T + A_i\chi - (B_i Y_{jl})^T - (B_i Y_{jl}) = -\sigma I \tag{3.30}$$

$$A_i^T P_2 + P_2 A_i - (O_i C_j)^T - (O_i C_j) = -\sigma I \tag{3.31}$$

where $\chi = P_1^{-1}$, σ is the robustness index. By solving (3.30) and (3.31) related to the wind turbine system, the observer gain ($N_i = P_2^{-1}O_i$) and controller gains ($G_{jl} = Y_{jl}\chi^{-1}$) can be easily determined and we can see that the uncertainty is affected by robustness index by the same manner as shown in Fig. 2 in chapter 2. According to the analysis above, the procedure for finding the FSFTC and the fuzzy observer are summarized as follows:

a) Obtain the mathematical model of the WES to be controlled

b) Solve (3.30) and (3.31) to obtain χ, P_2, O_i and Y_{jl} thus ($G_{jl} = Y_{jl}\chi^{-1}$ and $\mathrm{N_i} = P_2^{-1}O_i$).

c) Construct the FDOS (3.6) and the FSFTC (3.22).

3.3.4. Application Example B

The WES model system with DFIG system (2.48) used in application example A, in chapter 2 will be used as an application example. The nonlinear systems are subject to large parameter uncertainties, wind disturbance and sensor faults. The objective here is to conceive a sensor fault tolerant control for WES with parameters uncertainties within 40% of the nominal values and disturbance (20% of wind speed). Where ΔA_i (i=1,2,…,8) represent the non time varying system parameters uncertainties (R_s and R_r) but bounded, the elements of ΔA_i *(i=1,2,…,8)* randomly achieve the values within 40% of their nominal values corresponding to A_i (i=*1,2,…,8*), ΔB_i (i=*1,2,…,8*) = 0. A proportional error on the generator speed sensors changes the sensor gain as in (3.20).

3.3.5. Simulations and Results

The proposed controller is tested for a same random variation of wind speed as shown in Fig. 2.4. For the testing purpose, it is required that at least one sensor fail every time. Faults are modeled as proportional signals to sensor outputs as shown in Fig. 3.7 and the parametric uncertainties R_s and R_r are considered within 40% of their nominal values.

Fig. 3.8 and Fig. 3.9 show the rotational speed of the wind turbine and generator (dashed line), respectively, and their estimates (dotted lines) in the presence of parametric uncertainties, sensor faults and wind disturbance. A simulation without the FSFTC scheme strategy is shown at left and one with the FSFTC scheme strategy is shown at right. In order to obtain optimality, the $r(t)=\Omega_{gref}=\Omega_{opt}=\omega_s-n_b\lambda_{opt}v/R$ profile is chosen in such a way as to follow the optimal tip speed ratio (λ_{opt}) (solid line). From the simulation results using the proposed control scheme, it can be seen that the outputs of the system are

bounded and good tracking performance can be obtained though the uncertain nonlinearities of the system, sensor faults and the wind disturbance.

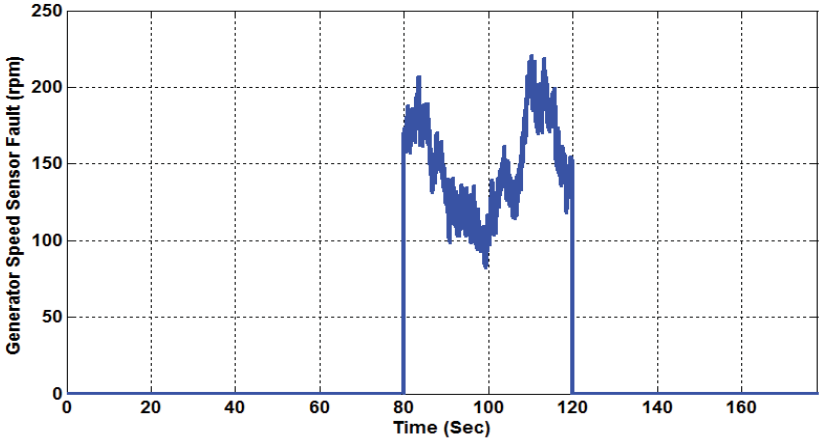

Fig. 3.7. Proportional error on the generator speed sensor

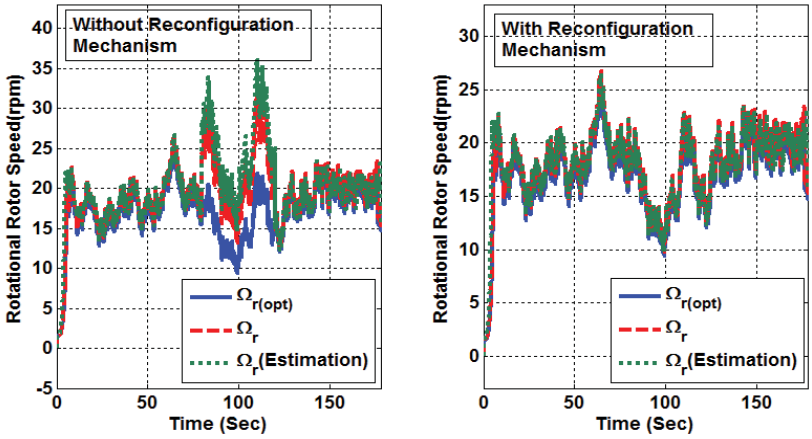

Fig. 3.8. The trajectories of Ω_r and its estimate without (left) and with (right) FSFTC strategy

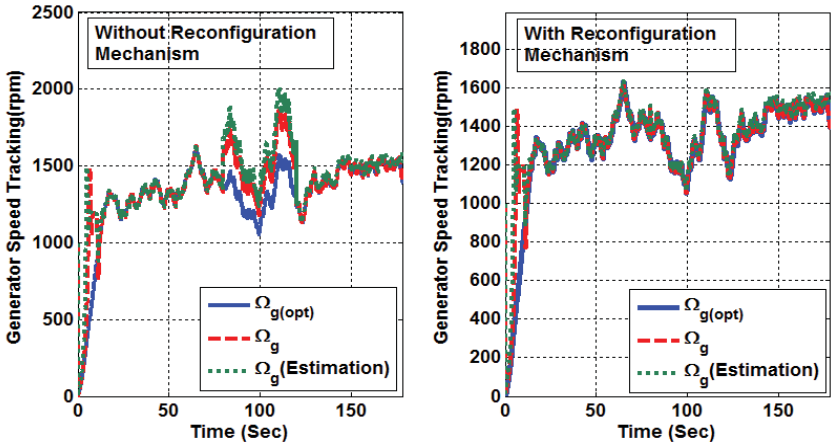

Fig. 3.9. The trajectories of Ω_g and its estimate without (left) and with (right) FSFTC strategy

Fig. 3.10 and Fig. 3.11 show the active power P_s (dashed line) and its estimate (dotted line) and the reactive power Q_s (dashed line) and its estimate (dotted line), respectively, without FSFTC scheme strategy (left) and with FSFTC scheme strategy (right).

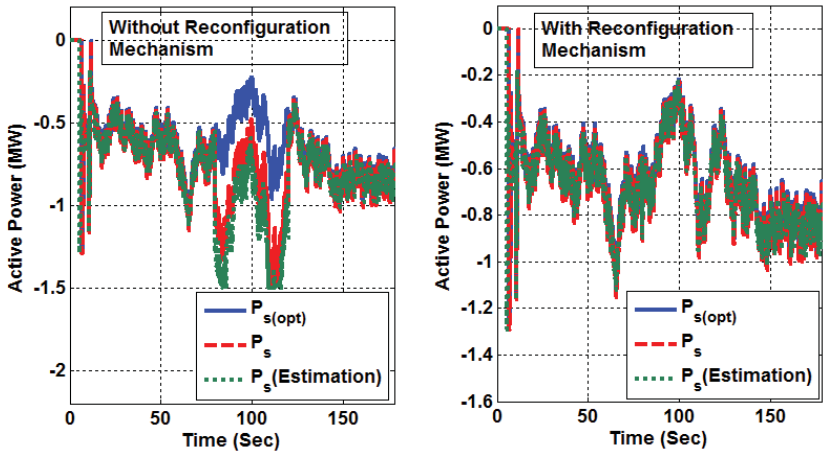

Fig. 3.10. The trajectories of P_s and its estimate without (left) and with (right) FSFTC strategy

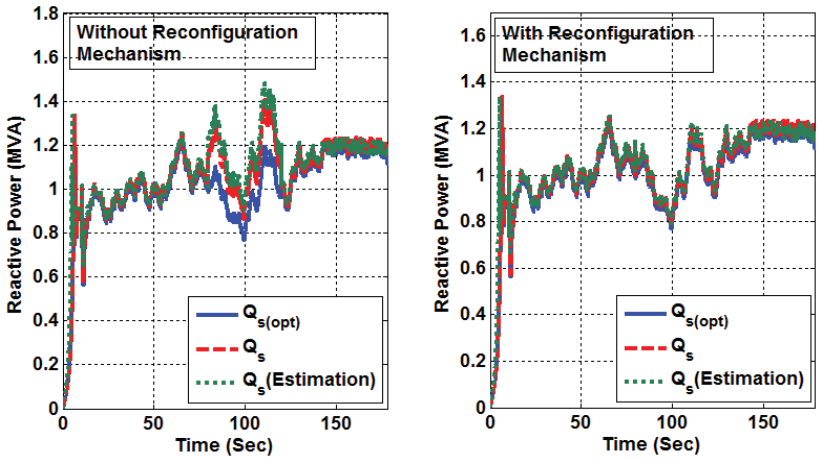

Fig. 3.11. The trajectories of Q_s (dashed line) and its estimate (dotted line) without (left) and with (right) FSFTC strategy

From the simulation, it can be seen that without the reconfiguration mechanism, the WES lost performance just after the generator speed sensor became faulty, whereas for the same reference input and by using the FSFTC scheme strategy proposed, the WES remains stable in the presence of sensor faults, parameter uncertainties and wind disturbance which demonstrates the effectiveness of the proposed FSFTC strategy.

In summary, it has been shown that the proposed scheme is able to detect and isolate sensor faults, through a proper and feasible selection of the healthy observed variables. The simulation results demonstrate the effectiveness of the proposed control approach. The proposed control scheme can guarantee the stability of the closed-loop system and the convergence of the output tracking error.

3.4. DFFTC for HWDSS Subject to Sensor Faults and Parameter Uncertainties

A new Dynamic Fuzzy Fault Tolerant Control (DFFTC) algorithm is proposed for nonlinear TS systems with parameter uncertainties. The modifications made in this approach enable robust handling of multiple simultaneous sensor failures. The control law aims to compensate for sensor faults and allows the system states to track a reference corresponding to a fault free situation. The proposed strategy is based on the fault estimate and the error between the faulty system state and a reference system state. FPIO design is proposed to estimate the state and sensor faults. Sufficient conditions are derived for robust stabilization in the sense of Lyapunov asymptotic stability and are formulated in the format of LMIs. The gains of the FFTC and FPIO are obtained by solving these LMIs. The proposed algorithm stabilizes the system over a wide range of sensor faults and parameter uncertainties while both reducing the bus-voltage and bus-frequency ripple and maximizing the power output of a variable-speed wind energy conversion system. Simulation results for a HWDSS are presented to illustrate the effectiveness of the proposed method.

This approach is an extension of the work proposed in [12]. This paper addresses the problem of Robust Fault Estimation and DFFTC for a system based on the TS fuzzy model. A FPIO design is proposed to estimate faults in TS models with sensor faults and parameter uncertainties. Furthermore, based on the information of online fault estimation, an observer-based DFFTC is designed to compensate for the effects of faults by stabilizing the closed-loop system. The closed-loop system will follow those of a user-defined stable reference model in the presence of bounded sensor faults and parameter

uncertainties. Sufficient conditions for the existence of both FPIO and DFFTC are given in terms of LMIs and Lyapunov theory. Simulation results of a HWDSS are presented to illustrate the effectiveness of the proposed method.

Based on the aforementioned works, the contributions of the proposed approach is in the use of the FPIO to estimate time-varying sensor faults and unmeasured states in a class of WES. Once the fault is estimated, the FTC controller is implemented as a state feedback controller. This controller is designed such that it can handle multiple simultaneous sensor failures. Therefore the proposed algorithm combines the merits

- The modifications approach is designed such that to handle multi-sensor failure at any time but the authors in section 3.2 and section 3.3 assumed only one faulty sensor, so section 3.2 and section 3.3, if the two sensors fail simultaneously, the controller cannot use the healthy one.
- The problem of robust fault estimation and DFFTC for system based on TS fuzzy model is addressed.
- A FPIO design is proposed to achieve fault estimation of TS models with sensor faults and parameter uncertainties.
- Based on the information of online fault estimation, an observer-based DFFTC is designed to compensate the effect of faults by stabilizing the closed-loop system.
- The closed-loop system will follow those of a user-defined stable reference model in the presence of bounded sensor faults and parameter uncertainties.
- The algorithm reduces the bus-voltage and bus-frequency ripple and maximization of the output power for a variable-speed wind energy conversion system.

This section is organized as follows. In section 3.4.1, the reference model, a TS Fuzzy plant model with sensor faults and FPIEO are introduced. In section 3.4.2, a fuzzy fault tolerant algorithm is proposed to close the feedback loop and HWDSS stability conditions will be derived and formulated as LMIs.

Section 3.4.3 presents the dynamic modeling of the HWDSS and the TS Fuzzy Description. In section 3.4.4, the procedures for finding the FPIEO and the proposed DFFTC are presented. Section 3.4.5 shows simulation results to illustrate the effectiveness of the proposed control method for wind systems.

3.4.1. Reference Model, TS Fuzzy Plant Model and FPIEO

This section presents the reference model, the TS fuzzy model with sensor faults and FPIEO.

3.4.1.1. Reference Model

Consider the stable linear model without faults described as follows [113]

$$\dot{\bar{x}}(t) = A_r\,\bar{x}(t) + B_r r(t)$$
$$\bar{y}(t) = C_r\,\bar{x}(t) \tag{3.32}$$

where $\bar{x}(t) \in \kappa^{nx1}$ is the state vector of the reference model, $r(t) \in \kappa^{nx1}$ is the bounded reference input, $A_r \in \kappa^{nxn}$ is the constant stable system matrix, $B_r \in \kappa^{nxn}$ is the constant input matrix, $C_r \in \kappa^{mxn}$ is the constant output matrix and $\bar{y}(t) \in \kappa^{mx1}$ is the reference output.

3.4.1.2. TS Fuzzy Plant Model With Sensor Faults and Parameter Uncertainties

The TS fuzzy model is described by fuzzy IF-THEN rules, which represent local linear input-output relationships of nonlinear systems [56]. The ith rule of the TS fuzzy model with sensor faults and parametric uncertainties is given in the following form [53].

Plant Rule i: IF $q_1(x(t))$ is M_{1i} AND … AND $q_\varepsilon(x(t))$ is $M_{\varepsilon i}$

Then $\dot{x}(t) = (A_i + \Delta A_i)\,x(t) + B_i u(t)$,

$$y(t) = C_i x(t) + E_{si} f_s(t) \tag{3.33}$$

where $x(t) \in \kappa^{nx1}$ is the state vector, $u(t) \in \kappa^{nx1}$ is the input vector, $y(t) \in \kappa^{mx1}$ is the output vector, $f_s(t) \in \kappa^{rx1}$ represents the fault which is assumed to be bounded, $A_i \in \kappa^{nxn}$ and $B_i \in \kappa^{nxn}$, $C_i \in \kappa^{mxn}$, $E_{si} \in \kappa^{mxr}$ are the system matrix, input matrix, output matrix and fault matrix, respectively, all of which are assumed to be known. It is supposed that the matrix E_{si} is full column rank, i.e. rank(E_{si})= r, $\Delta A_i \epsilon \kappa^{nxn}$ are the parameter uncertainties of A_i within known bounds, p is the number of IF-THEN rules, and $q_1(x(t)),\ldots, q_\varepsilon(x(t))$ are also assumed measurable variables and do not depend on the sensor faults [56]. The defuzzified output of (3.33) subject to sensor faults is represented as follows [93]:

$$\dot{x}(t) = \sum_{i=1}^{p} \mu_i(q(x(t)))[(A_i + \Delta A_i)x(t) + B_i u(t)] \quad ,$$

$$y(t) = \sum_{i=1}^{p} \mu_i(q(x(t)))[C_i x(t) + E_{si} f_s(t)] \tag{3.34}$$

3.4.1.3. FPIEO Observer Design

Definition 3.1: The fuzzy system (3.33) is called locally observable if the matrices (A_i,C_i), $i=1$, 2,…,p are observable [114].

For the fuzzy observer design, it is assumed that the fuzzy system (3.33) is locally observable. In order to detect and estimate faults, the following fuzzy proportional-integral estimation observer for TS fuzzy model with sensor faults (3.33) is formulated as follows [93], [51]:

Observer Rule i: IF $q_1(x(t))$ is M_{1i} AND … AND $q_\varepsilon(x(t))$ is $M_{\varepsilon i}$

Then
$$\dot{\hat{x}}(t) = A_i \hat{x}(t) + B_i u(t) + K_i (y(t) - \hat{y}(t)) \,,$$

$$\dot{\hat{f}}_s(t) = L_i(y(t) - \hat{y}(t)) = L_i \tilde{y}(t)$$

$$\hat{y}(t) = C_i \hat{x}(t) + E_{si} \hat{f}_s(t) \quad i=1, 2,\ldots,p \tag{3.35}$$

where K_i is the proportional observer gain and L_i is their integral gain for the ith observer rule, $\hat{y}(t)$ is the final output of the fuzzy observer and $\tilde{y}(t)$ is the estimation error. The defuzzified output of (3.35) subject to sensor faults is represented as follows:

$$\dot{\hat{x}}(t) = \sum_{i=1}^{p} \mu_i [A_i \hat{x}(t) + B_i u(t) + K_i \tilde{y}(t)]$$

$$\dot{\hat{f}}_s(t) = \sum_{i=1}^{p} \mu_i L_i \tilde{y}(t)$$

$$\hat{y}(t) = \sum_{i=1}^{p} \mu_i [C_i \hat{x}(t) + E_{si} \hat{f}_s(t)] \tag{3.36}$$

3.4.2. Proposed DFFTC Algorithm Design and Stability Analyses

In this section, we present LMIs-based solutions to the fuzzy FTC controller synthesis problems for nonlinear systems with sensor faults described by the TS fuzzy model. The proposed fuzzy FTC controller can be designed such that the states of the closed-loop system will follow those of a user-defined stable reference model (3.32) despite the presence of sensor faults.

3.4.2.1. Proposed DFFTC

Definition 2: The fuzzy system (3.33) is called locally controllable if the matrices (A_i,B_i), $i=1,2,\ldots,p$, are controllable [114].

For the fuzzy controller design, it is assumed that the fuzzy system (3.33) is locally controllable. Using PDC the ith rule of the fuzzy controller is given by:
Controller Rule i: IF $q_1(x(t))$ is M_{1i} AND … AND $q_\varepsilon(x(t))$ is $M_{\varepsilon i}$

$$\text{Then} \quad u(t)=u_i(t) \tag{3.37}$$

where $u_i(t) \in \kappa^{nx1}$ is the output of the ith rule controller that will be defined in the next sub-section. The global output of the fuzzy controller is given by

$$u(t) = \sum_{i=1}^{p} \mu_i u_i(t) \tag{3.38}$$

From (2.6), (2.7) and (3.38),

$$\dot{x}(t) = \sum_{i=1}^{p} \mu_i (A_i + \Delta A_i)\, x(t) + \sum_{i=1}^{p} \mu_i B_i \sum_{i=1}^{p} \mu_i u_i(t) \tag{3.39}$$

Let $B=B_1=B_2=\ldots=B_p$ (3.40)

$$\dot{x}(t) = \sum_{i=1}^{p} \mu_i (A_i + \Delta A_i)\, x(t) + B \sum_{i=1}^{p} \mu_i u_i(t) \tag{3.41}$$

Then, from (3.34) and (3.39)-(3.41),

$$\dot{x}(t) = \sum_{i=1}^{p} \mu_i [(A_i + \Delta A_i)\, x(t) + B u_i(t)]$$

$$y(t) = \sum_{i=1}^{p} \mu_i [C_i\, x(t) + E_{si}\, f_s(t)] \tag{3.42}$$

Note that B and E_{si} are known. In the same way, from (3.36), (3.38), and (3.44), we have

$$\dot{\hat{x}}(t) = \sum_{i=1}^{p} \mu_i [A_i \hat{x}(t) + B u_i(t) + K_i (y(t)-\hat{y}(t))] \tag{3.43}$$

$$\dot{\hat{f}}_s(t) = \sum_{i=1}^{p} \mu_i L_i (y(t)-\hat{y}(t)) \tag{3.44}$$

$$\hat{y}(t) = \sum_{i=1}^{p} \mu_i [C_i \hat{x}(t) + E_{si} \hat{f}_s(t)] \tag{3.45}$$

Let $e_1(t) = x(t)-\bar{x}(t)$ (3.46)

$$e_2(t) = x(t)-\hat{x}(t), \quad \tilde{f}_s(t) = f_s(t)-\hat{f}_s(t) \tag{3.47}$$

The dynamics of $e_1(t)$ are given by :

$$\dot{e}_1(t) = \dot{x}(t)-\dot{\bar{x}}(t) \tag{3.48}$$

$$\dot{e}_1(t) = \sum_{i=1}^{p} \mu_i [(A_i + \Delta A_i)\, x(t) + B u_i(t) - A_r\, \bar{x}(t) - B_r r(t)] \tag{3.49}$$

The dynamics of $e_2(t)$ are expressed as:

$$\dot{e}_2(t) = \dot{x}(t)-\dot{\hat{x}}(t) \tag{3.50}$$

$$= \sum_{i=1}^{p} \mu_i [(A_i + \Delta A_i)\, x(t) + B u_i(t)] - \sum_{i=1}^{p} \mu_i [A_i \hat{x}(t) + B u_i(t) + K_i (y(t)-\hat{y}(t))]$$

$$= \sum_{i=1}^{p} \mu_i A_i\, e_2(t) - \sum_{i=1}^{p} \mu_i K_i [\sum_{i=1}^{p} \mu_i (C_i e_2(t) + E_{si} \tilde{f}_s(t))] + \sum_{i=1}^{p} \mu_i \Delta A_i\, x(t)$$

$$\dot{e}_2(t) = \sum_{i=1}^{p} \mu_i[(A_i - K_i C)e_2(t) - K_i E_s \tilde{f}_s(t) + \Delta A_i\, x(t)] \tag{3.51}$$

Let $E_s = E_{s1} = E_{s2} = \ldots = E_{sp}$, $C = C_1 = C_2 = \ldots = C_p$ (3.52)

where E_s and C are fault matrix and the output matrix, respectively. The dynamics of the fault error estimation can be written as

$$\dot{\tilde{f}}_s(t) = \dot{f}_s(t) - \dot{\hat{f}}_s(t) \tag{3.53}$$

The assumption that the fault signal is constant over is restrictive, since in many practical situations, the faults are time-varying signals. So, time-varying faults are considered rather than constant faults. From (3.44), and (3.53), the derivative of $\tilde{f}(t)$ w.r.t time is derived as follows

$$\dot{\tilde{f}}_s(t) = \dot{f}_s(t) - \dot{\hat{f}}_s(t) = \dot{f}_s(t) - \sum_{i=1}^{p} \mu_i L_i (y(t) - \hat{y}(t))$$

$$= \dot{f}_s(t) - \sum_{i=1}^{p} \mu_i L_i \Big(\sum_{i=1}^{p} \mu_i [C_i e_2(t) + E_{si} \tilde{f}(t)] \Big) \tag{3.54}$$

From (3.52), we obtain

$$\dot{\tilde{f}}_s(t) = \dot{f}_s(t) - \sum_{i=1}^{p} \mu_i L_i [C e_2(t) + E_s \tilde{f}(t)] \tag{3.55}$$

From (3.51) and (3.55), is obtained:

$$\dot{\varphi} = A_o \varphi + B_o \dot{f}_s(t) + B_a x(t) \tag{3.56}$$

with $\varphi = \begin{bmatrix} e_2(t) \\ \tilde{f}_s(t) \end{bmatrix}$, $B_o = \begin{bmatrix} 0 \\ I \end{bmatrix}$, $A_o = \sum_{i=1}^{p} \mu_i A_{oi}$, $A_{oi} = \begin{bmatrix} A_i - K_i C & -K_i E_s \\ -L_i C & -L_i E_s \end{bmatrix}$, $B_a = \sum_{i=1}^{p} \mu_i B_{ai}$, $B_{ai} = \begin{bmatrix} \Delta A_i \\ 0 \end{bmatrix}$

3.4.2.2. Stability Analyses of the Proposed Fuzzy DFFTC Controller

The stability conditions for a generalized class of WES with sensor faults described by (3.42) are derived. The results of this sub-section can be summarized by the lemma 3.2 and theorem 3.3 and the lemma 3.1 [48]. The fuzzy control system (3.42) is stable if the lemma 3.2 and theorems 3.3 are satisfied.

Lemma 3.1 [48]: Given constant matrices J and O_a appropriate dimensions for $\forall \varepsilon_a > 0$, the following inequality holds:

$$J^T O_a + O_a^T J \le \varepsilon_a J^T J + \varepsilon_a^{-1} O_a^T O_a$$

Lemma 3.2: The fuzzy control system of (3.42) subject to plant sensors faults is guaranteed to be asymptotically stable, and its states will follow those of a stable reference model of (3.32) in the presence of bounded sensor, if B is an invertible square matrix and the fuzzy FTC is given by;

$$u_i(t) = B^{-1}\{He_1(t) + A_r\,\bar{x}(t) + B_r r(t) - A_i\,x(t) + S\hat{f}_s(t) - [0.5e_1(t)\|\hat{f}_s(t)\|\|S_E\|_{\max}\|\hat{f}_s(t)\|/e_1(t)^T P_1 e_1(t)]$$
$$- e_1(t)\|e_1(t)\|\|P_1\|\|\Delta A_i\|_{\max}\|x(t)\|/e_1(t)^T P_1 e_1(t) - e_1(t)\|x(t)\|\|D\|_{\max}\|x(t)\|/e_1(t)^T P_1 e_1(t)\} \quad (3.57)$$

Theorem 3.3: The TS fuzzy system (3.49) and (3.56) describing the evolution of the errors $e_1(t)$,$e_2(t)$ and $\tilde{f}(t)$ is asymptotically stabilizable via the TS fuzzy model based output-feedback controller (3.38) and (3.57), if there exist symmetric and positive definite matrices P_{11}, P_{22}, some matrices K_i and L_i, and matrices X_i , Y_i, such that the following LMIs are satisfied,

$$A_i^T P_{11} + P_{11} A_i - (Y_i C)^T - Y_i C + P_{11} P_{11} < -\delta I \quad (3.58)$$

$$(X_i E)^T + X_i E + P_{22} P_{22} < -\delta I \quad (3.59)$$

Proof. We define the following Lyapunov function,

$$V(e_1(t), \varphi(t)) = 0.5 e_1(t)^T P_1 e_1(t) + \varphi(t)^T P_2 \varphi(t) \quad (3.60)$$

where P_1 and P_2 are time-invariant, symmetric and positive definite matrices. Let

$$V_1(e_1(t)) = 0.5 e_1(t)^T P_1 e_1(t)\ ,\ \ V_2(\varphi(t)) = \varphi(t)^T P_2 \varphi(t) \quad (3.61)$$

The time derivative of $V_1(e_1(t))$ is

$$\dot{V}_1(e_1(t)) = \frac{1}{2}\dot{e}_1(t)^T P_1 e_1(t) + \frac{1}{2} e_1(t)^T P_1 \dot{e}_1(t) \tag{3.62}$$

By substituting (3.49) into (3.62), one obtain

$$\dot{V}_1(e_1(t)) = \frac{1}{2}\left\{ \sum_{i=1}^{p} \mu_i [(A_i + \Delta A_i)\,x(t) + B u_i(t) - A_r\,\bar{x}(t) - B_r r(t)] \right\}^T \times P_1 e_1(t)$$

$$+ \frac{1}{2} e_1(t)^T P_1 \left\{ \sum_{i=1}^{p} \mu_i [(A_i + \Delta A_i)\,x(t) + B u_i(t) - A_r\,\bar{x}(t) - B_r r(t)] \right\} \tag{3.63}$$

we design $u_i(t)$, $i = 1, 2, \ldots, p$, as follows,

$$u_i(t) = B^{-1}\{He_1(t) + A_r\,\bar{x}(t) + B_r r(t) - A_i\,x(t) + S\hat{f}_s(t) - [0.5 e_1(t)\|\hat{f}_s(t)\|\|S_E\|_{\max}\|\hat{f}_s(t)\|/e_1(t)^T P_1 e_1(t)]$$

$$- e_1(t)\|e_1(t)\|\|P_1\|\|\Delta A_i\|_{\max}\|x(t)\| / e_1(t)^T P_1 e_1(t) - e_1(t)\|x(t)\|\|D\|_{\max}\|x(t)\| / e_1(t)^T P_1 e_1(t)\} \quad \text{if } e_1(t) \neq 0 \tag{3.64}$$

$$u_i(t) = B^{-1}\{He_1(t) + A_r\,\bar{x}(t) + B_r r(t) - A_i\,x(t) + S\hat{f}_s(t)\} \quad \text{if } e_1(t) = 0 \tag{3.65}$$

where $\|\cdot\|$ denotes the l_2 norm for vectors and l_2 induced norm for matrices, $\|S_E\| \le \|S_E\|_{\max}$, $S_E = S^T S$, $\|\Delta A_i\| \le \|\Delta A_i\|_{\max}$, $\|D\| \le \|D\|_{\max}$, $D = B_{ai}^T B_{ai}$, $H \in \kappa^{nxn}$ is chosen as stable matrix to be designed. It is assumed that B^{-1} exists (B is nonsingular and rank $B = n$) and S is chosen such that $S = \sum_{i=1}^{p} \mu_i E_{si}$. From (3.63), (3.64) and assuming that $e_1(t) \neq 0$, one obtain

$$\dot{V}_1(e_1(t)) = \frac{1}{2} e_1(t)^T (H^T P_1 + P_1 H) e_1(t) + \frac{1}{2}\sum_{i=1}^{p} \mu_i [\hat{f}_s(t)^T S^T P_1 e_1(t) + e_1(t)^T P_1 S\hat{f}_s(t) - \|\hat{f}_s(t)\|\|S_E\|_{\max}\|\hat{f}_s(t)\|]$$

$$+ \frac{1}{2}\sum_{i=1}^{p} \mu_i \|e_1(t)\|\|P_1\|(\|\Delta A_i\| - \|\Delta A_i\|_{\max})\|x(t)\| + \frac{1}{2}\|x(t)\|\|D\|_{\max}\|x(t)\| \tag{3.66}$$

From (3.66), we replace the term $\hat{f}_s(t)^T S^T P_1 e_1(t) + e_1(t)^T P_1 S\hat{f}_s(t)$ by the following;

$$\hat{f}_s(t)^T S^T P_1 e_1(t) + e_1(t)^T P_1 S\hat{f}_s(t) = (S\hat{f}_s(t))^T P_1 e_1(t) + (P_1 e_1(t))^T S\hat{f}_s(t) \tag{3.67}$$

Using Lemma 1 and (3.67), we obtain

$$\hat{f}_s(t)^T S^T P_1 e_1(t) + e_1(t)^T P_1 S\hat{f}_s(t) \le \varepsilon_a (S\hat{f}_s(t))^T S\hat{f}_s(t) + \varepsilon_a^{-1}(P_1 e_1(t))^T P_1 e_1(t) \tag{3.68}$$

Assume $\varepsilon = 1$, then from (3.68)

$$\hat{f}_s(t)^T S^T P_1 e_1(t) + e_1(t)^T P_1 S \hat{f}_s(t) \le \hat{f}_s(t)^T S^T S \hat{f}_s(t) + e_1(t)^T P_1 P_1 e_1(t) \tag{3.69}$$

From (3.66) and (3.69), we have

$$\dot{V}_1 = \frac{1}{2} e_1(t)^T (H^T P_1 + P_1 H + P_1 P_1) e_1(t) + \frac{1}{2} \sum_{i=1}^{p} \mu_i \left\| e_1(t) \right\| \left\| P_1 \right\| (\left\| \Delta A_i \right\| - \left\| \Delta A_i \right\|_{\max}) \left\| x(t) \right\|$$

$$+ \frac{1}{2} (\left\| \hat{f}_s(t) \right\| (\left\| S_E \right\| - \left\| S_E \right\|_{\max}) \left\| \hat{f}_s(t) \right\| - \left\| x(t) \right\| \left\| D \right\|_{\max} \left\| x(t) \right\|) \tag{3.70}$$

Let $Q_1 = -(H^T P_1 + P_1 H + P_1 P_1)$, Q_1 is symmetric positive definite matrix

$$\dot{V}_1(e_1(t)) = -0.5 e_1(t)^T Q_1 e_1(t) + \frac{1}{2} \sum_{i=1}^{p} \mu_i \left\| e_1(t) \right\| \left\| P_1 \right\| (\left\| \Delta A_i \right\| - \left\| \Delta A_i \right\|_{\max}) \left\| x(t) \right\|$$

$$+ \frac{1}{2} (\left\| \hat{f}(t) \right\| (\left\| S_E \right\| - \left\| S_E \right\|_{\max}) \left\| \hat{f}_s(t) \right\| - \left\| x(t) \right\| \left\| D \right\|_{\max} \left\| x(t) \right\|) \tag{3.71}$$

The time derivative of $V_2(\varphi(t))$ is

$$\dot{V}_2(\varphi(t)) = \dot{\varphi}(t)^T P_2 \varphi(t) + \varphi(t)^T P_2 \dot{\varphi}(t) \tag{3.72}$$

In the same manner, $\dot{V}_2(\varphi(t))$ can be obtained by substituting (3.56) into (3.72),

$$\dot{V}_2(\varphi(t)) = \sum_{i=1}^{p} \mu_i \varphi(\mathrm{t})^{\mathrm{T}} (A_{oi}^T \mathrm{P}_2 + \mathrm{P}_2 A_{oi}) \varphi(\mathrm{t})$$

$$+ \sum_{i=1}^{p} \mu_i [\dot{f}_s(t)^T B_o^T P_2 \varphi(t) + \varphi(t)^T P_2 B_o \dot{f}_s(t)] + x(t)^T D x(t) \tag{3.73}$$

Using Lemma 1

$$\dot{V}_2(\varphi(t)) = \sum_{i=1}^{p} \mu_i \varphi(t)^T (A_{oi}{}^T P_2 + P_2 A_{oi} + P_2 P_2) \varphi(t) + \dot{f}_s(t)^T B_o^T B \dot{f}_s(t) + x(t)^T D x(t) \tag{3.74}$$

It is assumed that the derivative of $f_s(t)$ w.r.t time is norm bounded, i.e. $\left\| \dot{f}_s(t) \right\| \le d_1$ and $0 \le f_1 < \infty$, [56], [115] therefore, $\dot{f}_s(t)^T B_o^T B \dot{f}(t) \le f_1^2 \lambda_{\max}(B_o^T B_o)$, allows the derivation of:

$$\dot{V}_2(\varphi(t)) \le \sum_{i=1}^{p} \mu_i \varphi(t)^T (A_{oi}{}^T P_2 + P_2 A_{oi} + P_2 P_2) \varphi(t) + f_1^2 \lambda_{\max}(B_o^T B_o) + x(t)^T D x(t) \tag{3.75}$$

where $\lambda_{\max}(.)$ denotes the largest eigenvalue

Let $Q_2 = -(A_{oi}{}^T P_2 + P_2 A_{oi} + P_2 P_2)$, Q_2 is symmetric positive definite matrix

$$\dot{V}_2(\varphi(t)) = -\sum_{i=1}^{p} \mu_i \varphi(t)^T Q_2 \varphi(t) + f_1^2 \lambda_{\max}(B_o^T B_o) + \left\| x(t) \right\| D \left\| x(t) \right\| \tag{3.76}$$

Combining (3.71) with (3.76), the time derivative of $V(e_1(t),\varphi(t))$ can be expressed as

$$\dot{V}(e_1(t),\varphi(t)) \le -\frac{1}{2}e_1(t)^T Q_1 e_1(t) - \varphi(t)^T Q_2 \varphi(t) - \delta I + \frac{1}{2}\left\|\hat{f}_s(t)\right\|\left(\|S_E\| - \|S_E\|_{\max}\right)\left\|\hat{f}_s(t)\right\|$$

$$+\|x(t)\|\left(\|D\| - \|D\|_{\max}\right)\|x(t)\| + \sum_{i=1}^{p}\mu_i\|e_1(t)\|\|P_1\|\left(\|\Delta A_i\| - \|\Delta A_i\|_{\max}\right)\|x(t)\| \qquad (3.77)$$

where I is the identity matrix, $\delta = -f_1^2\lambda_{\max}(B_o^T B_o)$, $\|S_E\| - \|S_E\|_{\max} \le 0$, $\|\Delta A_i\| \le \|\Delta A_i\|_{\max}$, and $\|D\| \le \|D\|_{\max}$. From (3.77),

$$\dot{V}(e_1(t),\varphi(t)) \le -0.5\, e_1(t)^T Q_1 e_1(t) - \varphi(t)^T Q_2 \varphi(t) - \delta I \qquad (3.78)$$

$e_1(t)$ and $\varphi(t)$ converge to zero if $\dot{V} < 0$. $\dot{V} < 0$ if there exist a symmetric positive definite matrices P_1 and P_2 such that

$$H^T P_1 + P_1 H + P_1 P_1 < 0 \qquad (3.79)$$

$$A_{oi}{}^T P_2 + P_2 A_{oi} + P_2 P_2 < \delta I \qquad i=1,2,\ldots,p \qquad (3.80)$$

For the convenience of design, without loss of generality, we assume that $P_2 = \begin{bmatrix} P_{11} & 0 \\ 0 & P_{22} \end{bmatrix}$ [5], this choice is suitable for simplifying the design of fuzzy FTC and fuzzy observer. By multiplying (3.80) from left and right by P_{11}^{-1} and apply the change of variables $Y_i = P_{11}K_i$ and $X_i = -P_{22}L_i$, one obtain the LMIs (3.58) and (3.59) in the theorem.

From (3.77) and (3.79), we have

$$\dot{V} \le -0.5\, e_1(t)^T Q_1 e_1(t) - \varphi(t)^T Q_2 \varphi(t) - \delta I \le 0 \qquad (3.81)$$

If the time derivative of (3.61) is uniformly negative for all $e_1(t),\varphi(t)$ and for all $t \ge 0$ except at $e_1(t)=0$, $\varphi(t)=0$, then the controlled fuzzy system (3.42) is asymptotically stable about its zero equilibrium. Since each sum of the equation in (3.81) is negative definite, then the controlled TS fuzzy system is asymptotically stable. Also, from the proof procedure it can be seen that

if $\dot{f}_s(t)=0$, i.e. $f_1 = 0$, the proposed algorithm can achieve an asymptotic estimate for constant fault.

The block diagram of the closed-loop system is shown in Fig. 3.12.

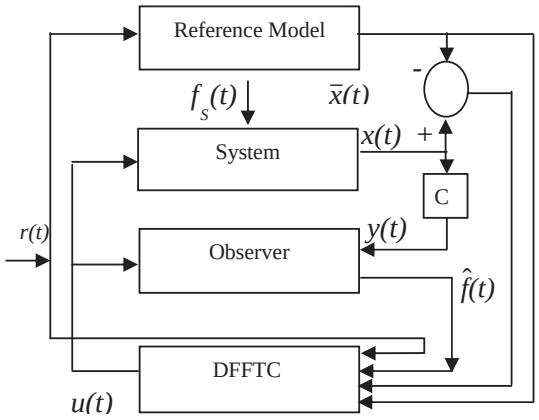

Fig. 3.12. Block diagram of DFFTC scheme

3.4.3. Application Example C

In this section, we present the description the HWDSS and its input and output relationship from the control point of view and TS Fuzzy model for HWDSS Description

3.4.3.1. HWDSS Description

The HWDSS consists of a horizontal axis, 3-bladed, stall regulated Wind Turbine (WT) with a rotor of 16.6 m diameter, and equipped with an Induction Generator (IG) rated at 55 KW connected to an ac bus-bar in parallel with a Diesel-generator set consisting of a 50 KW Turbocharged Diesel Engine (DE) driving a 65 KVA brushless Synchronous Generator (SG) and an energy storage system. The two generators are connected to a common ac bus-bar. The

overall structure of the wind-battery system is shown in Fig.3.13 [2], [14], [103].

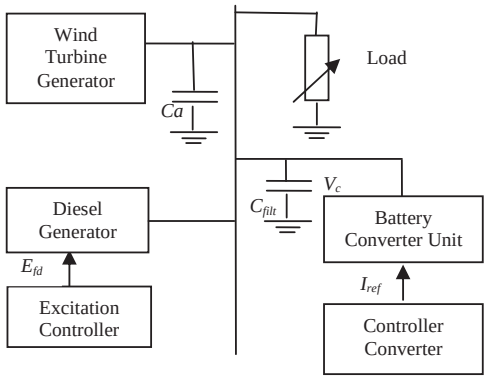

Fig. 3.13. Structural diagram of hybrid wind-diesel storage system

The dynamics of the nonlinear HWDSS can be characterized by the following equations [2], [14], [103]:

$$\dot{x} = A(x)x(t) + B(x)u(t), \quad y = Cx(t) \tag{3.82}$$

where $x(t) = [V_b \quad \omega_s]^T = [x_1(t) \quad x_2(t)]^T$,

$u(t) = [E_{fd} \quad I_{ref}]^T = [u_1(t) \quad u_2(t)]^T$

$$A(x) = \begin{bmatrix} 1 & 1 \\ 0 & 1 \end{bmatrix} \begin{bmatrix} \frac{L_f}{\tau L_{md}} q_1(x) & \frac{L_f}{\tau L_{md}} q_1(x)(L_d i_{sd} - r_a i_{sq} q_1(x)) \\ \frac{P_{ind} - P_{load}}{J_s} q_2(x) & -\frac{D_s}{J_s} \end{bmatrix} \quad B(x) = \begin{bmatrix} 1 & -V_c q_1(x)/J_s \\ 0 & -V_c q_1(x)/J_s \end{bmatrix}, C = \begin{bmatrix} 1 & 0 \\ 0 & 1 \end{bmatrix}$$

where $q_1(x(t))=1/\omega_s$ and $q_2(x(t))=1/V_b\omega_s$ are the nonlinear terms, V_c is the AC side voltage of the converter, E_{fd} is the SG field voltage, ω_s is the angular speed, which is proportional to frequency f_r, J_s and D_s are the inertia and frictional damping of SG, respectively, i_{sd} and i_{sq} are the direct and quadrature current components of SG, respectively, L_d and L_f are the stator d-axis and rotor inductances of SG, respectively, L_{md} is the d-axis field mutual inductance, τ is the transient open circuit time constant, r_a is the rotor resistance of SG, P_{ind} is the power of the induction generator, P_{load} is the power of the load, I_{ref} is the direct current set point, and V_b is the bus voltage, C_a is the

capacitor bank. Equation (3.82) indicates that the matrices *A(x)* and *B(x)* are not fixed, but change as functions of state variables, thus making the model nonlinear. The selected system parameters for the detailed wind turbine and machines are shown in Table 3.1 [2], [14], [103].

TABLE 3.1
HWDSS PARAMETERS

Symbol	Quantity	Conversion from Gaussian and CGS EMU to SI
	Rated power	55 [KW]
R	Blade radius	16.6 [m]
ρ	Air density	0.55 [kg /m^3]
	Rated line ac voltage	230 [V]
	AC rated current	138 [A]
	DC rated current	239 [A]
	Power rated of the IG	55kW
	Power rated of the SG	55kW
P_{load}	Rated Load power	40 [kW]
J_s	The inertia of SG	1.11 [kg m^2]
J_t	The inertia of the IG	1.40 [kg m^2]
D_s	Torsional damping	0.557 [Nm/ rad]
r_a	Rotor resistance of SG	0.96 [Ω]
L_f	Stator *d-axis* inductance of SG	1.33 [mH]
L_d	Rotor inductance of SG	3.06 [mH]
L_{md}	*d*-axis field mutual inductance	3 per unit
τ	The transient open circuit time constant	2.16 [ms]
	Nominal system frequency	50Hz
	Frequency/Angular speed	2π50 rad/sec

3.4.3.2. The Structure of the HWDSS Control

Fig. 3.14 depicts the input and output relationship of the wind-battery system from the control point of view. The control inputs are E_{fd}, the excitation field voltage and I_{ref}, the direct-current set point of the converter. The measurements are the voltage amplitude V_b of the common ac bus-bar and the frequency f_r. The wind speed v is considered to be a disturbance. From the control point of view, this is a coupled nonlinear system with two inputs and two outputs.

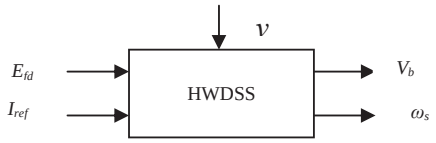

Fig. 3.14. Control structure of the HWDSS

3.4.3.3. TS Fuzzy HWDSS Description

To design the fuzzy FTC and the FPIEO, a fuzzy model that represents the dynamics of the HWDSS is necessary. Therefore, the system is first represented with a TS fuzzy model. The system (3.82) is described by a TS fuzzy representation with the angular speed of SG ω_s and the bus voltage V_b as the premise variables and do not depend on the sensor faults [56]. Next, calculate the minimum and maximum values of $q_1(t)$ and $q_2(t)$ under $q_{1min} \leq q_1(t) \leq q_{1max}$, $q_{2min} \leq q_2(t) \leq q_{2max}$. From the maximum and minimum values $q_1(t)$ and $q_2(t)$, one can obtain the sector nonlinearity as follow:

$$q_1(t)=q_{1max}N_1(q_1(t))+q_{1min}N_2(q_1(t))$$
$$q_2(t)=q_{2max}M_1(q_2(t))+q_{2min}M_2(q_2(t))$$

where $N_1(q_1(t))+N_2(q_1(t))=1$, $M_1(q_2(t))+M_2(q_2(t))=1$, N_{1i} and M_{1i} are a fuzzy term of rule i. The membership functions for $q_1(t)$ and $q_2(t)$ are depicted in Fig. 3.15. In the case of parametric uncertainties, the dynamic equations of the model are known but some parameters (L_f, L_d, and r_a) are uncertain. This kind of uncertainty is common in models obtained by linearization. Then, the nonlinear HWDSS is represented by the following fuzzy model.

Rule i: IF $q_1(t)$is N_{ji} and $q_2(t)$is M_{ji}

Then $\dot{x}(t) = (A_i + \Delta A_i)\, x(t) + B_i u(t)$,

$$y(t) = C_i\, x(t) + E_{si}\, f_s(t) \qquad j=1,2;i=1,2,\ldots,4$$

Referring to (3.33) the fuzzy plant model given by:

$$\dot{x}(t) = \sum_{i=1}^{4} \mu_i [(A_i + \Delta A_i) x(t) + B_i u(t)]$$

$$y(t) = \sum_{i=1}^{4} \mu_i [C_i\ x(t) + E_{si}\ f_s(t)] \qquad i=1,2,3,4 \tag{3.83}$$

where $x(t) \in \kappa^{2x1}$, $u(t) \in \kappa^{2x1}$ are the state vectors and the control input, respectively, where

$$A_1 + \Delta A_1 = \begin{bmatrix} 1 & 1 \\ 0 & 1 \end{bmatrix} \begin{bmatrix} \frac{\bar{L}_f}{\tau L_{md}} q_{1\max} & \frac{\bar{L}_f}{\tau L_{md}} q_{1\max} (\bar{L}_d i_{sd} - \bar{r}_a i_{sq} q_{1\max}) \\ \frac{P_{ind} - P_{load}}{J_s} q_{2\min} & -\frac{D_s}{J_s} \end{bmatrix}$$

$$A_2 + \Delta A_2 = \begin{bmatrix} 1 & 1 \\ 0 & 1 \end{bmatrix} \begin{bmatrix} \frac{\bar{L}_f}{\tau L_{md}} q_{1\max} & \frac{\bar{L}_f}{\tau L_{md}} q_{1\max} (\bar{L}_d i_{sd} - \bar{r}_a i_{sq} q_{1\max}) \\ \frac{P_{ind} - P_{load}}{J_s} q_{2\max} & -\frac{D_s}{J_s} \end{bmatrix}$$

$$A_3 + \Delta A_3 = \begin{bmatrix} 1 & 1 \\ 0 & 1 \end{bmatrix} \begin{bmatrix} \frac{\bar{L}_f}{\tau L_{md}} q_{1\min} & \frac{\bar{L}_f}{\tau L_{md}} q_{1\min} (\bar{L}_d i_{sd} - \bar{r}_a i_{sq} q_{1\min}) \\ \frac{P_{ind} - P_{load}}{J_s} q_{2\max} & -\frac{D_s}{J_s} \end{bmatrix}$$

$$A_4 + \Delta A_4 = \begin{bmatrix} 1 & 1 \\ 0 & 1 \end{bmatrix} \begin{bmatrix} \frac{\bar{L}_f}{\tau L_{md}} q_{1\min} & \frac{\bar{L}_f}{\tau L_{md}} q_{1\min} (\bar{L}_d i_{sd} - \bar{r}_a i_{sq} q_{1\min}) \\ \frac{P_{ind} - P_{load}}{J_s} q_{2\min} & -\frac{D_s}{J_s} \end{bmatrix} \quad B_1 = B_2 = \begin{bmatrix} 1 & -\frac{V_c}{J_s} q_{1\max} \\ 0 & -\frac{V_c}{J_s} q_{1\max} \end{bmatrix},$$

$$B_3 = B_4 = \begin{bmatrix} 1 & -\frac{V_c}{J_s} q_{1\min} \\ 0 & -\frac{V_c}{J_s} q_{1\min} \end{bmatrix} \quad E_{si} = \begin{bmatrix} 1 & 2 \\ 5 & 1 \end{bmatrix}, \quad f_s(t) = \begin{bmatrix} f_{s1}(t) \\ f_{s2}(t) \end{bmatrix}$$

The choice of E_{si} depends on the two inputs of the system. where $\bar{L}_f = L_f + \Delta L_f$, $\bar{L}_d = L_d + \Delta L_d$, and $\bar{r}_a = r_a + \Delta r_a$, where L_f, L_d, and r_a are the nominal values and ΔL_f, ΔL_d, and Δr_a are the parameter uncertainties, ΔA_i represents the bounded system parameter uncertainties. The elements of ΔA_i randomly achieve the values within 40% of their nominal values corresponding to A_i, which represent the change of parameter uncertainties L_f, L_d, and r_a within 40% of their nominal values and $\Delta B_i = 0$ ($i=1,2,3,4$). The choice of E_{si} depends on the two inputs of the system.

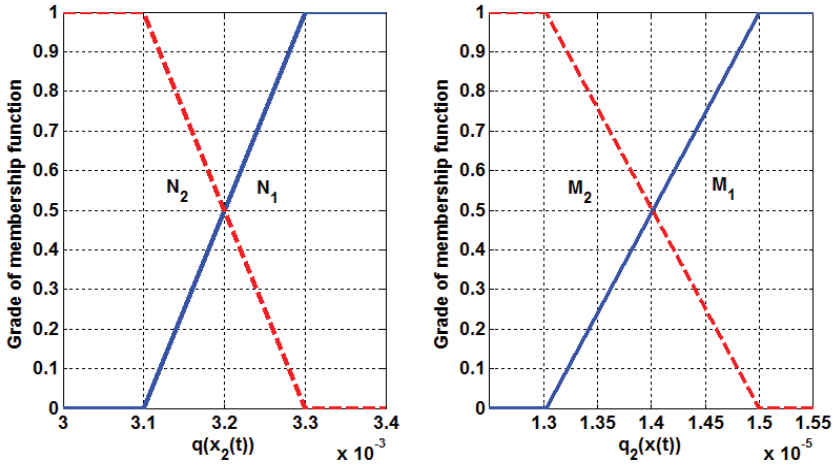

Fig. 3.15. Membership functions of state variables

Two sensor faults are considered: bus voltage and generator speed sensors which are modeled as follow:

$$f_{s1}(t) = \begin{cases} 0 & t < 6.22\text{sec} \\ 3\sin(\pi t) & t \geq 6.22\text{sec} \end{cases}, f_{s2}(t) = \begin{cases} 0 & t < 6.22\text{sec} \\ 2\sin(\pi t) & t \geq 6.22\text{sec} \end{cases} \quad (3.84)$$

where $f_{s1}(t)$ is the bus voltage sensor fault and $f_{s2}(t)$ is the generator speed sensor fault. Consider, $H = \begin{bmatrix} -4 & -4 \\ 0 & -1 \end{bmatrix}$ which is a stable matrix. The stable linear model is chosen as

$$A_r = \begin{bmatrix} -4 & -4 \\ 0 & -4 \end{bmatrix}, B_r = \begin{bmatrix} 1 & 1 \\ 0 & 1 \end{bmatrix}, C_r = \begin{bmatrix} 1 & 0 \\ 0 & 1 \end{bmatrix}$$

3.4.4. Procedures for Design FPIEO and DFFTC

According to the analysis above, the procedure for finding the proposed fuzzy FTC controller and the FPIEO observer are summarized as follows.

1. Obtain the mathematical model of the HWDSS to be controlled.
2. Obtain the fuzzy plant model for the system stated in step (1) by means of a fuzzy modeling method.

3. Check if there exists B^{-1} by determining its rank
4. Choose a stable reference model.
5. Solve LMIs (3.58)and (3.59) to obtain X_i, Y_i, P_{11}, K_i and L_i thus (K_i=- $P_{11}^{-1}Y_i$ and L_i=- $P_{22}^{-1}X_i$)
6. Construct fuzzy observer (3.36) according to the Theorem and fuzzy controller (3.38) according to the Lemma 3.2.

3.4.5. Simulation Studies

The system under study consists of a three-bladed horizontal axis, the simulations are performed on a HWDSS model [2], [14], [103]. The proposed DFFTC is tested for random variations of wind speed as shown in Fig.3.16 and compared to the proposed FSFTC in section 3.3 to prove the effectiveness of the proposed algorithm. If λ_{opt} is specified by the wind turbine producer, the optimal control may be implemented by tracking the desired value of the shaft speed $\omega_{t(opt)}=v\lambda_{opt}/R$. The reference input ($r(t)=\omega_{t(opt)}$) is applied to the reference model and the controller to obtain the maximum power coefficient from the wind energy. Consider the nonlinear WDSHS affected by sensor faults described by (3.84) and 40% of the parameter uncertainties (L_f, L_d, and r_a).

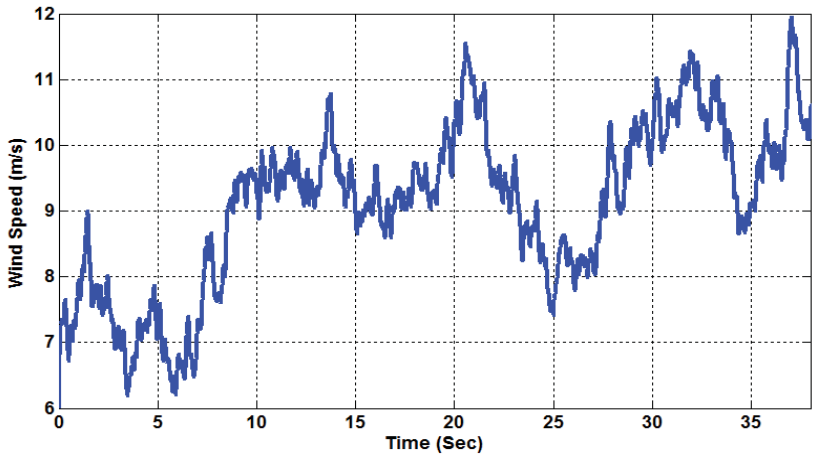

Fig. 3.16. Wind speed profile

Fig.3.17 shows the time evolution of the sensor fault (solid lines) and its estimate (dashed lines) based on (3.84) (bus voltage sensor fault $f_{s1}(t)$(left) and its estimate, and the generator speed sensor fault $f_{s2}(t)$ (right) and its estimate).

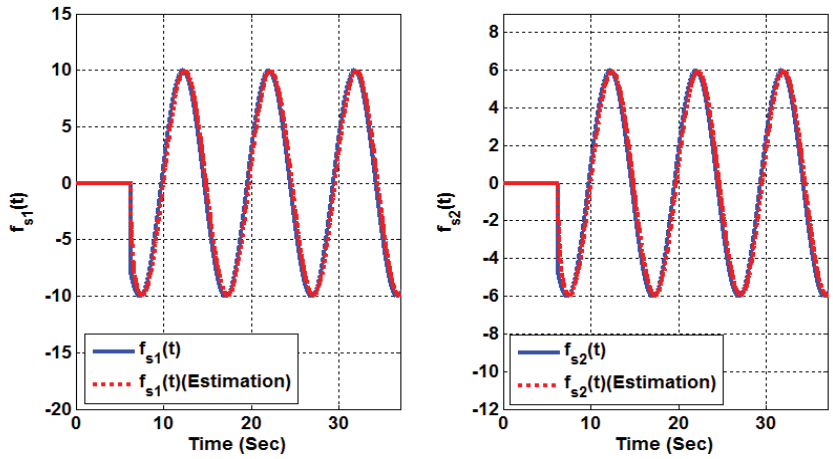

Fig. 3.17. Faults and their estimations

The variations of frequency and voltage of the system for the proposed DFFTC (left) and proposed FSFTC (right) are shown in Figs 3.18 and 3.19, respectively. From these figures (left), it can be seen that the states of the system (dashed line) for the DFFTC are bounded and good tracking for the reference model (solid line) is obtained in the presence of multi-sensor faults, but in Figs 3.18 and 3.19 (right) with FSFTC cannot use the healthy one so the system will become unstable

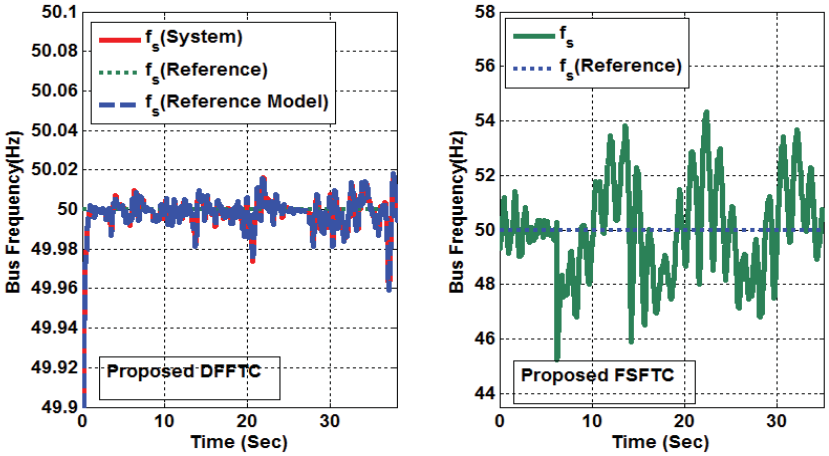

Fig. 3.18. Response of bus-bar frequency of the fuzzy control for the proposed DFFTC (left) and proposed FSFTC (right) with sensor faults based on (3.84)

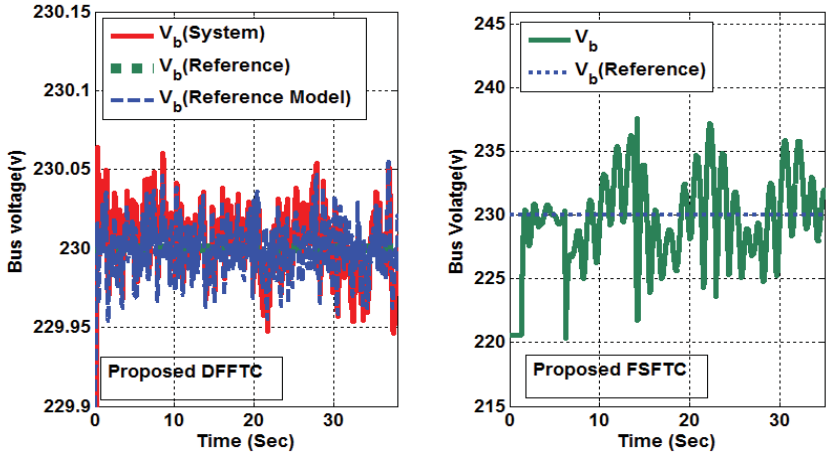

Fig. 3.19. Response of bus-bar voltage of the fuzzy control system for the proposed DFFTC (left) and proposed FSFTC (right)

As the wind speed varies randomly, the produced power curve for the proposed DFFTC (left) and proposed FSFTC (right) as shown in Fig. 3.20, we can see for the DFFTC the produced power nearly follows the wind speed curve, except for a spike when the fault is detected at 6.22 sec.

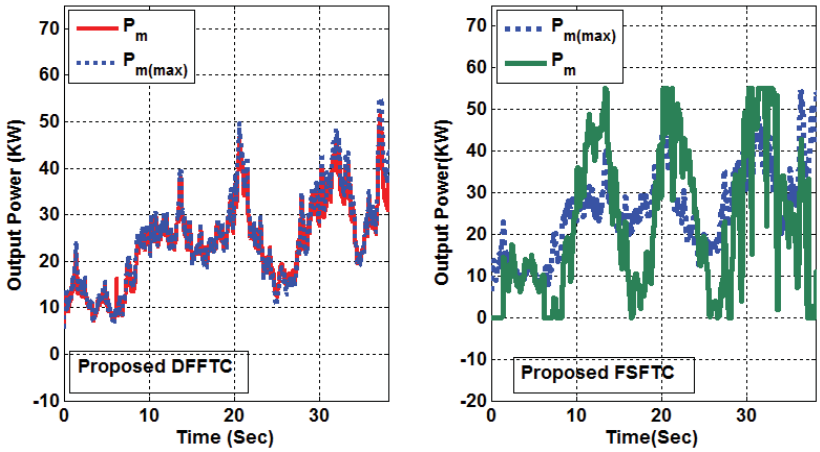

Fig. 3.20. The output power for the proposed DFFTC (left) and proposed FSFTC (right)

From Figs 3.18 and 3.19 (left) with the DFFTC, we can be observing that the states of the nonlinear HWDSS system follow those of the reference model and the tracking performance is good in presence the parameter uncertainties and the two sensors become faulty at the same time, on the other hand, from Figs 3.18 and 3.19 (right) with FSFTC cannot keep the system stable when the bus voltage sensor and the generator speed sensor become faulty at the same time. Moreover, the standard deviation of voltage and frequency for the DFFTC controller are 0.1 V and 0.05 Hz, respectively. Those corresponding to the PI are 2V and 0.2Hz, the Fuzzy-Linear Quadratic Regulator (F-LQR) are 1V and 0.1Hz [1], [2] and the adaptive network based inference system (ANFIS) are 0.2999 V and 0.0551 [13].

In summary, it can be seen that the system trajectory follows the trajectory of the reference model which represents the trajectory of the HWDSS in the fault free situation. Thus, the TS fuzzy model based controller through fuzzy observer is robust against norm-bounded sensor faults and parameter uncertainties. We can see from the simulation, there is spike when the fault is detected at 6.22 sec and then the HWDSS trajectory follows the trajectory of

the reference model. Comparing the proposed DFFTC controller with that given in the previous algorithms in section 3.2 and section 3.3, it can be seen that the proposed DFFTC controller can control the plant well over a multi and time varying sensor faults and parameter uncertainties. In addition, the proposed DFFTC performs is better than FFTC and FSFTC. The criteria considered for bus voltage and frequency deviation is less than [14], [103].

3.5. Chapter Conclusion

In section 3.2 and section 3.3 modified algorithms to control WES with parametric uncertainties, wind disturbance and sensor faults is presented under conditions where by state variables are unavailable for measurement. The basic approach is based on rigorous Taylor series, Lyapunov stability and LMIs. A set of sufficient conditions for robust stabilization of the TS fuzzy model is presented. Simulation studies clearly indicate that performance is satisfactory and regulation is achieved over the entire range of wind velocities tested. The implementation of the proposed controller in a wind energy conversion system showed that the system is kept stable over a wide range of uncertainties up to 40%. The problem of a switching mechanism we assumed one sensor fault at instant time, we solved this constraints in section 3.4, by detection and cancellation the fault by the controller. Thus, a FPIO design can be used to estimate the fault of TS models with time-varying sensor faults and parameter uncertainties. As such, an observer-based DFFTC, based on the information of online fault estimation, can be designed to compensate the effect of faults by stabilizing the closed-loop system. This modifications approach is designed such that to handle multi-sensor faults at any time but the FFTC and FSFTC in section 3.2 and section 3.3 assumed only one faulty sensor.

CHAPTER 4

CHAPTER 4

INTELLIGENT RFFTC OF WES SUBJECT TO ACTUATOR AND SENSOR FAULTS

4.1. Introduction

Nonlinearities and system uncertainties are the most important difficulties in designing controllers that ensure stability and acceptable closed-loop performance. Many significant results on the stability and robust control of uncertain nonlinear systems using TS fuzzy model have been reported [51], [59], [52], [116]-[124] over the past decades, and considerable advances have been made. However, as stated in [123], many approaches for stability and robust control of uncertain systems are often characterized by conservatism when dealing with uncertainties. It has been well known that the TS fuzzy model is very effective representation of complex nonlinear systems. In TS fuzzy model, the state space of a nonlinear system is divided into different fuzzy regions with a local linear model being used in each region. The overall model output is obtained by defuzzification using the Center of Gravity (COG) method. Once the fuzzy model is obtained, control design can be carried out via the so called PDC approach, which employs multiple linear controllers corresponding to the locally linear plant models [53]. This class of systems is described as a weighted sum of some simple linear subsystems, and thus is easily analyzable.

Commonly seen practice, many control systems are subjected to faults which can be caused by sensors, actuators or systems faults. Therefore, it is an important issue in control system design as to how the system is kept stable and acceptable performance levels maintained when a failure occurs. Generally speaking, FTC can be achieved either passively or actively. In passive FTC, the formed may be viewed as robust control. It requires a priori knowledge of possible faults which may affect the system and its controller is based on treating all possible faults as uncertainties which are taken into account for the design of tolerant control by using different techniques such as H_∞ [126], [127]. The interest of this approach lies in the fact that no online information is needed and the structure of the control law remains unchanged. Generally, the structure of the uncertainties (faults) is not taken into account in order to lead to a convex optimization problem. Furthermore, the class of the faults considered is limited and it then becomes risky to use only passive FTC [128]. While in active FTC, the controller is designed to be reconfigurable for occurring faults according to the fault detection and estimation performed by an observer to allow the faulty system to accomplish its mission. Indeed, the active FTC has been introduced to overcome the passive control drawbacks. In addition, the active FTC can usually get better control performances, it has attracted more attentions in recent years. The knowledge of some information about these is required and obtained from a Fault Detection and Diagnosis (FDD) block. Different ideas are developed in the literature, e.g., control law re-scheduling [129]-[131]. This approach requires a very robust FDI block, which constitutes its major disadvantage. Indeed, a false alarm or an undetected fault may lead to degraded performance or even to instability. The linear framework, the FTC problem is widely treated [132]-[134]. However in practice, most of physical systems are nonlinear, hence, it is primary to consider the FTC design for nonlinear systems. Some approaches dealing with this problem are proposed by [135], [136]. The proposed methods in [56] are

confined to the actuator failures and didn't consider the fuzzy systems with sensor failures. Afterwards, several FTC methods have been extended to the nonlinear systems with sensor faults [46]. In the above studies, the considered faults affecting the system behavior are modeled by a constant function. However, in practice, the faults are often time variant and as we know, in practice, many control systems are subjected to faults which can be caused by actuators, sensors or systems faults and parameter uncertainties. In addition, the problem of control in the maximization of power generation in VS-WES has been greatly studied and such control still remains an active research area [20]-[28].

However, in this chapter, our goal is to present three different proposed approaches, namely, Robust Fuzzy Fault Tolerant Control (RFFTC), Robust Fuzzy Scheduled Fault Tolerant Control (RFSFTC) and Robust Dynamic Fuzzy Fault Tolerant Control (RDFFTC) for TS models subject to time varying actuator faults, sensor faults, and parameter uncertainties, and maximize the output power from the wind turbine.

The chapter is organized as follows, the RFFTC control for the WES subject to time varying actuator faults, time varying sensor faults, and parameter uncertainties are presented in section 4.2. The RFSFTC control for the WES subject to actuator faults, sensor faults with time varying, and parameter uncertainties are presented in section 4.3. Intelligent RDFFTC of WES in the presence the parameter uncertainties, sensor fault and actuator faults are studied in section 4.4. Chapter conclusion will be given in section 4.5.

4.2. RFFTC of WES With DFIG

This section presents a new method for RFFTC of nonlinear systems described by TS fuzzy systems subject to sensor faults, parameter uncertainties, and time varying actuator faults. The algorithm based on reconfiguration

mechanism is then investigated for detection, isolation and accommodation of faults. The idea is to use a Fuzzy FDOS, FPIEO and design a new control law to minimize the state deviation between a healthy observer and the eventually faulty actual model. This scheme requires the knowledge of the system states and the occurring faults. These signals are estimated from a FDOS and FPIEO Observers. TS fuzzy systems are classified into three families based on the input matrices and a design RFFTC for each family. In each family, the fault tolerant control law is designed by using the Lyapunov method to obtain conditions which are given in LMIs formulation. The effectiveness of the proposed controller design methodology is finally demonstrated through a wind energy system with DFIG to illustrate the effectiveness of the proposed method.

This section is organized as follows. Section 4.2.1 provides the proposed RFFTC scheme, TS fuzzy model FDOS and FPIEO. The proposed algorithm and the augmented system are presented in section 4.2.2. Section 4.2.3 shows the stability and robustness conditions for the proposed algorithm followed by the calculation of state RFFTC, FDOS and FPIEO gains. Section 4.2.4 shows WES model system with DFIG. Simulation and results are shown in section 4.2.5.

4.2.1. TS Fuzzy Model With Parameter Uncertainties and Fuzzy Observer

In this sub-section, we will present the TS fuzzy plat model subject to sensor faults, parametric uncertainties and time varying actuator faults. In addition, we will present the FDOS and FPIEO and the RFFTC Scheme Design.

4.2.1.1. TS Fuzzy Plant Model With Parameter Uncertainties, Sensor Faults and Actuator Faults

Since this work considers the occurrence of actuator and sensor faults. For the first family, if we take the non time varying the parameter uncertainties in consideration we rewrite the plant dynamics (3.3) as the following [104], [105],

$$\dot{x}(t) = \sum_{i=1}^{p} \mu_i(q(x(t)))[A_i x(t) + \alpha_i B u(t) + \overline{D}_i f_a(t)] + \sum_{i=1}^{p} \mu_i(q(x(t)))\Delta A_i x(t)$$

$$y(t) = \sum_{i=1}^{p} \mu_i(q(x(t)))[(I + F_s) C_i x(t)] \quad (4.1)$$

where $\overline{D}_i \in \kappa^{nxk}$ are known matrices of actuator faults and $f_a(t) \epsilon \kappa^{kx1}$ is actuator faults time varying signal ($k<n$), $\overline{D}_i = B_i D_i$, $D_i \epsilon \kappa^{mxk}$ actuator faults which are be known.

For the second family, the plant dynamics can be described by

$$\dot{x}(t) = \sum_{i=1}^{p} \mu_i(q(x(t)))[(A_i x_i(t) + B_i u(t) + \overline{D}_i f_a(t)] + \sum_{i=1}^{p} \mu_i(q(x(t)))\Delta A_i x_i(t)$$

$$y(t) = \sum_{i=1}^{p} \mu_i(q(x(t)))[(I + F_s) C_i x(t)] \quad (4.2)$$

For the third family, the plant dynamics are then given by:

$$\dot{x}(t) = \sum_{i=1}^{p} \mu_i(q(x(t)))[(A_i x_i(t) + Bu(t) + \overline{D}_i f_a(t)] + \sum_{i=1}^{p} \mu_i(q(x(t)))\Delta A_i x_i(t)$$

$$y(t) = \sum_{i=1}^{p} \mu_i(q(x(t)))[(I + F_s) C_i x(t)] \quad (4.3)$$

4.2.1.2. TS Fuzzy Observer and the RFFTC Scheme Design

In this sub-section we presented the proposed RFFTC Scheme Design, FPIEO and FDOS.

4.2.1.2.1. Nonlinear FPIEO and FDOS

This sub-section presents FPIEO and FDOS design methodologies involving actuator faults estimation for TS fuzzy models. PDC structure is employed to achieve the following unknown fuzzy observer structures [104], [137]. Based on the analysis given in chapter 3 in section 3.4.1.3, the structure of the FPIEO that be given in (3.36) for estimate the actuator faults and the dynamic of the fault error estimation ***for the first family***, can be written is chosen as follows:

$$\dot{\hat{x}}_u(t) = \sum_{i=1}^{p} \mu_i [A_i \hat{x}_u(t) + \alpha_i Bu(t) + K_i(y(t)-\hat{y}_u(t)) + \overline{D}_i \hat{f}_a(t)]$$

$$\dot{\hat{f}}_a(t) = \sum_{i=1}^{p} \mu_i L_i(y(t)-\hat{y}_u(t)) = \sum_{i=1}^{p} \mu_i L_i \tilde{y}(t)$$

$$\hat{y}_u(t) = \sum_{i=1}^{p} \mu_i C_i \hat{x}_u(t) \qquad (4.4)$$

where $\hat{x}_u(t)$ is the estimated state vector by unknown fuzzy observer, K_i *(1,2,…,p)* are observation error matrices, L_i are their corresponding integral gains to be determined, $y(t)$ is the output vector, and $\hat{y}_u(t)$ is the final output of the unknown fuzzy observer, $\tilde{y}(t) = y(t)-\hat{y}_u(t)$ is the output estimation error and $\hat{f}_a(t)$ is the estimated actuator faults.

In the same manner and from (4.2) and (4.3), we can induce the inferred output of the FPIEO for the other two cases.

Also in this sub-section presents FDOS based on the observer that are stated in chapter 3 (3.6). The inferred modified FDOS states are governed by:

$$\dot{\hat{x}}_o(t) = \sum_{i=1}^{p} \mu_i [A_i \hat{x}_o(t) + \alpha_i Bu(t) + N_i(y(t)-\hat{y}_o(t)) + \overline{D}_i \hat{f}_a(t)]$$

$$\hat{y}_o(t) = \sum_{i=1}^{p} \mu_i C_i \hat{x}_o(t) \qquad (4.5)$$

where $\hat{x}_o(t)$ is the estimated state vector by the FDOS, $\hat{y}_o(t)$ is the final output of the FDOS, and $N_i \epsilon \kappa^{nxg}$ are the FDOS gains. From (4.2) and (4.3), in the same manner, we can induce the inferred output of the FDOS for the other two cases.

4.2.1.2.2. The Structure of the Proposed RFFTC Scheme

The proposed scheme, illustrated in Fig. 4.1, is based on the proposed RFFTC scheme that discussed in chapter 3 as given in Fig. 3.1, which detect and isolate the sensor faults and an unknown input observer which estimates the actuator faults and reconstructs the state of the WES from a healthy estimate. Each one of the FDOS is driven by all sensed to generate residual signals. The estimated actuator faults from the FPIEO are fed to the FDOS. Through the decision and switcher mechanism, detecting and identifying the faulty sensor is possible [106]-[111]. Finally, by using a switcher, selecting the healthy observer for reconstructing the controller input is enabled.

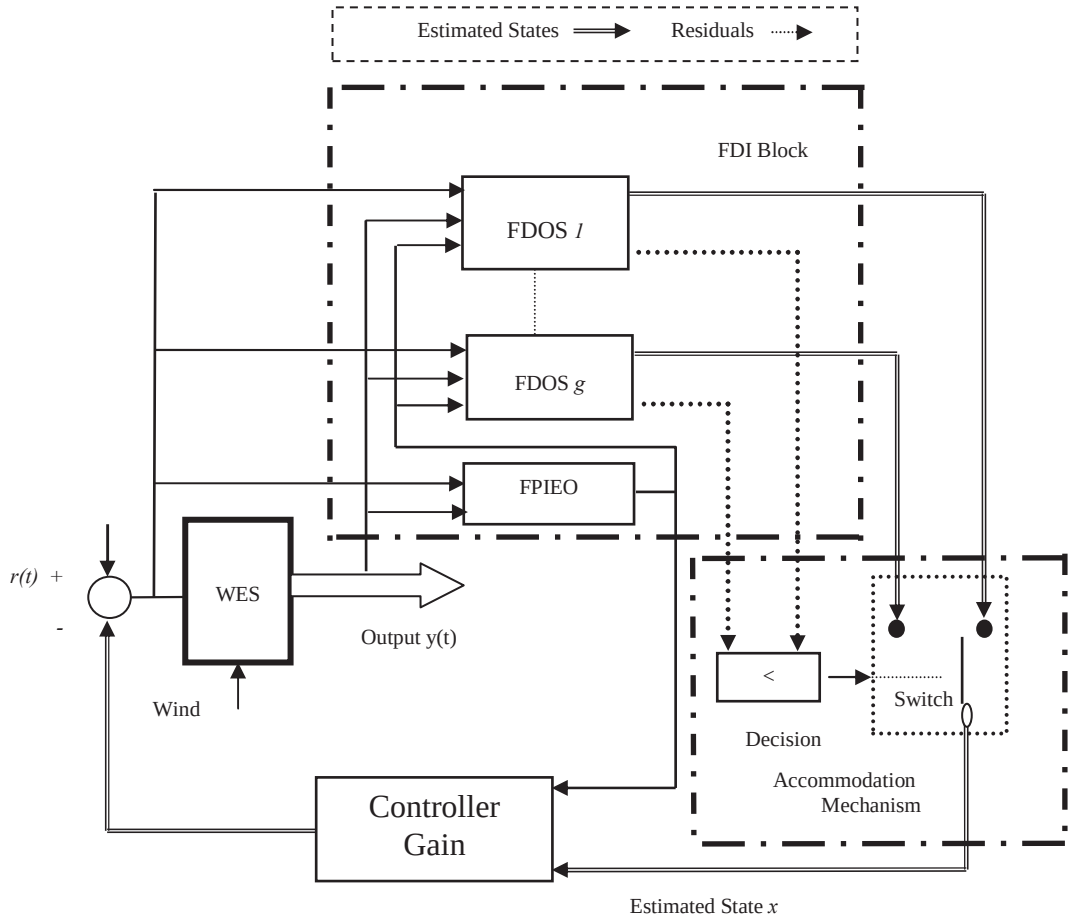

Fig. 4.1. Block diagram of the proposed RFFTC scheme

4.2.2. Proposed RFFTC Based on FPIEO and FDOS

In this sub-section, a unique RFFTC synthesis procedure is developed for each member of the TS family to deal with a wide range of uncertainties, sensor faults, and actuator faults while maintaining the stability of the closed loop system.

4.2.2.1. Nonlinear RFFTC

For the fuzzy model (4.1), we construct the following RFFTC via the PDC. It is assumed that the fuzzy system (4.1) is locally controllable. A state-feedback with LMIs is used to design a controller for each subsystem.

For the first family, the modified RFFTC is defined by base on (3.8) [53]

Rule *j:* IF $q_1(x(t))$ is M_{1i} AND … AND $q_\varepsilon(x(t))$ is $M_{\varepsilon i}$

Then $u(t)=[-G_j x(t) - D_j \hat{f}_a(t) + r(t)]/\alpha_j \qquad j=1,2,..,c$ (4.6)

From (4.5) the estimated state by the healthy observer from FDOS is used, then, the final output of the modified RFFTC becomes

$$u(t) = \frac{\sum_{j=1}^{c} \mu_j [-G_j \hat{x}_o(t) - D_j \hat{f}_a(t) + r(t)]}{\sum_{j=1}^{c} \alpha_j \mu_j} \tag{4.7}$$

For the second family, the overall output of the RFFTC is given by,

$$\dot{u}(t) = z_k\, u(t) + \sum_{j=1}^{c} \mu_j [-G_j \hat{x}_o(t) - D_j \hat{f}_a(t) + r(t)] \tag{4.8}$$

For the last family, the RFFTC is given by,

$$u(t) = \sum_{j=1}^{c} \mu_j [-G_j \hat{x}_o(t) - D_j \hat{f}_a(t) + r(t)] \tag{4.9}$$

4.2.2.2. The Augmented Fuzzy Control System

In order to carry out the analysis, the closed-loop fuzzy system should be obtained first by establishing the conditions for the asymptotic convergence of the observers (4.4) and (4.5).

For the first family, the fuzzy control system of the state and the errors can be obtained.

Let $$e_1(t) = x(t) - \hat{x}_o(t) \tag{4.10}$$

$$\dot{x}(t) = \sum_{i=1}^{p} \mu_i A_i x_i(t) + \left\{ \sum_{i=1}^{p} \alpha_i \mu_i \right\} Bu(t) + \sum_{i=1}^{p} \mu_i \overline{D}_i f_a(t) + \sum_{i=1}^{p} \mu_i \Delta A_i x_i(t) \tag{4.11}$$

With the modified TS fuzzy fault tolerant controller (4.7) employed, the TS fuzzy system (4.10) has the following closed-loop:

$$\dot{x}(t) = \sum_{i=1}^{p} \mu_i A_i x(t) + \sum_{i=1}^{p} \mu_i \overline{D}_i f_a(t) + \sum_{i=1}^{p} \mu_i \Delta A_i x_i(t) + \left\{ \sum_{i=1}^{p} \alpha_i \mu_i \right\} B \left\{ \sum_{j=1}^{p} \mu_j [-G_j \hat{x}_o(t) - D_j \hat{f}_a(t) + r(t)] \right\} / \left\{ \sum_{j=1}^{p} \alpha_j \mu_j \right\} \tag{4.12}$$

Let $$\tilde{f}_a(t) = f_a(t) - \hat{f}_a(t) \tag{4.13}$$

From (4.10) and (4.13), a TS fuzzy closed-loop can be observed:

$$\dot{x}(t) = \sum_{i=1}^{p} \sum_{j=1}^{c} \mu_i \mu_j [(A_i - BG_j) x_i(t) + BG_j e_1(t) + \overline{D}_j \tilde{f}_a(t) + Br(t)] + \sum_{i=1}^{p} \mu_i \Delta A_i x_i(t) \tag{4.14}$$

By taking the derivative of (4.10) and substituting from (4.1), (4.6) and (4.13), the following is obtained:

$$\dot{e}_1(t) = \sum_{i=1}^{p} \sum_{j=1}^{c} \mu_i \mu_j [(\Delta A_i - N_i F_s C_j) x_i(t) + (A_i - N_i C_j) e_1(t) + \overline{D}_i \tilde{f}_a(t)] \tag{4.15}$$

Using $$e_2(t) = x(t) - \hat{x}_u(t) \tag{4.16}$$

Then taking the derivative of (4.16) and substituting from (4.1), (4.4) and (4.13), the following is obtained:

$$\dot{e}_2(t) = \sum_{i=1}^{p} \sum_{j=1}^{c} \mu_i \mu_j [(\Delta A_i - K_i F_s C_j) x_i(t) + (A_i - K_i C_j) e_2(t) + \overline{D}_i \tilde{f}_a(t)] \tag{4.17}$$

we assume the actuator fault is not constant but time varying, the derivative of $\dot{\tilde{d}}(t)$ can be written as,

$$\dot{\tilde{f}}_a(t) = \dot{f}_a(t) - \dot{\hat{f}}_a(t) = \dot{f}_a(t) - \sum_{i=1}^{p} \mu_i [L_i C_i e_2(t) + L_i F_s C_i x(t)] \tag{4.18}$$

The equations (4.14), (4.15), (4.17) and (4.18) can be written:

$$\dot{X}(t) = \sum_{i=1}^{p} \sum_{j=1}^{c} \mu_i \mu_j (H_{ij} + \Delta H_{ij}) X(t) + Sr(t) + \Psi_a \phi(t) \tag{4.19}$$

with $X(t) = \begin{bmatrix} x(t) \\ e_1(t) \\ e_2(t) \\ \tilde{f}_a(t) \end{bmatrix}$, $\phi(t) = \left[\dot{f}_a(t)\right]$, $S = \begin{bmatrix} B \\ 0 \\ 0 \\ 0 \end{bmatrix}$, $\Psi_a = \begin{bmatrix} 0 \\ 0 \\ 0 \\ I \end{bmatrix}$, $\Delta H_{ij} = \begin{bmatrix} \Delta A_i & 0 & 0 & 0 \\ \Delta A_i - N_i F_s C_j & 0 & 0 & 0 \\ \Delta A_i - K_i F_s C_j & 0 & 0 & 0 \\ L_i F_s C_i & 0 & 0 & 0 \end{bmatrix}$,

$$H_{ij} = \begin{bmatrix} (A_i - BG_j) & BG_j & 0 & \overline{D}_j \\ 0 & (A_i - N_i C_j) & 0 & \overline{D}_i \\ 0 & 0 & (A_i - K_i C_j) & \overline{D}_i \\ 0 & 0 & -L_i C_i & 0 \end{bmatrix}$$

For the second family, when the input matrices are different, using (4.2), (4.8), (4.15), (4.17) and (4.18), the augmented fuzzy system is given by,

$$\dot{X}(t) = \sum_{i=1}^{p} \sum_{j=1}^{c} \mu_i \mu_j (H_{ij} + \Delta H_{ij}) X(t) + S_i r(t) + \Psi_a \phi(t) \tag{4.20}$$

with $X(t) = \begin{bmatrix} x(t) \\ u(t) \\ e_1(t) \\ e_2(t) \\ \tilde{f}_a(t) \end{bmatrix}$, $\phi(t) = \begin{bmatrix} \dot{f}_a(t) \\ \hat{f}_a(t) \end{bmatrix}$ $S_i = \begin{bmatrix} 0 \\ B_i \\ 0 \\ 0 \\ 0 \end{bmatrix}$, $\Psi_a = \begin{bmatrix} 0 & \overline{D}_i \\ 0 & 0 \\ 0 & 0 \\ 0 & 0 \\ I & 0 \end{bmatrix}$,

$$H_{ij} = \begin{bmatrix} A_i & B_i & 0 & 0_i & \overline{D}_j \\ G_j & Z_k & -G_j & 0 & \overline{D}_j \\ 0 & 0 & (A_i - N_i C_j) & 0 & \overline{D}_i \\ 0 & 0 & 0 & (A_i - K_i C_j) & \overline{D}_i \\ 0 & 0 & 0 & -L_i C_j & 0 \end{bmatrix}, \Delta H_{ij} = \begin{bmatrix} \Delta A_i & 0 & 0 & 0 & 0 \\ 0 & 0 & 0 & 0 & 0 \\ \Delta A_i - N_i F_s C_j & 0 & 0 & 0 & 0 \\ \Delta A_i - K_i F_s C_j & 0 & 0 & 0 & 0 \\ L_i F_s C_i & 0 & 0 & 0 & 0 \end{bmatrix}$$

In the same manner, the augmented fuzzy system for the third family can be

deduced.

4.2.3. Proposed RFFTC Stability and Robustness Analysis

The analysis procedures are also the same as those in chapter 2, section 2.2.3, and so the analysis results will be presented without proof. The main result for the global asymptotic stability of a TS fuzzy model with parameter uncertainties, sensor faults, and actuator faults are summarized by the following theorem 4.1. The sufficient and necessary stability condition of the nonlinear control system (4.19) is summarized by the following lemma 2.1 and theorem 4.1.

Theorem 4.1: The fuzzy control system as given by (4.19) is stable if the controller and the observer gains are set to $G_j = M_{a11}^{-1} Y_j$ and $N_i = P_{a22}^{-1} O_i$ and $\overline{E}_i = P_2^{-1} X_i$ with the matrices X_i, M_{a11}, Y_j and O_i satisfying the following LMIs.

$$M_{a11} A_i^T + A_i M_{a11} - (B_i Y_j)^T - (B_i Y_j) < 0 \tag{4.21}$$

$$A_i^T P_{a22} + P_{a22} A_i - (O_i C_j)^T - (O_i C_j) < 0 \tag{4.22}$$

$$H_{bij}^T P_2 + P_2 H_{bij} - (X_i \overline{C}_j)^T - (X_i \overline{C}_j) < 0 \tag{4.23}$$

where,

$$H_{bij} = \begin{bmatrix} A_i & \overline{D}_i \\ 0 & 0 \end{bmatrix}, \overline{E}_i = \begin{bmatrix} K_i \\ L_i \end{bmatrix}, \overline{C}_j = \begin{bmatrix} C_j \\ 0 \end{bmatrix}^T, P = \begin{bmatrix} P_1 & 0_{2x2} \\ 0_{2x2} & P_2 \end{bmatrix}, P_1 = \begin{bmatrix} P_{a11} & 0 \\ 0 & P_{a22} \end{bmatrix}, M_{a11}=P_{a1} \tag{4.24}$$

4.2.4. WES With DFIG Application

The WES model system with DFIG system used in application example A, in chapter 2 will be used as an application example. The nonlinear systems are

subject to large parameter uncertainties, actuator faults and sensor faults. The objective here is to conceive a actuator and sensor fault tolerant control for WES with parameters uncertainties within 35% of the nominal values and disturbance (20% of wind speed). Based on (2.55), we can generalize that the *i-th* rule of the continuous TS fuzzy models including actuator faults and sensor faults are of the following forms:

Rule i: IF $q_1(x_5(t))$ is $M_{э\,i}$ and $q_2(x_6(t))$ is $D_{э\,i}$ and $q_3(x_3(t))$ is $N_{э\,i}$

Then $\dot{x}(t) = (A_i + \Delta A_i)x(t) + B_i u(t) + \overline{D}_i f_a(t)$

$$y(t) = (I + F_s)\, C_i x(t) \qquad i=1,2,\ldots,8\ ;\ э=1,2 \qquad (4.25)$$

where the subsystems are determined as: $\overline{D}_i = \begin{bmatrix} 0 & 0 & 0 & 1 & 0 \\ 0 & 1 & 0 & 1 & 0 \end{bmatrix}^T$

$$A_i = \begin{bmatrix}
\frac{-R_s}{\xi L_s} & \omega_s + \frac{(1-\xi)n_p q_{2i}}{\xi} & \frac{L_m R_r}{\xi L_r L_s} & \frac{L_m}{\xi L_s} n_p q_{2i} & 0 & 0 & 0 & 0 \\
\frac{-R_s}{\xi L_s} & -(\omega_s + \frac{1-\xi}{\xi} n_p q_{2i}) & \frac{R_r L_m}{\xi L_r L_s} & -\frac{L_m}{\xi L_s} n_p q_{2i} & 0 & 0 & 0 & 0 \\
\frac{R_s L_m}{\xi L_r L_s} & -\frac{L_m}{\xi L_r} n_p q_{2i} & -\frac{R_r}{\xi L_r} & \omega_s - \frac{1}{\xi} n_p q_{2i} & 0 & 0 & 0 & 0 \\
\frac{R_s L_m}{\xi L_r L_s} & \frac{L_m}{\xi L_r} n_p q_{2i} & -\frac{R_r}{\xi L_r} & -\omega_s + \frac{1}{\xi} n_p q_{2i} & 0 & 0 & 0 & 0 \\
0 & 0 & 0 & 0 & (\frac{D_r}{J_r} + \frac{K_{opt}}{J_r} q_{1i}) & 0 & -\frac{n_b}{J_r} & 0 \\
0 & 0 & 0 & 0 & 0 & \frac{-D_g}{J_g} & \frac{1}{J_g} & -\frac{1}{J_g} \\
0 & 0 & 0 & 0 & a75 + \frac{D_{lse} K_{opt}}{n_b J_r} q_{1i} & a76 & a77 & \frac{D_{ls}}{n_b^2 J_g} \\
0 & 0 & 0 & 0 & 0 & 0 & 0 & -\frac{1}{\tau_g}
\end{bmatrix},$$

$$B_i = \begin{bmatrix} -\frac{1}{\xi L_s} & 0 & \frac{L_m}{\xi L_r L_s} & 0 & 0 \\ 0 & -\frac{1}{\xi L_s} & 0 & \frac{L_m}{\xi L_r L_s} & 0 \\ \frac{L_m}{\xi L_r L_s} & 0 & -\frac{1}{\xi L_r} & 0 & 0 \\ 0 & \frac{L_m}{\xi L_r L_s} & 0 & -\frac{1}{\xi L_r} & 0 \\ 0 & 0 & 0 & 0 & 0 \\ 0 & 0 & 0 & 0 & 0 \\ 0 & 0 & 0 & 0 & 0 \\ 0 & 0 & 0 & 0 & \frac{1}{\tau_g} \end{bmatrix}, C_i = \begin{bmatrix} 0 & 0 & 0 & 0 & 1 & 0 & 0 \\ 0 & 0 & 0 & 0 & 0 & 1 & 0 \\ 0 & 0 & 0 & -\frac{L_m V_s}{L_s} & 0 & 0 & 0 \\ 0 & 0 & \frac{V_s^2}{\omega_s L_s} q_{3i} & -\frac{L_m V_s}{L_s} & 0 & 0 & 0 & 0 \end{bmatrix},$$

Where ΔA_i (i=1,2,…,8) represent the non time varying system parameters uncertainties (J_r, J_g, R_s and R_r) but bounded, the elements of ΔA_i (i=1,2,…,8) randomly achieve the values within 35% of their nominal values corresponding to A_i (i=1,2,…,8); ΔB_i (i=1,2,…,8) = 0. The actuator faults $f_a(t)=[f_{a1}(t) \ \ f_{a2}(t)]^T$ are time varying and defined as follows

$$f_{a1}(t) = \begin{cases} 0 & t < 120\sec \\ 4\sin(\pi t) & t \geq 120 \text{ sec} \end{cases}, \quad f_{a2}(t) = \begin{cases} 0 & t < 120 \text{ sec} \\ 2\sin(\pi t) & t \geq 120 \text{ sec} \end{cases} \tag{2.26}$$

Faults are modelled as additive signals to generator speed sensor outputs based on (3.20).

According to the analysis above, the procedure for finding the proposed RFFTC with a nonlinear unknown input observer and the FDOS observer is summarized as follows.

1. Obtain the mathematical model of the WES to be controlled (2.38).
2. Obtain the fuzzy plant model for the system stated in step (1) by means of a fuzzy modelling method.
3. Solve LMIs (4.21)-(4.23) to obtain X_i , Y_j , P_{a22} ,P_2 ,K_i, L_i, N_i ,and $\overline{E}_i$ thus ($G_j = M_{a11}^{-1} Y_j$ and $N_i = P_{a22}^{-1} O_i$ and $\overline{E}_i = P_2^{-1} X_i$).

4. Construct fuzzy observers (4.4), (4.5) and the fuzzy controller (4.7)-(4.9)

4.2.5. Simulations and Results

The proposed controller for the WES is tested for the same random variation of wind speed as shown in Fig.2.4 in chapter 2 to illustrate the effectiveness of the proposed method. The control objective of this chapter is to design a RFFTC law for the system (2.48) to ensure that all signals in the closed-loop system are bounded. Fig. 4.3 shows the time evolution of the time varying actuator faults $f_a(t)$ and its estimate $\hat{f}_a(t)$,which occur after 120sec. Fig. 4.4 shows the proportional signals that represent sensor failures which has been added to the output of sensor 6 between $t=40sec$ and $t=80sec$. The magnitudes of faults are between ≈10% to ≈20% of the nominal values of the variables and the parametric uncertainties J_r, J_g, R_s and R_r are considered within 35% of their nominal values.

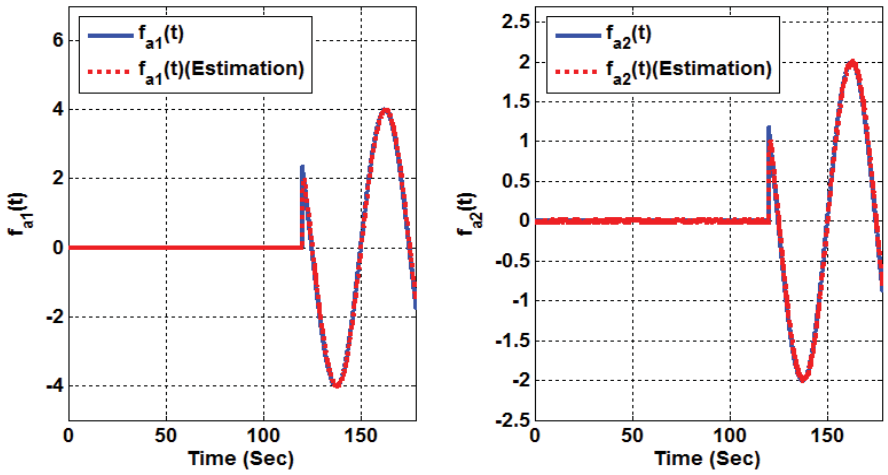

Fig. 4.3. Actuator faults ($f_{a1}(t)$ and $f_{a2}(t)$) and their estimations

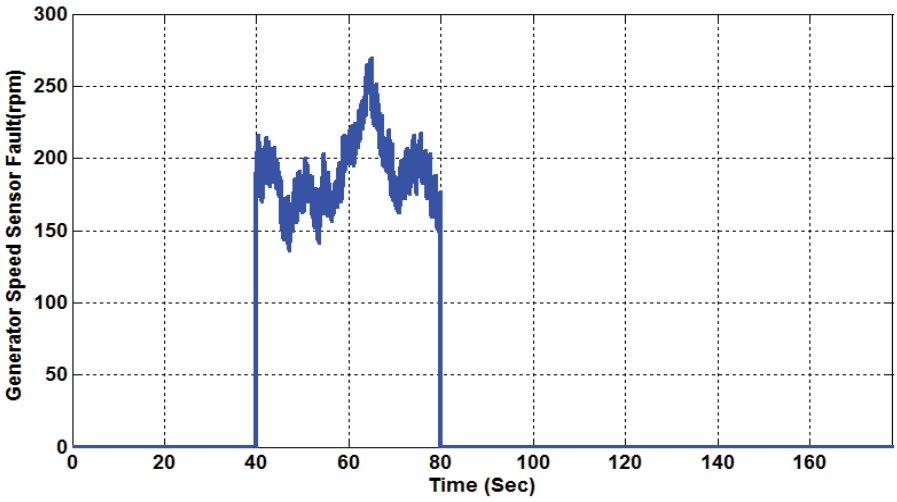

Fig. 4.4. Proportional error on the generator speed sensor

The simulation results are given in Figs. 4.5-4.8 with (left) and without (right) the RFFTC strategy and all the simulations are realized on the nonlinear model given in (2.48) with the presence of non time varying parametric uncertainties, sensor faults and time varying actuator faults. In Figs. 4.5-4.8 (left) the control law is based on one observer (observer 2) without using the switching block and the unknown observers. We can observe that between t =0 sec to t ≈<40 sec and t >≈80sec to t ≈<120 sec there are no faults, providing good tracking performance. However between *t=40sec* to t=*80sec* and after *t=120 sec*, we can see that the WES's performance is reduced right after the generator speed sensor and actuators became faulty. Figs. 4.5 and 4.6 (right) shows WES state variables and their estimated signals, when the law control is based on the bank observers (observer 1) with the switch block and the unknown observers. We can note that the WES remains stable despite the presence of faults and parameter uncertainties, which shows the effectiveness of the proposed RFFTC strategy. The rotational speed of the wind turbine and generator (dashed line), respectively, and their estimates (dotted lines) in the presence of parametric uncertainties, sensor faults and actuator faults, are

shown in Figs. 4.5 and 4.6. In order to obtain optimality, the $r(t)=\Omega_{gref}=\Omega_{opt}=\omega_s-n_b\lambda_{opt}V/R$ profile are chosen in such a way to follow the optimal tip speed ratio (λ_{opt}) (solid line).

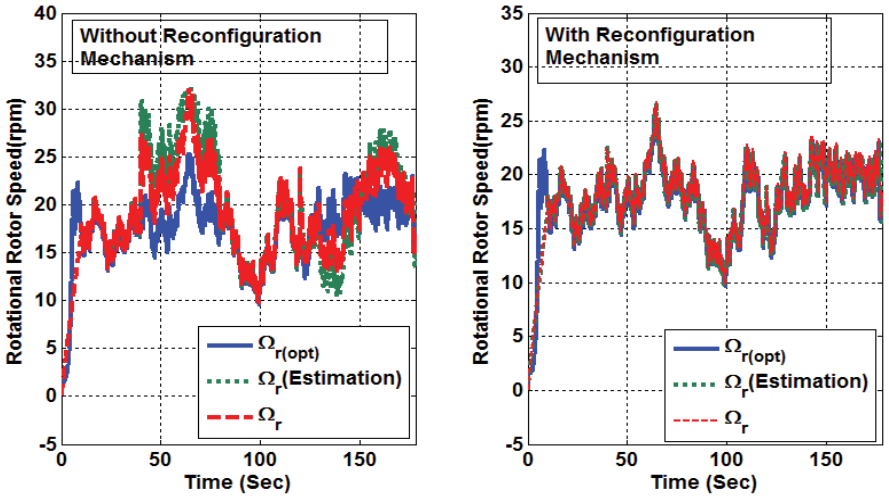

Fig. 4.5. The trajectories of Ω_r and its estimate without (left) and with (right) RFFTC strategy

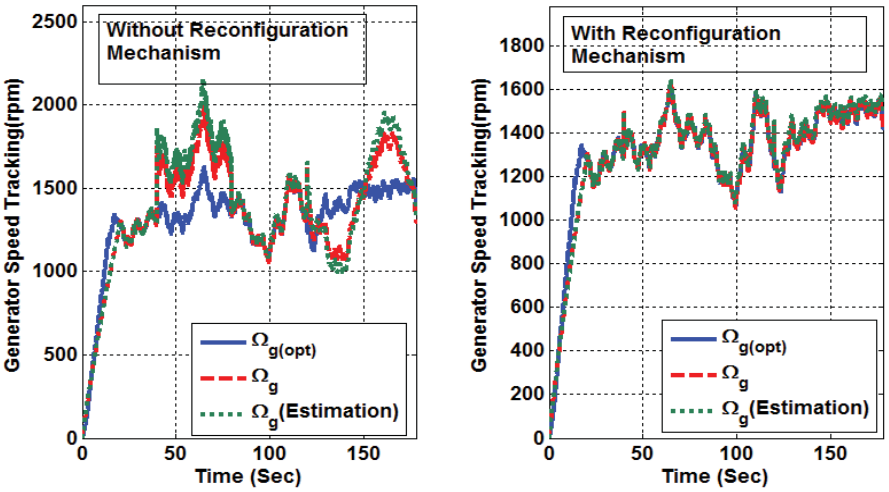

Fig. 4.6. The trajectories of Ω_g and its estimate without (left) and with (right) RFFTC strategy

The switching from observer 6 to observer 5 is visualized clearly at t ≈ 40sec (Figs. 4.5-4.8 (right)). We notice that switching observers is carried out without loss of control of the system state.

Fig. 4.7 and Fig. 4.8 show the active power P_s (dashed line) and its estimate (dotted line) and the reactive power Q_s (dashed line) and its estimate (dotted line), respectively. It can be seen that our design can get good tracking performance, although there are severe actuator faults and sensor fault entering into the system.

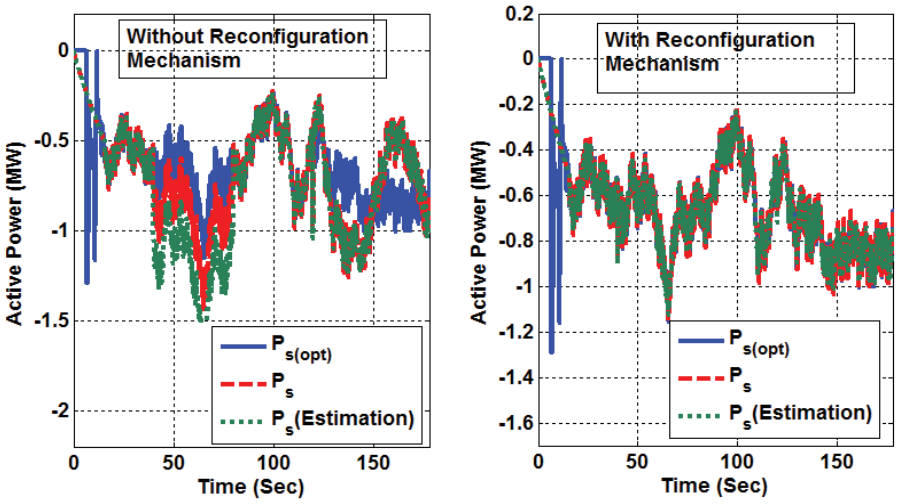

Fig. 4.7. The trajectories of P_s and its estimate without (left) and with (right) RFFTC strategy

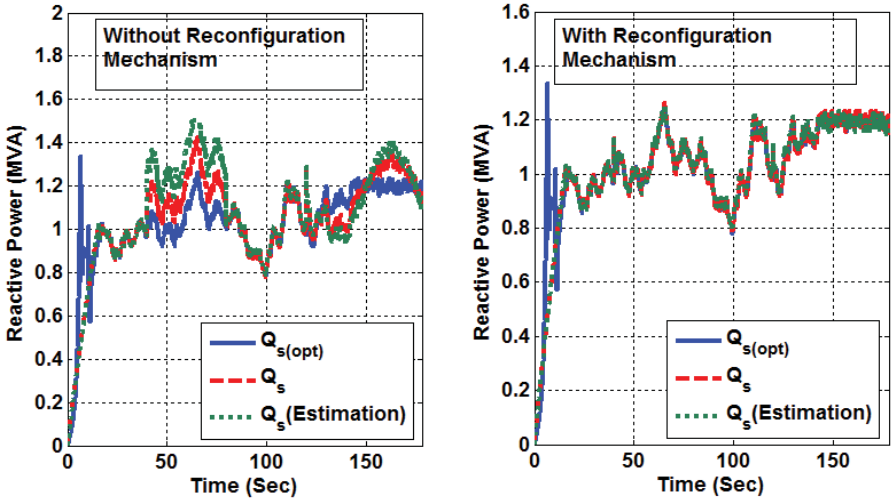

Fig. 4.8. The trajectories of Q_s (dashed line) and its estimate (dotted line) without (left) and with (right) RFFTC strategy

From the simulation, it can be seen that without the reconfiguration mechanism, the WES lost its performance after the generator speed sensor and the actuator became faulty. Whereas for the same reference input and by using the RFFTC scheme strategy proposed, the WES remains stable in the presence of sensor faults, parameter uncertainties and actuator faults. This demonstrates the effectiveness of the proposed RFFTC strategy.

In summary, it has been shown that the proposed scheme is able to detect and isolate sensor faults, through a proper and feasible selection of the healthy observed variables. It can also compensate the actuator faults using the nonlinear unknown input observers. The simulation results demonstrate the effectiveness of the proposed control approach. The proposed control scheme can guarantee the stability of the closed-loop system and the convergence of the output tracking error.

4.3. RFSFTC of WES With DFIG Subject to Sensor and Actuator faults

This chapter proposes a FDOS method using a nonlinear FPIEO with a RFSFTC algorithm for fuzzy TS systems subject to sensor faults, parametric uncertainties, and time varying actuator faults. FDOS provide residuals for detection and isolation of sensor faults which can affect a TS model. The TS fuzzy model is adopted for fuzzy modeling of the uncertain nonlinear system and establishing fuzzy state observers. The concept of PDC is employed to design RFSFTC and fuzzy observers from the TS fuzzy models. TS fuzzy systems are classified into three families based on the input matrices and a RFSFTC synthesis procedure is given for each family. In each family,

sufficient conditions are derived for robust stabilization, in the sense of Taylor series stability and Lyapunov method, for the TS fuzzy system with parametric uncertainties, sensor faults, and actuator faults. The sufficient conditions are formulated in the format of LMEs. The effectiveness of the proposed controller design methodology is finally demonstrated through a WES with Doubly DFIG to illustrate the effectiveness of the proposed method.

This section is organized as follows. Section 4.3.1 provides the proposed RFSFTC scheme, TS fuzzy model FDOS and FPIEO. Section 4.3.2 shows the stability and robustness conditions for the proposed algorithm followed by the calculation of state RFSFTC, FDOS and FPIEO gains. Section 4.3.3 shows simulation and results on WES model system with DFIG.

4.3.1. TS Fuzzy Plant Model With Actuator Faults, Sensor Faults and Parameter Uncertainties

In this section, the TS fuzzy plant model subject to parameter uncertainties, sensor faults, and actuator faults will be expressed as a weighted sum of a number of fuzzy systems. An augmented TS fuzzy plant model is formed by adding a FRU. The inferred outputs of the fuzzy scheduler fault system for three families have been introduced in chapter 3. Since in this chapter considers the occurrence of sensor faults, and actuator faults in presence the parameter uncertainties, for the first family based on (2.66) and (3.21), the dynamics of fuzzy scheduler fault system for the first family is given by,

$$\dot{x}(t) = \sum_{i=1}^{p} \sum_{l=1}^{s} \mu_i h_l [(A_i + \Delta\tilde{A}_l)\, x(t) + \alpha_l B\, u(t) + \overline{D}_i f_a(t)]$$

$$y(t) = \sum_{i=1}^{p} \mu_i (q(t))(I + F_s) C_i\, x(t) \qquad (4.27)$$

In the same manner we can induce the inferred output of the fuzzy scheduler

for the other two cases.

4.3.2. Proposed RFSFTC Algorithm Based on FPIEO and FDOS

In this section, RFSFTC is developed for each member of the TS family to deal with a wide range of parameter uncertainties, sensor faults, and actuator faults such that the closed loop system is stable. We use the same proposed scheme, illustrated in Fig. 4.1, but we will change the RFFTC to RFSFTC.

4.3.2.1. Proposed RFSFTC Controllers

Based on the analysis in chapter 2 to obtain the RFSFTC and based on the FPIEO (4.4) and FDOS (4.5), we can obtain the fuzzy scheduler fault tolerant controller, ***for the first family***, the inferred output of the modified RFSFTC in (3.22) will be as the following:

$$u(t)=\frac{\sum_{l=1}^{s}\sum_{j=1}^{c} h_l\mu_j[-G_{jl}\,\hat{x}_o(t)-D_j\hat{f}_a(t)+r(t)]}{\sum_{l=1}^{s}\sum_{j=1}^{c}\alpha_j h_l\mu_j} \tag{4.28}$$

In the same manner we can induce the inferred output of the RFSFTC for the other two cases as follows

For the second family, the modified RFSFTC in (3.23) becomes

$$\dot{u}(t)=z_k\,u(t)+\sum_{l=1}^{s}\sum_{j=1}^{c}h_l\mu_j[-G_{jl}\hat{x}_o(t)-D_j\hat{f}_a(t)+r(t)] \tag{4.29}$$

For the last family, the RFSFTC in (3.24) becomes

$$u(t)=\sum_{l=1}^{s}\sum_{j=1}^{c}h_l\mu_j[-G_{jl}\hat{x}_o(t)-D_j\hat{f}_a(t)+r(t)] \tag{4.30}$$

4.3.2.2. Stability Analysis for the Proposed RFSFTC Algorithm

In order to carry out the analysis, the closed-loop fuzzy system should be obtained first by establishing the conditions for the asymptotic convergence of the observers.

For the first family, based on (4.10), (4.13), (4.16) and (4.27), we can obtain the augmented fuzzy system.

$$\dot{X}(t) = \sum_{i=1}^{p}\sum_{j=1}^{p}\sum_{l=1}^{s} \mu_i \mu_j h_l [(H_{ijl} + \Delta\tilde{H}_{ijl})\mathrm{X(t)} + Sr(t) + \Psi_a \phi(t)] \tag{4.31}$$

with $X(t) = \begin{bmatrix} x(t) \\ e_1(t) \\ e_2(t) \\ \tilde{f}_a(t) \end{bmatrix}$, $\phi(t) = \left|\dot{f}_a(t)\right|$, $\Delta H_{ijl} = \begin{bmatrix} \Delta\tilde{A}_l & 0\ 0\ 0 \\ \Delta\tilde{A}_l - N_i F_s C_j & 0\ 0\ 0 \\ \Delta\tilde{A}_l - K_i F_s C_j & 0\ 0\ 0 \\ L_i F_s C_j & 0\ 0\ 0 \end{bmatrix}$, $S = \begin{bmatrix} B \\ 0 \\ 0 \\ 0 \end{bmatrix}$,

$\Psi_a = \begin{bmatrix} 0 \\ 0 \\ 0 \\ I \end{bmatrix}$, $H_{ijl} = \begin{bmatrix} (A_i - B G_{jl}) & B G_{jl} & 0 & \overline{D}_j \\ 0 & (A_i - N_i G_{jl}) & 0 & \overline{D}_i \\ 0 & 0 & (A_i - K_i C_j) & \overline{D}_i \\ 0 & 0 & -L_i C_i & 0 \end{bmatrix}$

In the same manner, the augmented fuzzy system for the second and the third families can be deduced.

4.3.3. Derivation of the Stability and Robustness Conditions

Based on the analysis before, the main result for the global asymptotic stability of a TS fuzzy model with parameter uncertainties, sensor faults, and actuator faults input are summarized by the following theorem 4.2. The sufficient and necessary stability condition of the nonlinear control system (4.31) is summarized by the following lemma 2.2 and theorem 4.2.

Theorem 4.2: The fuzzy control system as given by (4.31) is stable if the controller and the observer gains are set to $G_j = M_{a11}^{-1} Y_j$ and $N_i = P_{a22}^{-1} O_i$ and $\overline{E}_i = P_2^{-1} X_i$ with the matrices X_i, M_{a11}, Y_j and O_i satisfying the following LMEs.

$$M_{a11} A_i^T + A_i M_{a11} - (B_i Y_{jl})^T - (B_i Y_{jl}) = -\sigma I \tag{4.32}$$

$$A_i^T P_{a22} + P_{a22} A_i - (O_i C_j)^T - (O_i C_j) = -\sigma I \tag{4.33}$$

$$H_{bi}^T P_2 + P_2 H_{bi} - (X_i \overline{C}_j)^T - (X_i \overline{C}_j) = -\sigma I \tag{4.34}$$

where $P = \begin{bmatrix} P_1 & 0_{2x2} \\ 0_{2x2} & P_2 \end{bmatrix}$, $H_{bi} = \begin{bmatrix} A_i & \overline{D}_i \\ 0 & 0 \end{bmatrix}$, $\overline{E}_i = \begin{bmatrix} K_i \\ L_i \end{bmatrix}$, $\overline{C}_j = \begin{bmatrix} C_j \\ 0 \end{bmatrix}^T$, $P_1 = \begin{bmatrix} P_{a11} & 0 \\ 0 & P_{a22} \end{bmatrix}$

$M_{a11}=P_{a11}^{-1}$, σ is the robustness index and is determine by the same manner in sub-section 2.3.3.2 in chapter 2.

4.3.4. WES With DFIG Application and Simulations and Results

We use the random variation of wind speed as shown in Fig.2.4 in chapter 2 also to test the proposed controller and the WES model system with DFIG system (2.48). The nonlinear systems are subject The actuator fault $f_a(t)$ as shown in Fig. 4.9 (left), represents the actuator fault signals. For the testing purpose, it is required that at least one sensor fail every time. Faults are modeled as proportional signals to sensor outputs as shown in Fig. 4.9 (right) and the parametric uncertainties R_s and R_r are considered within 40% of their nominal values. The actuator fault $f_a(t)$ is time varying and defined as follows

$$f_a(t) = \begin{cases} 0 & t < 40\,\text{sec} \\ 4\sin(\pi t) & t \geq 40\ \text{sec} \end{cases} \tag{4.35}$$

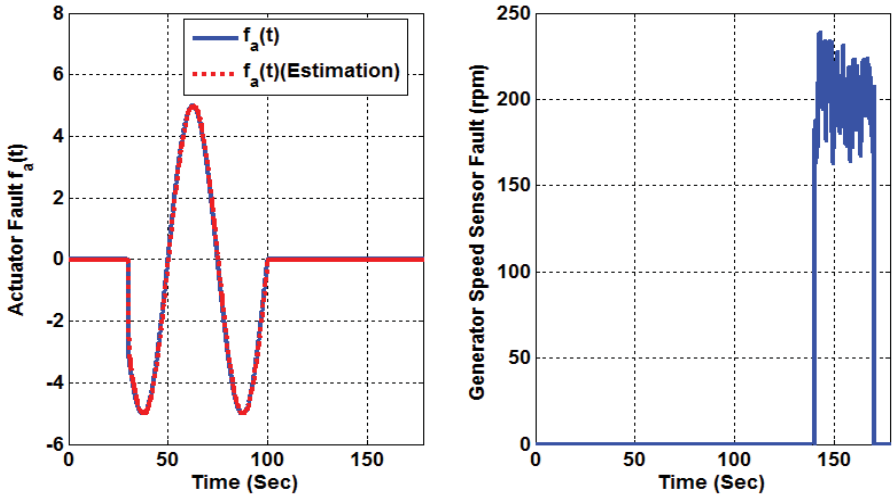

Fig.4.9. The actuator fault $f_a(t)$ and its estimate(left) and the proportional error on the generator speed sensor(right)

Fig. 4.10 and Fig. 4.11 show the rotational speed of the wind turbine and generator (dashed line), respectively, and their estimates (dotted lines) in the presence of parametric uncertainties, sensor faults and actuator fault. A simulation without the RFSFTC scheme strategy is shown at left and one with the RFSFTC scheme strategy is shown at right. In order to obtain optimality, the $r(t)=\Omega_{gref}=\Omega_{opt}=\omega_s-n_b\lambda_{opt}v/R$ profile is chosen in such a way as to follow the optimal tip speed ratio (λ_{opt}) (solid line). From the simulation results using the proposed control scheme, it can be seen that the outputs of the system are bounded and good tracking performance can be obtained though the uncertain nonlinearities of the system, sensor faults and the actuator fault.

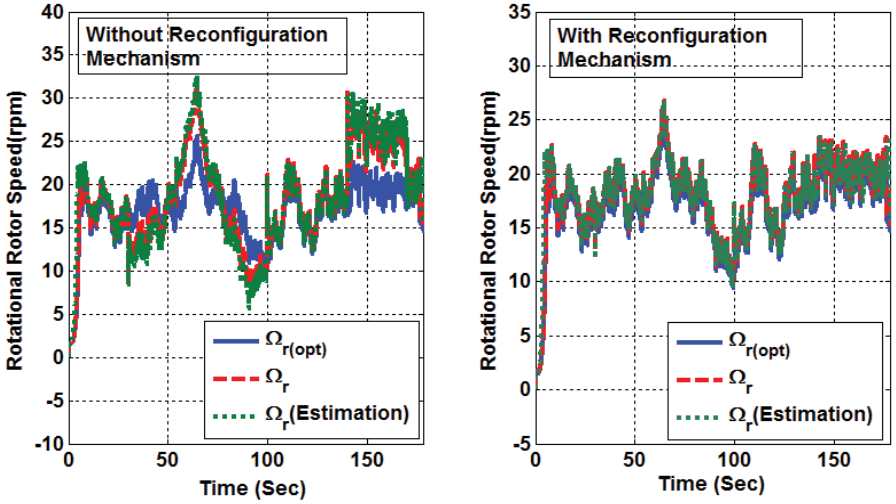

Fig. 4.10. The trajectories of Ω_r and its estimate without (left) and with (right) RFSFTC strategy

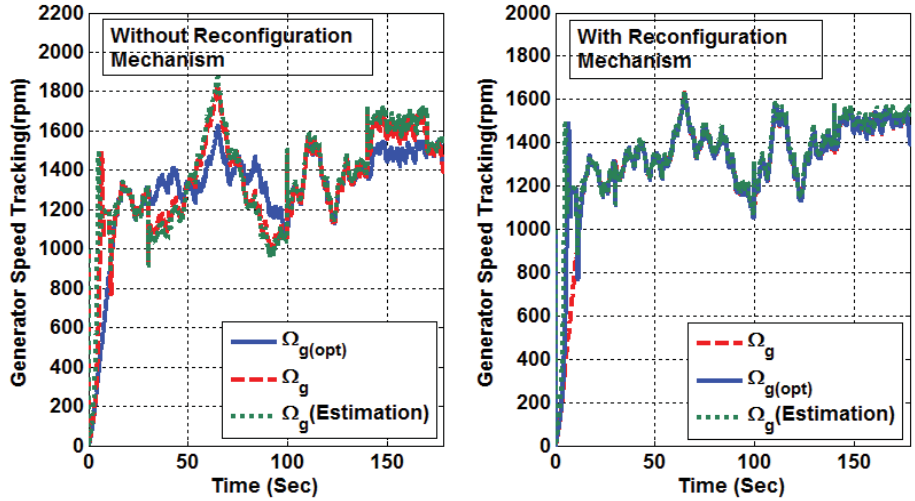

Fig. 4.11. The trajectories of Ω_g and its estimate without (left) and with (right) RFSFTC strategy

Fig. 4.12 and Fig. 4.13 show the active power P_s (dashed line) and its estimate (dotted line) and the reactive power Q_s (dashed line) and its estimate (dotted line), respectively, without RFSFTC scheme strategy (left) and with RFSFTC scheme strategy (right).

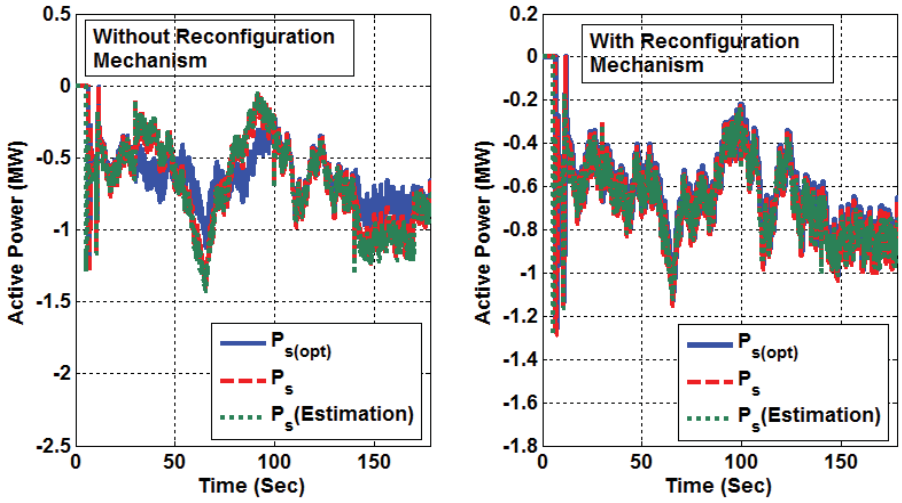

Fig. 4.12. The trajectories of P_s and its estimate without (left) and with (right) RFSFTC strategy

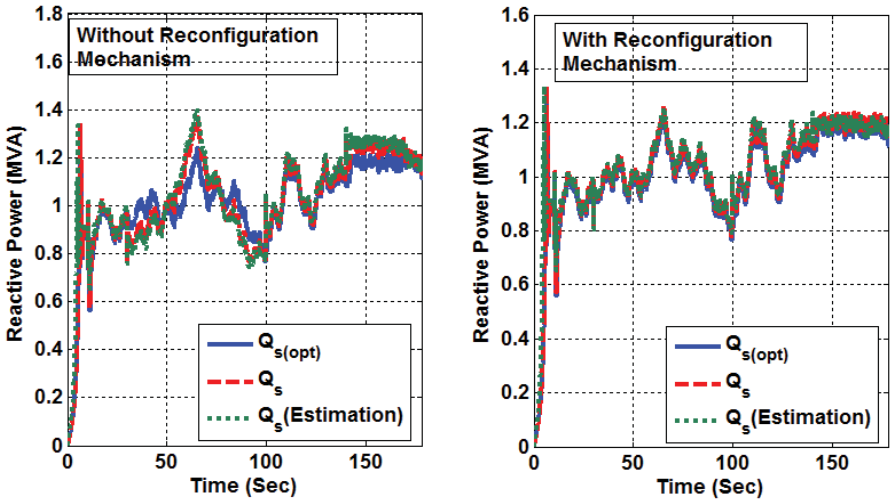

Fig. 4.13. The trajectories of Q_s (dashed line) and its estimate (dotted line) without (left) and with (right) RFSFTC strategy

From the simulation, it can be seen that without the reconfiguration mechanism, the WES lost performance just after the generator speed sensor became faulty, whereas for the same reference input and by using the RFSFTC scheme strategy proposed, the WES remains stable in the presence of sensor

faults, parameter uncertainties and actuator fault which demonstrates the effectiveness of the proposed RFSFTC strategy.

In summary, it has been shown that the proposed scheme is able to detect and isolate sensor faults, through a proper and feasible selection of the healthy observed variables. It can also compensate for the actuator fault using the nonlinear FPIEO. The simulation results demonstrate the effectiveness of the proposed control approach. The proposed control scheme can guarantee the stability of the closed-loop system and the convergence of the output tracking error.

4.4. RDFFTC of HWDSS Subject to Actuator and Sensor Faults

This section extends the general ideas proposed in section 3.4. A fuzzy FTC approach is proposed for WES with norm-bounded parameter uncertainties, sensor faults and actuator faults. The algorithm utilizes fuzzy systems based on TS fuzzy models to approximate uncertain nonlinear systems with sensor faults and actuator faults. Sufficient stabilization conditions of the fuzzy fault tolerant control systems are given, which are formulated in terms of LMEs. The proposed algorithm combines the merits of: (i) The states of the closed-loop system will follow those of a user-defined stable reference model despite the presence of bounded magnitude sensor faults, actuator faults and parameter uncertainties; (ii) The algorithm maximizes the power coefficient for a fixed pitch and reduces the voltage ripple.

This section is organized as follows: Section 4.4.1 describes the fuzzy system subject to sensor and actuator faults with parameter uncertainties. The proposed fault tolerant controller and the condition for stability are presented in section 4.4.2. Section 4.4.3 presents TS fuzzy description for the WES and simulations of sensor and actuator faults and results analysis.

4.4.1. Fuzzy Observer Scheme for the Uncertain System With Sensor and Actuator Faults

The objective is to design a fuzzy observer for nonlinear system with parametric uncertainties, sensor fault and actuator faults. Consider initially the i-th rule of the TS fuzzy model with parametric uncertainties, sensor and actuator faults [46], [138] is given by.

Plant Rule i: IF $q_1(x(t))$ is M_{1i} AND … AND $q_\varepsilon(x(t))$ is $M_{\varepsilon i}$

Then $\dot{x}(t) = (A_{fi} + \Delta A_{fi})x(t) + B_{fi}u(t) + E_{ai}f_a(t)$,

$$y(t) = C_{fi}x(t) + E_{si}f_s(t) \qquad i=1,\ldots,p \tag{4.36}$$

Where $q(x(t))=[\ q_1(x(t)),\ldots,q_\varepsilon(x(t))\ ]$ are also measurable variables and do not depend on the faults [138]., i.e., the premise variables, $x(t)\epsilon\kappa^{nx1}$ is the state vector, $u(t)\epsilon\kappa^{mx1}$ is the control input vector, $y(t)\epsilon\kappa^{gx1}$ is the output vector, $A_{fi}\epsilon\kappa^{nxn}$, $B_{fi}\epsilon\kappa^{nxm}$ and $C_{fi}\epsilon\kappa^{gxn}$ are system, input and output matrices, respectively, $\Delta A_{fi}\epsilon\kappa^{nxn}$ is the parametric uncertainties in the plant model, E_{ai} and E_{si} are actuator and sensor faults matrices, respectively, and $f_a(t)$ and $f_s(t)$ represents actuator and sensor faults, respectively, which is assumed to be bounded. The inferred system is given by,

$$\dot{x}(t) = \sum_{i=1}^{p}\mu_i[(A_{fi} + \Delta A_{fi})x(t) + B_{fi}u(t) + E_{ai}f_a(t)] \quad ,$$

$$y(t) = \sum_{i=1}^{p}\mu_i[C_{fi}x(t) + E_{si}f_s(t)] \tag{4.37}$$

Consider also the state $Z(t)\epsilon\kappa^{rx1}$ that is a filtered version of the output $y(t)$ [139]. This state is given by:

$$\dot{Z}(t) = \sum_{i=1}^{p}\mu_i[-A_{zi}z(t) + A_{zi}C_{fi}x(t) + A_{zi}E_{si}f_s(t)] \tag{4.38}$$

where $-A_{zi}\epsilon\kappa^{rxr}$ is the stable matrix, from the (4.37) and (4.38), one can obtain the augmented system:

$$\dot{X}(t) = \sum_{i=1}^{p} \mu_i [(A_i + \Delta A_i) X(t) + B_i u(t) + E_i f(t)] \quad ,$$

$$Y(t) = \sum_{i=1}^{p} \mu_i C_i X(t) \tag{4.39}$$

where

$$X(t) = \begin{bmatrix} x(t) \\ Z(t) \end{bmatrix}, f(t) = \begin{bmatrix} f_a(t) \\ f_s(t) \end{bmatrix} A_i = \begin{bmatrix} A_{fi} & 0 \\ A_{zi} C_{fi} & -A_{zi} \end{bmatrix}, \Delta A_i = \begin{bmatrix} \Delta A_{fi} & 0 \\ 0 & 0 \end{bmatrix}, B_i = \begin{bmatrix} B_{fi} \\ 0 \end{bmatrix}, E_i = \begin{bmatrix} E_{ai} & 0 \\ 0 & A_{zi} E_{si} \end{bmatrix},$$

$$C_i = [0 \quad I]$$

Based on the (4.4), the overall fuzzy observer is represented as follows:

$$\dot{\hat{X}}(t) = \sum_{i=1}^{p} \mu_i [A_i \hat{x}(t) + B_i u(t) + E_i \hat{f}(t) + K_i (Y(t) - \hat{Y}(t))] \quad ,$$

$$\dot{\hat{f}}(t) = \sum_{i=1}^{p} \mu_i L_i (Y - \hat{Y}) = \sum_{i=1}^{p} \mu_i L_i \tilde{Y} \ ,$$

$$\hat{Y}(t) = \sum_{i=1}^{p} \mu_i C_i \hat{x}(t) \tag{4.40}$$

where K_i is the proportional observer gain and L_i is its integral gain for the i-th observer rule. $Y(t)$ and $\hat{Y}(t)$ are the final output of the fuzzy system and the fuzzy observer respectively.

4.4.2. Proposed RDFFTC, Reference Model and Stability Analysis

In order to establish the conditions for the asymptotic convergence of the observers (4.40), consider the stable linear model without faults described as in (3.32). The proposed FTC scheme depends on the scheme of Fig. 3.16.

4.4.2.1. Proposed RDFFTC

Based on the analysis given in section 3.4.2.2, we construct the following fuzzy controller based on (3.38), the global output of the fuzzy fault tolerant controller is given by

$$u(t) = \sum_{i=1}^{p} \mu_i u_i(t) \tag{4.41}$$

From (4.38), (4.39) and (4.41), we have,

$$\dot{X}(t) = \sum_{i=1}^{p} \mu_i (A_i + \Delta A_i) X(t) + Bu(t) + Ef(t)]$$

$$Y(t) = \sum_{i=1}^{p} \mu_i C_i X(t) \tag{4.42}$$

Note that B and E are known, and defined as given in (3.40) and (3.52)

4.4.2.2. Stability Analyses of the Proposed RDFFTC

The analysis procedures are the same as those in section 3.4.2.3, so the analysis results will be presented without proof. The main result for the global asymptotic stability of a TS fuzzy model with parameter uncertainties, sensor faults, and actuator faults are summarized by the following lemma 4.1 and theorem 4.3. The sufficient and necessary stability condition of the nonlinear control system (4.42) is summarized by the following lemma 4.1 and theorem 4.3.

Lemma 4.1: The fuzzy control system as given by (4.42) is stable if B_i is nonsingular and the control laws of fuzzy controller of (4.41) are designed as,

$$u_i(t) = B_i^{-1}\Big\{[He_1(t) + \bar{A}\,\bar{x}(t) + \bar{B}r(t) - A_i x(t) - S\hat{f}(t) \; - \frac{e_1(t)\|e_1(t)\|\|P_1\|\|\Delta A_i\|_{\max}\|x(t)\|}{e_1(t)^T P_1 e_1(t)} - \frac{e_1(t)\|x(t)\|\|D\|_{\max}\|x(t)\|}{e_1(t)^T P_1 e_1(t)}$$

$$- \frac{e_1(t)\|e_1(t)\|\|P_1\|\|E\|_{\max}\|\tilde{f}(t)\|}{e_1(t)^T P_1 e_1(t)} J\Big\} \tag{4.43}$$

$\|\cdot\|$ denotes the l_2 norm for vectors and l_2 induced norm for matrices, $\|\Delta A_i\| \le \|\Delta A_i\|_{\max}$, $\|E\| \le \|E\|_{\max}$, $\|D\| \le \|D\|_{\max}$, $H \in \kappa^{nxn}$ is a stable matrix to be designed and choosing S so that $S=E$ and $D=B_{oi}{}^T B_{oi}$.

Theorem 4.3: If there exist symmetric and positive definite matrices P_{11}, some matrices K_i and L_i ,and matrices Z_{qi} , Q_i, such that the following LMEs are satisfied, then the TS fuzzy system (4.42) is asymptotically stabilizable via the TS fuzzy model based output-feedback controller (4.41) and (4.43)

$$A_i{}^T P_{11} + P_{11} A_i + (Z_{qi} C_i)^T + (Z_{qi} C_i) = -\sigma I \tag{4.44}$$

$$(Q_iC_i)^T + (Q_iC_i) = -\sigma I \tag{4.45}$$

According to the analysis above, the procedure for finding the proposed fuzzy FTC controller and the FPIEO observer are summarized as follows.

1. Obtain the mathematical model of the HWDSS to be controlled.
2. Obtain the fuzzy plant model for the system stated in step (1) by means of a fuzzy modeling method.
3. Check if there exists B^{-1} by determining its rank
4. Choose a stable reference model.(3.32)
5. Solve LMEs (4.44) and (4.45) to obtain Q_i, Z_{qi}, P_{11}, K_i and L_i thus ($Z_{qi}=-P_{11}K_i$ and $Q_i=-P_{11}L_i$)
6. Construct fuzzy observer (4.40) according to the theorem 4.1 and fuzzy controller (4.41) according to the Lemma 4.1.

In the same manner as given in chapter 2, by solving (4.44) and (4.45) related to HWDSS, the robustness index σ as shown in the Fig.4.14.

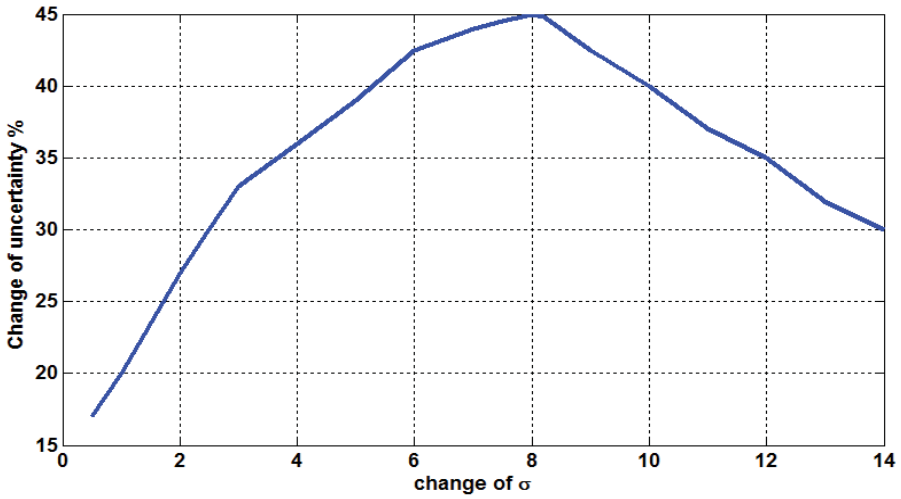

Fig. 4.14. Change of uncertainty with σ

4.4.3. HWDSS Application and Simulations and Results

In this section the HWDSS (3.82) used in application example C, in chapter 3 will be used as an application example and we study the simulations of sensor and actuator faults and results analysis.

4.4.3.1. TS Fuzzy HWDSS Description

We first represent the system (3.82) by a TS fuzzy representation with the angular speed of SG (ω_s) and the bus voltage (V_b) as the measurable premise variables. Consequently the HWDSS can be represented by a TS-fuzzy plant model having four rules. The *ith* rule can be written as follow ($i=1,2,3,4$):

Rule i: IF $q_1(t)$is N_{ji} and $q_2(t)$is M_{ji}

Then $\dot{x}(t) = (A_i + \Delta A_i)x(t) + B_i u(t) + E_{ai} f_a(t)$,

$$y(t) = C_i x(t) + E_{si} f_s(t) \qquad j=1,2;i=1,2,...,4 \tag{4.46}$$

Referring to (4.36) the fuzzy plant model given by:

$$\dot{x}(t) = \sum_{i=1}^{4} \mu_i [(A_i + \Delta A_i) x(t) + B_i u(t) + E_{ai} f(t)] \ ,$$

$$y(t) = \sum_{i=1}^{4} \mu_i [C_i x(t) + E_{is} f_s(t)] \tag{4.47}$$

Where $x(t) \in \kappa^{2x1}, u(t) \in \kappa^{2x1}$ are the state vectors and the control input, respectively, ΔA_i represents the system parameters uncertainties but bounded, the elements of ΔA_i randomly achieve the values within 30% of their nominal values corresponding to A_i, which represent the change of parameter uncertainties L_f, L_d, and D_s within 30% of their nominal values and ΔB_i =0. The minimum and maximum values of $q_1(t)$ and $q_2(t)$ are given by $q_1(t) \in [q_{1min}\ q_{1max}] \in [1/240\ \ 1/220]$ and $q_2(t) \in [q_{2min}\ \ q_{2max}] \in [1/3\ \ 1/0.1]$, the membership functions ($N_i(q_1(t))$, $M_i(q_2(t))$) are related to the uncertain system parameters are shown in Fig. 3.19 in chapter 3 and given by

$$N_1(q_1(t)) = \frac{q_1(t) - q_{1\min}}{q_{1\max} - q_{1\min}},\ N_2(q_1(t)) = 1 - N_1(q_1(t)) \tag{4.48}$$

$$M_1(q_2(t)) = \frac{q_2(t) - q_{2\min}}{q_{2\max} - q_{2\min}},\ M_2(q_2(t)) = 1 - M_1(q_2(t)) \tag{4.49}$$

$$A_1 + \Delta A_1 = \begin{bmatrix} 1 & 1 \\ 0 & 1 \end{bmatrix} \begin{bmatrix} \frac{L_f + \Delta L_f}{\tau L_{md}} q_{1\max} & \frac{L_f + \Delta L_f}{\tau L_{md}} q_{1\max}((L_d + \Delta L_d) i_{sd} - r_a i_{sq} q_{1\max}) \\ \frac{P_{ind} - P_{load}}{J_s} q_{2\min} & -\frac{D_s + \Delta D_s}{J_s} \end{bmatrix}$$

$$A_2 + \Delta A_2 = \begin{bmatrix} 1 & 1 \\ 0 & 1 \end{bmatrix} \begin{bmatrix} \frac{L_f + \Delta L_f}{\tau L_{md}} q_{1\max} & \frac{L_f + \Delta L_f}{\tau L_{md}} q_{1\max}((L_d + \Delta L_d) i_{sd} - r_a i_{sq} q_{1\max}) \\ \frac{P_{ind} - P_{load}}{J_s} q_{2\max} & -\frac{D_s + \Delta D_s}{J_s} \end{bmatrix}$$

$$A_3 + \Delta A_3 = \begin{bmatrix} 1 & 1 \\ 0 & 1 \end{bmatrix} \begin{bmatrix} \frac{L_f + \Delta L_f}{\tau L_{md}} q_{1\min} & \frac{L_f + \Delta L_f}{\tau L_{md}} q_{1\min}((L_d + \Delta L_d) i_{sd} - r_a i_{sq} q_{1\min}) \\ \frac{P_{ind} - P_{load}}{J_s} q_{2\min} & -\frac{D_s + \Delta D_s}{J_s} \end{bmatrix}$$

$$A_4 + \Delta A_4 = \begin{bmatrix} 1 & 1 \\ 0 & 1 \end{bmatrix} \begin{bmatrix} \frac{L_f + \Delta L_f}{\tau L_{md}} q_{1\min} & \frac{L_f + \Delta L_f}{\tau L_{md}} q_{1\min}((L_d + \Delta L_d) i_{sd} - r_a i_{sq} q_{1\min}) \\ \frac{P_{ind} - P_{load}}{J_s} q_{2\max} & -\frac{D_s + \Delta D_s}{J_s} \end{bmatrix}$$

$$B_1 = B_2 = \begin{bmatrix} 1 & -\frac{V_c}{J_s} q_{1\max} \\ 0 & -\frac{V_c}{J_s} q_{1\max} \end{bmatrix},\ B_3 = B_4 = \begin{bmatrix} 1 & -\frac{V_c}{J_s} q_{1\min} \\ 0 & -\frac{V_c}{J_s} q_{1\min} \end{bmatrix}\ E_{ai} = \begin{bmatrix} 1 & 1 \\ 0.1 & 0.1 \end{bmatrix}$$

$$E_{si} = \begin{bmatrix} 10 & 1 \\ 0.1 & 0.01 \end{bmatrix}$$

To define the state *Z*, one choose $A_{iz} = 20 \times I$, where *I* is the identity matrix. Consider $H = \begin{bmatrix} -4 & -4 \\ 0 & -1 \end{bmatrix}$ is a stable matrix. The stable reference model is chosen as follows,

$$\overline{A} = \begin{bmatrix} -4 & -4 \\ 0 & -4 \end{bmatrix}, \overline{B} = \begin{bmatrix} 1 & 1 \\ 0 & 1 \end{bmatrix}, \overline{C} = \begin{bmatrix} 1 & 0 \\ 0 & 1 \end{bmatrix}$$

Solve LMEs (4.44) and (4.45) give the computation of the matrices K_i and L_i. Based on the lemma 1, construct the fuzzy fault tolerant controller (4.41) and based on the theorem construct the fuzzy observer (4.40).

4.4.3.2. Simulation Studies

The proposed RDFFTC for the HWDSS (3.82) is tested and we study the responses for the HWDSS subject to sensor faults, actuator faults and parameter uncertainties. The proposed controller is tested for same random profiles of wind speed signal as shown in Fig.3.16 in chapter 3 to prove the effectiveness of the proposed algorithm. The actuator fault $f_a(t)=[f_{a1}\ f_{a2}]^T$ are modeled as the following

$$f_{a1}(t) = \begin{cases} 0 & t < 13.34\text{sec} \\ 3\sin(\pi t) & t \geq 13.34\ \text{sec} \end{cases}, f_{a2}(t) = \begin{cases} 0 & t \leq 13.34\ \text{sec} \\ \sin(\pi t) & t \geq 13.34\ \text{sec} \end{cases} \quad (4.50)$$

where $f_{a1}(t)$is the excitation field voltage actuator fault of the SG and the direct-current set point actuator fault of the converter is $f_{a2}(t)$. The sensor faults $f_s(t)=[f_{s1}\ f_{s2}]^T$ are modeled as follow

$$f_{s1}(t) = \begin{cases} 0 & t < 22.22\,s \\ 10\sin(\pi t) & t \geq 22.22\,s \end{cases}, f_{s2}(t) = \begin{cases} 0 & t < 22.22\,s \\ 5\sin(\pi t) & t \geq 22.22\,s \end{cases} \quad (4.51)$$

where f_{s1} is the bus voltage sensor and f_{s2} is the generator speed sensors. Fig. 4.15 shows the actuator fault (top) and sensor faults (bottom) and their estimations based on (4.50) and (4.51), respectively. The frequency and bus voltage of the system (dashed line), observer states (dotted line) and reference states (solid line) are shown in Fig.4.16 and Fig.4.17, respectively. When the wind speed is varying, the produced power curve takes almost the wind speed curve as shown in Fig. 4.18, but there is only spike when the fault is detected at 13.34sec and 22.22 sec, it is clear that a 35 % increase is obtained in the maximum value compared with [13].

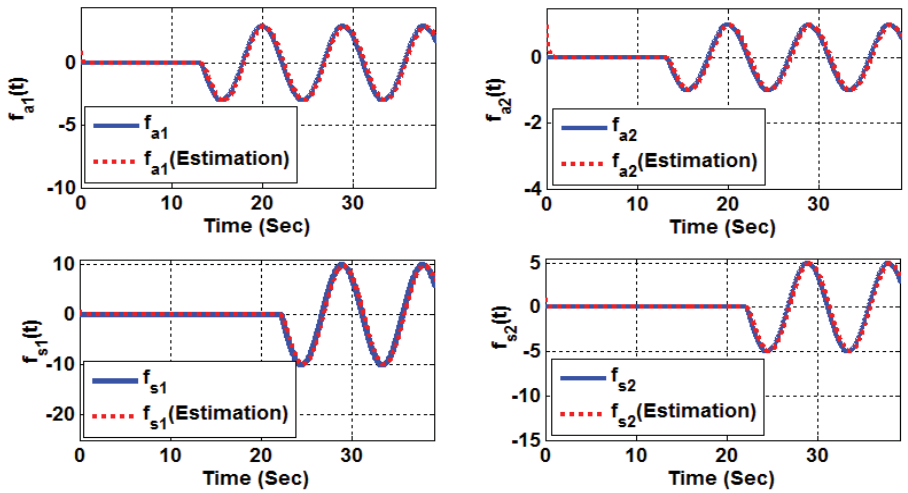

Fig.4.15. Actuator faults ($f_{a1}(t)$ and $f_{a2}(t)$) and their estimations (top) and sensor faults ($f_{s1}(t)$ and $f_{s2}(t)$) and their estimations (bottom)

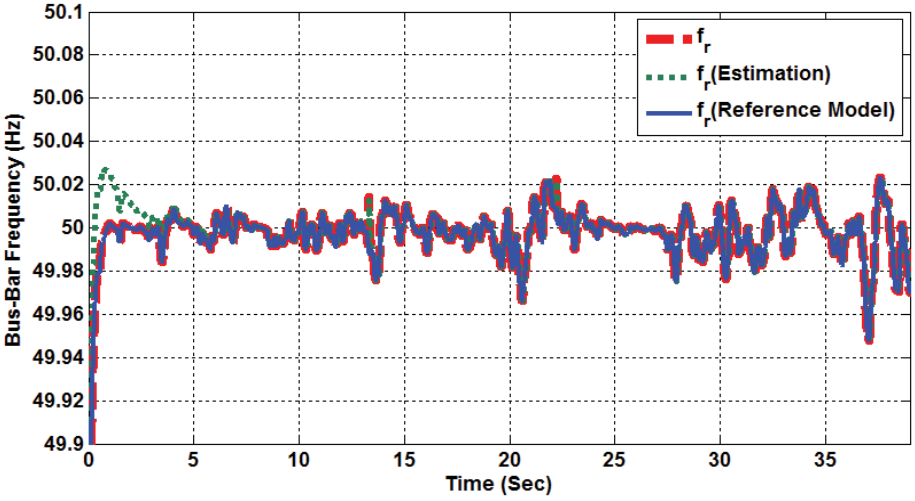

Fig. 4.16. The frequency of the system (dashed line), observer (dotted line) and reference model (solid line)

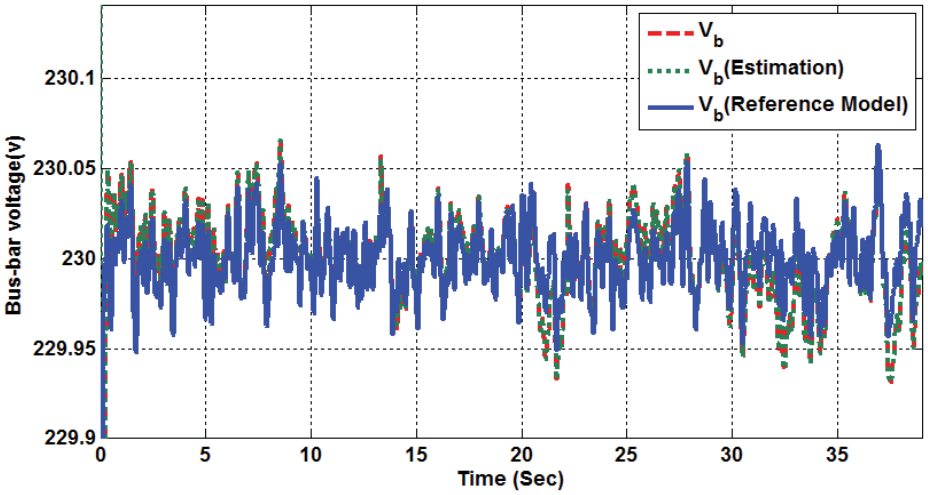

Fig. 4.17. The bus voltage of the system (dashed line), observer (dotted line) and reference model (solid line)

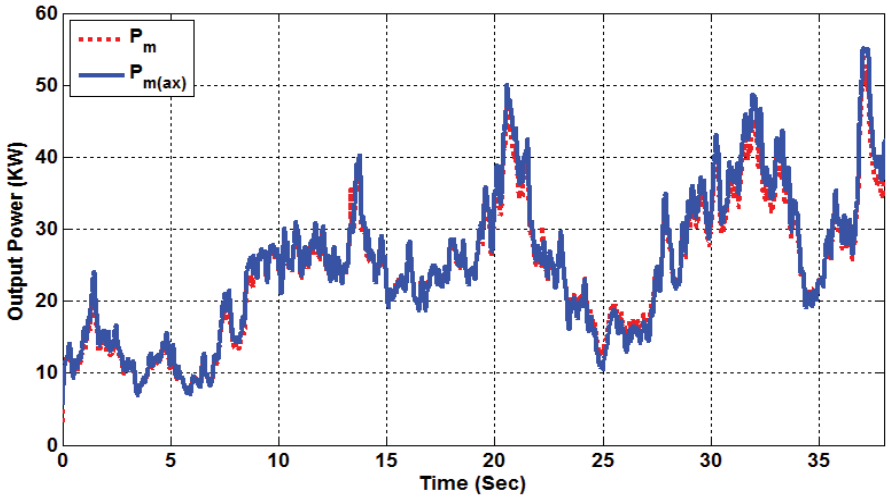

Fig. 4.18. Produced power with the proposed control law

It can be seen from the simulation results there is a good tracking between the states of the nonlinear HWDSS subject to the norm-bounded parametric uncertainties, sensor faults and actuator faults and the reference model.Thus, the TS fuzzy model based controller through fuzzy observer is robust against norm-bounded parametric uncertainties, sensor faults and actuator faults.

Comparing the results of the proposed algorithm, with that given in the previous algorithms, we can be seen that the proposed controller has the following advantages, (i) is stable over a wide range of uncertainty up to 30 % compared with [53] and when the actuators and sensors become faulty at any time, (ii) the generated power is increased and bus voltage is nearly constant compared with [14].

4.5. Chapter Conclusion

An augmented TS fuzzy plant model has been proposed to model the nonlinear plant subject to large parameter uncertainties, sensor faults and actuator faults. Based on this augmented TS fuzzy plant model, three different methods to design the fuzzy fault tolerant control has been proposed to tackle this nonlinear system. A design procedure of fuzzy fault tolerant controllers has been developed. The stability and robustness of the fuzzy fault tolerant control systems have been investigated based on the results of chapter 2 and chapter 3. An application example on stabilizing a WES with sensor faults, actuator faults and parameter uncertainties has been given to illustrate the design procedure and merits of the proposed fuzzy fault tolerant controller.

CHAPTER 5

CHAPTER 5

CONCLUSIONS

Multivariable multi-sources of energy systems subject to parameter uncertainties, sensor faults, actuator faults, unknown inputs and wind disturbance can be represented by a TS fuzzy plant model. To control this plant, a FFTC can be used to close the feedback loop and form a closed-loop system. In this thesis, the stability and robustness analysis of this class of uncertain fuzzy control systems under various robust fuzzy controllers and robust fuzzy fault tolerant controllers have been presented and some design issues have been addressed. In chapter 2, chapter 3 and chapter 4, a RFC and RFSC, FFTC and FSFTC, RFFTC and RFSFTC controller for multivariable nonlinear WES plants subject to sensor, actuator faults and parameter uncertainties have been developed, respectively.

To tackle a multivariable nonlinear plant subject to parameter uncertainties, a robust fuzzy controller has been proposed. Three designs proposed approaches of the robust fuzzy controller have been employed to close the feedback loop under different situations. Stability and robustness conditions have been derived by different methods of the system parameters of the fuzzy control system and the norm values of the parameter uncertainties. The ways of meeting the stability and robustness conditions have been formulated into LMIs and LMEs problems. A nonlinear controller designed based on TS fuzzy plant models has been proposed. The number of linear matrix inequalities involved is reduced. For multivariable nonlinear WES plant subject to large parameter uncertainties, a RFSC has been proposed. This RFSC can deduce the control signal by inferring those from the RFC. The stability and robustness conditions have been derived for the fuzzy scheduled system. Based on the

analysis results, systematic design procedures have been developed for both controllers. For multivariable nonlinear WES with to parameter uncertainties, time varying sensor faults, time varying actuator faults, unknown inputs and wind disturbance within given ranges, a fuzzy fault tolerant controller has been proposed. Three proposed approaches design method of the fault tolerant controller has been developed based on the TS fuzzy plant model. To verify the results of the derived stability and robustness conditions, and the developed design procedures, the proposed fuzzy fault tolerant controllers have been applied to stabilize and control some uncertain nonlinear plants subject to time varying sensor faults or/and actuator faults, namely HWDSS, WES with DFIG and PV generation system.

The proposed algorithm combines the merits of: 1) the capability for dealing with uncertain nonlinear systems; 2) the LMIs and LMEs approaches are used to obtain control gains and observer gains; 3) The stability and robustness analyses throughout this thesis are based on the TS fuzzy plant model and formulated by LMIs and LMEs; 4) Control of the plant over a wide range of wind speeds; 5) Stability over a wide range of uncertainties up to 40% compared with [73] and in the presence of sensor faults and actuator faults; 6) Increased robustness over conventional controllers such as PI [91] and the Linear Quadratic Gaussian (LQG) [73]; 7) The algorithm maxim izes the power coefficient for a fixed pitch. Moreover, it reduces the voltage ripple and stabilizes the system over a wide range of wind speed variations.

For future research, the analysis results and design methodologies of the robust fuzzy controllers and fault tolerant control presented in this thesis can be extended to plants with the premise variables affected by faults and unmeasurable based on the neural fuzzy algorithm. In view of the growing importance of information technology, extending the work reported by this thesis to digital systems should be investigated. In practice, many plants are analog systems; thus, work on sampled-data control systems is equally

important. In addition, the analysis results can be also extended to control for energy management of wind/fuel cell/solar/super-capacitors/batteries hybrid power sources and implemented by real system application.

REFERENCES

REFERENCES

[1] H.-S. Ko, and J. Jatskevich, "Power quality control of wind-hybrid power generation using Fuzzy-LQR controller," *IEEE Trans. Energy Convers.*, vol.22, no.2, pp.516-27, 2007.

[2] H.-S. Ko, T. Niimura, J. Jatskevich, H. C. Kim, and K. Y. Lee, "Power quality control of hybrid wind power generation with battery storage using fuzzy-LQR controller," in *IEEE Power Engineering Society Meeting*, Denver, Colorado, Jun. 2004, pp. 1722–1728.

[3] G. X. Athanasius and J. G. Zhu, "Design of Robust Controller for Wind Turbines," *2nd International Conference on Emerging Trends in Engineering and Technology (ICETET)*, pp.7-12, 2009.

[4] P. Schegner and P. La Seta, "Stability of Asynchronous Wind Generators Using Lyapunov's Direct Method," *Bulk Power System Dynamics and Control - VI*, pp.144-150, 2004.

[5] S. C. Tripathy, "Dynamic simulation of hybrid wind-diesel power generation system with superconducting magnetic energy storage," *Energy Convers. Manage.*, vol.38, no. 9, 1997, pp. 919-930, 1997.

[6] E. Billy Muhando, T Senjyu, A. Uehara and T. Funabashi, "Gain-Scheduled H∞ Control for WECS via LMI Techniques and Parametrically Dependent Feedback Part I: Model Development Fundamentals,"*IEEE Trans. Ind. Electron.*, vol.58, no.1, pp.48-56, 2011.

[7] E. Billy Muhando, T Senjyu, A. Uehara and T. Funabashi, "Gain-Scheduled H∞ Control for WECS via LMI Techniques and Parametrically Dependent Feedback Part II: Controller Design and Implementation," *IEEE Trans. Ind. Electron.*, vol.58, no.1, pp.57-65, 2011.

[8] F. Lescher, J. Y. Zhao and P. Borne, “Robust Gain Scheduling Controller for Pitch Regulated Variable Speed Wind Turbine,” *Studies in Informatics and Control*, vol. 14,no. 4, pp 299-315, 2005.

[9] F. Lescher, J. Y. Zhao and P. Borne, “Switching LPV Controllers for a Variable Speed Pitch Regulated Wind Turbine,” *In. J. Comput., Commun. Control*, vol. 1, no.4, pp.73-84, 2006.

[10] Z. Chen and Y. Hu, “A Hybrid Generation System Using Variable Speed Wind Turbines and Diesel Units,” *IEEE Trans. Energy Convers.*, pp. 2729-2734, 2003.

[11] E. Muljadi and H. Edward McKenna, “Power Quality Issues in a Hybrid Power System,” *IEEE Trans. Ind. Appl.*, vol.38, no.3, pp.803-809, 2002.

[12] B. Boukhezzar and H. Siguerdidjane, “Nonlinear control with wind estimation of a DFIG variable speed wind turbine for power capture optimization,” *Energy Convers. Manage.*, vol. 50, pp.885–892, 2009.

[13] R. B. Chedid, S. H. Karaki and C. El-Chamali, “Adaptive Fuzzy Control for Wind Diesel Weak Power Systems,” *IEEE Trans. Energy Convers.*, vol. 15, no. 1, pp. 71-78, 2000.

[14] E. Kamal, M. Koutb, A. A. Sobaih, and B. Abozalam, "An intelligent maximum power extraction algorithm for hybrid wind-diesel-storage system," *Int. J. Electr. Power Energy Syst.*, vol. 32, no.3, pp. 170-177, 2010.

[15] K. Uhlen, B. A. Foss and O. B. Gjosaeter, “Robust control and analysis of a wind-Diesel hybrid power plant,” *IEEE Trans. Energy Convers.*, vol. 9, no.4, pp.701-708, 1994.

[16] H. Battista and R. J. Mantz, “Dynamical Variable Structure Controller for Power Regulation of Wind Energy Conversion Systems,” *IEEE Trans. Energy Convers.*, vol.19, no.4, pp.756-763, 2004.

[17] C. Sloth, T. Esbensen, O. K. Niss Michae, J. Stoustrup and P. F. Odgaard, "Robust LMI-Based Control of Wind Turbines with Parametric Uncertainties,"*18th IEEE International Conference on Control Applications Part of 2009 IEEE Multiconference on Systems and Control Saint Petersburg*, pp.776-781, 2009.

[18] B. Boukhezzar and H. Siguerdidjane, "Comparison between linear and nonlinear control strategies for variable speed wind turbines," *Control Eng. Pract.*, vol.18, pp.1357-1368, 2010.

[19] M. M. Prats, J. Carrasco, E. Galvan, J. Sanchez, L. Franquelo and C. Batista, "Improving transition between power optimization and power limitation of variable speed, variable pitch wind turbines using fuzzy control techniques," *Proc. IECON 2000, Nagoya*, Japan, vol.3, pp.1497-1502, 2000.

[20] A. G. Abo-Khalil and L. Dong-Choon, "MPPT Control of Wind Generation Systems Based on Estimated Wind Speed Using SVR," *IEEE Trans. Ind. Electron.*, vol.55, no.3, pp.1489-1490, 2008.

[21] V. Aggarwal, R. K. Patidar and P. Patki, "A Novel Scheme for Rapid Tracking of Maximum Power Point in Wind Energy Generation Systems," *IEEE Trans. Energy Convers.*, vol.25, no.1, pp. 228-236, 2010.

[22] H. Camblong, I. Martinez de Alegria, M. Rodriguez and G. Abad, "Experimental evaluation of wind turbines maximum power point tracking controllers," *Energy Convers. Manage.*, vol.47, no.18-19, pp.2846-2858, 2006.

[23] R. Datta and V. T. Ranganathan, "A method of tracking the peak power points for a variable speed wind energy conversion system," *IEEE Trans. Energy Convers.*, vol.18 no.1, pp.163-168, 2003.

[24] L. Whei-Min and H. Chih-Ming, "Intelligent approach to maximum power point tracking control strategy for variable-speed wind turbine generation system," *Energy*, vol.35 no.6, pp.2440-2447, 2010.

[25] V. Galdi, A. Piccolo and P. Siano, “Exploiting maximum energy from variable speed wind power generation system by using an adaptive Takagi-Sugeno-kang fuzzy model,” *Energy Convers. Manage.*, vol.50, pp.413-420, 2009.

[26] S. Masoud Barakati, M. Kazerani and J. Dwight Aplevich, “Maximum Power Tracking Control for a Wind Turbine System Including a Matrix Converter,” *IEEE Trans. Energy Convers.*, vol.24, no.3, pp.705-713, 2009.

[27] E. Koutroulis and K. Kalaitzakis, “Design of a maximum power tracking system for wind-energy-conversion applications,” *IEEE Trans. Ind. Electron.*, vol.53, no.2, pp.486-494, 2006.

[28] A. Z. Mohamed, M. N. Eskander and F. A. Ghali, “Fuzzy logic control based maximum power tracking of a wind energy system,” *Renewable Energy*, vol.23, no.2, pp. 235-245, 2001.

[29] M. M. Prats, J. M. Carrasco, E. Galvan, J. A. Sanchez and L. G. Franquelo, “A new fuzzy logic controller to improve the captured wind energy in a real 800 kW variable speed-variable pitch wind turbine,” *IEEE 33th Annual power Electronics Specialists Conference*, vol.1, pp.101-105, 2002.

[30] A. Hussien Besheer, H. M. Emara and M. M. Abdel-Aziz, “Wind energy conversion system regulation via LMI fuzzy pole cluster approach,” *Electr. Power Syst. Res.*, vol.79, pp. 531-538, 2009.

[31] E. Iyasere, M. Salah, D. Dawson and J. Wagner, “Nonlinear robust control to maximize energy capture in a variable speed wind turbine,” *American Control Conference*, pp. 1824-1829, 2008.

[32] E. Koutroulis, K. Kalaitzakis and N. C. Voularis , “Development of a microcontroller-based, photovoltaic maximum power point tracking control system,” *IEEE Trans. Power Electron.*, vol. 16, no. 1, pp. 46–54, 1995.

[33] V. Salas, E. Olias, A. Barrado, and A. Lazaro, "Review of the maximum power point tracking algorithms for stand-alone photovoltaic systems," *Solar Energy Mater. Solar Cells*, vol. 90, pp. 1555–1578, 2006.

[34] K. H. Hussein, I. Muta, T. Hoshino, M. Osakada, "Maximum photovoltaic power tracking: An algorithm for rapidly changing atmospheric condition," *Proc. Inst. Electr. Eng., Gen. Transmiss. Distrib.*, vol. 142, no. 1, pp.59–64, 1995.

[35] G.J. Yu, Y.S. Jung, J.Y. Choi, I. Choy, J.H. Song and G.S. Kim, "A Novel Two-Mode MPPT Control Algorithm Based on Comparative Study of Existing Algorithms," Proc. *Photovoltaic Specialists Conference*, pp. 1531-1534, 2002.

[36] T. Noguchi, S. Togashi and R. Nakamoto, "Short-Current Pulse-Based Maximum-Power-Point Tracking Method for Multiple Photovoltaic-and-Converter Module System," *IEEE Trans. Ind. Electron*., vol.49, no.1, pp.217-223, 2002.

[37] E. Kamal, A. Azim Sobaih, "Fuzzy Logic Control of Nonlinear Systems with Parametric Uncertainties," Electronic Engineering Research Journal, vol.20, no.1,2 , 2007, Master thesis, Menoufia, 2007.

[38] M. Park and I. K. Yu, "A Study on Optimal Voltage for MPPT Obtained by Surface Temperature of Solar Cell," *Proc. IECON*, pp. 2040-2045, 2004.

[39] X. Wei, M. Verhaegen and T. van Engelen, "Sensor fault detection and isolation for wind turbines based on subspace identification and Kalman filter techniques," *Int. J. Adapt. Control Signal Process*, vol. 24, pp.687-707, 2010.

[40] P. F. Odgaard, J. Stoustrup, R. Nielsen and C. Damgaard, "Observer based detection of sensor faults in wind turbines," *In Proceedings of European Wind Energy Conference*, 2009.

[41] A. Gaillard, S. Karimi, P. Poure, S. Saadate and E. Gholipour, "A fault tolerant converter topology for wind energy conversion system with doubly fed induction generator," *Power Electronics and Application European Conference*, pp.1-6, 2007.

[42] P. J. Ribrant, "Reliability Performance and Maintainance: A Survey of Failure in Wind Power Systems," *KTH school of Electrical Engineering, KTH*, 2006.

[43] X. Wang, Y. Wang, J. Zhicheng and W. Dinghui, "Design of Two-Frequency-Loop Robust Fault Tolerant Controller for Wind Energy Conversion Systems," *5th IEEE Conference on Industrial Electronics and Applicationsis*, pp. 718- 723, 2010.

[44] O. Bennouna, N. Hèraud, H. Camblong, M. Rodriguez and M. Kahyeh, "Diagnosis and Fault Signature Analysis of a Wind Turbine at a Variable Speed," *Proc. I. Mech*, vol. 223, pp.41-50, 2009.

[45] A. Khedher, K. Ben Othman, D. Maquin and M. Benrejeb, "State and Sensor Faults Estimation via a Proportional Integral Observer," *International Multi-Conference on Systems, Signals and Devices*, 2009.

[46] M. Chadli and A. El Hajjaji, "Observer-based robust fuzzy control of nonlinear systems with parametric uncertaintie," *Fuzzy Sets Syst.*, vol. 157, no.9, pp.1276-1281, 2006.

[47] S. Tong, T. Wang and T. Wang, "Observer Based Fault-Tolerant Control for Fuzzy Systems with Sensor and Actuator Failures," *Int. J. of Innovative Computing, Information and Control*, vol.5, no.10, pp. 3275-3286, 2009.

[48] Y. Wang, D. Zhou, S. Joe Qin and H. Wang, "Active Fault-Tolerant Control for a Class of Nonlinear systems with Sensor faults," *International Journal of Control, Automation, and System*, vol.6, no. 3, pp. 339-350, 2008.

[49] C. Yong-Qi, "Design and application of fault observer for variable speed wind turbine system," *Computer Engineering and Applications*, vol. 45, no. 14, pp. 223-227, 2009.

[50] K. Zhang, B. Jiang and P. Shi, "A New Approach to Observer-Based Fault-Tolerant Controller Design for Takagi-Sugeno Fuzzy Systems with State Delay," *Circuits Syst Signal Process* , vol. 28, pp. 679-697, 2009.

[51] H. O. Wang, K. Tanaka, and M. F. Griffin, "An approach to fuzzy control of nonlinear systems: stability and the design issues," *IEEE Trans. Fuzzy Syst.*, vol. 4, no. 1, pp. 14-23, Feb., 1996.

[52] J. Park, J. Kim and D. Park, "LMI-based design of stabilizing fuzzy controllers for nonlinears systems described by Takagi-Sugeno fuzzy model," *Fuzzy Sets Syst.*, vol.122, pp.73-82, 2001.

[53] K. Tanaka, T. Ikeda and H. O. Wang, "Robust stabilization of a class of uncertain nonlinear systems via fuzzy control: Quadratic stability, H∞ control theory, and linear matrix inequalities," *IEEE Trans. Fuzzy Syst.,* vol.4, no.1, pp.1-13, 1996.

[54] H. K. Lam, "Studies on the Stability and Robustness of Uncertain Nonlinear Systems Based on a Fuzzy Logic Approach," Ph.D., Dept. of Electronic and Information Engineering, The Hong Kong Polytechnic University, 2000.

[55] F. D. Bianchi, H. De Battista and R. J. Mantz, "Robust Multivariable Gain-Scheduled Control of Wind Turbines for Variable Power Production," *Int. J. Syst. Control*, vol.1, no.3, pp.103-112, 2010.

[56] X. Yao, S. Liu, G. Shan, Z. Xing, C. Guo and C. Yi, "LQG Controller for a Variable Speed Pitch Regulated Wind Turbine," *International Conference on Intelligent Human-Machine Systems and Cybernetics*, pp. 210-213, 2009.

[57] Y. Xiyun1, L. Xinran, "Sliding Mode Control using Integral Fuzzy Method to Variable Speed Wind Turbine," *Proceedings of the 29th Chinese Control Conference*, pp.4918-4922, 2010.

[58] B. Connor, S. N. Iyer, W.E. Leithead and M. J. Grimble, "Control of a horizontal axis wind turbine using H∞ control," *In Proceedings of the first IEEE Conference on Control Applications*, vol.1, pp.117-122, 1992.

[59] R. Rocha, L. S. M. Filho and M. V. Bortolus, "Optimal Multivariable Control for Wind Energy Conversion System - A comparison between H2 and H∞ controllers," *In Proceedings of the 44th IEEE Conference on Decision & Control*, pp.7906-7911, 2005.

[60] M. M. Hand, "Variable-speed wind turbine controller systematic design methodology: a comparison of nonlinear and linear model-based designs," *NREL report TP-500-25540, National Renewable Energy Laboratory*,1999.

[61] T. Knudsen, P. Andersen and S. Tiffner-Clausen, "Comparing PI and robust control pitch controllers on a 400KW wind turbine by full scale tests, Department of Control Engineering," Aalborg University, Aalborg, Denmark, Tech. Rep. R-97-4174, 1997.

[62] P. Bongers, "Modeling and identification of flexible wind turbines and a factorizational approach to robust control," PhD thesis, Delft University of Technology, June 1994.

[63] P. Bongers, W. Bierbooms , W. Dijkstra, and T. van Hoten, "An integrated dynamic model of a flexible wind turbine," Technical report, Delft University of Technology, 1990.

[64] E. Bossanyi, "The design of closed loop controllers for wind turbines," *Wind Energy*, vol.3, pp.149-163, 2000.

[65] E. L. Van der Hooft and T. G. van Engelen, "Estimated wind speed feed forward control for wind turbine operation optimisation," *Renewable Energy*, vol.32, pp.1273-1287, 2007.

[66] B. Boukhezzar, H. Siguerdidjane, and M. Maureen Hand, "Nonlinear Control of Variable-Speed Wind Turbines for Generator Torque Limiting and Power Optimization," *J. Sol. Energy Eng.*, vol.128, no.4, pp.516-530, 2006.

[67] G. C. Venkatesh and S. V. Kulkarni, "Energy yield of passive stall regulated fixed speed wind turbine with optimal rotor speed," *Electr. Power Syst. Res.*, vol.76, pp.1019-1026, 2006.

[68] T. Pan, Z. Ji and Z. Jiang, "Maximum Power Point Tracking of Wind Energy Conversion Systems Based on Sliding Mode Extremum Seeking Control," *IEEE Energy2030 Conference,* pp.1-5, 2008.

[69] A. Soetedjo, A. Lomi and W. P. Mulayanto, "Modeling of Wind Energy System with MPPT Control," *International Conference on Electrical Engineering and Informatics*, pp.1-5, 2011.

[70] T. Hawkins, W. N. White, G. Hu and F. D. Sahneh, "wind turbine power capture control with robust estimation," *Proceedings of the Dynamic Systems and Control Conference*, pp.1-8, 2010.

[71] F. Poitiers, T. Bouaouiche and M. Machmoum, "Advanced control of a doubly-fed induction generator for wind energy conversion," *Electr. Power Syst. Res.*, vol.79, no.7, pp.1085-1096, 2009.

[72] R. Fadaeinedjad, M. Moallem and G. Moschopoulos, "Simulation of a Wind Turbine With Doubly Fed Induction Generator by FAST and Simulink," *IEEE Trans. Energy Convers.*, vol.23, no.2, pp.690-700, 2008.

[73] M. Gálvez-Carrillo and M. Kinnaert, "Sensor fault detection and isolation in three-phase systems using a signal-based approach," *IET Control Theory Appl.*,, vol.4, no.9, pp.1838–1848, 2010.

[74] M. Gálvez-Carrillo and M. Kinnaert, "Sensor fault detection and isolation in doubly-fed induction generators accounting for parameter variations," *Renewable Energy*, vol.36, no.5, pp.1447-1457, 2011.

[75] N. Patcharaprakiti, S. Premrudeepreechacharnb and Y. Sriuthaisiriwong, "Maximum power point tracking using adaptive fuzzy logic control for grid-connected photovoltaic system," *Renewable Energy*, vol. 30, pp.1771-1788, 2005.

[76] K. H. Hussein, I. Muta, T. Hoshino and M. Osakada, "Maximum photovoltaic power tracking: an algorithm for rapidly changing atmospheric conditions," *lEE Proc.-Gener. Transm. Distrib.*, Vol. 142, pp.59-64, 1995.

[77] V. Salas, E. Olias, A. Barrado and A. Lazaro, "Review of the maximum power point tracking algorithms for stand-alone photovoltaic systems," *Sol. Energy Mater. Sol. Cells*, vol. 90, pp. 1555-1578, 2006.

[78] C.-S. Chiu and Y.-L. Ouyang, "Robust Maximum Power Tracking Control of Uncertain Photovoltaic Systems: A Unified T-S Fuzzy Model-Based Approach," *IEEE Trans. Control Systems Tech.*, vol.19, no.6, pp.1516-1526, 2011.

[79] I. S. Kim, "Robust maximum power point tracker using sliding mode controller for the three-phase grid-connected photovoltaic system," *Sol. Energy*, vol. 81, pp. 405-414, 2007.

[80] M. Veerachary, T. Senjyu and K. Uezato, "Neural-network-based maximum-power-point tracking of coupled-inductor interleavedboost-converter-supplied PV system using fuzzy controller," *IEEE Trans. Ind. Electron.*, vol. 50, no. 4, pp. 749–758, 2003.

[81] T. Takagi and M. Sugeno, "Fuzzy identification of systems and its applications to modeling and control," *IEEE Trans. Syst. Man Cybern*, vol.15, no.1,, pp.116-132, 1985.

[82] H. K. Lam, F. H. F. Leung and P. K. S. Tam, "Design of Fuzzy Observer-Controllers for Uncertain Nonlinear Systems Using Stability and Robustness Analyses," *Multiplevalued-logic*, pp. 391-405, 2000.

[83] Q. Wang and L. Chang, "An Intelligent Maximum Power Extraction Algorithm for Inverter-Based Variable Speed Wind Turbine Systems," *IEEE Trans. Power Electron.*, vol. 19, no. 5, pp. 1242-1249, 2004.

[84] B. Boukhezzar and H. Siguerdidjane, "Nonlinear Control of Variable Speed Wind Turbines for Power Regulation," *Proceedings of the 2005 IEEE Conference on Control Applications*, pp.114-119, 2005.

[85] Vas P., (1990), "Vector control of AC machines.", New York, Oxford Univ. Press.

[86] Slootweg J. G., (2003), "Wind power: modeling and impact on power system dynamics.", Ph.D. thesis, Technische Universiteit Delft.

[87] Tapia A., Tapia G., Ostolaza X., Saen J.R., (2003), "Modeling and control of wind turbine driven doubly fed induction generator.", IEEE Transaction on Energy Conversion, 18, 194-204.

[88] H. Xue and Y. Wang, "Fuzzy optimal control of doubly fed induction wind power generator systems," *International Conference Mechanic Automation and Control Engineering (MACE),* pp.3512-3515, 2010.

[89] J. J. E. Slotine W. Li, "Applied nonlinear control,"Prentice Hall, 1991.

[90] H. K. Khalil, "Nonlinear Systems, Prentice Hall, 1996.

[91] K. Tanaka and M. Sugeno, "Stability analysis and design of fuzzy control systems," *Fuzzy Sets Syst.*, vol. 45, no.2, pp. 135-156, 1992.

[92] K. Tanaka, T. Ikeda and H.O. Wang, "Fuzzy control system design via LMIs," Proceedings of the American Control Conference, pp.2873-2877, 1997.

[93] A. Khedher, K. Ben Othman, D. Maquin and M. Benrejeb, "Design of an adaptive faults tolerant control: case of sensor faults," *WSEAS Transactions on Systems*, vol.9, no.7, pp.794-803, 2010.

[94] X. Wei, M. Verhaegen, and T. van den Engelen, "Sensor fault diagnosis of wind turbines for fault tolerant," *The International Federation of Automatic Control*, pp. 3222-3227, 2008.

[95] H. Wang and S. Daley, "Actuator fault diagnosis: An adaptive observer-based technique," *IEEE Trans. Automat. Contr.,* vol.41, no.7, pp.1073–1078, 1996.

[96] K. Zhang, B. Jiang and V. Cocquempot, "Adaptive observer-based fast fault estimation," *Int. J. Control Autom. Syst.*, vol.6, no.3, pp.320–326, 2008.

[97] C. J. Lopez-Toribio and R. J. Patton, "Takagi-Sugeno fuzzy fault-tolerant control for a non-linear system," *in Proceedings of the 38th IEEE Conference on Decision and Control*, pp. 4368-4373, 1999.

[98] R. J. Patton, J. Chen and C. J. Lopez-Toribio, "Fuzzy observers for non-linear dynamic systems fault diagnosis," *in Proceedings of the 37th IEEE Conference on Decision and Control*, pp.84–89, 1998.

[99] G. Notton, C. Cristofari, P. Poggi, and M. Muselli, "Wind Hybrid Electrical Supply System: Behavior Simulation and Sizing Optimization," *Wind Energy*, vol. 4, pp.43-59, 2001.

[100] C. Protogeropoulos, B. J. Brinkworth and R. H. Marshall, "Sizing and techno-economical optimization for hybrid solar photovoltaic/wind power systems with battery storage," *Int. J. Energy Res.*, vol. 21, pp.465-479,1997.

[101] M. D. Mufti, R. Balasubramanian and S. C. Tripathy, "Dynamic performance assessment of an isolated wind-diesel power system with superconducting magnetic energy storage unit under turbulent wind and load disturbances," *Int. J. Energy Res.*, vol. 26, pp.185-201, 2002.

[102] I. J. Iglesias, L. Garcia-Tabarés, A. Agudo, I. Cruz and L. Arribas, "Design and simulation of a stand-alone wind-diesel generator with a

flywheel energy storage system to supply the required active and reactive power," *IEEE 31st Power Electronics Specialists Conference*, pp.1381-1386, 2000.

[103] A. K. Jindal, A. M. Gole and D. Muthumuni, "Modeling and Performance Analysis of an Integrated Wind/Diesel Power System for Off-Grid Locations," *15th National Power Systems Conference (NPSC)*, pp. 574-579, 2008.

[104] M. Oudghiri, M. Chadli, A. EL-Hajjaji, " Robust observer based fault-tolerant control for vehicle lateral dynamics," *International Journal of Vehicle Design*, vol. 48, no 3-4 ,pp. 167,2008

[105] W. Chen and M. Saif, "Design of a TS Based Fuzzy Nonlinear Unknown Input Observer with Fault Diagnosis Applications," *American Control Conference*, pp. 2545-2550, 2007.

[106] J. Chen and R. J. Patton, "Robust Model Based Fault Diagnosis for Dynamic Systems," Kluwer Academic Publishers, ISBN 0-7923-8411-3, 1999.

[107] S. X. Ding, S. Schneider, E. L. Ding and A. Rehm, "Advanced model-based diagnosis of sensor faults in vehicle dynamics control systems," IFAC, 16th Triennial World Congress, Prague, Czech Republic, 2005.

[108] R. Chen and J. S. Liu, "Mixture Kalman Filters," Journal of the Royal Statistical Society (B), Vol. 62, pp.493-508, 2000.

[109] R. Isermann, "Diagnosis methods for electronic controlled vehicles," International Journal of Vehicle Mechanics and Mobility, vol. 36, No. 2-3, pp. 77–117, 2001.

[110] J. Huang and M. Tomizuka, "LTV Controller Design for vehicle lateral control under fault in rear sensors," IEEE/ASME Trans. On Mechatronics, Vol 10, No 1, pp. 1-7, 2005.

[111] M. Oudghiri M. Chadli and A. El Hajjaji, "Observer-based fault tolerant control for vehicle lateral dynamics," European Control Conference ECC07, Kos, Greece 2-5 July, 2007.

[112] S.-L. Sun, "Multi-sensor optimal information fusion Kalman filters with applications," *Aerospace Sci. Technol.*, vol.8, no.1, pp.57-62; 2004.

[113] J. Huang and M. Tomizuka, "LTV Controller Design for vehicle lateral control under fault in rear sensors," *IEEE/ASME Trans. On Mechatronics*, vol.10, no.1, pp.1-7; 2005.

[114] M. Witczak, L. Dziekan, V. Puig and J. Korbicz, "Design of a fault-tolerant control scheme for Takagi-Sugeno fuzzy Systems," *16th Mediterranean Conference on Control and Automation Congress Centre*, pp. 280-285, 2008.

[115] X.-J. Ma, Z.-Q. Sun and Y.-Y. He, "Analysis and Design of Fuzzy Controller and Fuzzy Observer," *IEEE Trans. Fuzzy Syst.*, vol. 6, no.1, pp 41-51, 1998.

[116] D. Ichalal, B. Marx, D. Maquin and J. Ragot, "New fault tolerant control strategy for nonlinear systems with multiple model approach," *Control and Fault Tolerant Systems Conference*, pp.606-611, 2010.

[117] Y. Zhang, S. Xu, Y. Zou and J. Lu, "Delay-dependent robust stabilization for uncertain discrete-time fuzzy Markovian jump systems with mode-dependent time delays," *Fuzzy Sets Syst.*, vol.164, no.1, pp.66-81, 2011.

[118] B. Zhang, W. X. Zheng and S. Xu, "Passivity analysis and passive control of fuzzy systems with time-varying delays," *Fuzzy Sets Syst.*, vol.174, no.1, pp.83-98, 2011.

[119] S. He and F. Liu, "Filtering-based robust fault detection of fuzzy jump systems," *Fuzzy Sets Syst.*, vol.185, no.1, pp.95-110, 2011.

[120] I. Kar, P. Patchaikani and L. Behera, "Short Communication On balancing a cart-pole system using T-S fuzzy model," *Fuzzy Sets Syst.*, vol. 207 , pp. 94-110, 2012.

[121] C. Hu, H. Jiang and Z.Teng, "General impulsive control of chaotic systems based on a TS fuzzy model, *Fuzzy Sets Syst.*," vol.174, pp.66–82, 2011.

[122] T. M. Guerra, M. Bernal, K. Guelton and S. Labiod, "Non-quadratic local stabilization for continuous-time Takagi–Sugeno models," *Fuzzy Sets Syst.*," vol. 201, pp.40–54, 2012.

[123] O. M. Kwon, M. J. Park, S. M. Lee and J. H. Park, "Augmented Lyapunov–Krasovskii functional approaches to robust stability criteria for uncertain Takagi–Sugeno fuzzy systems with time-varying delays," *Fuzzy Sets Syst.*, vol.201, pp.1-19, 2012.

[124] Q. Gao, G. Feng, Y. Wang and J. Qiu, "Universal fuzzy controllers based on generalized T-S fuzzy models," *Fuzzy Sets Syst.*," vol. 201, pp.55–70, 2012.

[125] Q.-F. Liao, W.-J. Cai, S.-Y. Li and Y.-Y. Wang, "Interaction analysis and loop pairing for MIMO processes described by T-S fuzzy models," *Fuzzy Sets Syst.*, vol. 207, pp.64-76, 2012.

[126] S. X. Guo, "Robust reliability as a measure of stability of controlled dynamic systems with bounded uncertain parameters," *J. Vib. Control*, vol.16, no.9, pp.1351-1368, 2010.

[127] R. Patton, "Fault-tolerant control systems," The 1997 situation, 3rd IFAC Symposium on Fault Detection, Supervision and Safety of Technical Processes, pp. 1033–1054, 1997.

[128] H. Niemann and J. Stoustrup, "Passive fault tolerant control of a double inverted pendulum—A case study*," Control Eng. Pract*, vol.13, no.8, pp.1047–1059, 2005.

[129] M. M. Mufeed, J. Jiang and Z. Zhang, "Active Fault Tolerant Control Systems: Stochastic Analysis and Synthesis," Springer-Verlag, Berlin/Heidelberg, 2003.

[130] C. Ocampo-Martinez, J. De Dona and M. Seron, "Actuator fault-tolerant control based on set separation," *Int. J. Adapt Control Signal Process.*, vol.24, no.12, pp.1070–1090, 2010.

[131] D. J. Leith and W. E. Leithead, "Survey of gain scheduling analysis design," *Int. J. Control*, vol. 73, no.11, pp.1001-1025, 1999.

[132] D. J. Stilwell and W. J. Rugh, "Interpolation of observer state feedback controllers for gain scheduling," *IEEE Trans. Autom. Control*, vol.44, no.6, pp.1225-1229, 1997.

[133] B. Marx, D. Koenig and D. Georges, "A Robust fault tolerant control for descriptor systems," *IEEE Trans. Autom. Control,* vol.49, no.10, pp.1869-1875, 2004.

[134] Y. Zhang and J. Jiang, "Bibliographical review on reconfigurable fault tolerant control systems," *Annual Reviews in Control*, vol.32, no.2, pp.229-252, 2008.

[135] Z. Zuo, D. W.C. Ho and Y. Wang, "Fault tolerant control for singular systems with actuator saturation and nonlinear perturbation," *Automatica,* vol.46, no.3, pp.569-576, 2010.

[136] Y. Shtessel, J. Buffington and S. Banda, "Tailless aircraft flight control using multiple time scale reconfigurable sliding modes," *IEEE Trans. Control Systems Tech.*, vol.10, no.2, pp.288-296, 2002.

[137] S. A. Khan and M. I. Hossain, "Intelligent control based maximum power extraction strategy for wind energy conversion system," 24th Canadian Conference on Electrical and Computer Engineering (CCECE), pp.1040-1043, 2011.

[138] J. Chen, R. Patton and H. Zhang, “Design of unknown input observers and robust fault detection filters,” *Int. J. Control*, vol.63, pp.85–105, 1996.

[139] C. Edwards, “A comparison of sliding mode and unknown input observers for fault reconstruction,” *European journal of control*, vol.12, no.3, pp. 245-260, 2006.

RÉSUMÉ

Cette thèse présente une analyse de la stabilité pour une classe de systèmes non linéaires incertains et une méthode pour concevoir des contrôleurs flous robustes pour stabiliser les systèmes multi-sources d'énergie assujettis à des incertitudes paramétriques, des défauts de capteur, des défauts d'actionneurs, d'entrées inconnues et des perturbations. Tout d'abord, le modèle flou de Takagi-Sugeno (TS) est adopté pour la modélisation floue du système non linéaire incertain. Ensuite, nous proposons une méthode d'observateurs flous dédiés (OFD) et un Observateur Flou Proportionnel Intégral (OFPI) et une commande tolérante aux fautes pour les systèmes de type TS. Les observateurs dédiés fournissent des résidus pour la détection et la localisation des défauts de capteurs qui peuvent affecter un modèle TS et l'observateur proportionnel intégral permet d'estimer les défauts d'actionneurs qui alimentent le banc d'observateurs dédiés pour reconfigurer la loi de commande. Le concept de compensations distribuées parallèle (PDC) est utilisé pour concevoir une commande floue tolérante aux fautes et des observateurs à partir des modèles flous TS. Les systèmes flous TS sont classés en trois familles sur la base des matrices d'entrée et une synthèse de la commande est proposée pour chaque famille. Dans chaque famille, des conditions suffisantes sont établies pour la stabilisation robuste, dans le sens de Taylor et de Lyapunov, pour le système flou TS. Des conditions suffisantes sont formulées sous la forme d'inégalités matricielles linéaires (LMI) et d'égalités linéaires matricielles (LME). Des remarques importantes pour l'analyse de la stabilité et le concept sont données. L'efficacité de la méthodologie de conception de la commande proposée est finalement démontrée par un système hybride éolien-diesel (HWDS), système d'énergie éolienne (SEA) avec les machines asynchrones à double alimentation (MADA) et une installation photovoltaïque de nouvelle génération (PV).

Mots clés : MADA, l'énergie éolienne, photovoltaïque, MPPT, Observateur à entrées inconnues, Commande Tolérante aux Fautes, Détection de fuite, Diagnostic à base de modèle, LMI, Paramètres incertitudes, les défauts de sonde, défauts d'actionneurs